Development of an albumin-binding ligand for prolonging the plasma half-life of peptide therapeutics

THÈSE N^{O} 7728 (2017)

PRÉSENTÉE LE 2 JUIN 2017

À LA FACULTÉ DES SCIENCES DE BASE
LABORATOIRE DE PROTÉINES ET PEPTIDES THÉRAPEUTIQUES
PROGRAMME DOCTORAL EN CHIMIE ET GÉNIE CHIMIQUE

ÉCOLE POLYTECHNIQUE FÉDÉRALE DE LAUSANNE

POUR L'OBTENTION DU GRADE DE DOCTEUR ÈS SCIENCES

PAR

Alessandro ZORZI

acceptée sur proposition du jury:

Prof. S. Gerber, présidente du jury
Prof. C. Heinis, directeur de thèse
Prof. R. E. Kontermann, rapporteur
Prof. K. J. Jensen, rapporteur
Prof. B. E. Correia, rapporteur

ÉCOLE POLYTECHNIQUE
FÉDÉRALE DE LAUSANNE
Suisse
2017

Let me tell you the secret that has led me to my goal.

My strength lies solely in my tenacity.

- Louis Pasteur -

Acknowledgements

First of all, I would like to thank my supervisor Professor Christian Heinis. Thank you for accepting me as an Erasmus student in 2012, recognizing my potential and motivation, and giving me the opportunity to start a Ph.D. in your laboratory. I have appreciated all of your scientific advice as well as the support through the years.

I would like to thank Prof. Bruno Correia, Prof. Roland Kontermann and Prof. Knud Jensen for being part of the jury and evaluating my work, and to Prof. Sandrine Gerber for chairing the committee.

I am also very grateful to our secretaries Beatrice and Anne Lene for all the administrative help, their kindness and availability.

A huge thanks to all of the past and current members of the LPPT group for the nice, fun and helpful atmosphere at work. Thanks to the “old generation” Jeremy, Lisa, Silvia, Inma, Philippe, Mike, Vanessa, Charlotte, Ranga, and in addition Julia and Alessandro — not “official” colleagues in the laboratory but clearly fundamental pillars in its scientific development. You all accepted me as a simple student, taught me a lot, and then as a colleague, taught me even more. I have learned so many things from all of you that have contributes to my formation as scientist that I cannot even quantify or qualify this. Thanks to the “contemporary-new generation” consisting of Camille, Davide, Sangram, Jonas, Simon, Christina, Xudong, Manh, Kaycie and Vanessa, for all the help, feedback and constant support. I finally wish a good luck to the “freshly arrived” Patrick, Joao, Ganesh, Carl and YuTeng. Your positive joy and attitude is already improving the atmosphere in the lab.

A special mention goes to the Italian LPPT crew, composed of Silvia, Lisa, Beatrice, Davide and Vanessa. You were and still are the base of my survival at EPFL and in Lausanne.

Silvia, you were an amazing surprise in this experience, and you became one of my best friends. It was always too easy to share ideas with you and enjoy together the life in Lausanne. Thanks!

Lisa, you have been for me the first teacher in the lab and a “sister” who provided crucial suggestions for surviving all these years in the lab without getting in troubles and losing motivation.

Beatrice, we came here together as “Erasmus students/friends”, and we are still here, always fighting and laughing as in the past. Is it time to become older and move away from Lausanne?

Berti, Berti, Berti, you were always supportive and ready to help in the lab. Thanks for being “excessively” stubborn, precise, conservative, generous and a friend all at the same time.

Vanessa, you are the “youngest one” in the Italian LPPT crew, but you immediately demonstrated high maturity and loyalty, two aspects that I really appreciated. Please, don’t change!

A personal thanks to my two “personal” mentors Ranga and Kaycie. Thanks for being so altruistic and extremely precious for me. You guided me through several tricky moments of my Ph.D., provided me with a lot of critical scientific suggestions and careful English proofreading, and demonstrated your trust in me by asking me several scientific or unrelated questions as well.

I want to also thank the LIP laboratory members for their help and friendship, in particular Silvia S., Nico, Fay, Helen, Yann, Alberto and Rudolf.

My final and most important thoughts go to my family and Miriam. I will not use a lot of words here because I am not that kind of person — you know me. I simply want to tell you that if I am a better person than five years ago, it is thanks to you.

Thanks mum and dad for your constant support, not only during these 4 years of my Ph.D. but also years ago, when you gave me the opportunity to study and follow my personal passions. Thanks for coming to visit me twice per year and helping me in all the difficult moments that I had in my new everyday life outside of our safe home.

Thanks Miriam for your everyday presence in the bad moments as well as the good, even if the distance between us was not helping at all. You believe in me much more than I believe in myself. Thanks for your tenacity and for always pushing me to be stronger. Thanks, thanks, thanks for being part of my life…but, where should we go now?!!

Abstract

Peptides represent a promising format for the development of therapeutics since they combine the advantages of proteins and small molecules. Several techniques based on rational design or *in vitro* evolution can be used to develop peptides as therapeutics. A limitation of peptides is a rapid clearance from the blood circulation when applied intravenously, preventing their application in therapies that require prolonged drug exposure. Several methods have been tested to extend the *in vivo* half-life of peptides, including fusion to long-lived serum proteins, PEGylation and conjugation to non-covalent albumin-binding ligands.

A particularly attractive approach is a “piggy back” strategy in which peptides bind via a ligand to albumin without increasing significantly their small size. Acylation with fatty acids is the most successful strategy for delaying peptide clearance. The attachment of either myristic or palmitic acid to insulin and GLP-1 led to the approval of three acylated peptide drugs as daily injectable. Nevertheless, acylated conjugates generally present low solubility and weak affinity for albumin. Peptides have been explored as an alternative, as their format offers multiple approaches for affinity maturation as well as an easier synthesis of the conjugates. However, the albumin-binding peptides developed so far do not overcome the disadvantages faced with fatty acids.

The first aim of my project was the development of an albumin-binding tag that combines the favorable properties of both fatty acids and peptides, and overcomes at the same time their limitations. This tag was engineered in order to have i) a high affinity for human albumin, ii) a high solubility in physiological solutions, and iii) an efficient synthesis in conjunction with therapeutic peptides. Towards this goal, I created a chimeric format consisting of a fatty acid combined with a short linear peptide. After iterative rounds of affinity screening, an evolved peptide-fatty acid tag able to bind human, rat and rabbit albumin with K_d values of 39, 220 and 320 nM, respectively, was obtained. This makes it the best albumin-binding tag among all of the peptide- or fatty acid-based ligands that have been developed. This tag can be easily synthesized in conjugation with peptides on standard automated synthesizers. Finally, it exhibits a high solubility due to

four negatively charged amino acids in the peptide sequence, despite the presence of a 16-carbon palmitic hydrophobic tail.

The second aim of my project was the application of this tag to three bioactive bicyclic peptides, previously developed in the laboratory, in order to improve their *in vivo* half-lives. I demonstrated that the conjugation has, overall, a mild impact on peptides' binding affinity towards their targets and human albumin, and increases their proteolytic stability. Pharmacokinetic experiments showed that the tag extends the elimination half-life of bicyclic peptides in rats and rabbits approximately 25-fold to over seven and five hours, respectively. Tag conjugation to a bicyclic peptide targeting coagulation factor XII led to an efficient inhibition of coagulation in rabbits up to eight hours, suggesting a potential application in humans as anti-thrombotic drug. These results indicated that the tag will efficiently prolong the exposure of target proteins to bioactive peptides in humans due to its higher affinity for human albumin than that of rat and rabbit.

Keywords: peptide, half-life extension, human albumin, non-covalent binding, affinity, solubility, synthesis, fatty acid, tag, bioactive conjugates

Sommario

I peptidi hanno un formato promettente per la creazione di farmaci in quanto combinano molti vantaggi tipici delle proteine e dei classici farmaci chimici. Diverse tecnologie basate sullo sviluppo razionale o sull'evoluzione *in vitro* delle proprietà dei peptidi possono essere utilizzate per il loro sviluppo come farmaci. Tuttavia, un limite dei peptidi è la loro rapida eliminazione dalla circolazione sanguigna quando sono somministrati per via endovenosa, e ciò ne impedisce l'applicazione in terapie che richiedono una prolungata esposizione al farmaco. Diversi metodi sono stati testati per aumentare l'emivita dei peptidi *in vivo*, come ad esempio la fusione con proteine del siero, la modifica con polimeri idrofilici (PEG) e la coniugazione a molecole che legano l'albumina.

Un approccio particolarmente interessante si basa su una strategia "piggy back" in cui i peptidi legano l'albumina attraverso un ligando dell'albumina stessa, senza che ciò aumenti in modo significativo le loro piccole dimensioni. La modifica con gli acidi grassi è la strategia di maggior successo per ritardare l'eliminazione dei peptidi dal sangue. L'aggiunta di uno acido miristico o palmitico a polipeptidi come insulina e GLP-1 ha portato all'approvazione di tre peptidici acilati che possono essere iniettati una sola volta al giorno. Tuttavia, molti coniugati acilati generalmente hanno una bassa solubilità e una debole affinità di legame per l'albumina. I peptidi sono stati studiati come alternativa in quanto presentano una struttura che offre molteplici approcci per la maturazione dell'affinità di legame e permette una sintesi potenzialmente più semplice dei coniugati. Tuttavia, i peptidi sviluppati finora non hanno risolto i problemi degli acidi grassi.

Il primo scopo del mio progetto è stato lo sviluppo di un nuovo ligando dell'albumina che combini le migliori proprietà di acidi grassi e peptidi, superando nel contempo i loro limiti. Tale ligando è stato progettato in modo da avere i) un'elevata affinità di legame per l'albumina umana ii) un'elevata solubilità in soluzioni fisiologiche, e iii) un'efficiente sintesi in combinazione con i peptidi terapeutici. Con questo obiettivo, ho creato una chimera composta da un acido grasso legato ad un breve peptide lineare. Ripetute fasi di screening basate sull'affinità di legame della chimera per l'albumina hanno portato alla creazione di un elaborato tag acil-peptidico in grado di legare l'albumina umana, di ratto

e di coniglio con K_d uguali rispettivamente a 39, 220 e 320 nM. Al momento, questo tag risulta essere il miglior ligando dell'albumina tra tutti quelli sviluppati basandosi su formati peptidici e/o con acidi grassi. Questo tag può essere facilmente e direttamente sintetizzato in combinazione con peptidi terapeutici utilizzando sintetizzatori automatizzati. Infine, nonostante l'acido palmitico abbia una coda idrofobica di 16 carboni, il tag presenta una elevata solubilità grazie all'inserimento di quattro amminoacidi carichi negativamente nella sequenza del peptide.

Il secondo scopo del mio progetto è stata la coniugazione del ligando creato a tre peptidi biciclici bioattivi, precedentemente sviluppati in laboratorio, con il fine di migliorarne l'emivita *in vivo*. Ho dimostrato che la coniugazione ha, nel complesso, un lieve impatto sull'affinità di legame sia nei confronti del target dei peptidi biciclici che verso l'albumina umana, e ne aumenta la stabilità alla degradazione proteolitica. Esperimenti di farmacocinetica hanno dimostrato che il tag estende l'emivita dei peptidi biciclici in ratto e coniglio di circa 25 volte, raggiungendo rispettivamente valori di sette e cinque ore. La coniugazione del tag ad un peptide biciclico attivo contro il fattore di coagulazione XII ha portato ad un'inibizione efficace della coagulazione in coniglio fino ad otto ore, suggerendone un potenziale applicazione come farmaco anti-trombotico. Questi risultati indicano che il tag potrà efficientemente prolungare l'azione di peptidi attivi contro proteine di interesse farmacologico, grazie alla sua maggiore affinità di legame per l'albumina umana rispetto a quella di ratto e coniglio.

Parole chiave: peptide, estensione dell'emivita plasmatica, albumina umana, legame non covalente, affinità di legame, solubilità, sintesi, acidi grassi, tag, coniugati bioattivi

Contents

List of amino acids

Name	Three letter code	Single letter code	Side chains			
			Class	Polarity	Charge (pH 7.4)	pKa
Alanine	Ala	A	aliphatic	nonpolar	-	-
Arginine	Arg	R	basic	polar	positive	12.48
Asparagine	Asn	N	amide	polar	neutral	-
Aspartic acid	Asp	D	acidic	polar	negative	3.65
Cysteine	Cys	C	sulfuric	polar	neutral	8.18
Glutamic acid	Glu	E	acidic	polar	negative	4.25
Glutamine	Gln	Q	amide	polar	neutral	-
Glycine	Gly	G	hydrogen	nonpolar	-	-
Histidine	His	H	basic aromatic	polar	positive (10%) neutral (90%)	6.00
Isoleucine	Ile	I	aliphatic	nonpolar	-	-
Leucine	Leu	L	aliphatic	nonpolar	-	-
Lysine	Lys	K	basic	polar	positive	10.53
Methionine	Met	M	sulfuric	nonpolar	-	-
Phenylala-nine	Phe	F	aromatic	nonpolar	-	-
Proline	Pro	P	cyclic	nonpolar	-	-
Serine	Ser	S	hydroxylic	polar	neutral	-
Threonine	Thr	T	hydroxylic	polar	neutral	-
Tryptophan	Trp	W	aromatic	nonpolar	-	-
Tyrosine	Tyr	Y	aromatic	polar	neutral	10.07
Valine	Val	V	aliphatic	nonpolar	-	-

Data from http://www.sigmaaldrich.com/life-science/metabolomics/learning-center/amino-acid-reference-chart.html#prop

List of abbreviations

ABD	Albumin-Binding Domain	i.v.	intravenous
Ac	Acetyl	K_a	Association constant
aPTT	activated Partial Thromboplastin Time	K_d	Dissociation constant
Boc	Tert-butyloxycarbonyl	K_i	Inhibition constant
Da	Dalton	K_M	Michaelis-Menten constant
Dde	1-(4,4-dimethyl-2,6-dioxycyclo-hex-1-ylidene)theyl	LC-MS	Liquid Chromatography Mass Spectrometry
DNA	DeoxyriboNucleic Acid	mRNA	messenger RiboNucleic Acid
ELISA	Enzyme-Linked ImmunoSorbent Assay	MW	Molecular Weight
EMA	European Medicines Agency	NMR	Nuclear Magnetic Resonance
ESI-MS	ElectroSpray Ionization Mass Spectrometry	or	oral
Fc region	Fragment crystallizable region	PBS	Phosphate Buffered Saline
FcRn	Neonatal Fc receptor	PDB	Protein Data Bank
FDA	Food and Drug Administration	PEG	PolyEthylene Glycol
Fmoc	Fluorenylmethyloxycarbonyl	PK	Plasma Kallikrein
FXIIa	Activated coagulation factor XII	RP-HPLC	Reverse Phase High-Perfor-mance Liquid Chromatography
(F)	Fluorescein	rt	room temperature
GLP-1	Glucagon-Like Peptide-1	SPPS	Solid Phase Peptide Synthesis
IC_{50}	Half maximal inhibitory concentration	s.c.	subcutaneous
IgG	Gamma Immunoglobulin	Trt	Triphenylmethyl
IgBD	IgG-Binding Domain	UFLC	Ultra Fast Liquid Chromatography
ITC	Isothermal Titration Calorimetry	uPA	Urokinase-type Plasminogen Activator
i.m.	intramuscolar	USD	United States Dollar

Abbreviation of reagents, proteins and solvents used are listed in chapter 5 "Material and methods"

1. Introduction

NOTE: sub-section 1.1.2 of the introduction was adapted with permission from the review “Cyclic peptide therapeutics: past, present and future”, in which I am one of the authors with Deyle, K. and Heinis, C. Article published in *Current Opinion in Chemical Biology* (DOI: 10.1016/j.cbpa.2017.02.006). Reprinting license nr. 4057571248016.

1.1 Development of peptide therapeutics

Around one hundred linear and cyclic peptide drugs are currently used as therapeutics for the treatment of cancer, infective diseases, metabolic disorders, cardiovascular diseases and many other pathologies, and there are many other peptides currently in clinical trials.[1–3] Some of these peptide therapeutics recently reached the status of blockbusters, with annual sales higher than one billion USD. Examples include the insulin derivatives glargine (Lantus, Sanofi) and lispro (Humalog, Eli Lilly), and the GLP-1 analogues liraglutide (Victoza, Novo Nordisk) and exenatide (Byetta, Astrazeneca) for diabetes, glatiramer (Copaxone, Teva) for multiple sclerosis, teripatide (Forteo, Eli Lilly) for osteoporosis, octreotide (Sandostatin, Novartis) for acromegaly and daptomycin (Cubicin, Merck) for bacterial infections.[4]

Because a universal definition of a peptide-based drug is not-existent, in this thesis I arbitrarily define peptides as all of the molecules that contain at least three amino acids linked by two peptide bonds. All peptides of up to approximately 50-amino acids, insulin included, were placed into this class of therapeutics, applying the cut-off which is typically imposed as the boundary between peptides and proteins.[5,6]

The majority of the approved peptides are based on naturally evolved compounds that were initially isolated from different biological sources (humans, animals, bacteria and plants), and were chemically modified into analogues with improved potency, stability, safety, and activity against clinically validated targets.[7] Improvements in the characterization of protein structures as well as a better understanding of physiological processes in the human body and related pathologies directed new research fields (e.g. molecular biology, biotechnologies, and -omics) towards the identification of a great number of new biological targets against which peptides could play a crucial role.[3]

As a consequence, several *de novo* technologies that allow the combinatorial production and screening of millions of different peptide variants have been developed. In parallel, innovative solution- and solid-phase synthetic approaches and purification strategies have enabled the generation of complex peptides, encouraging the development of novel peptide-based drugs targeting diseases lacking clinical treatments.[1,5,6]

1.1.1 Properties of peptide therapeutics

Peptides have typically a molecular size between 0.5 and 5 kDa. They fill the gap between proteins and small molecules, and they combine several favorable properties of both formats (Fig. 1).[1,3,8,9] As proteins and antibodies, peptides exhibit high target selectivity and potency, thus reducing the risk of off-target side-effects. The improved binding properties are generally related to their larger surface of interaction with the target, which allows specific contacts and structural rearrangements. Similarly, peptide backbone also contains natural amino acid building blocks that undergo physiological catabolism without hepatic or renal accumulation of harmful metabolites. This property, combined with a small size, strongly decreases the chance of immunogenic reactions and toxicity.[3,8,9]

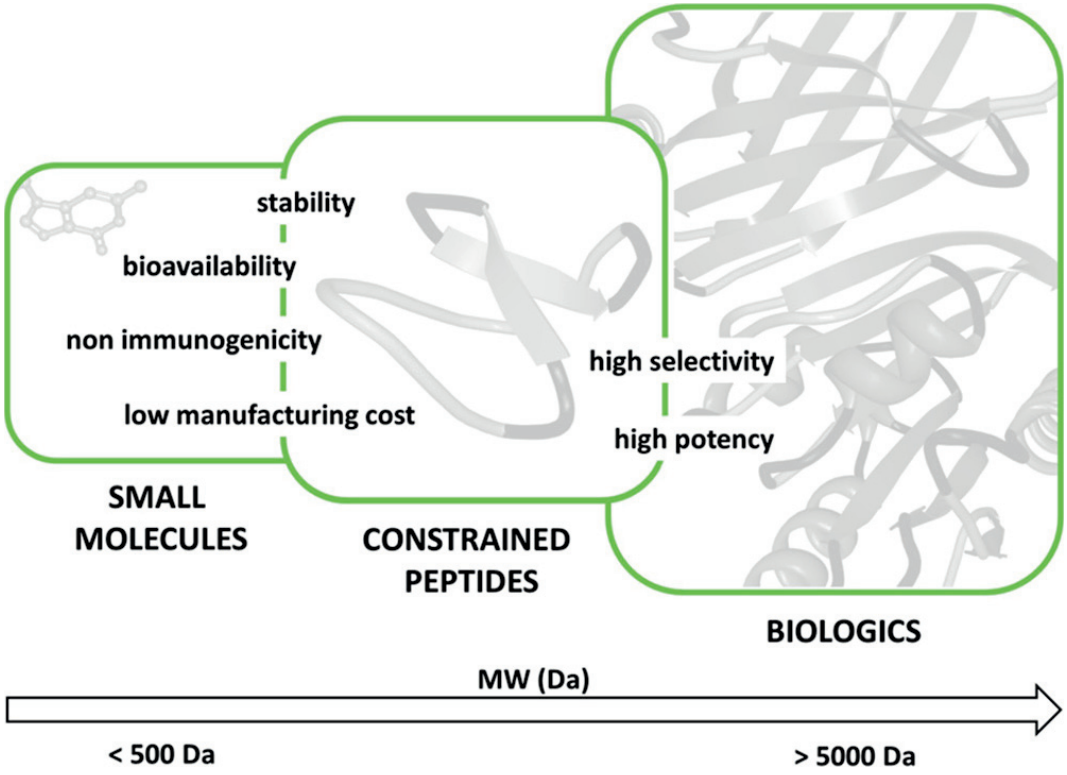

Figure 1. Peptides combine the advantages of biologics, namely high selectivity and potency, with those of small molecules, including stability, bioavailability, non-immunogenicity, and low manufacturing cost. Reprinted with permission from [9], copyright © 2014 American Chemical Society.

As small molecules, peptides can be chemically synthesized and modified (e.g. backbone cyclization, unnatural amino acid substitution, fluorophore labeling) in large scales with a much lower cost of production compared to biologicals. The small size

allows a deeper penetration into tissues, and could additionally enhance the cell membrane permeability. Analogously to small molecules, peptides can be lyophilized and have a long shelf-life thanks to a high stability at room temperature, and are thus easier to handle for clinicians and patients.[1,3,9]

According to their structure, peptide therapeutics can be classified as linear or cyclic. In the last decades, peptide macrocycles demonstrated strong advantages over their linear counterparts.[10,11] Differently from the linear format, cyclic peptides are characterized by a limited conformational flexibility that confers a higher binding affinity by reducing the entropic penalty upon binding, allowing therapeutic effects at lower drug concentrations. The cyclic format might also present multiple structures that adopt shapes which fit into binding pockets with great selectivity. Furthermore, cyclization increases peptide metabolic stability by both limiting the backbone accessibility to endopeptidases and protecting the termini from exopeptidases. This preserves them from fast degradation in the systemic circulation, a limitation commonly faced by many linear peptides. Peptide cyclization can be achieved by applying several methodologies such as head-to-tail, head-to-side chain, side chain-to-tail, or side chain-to-side chain (Fig. 2). The chemistry required for macrocyclization includes the formation of cyclic structure through disulfide bridges or different redox stable bonds, such as lactams, thioethers and other options.[9,12]

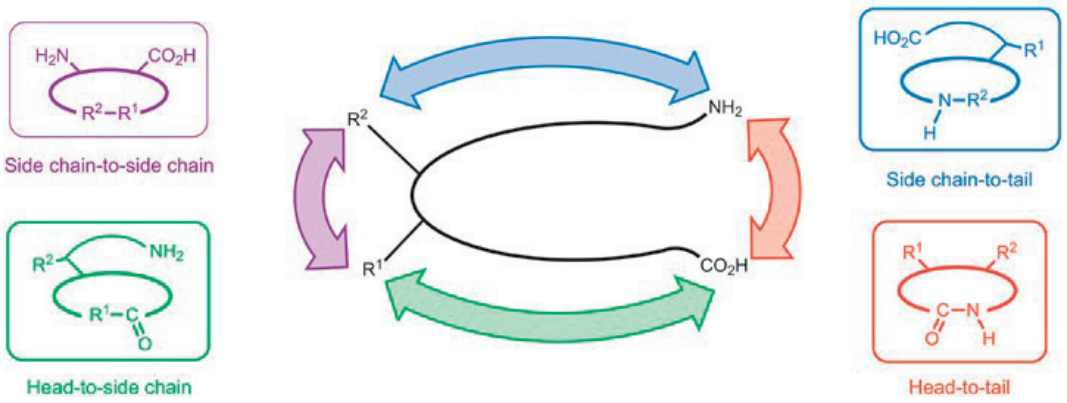

Figure 2. The four conventional synthetic approaches used for peptide macrocyclization: head-to-tail, head-to-side chain, side chain-to-tail or side chain-to-side chain. Adapted with permission from [12], reprinting license nr. 4047091488316, copyright © 2011 Nature Publishing Group.

1.1.2 Cyclic peptide therapeutics

As discussed in the previous sub-section, cyclic peptides are potentially a successful format since they possess several favorable properties that are ideal for the development of therapeutics. Examples of widely applied cyclic peptide drugs are the hormones or hormone analogues oxytocin, octreotide and vasopressin, the antibiotics vancomycin, daptomycin and polymyxin B or the immunosuppressant cyclosporine.[3,10] We actually counted that more than 40 cyclic peptide drugs entered in the market so far and, over the last decade, an average of one new entity has been added per year. Although many of these cyclic peptides are derivatives of naturally occurring compounds, there are clearly new opportunities for the *in vitro* development of novel peptides.[13]

In this sub-section, the first part (1.1.2.1) provides a look into the past by discussing the cyclic peptide therapeutics that have reached the market in the last ten years and details the techniques that were used to develop them. This part highlights that nearly all of these drugs are based on natural products or derivatives thereof. In a second part (1.1.2.2), we look at the present by discussing cyclic peptides that are currently undergoing clinical studies. This overview shows that there are several original cyclic peptide drug candidates developed *de novo* by rational design or *in vitro* evolution instead of through the modification of natural products. In a third part (1.1.2.3), we look to the future by discussing the most promising new cyclic formats and predict the technologies that will comprise the next generation of cyclic peptide therapeutics.

1.1.2.1 Peptide macrocycle drugs approved in the last ten years

In the last ten years, 2006-2015, the FDA and EMA have approved nine cyclic peptide drugs, which account for 3% of the new drugs that entered the market in this time period (Tab. 1, Fig. 3).[14–23] Four of these cyclic peptides, telavancin, dalbavancin, oritavancin and anidulafungin, are employed in bacterial and fungal infections. Three peptides, lanreotide, romidepsin, and pasireotide are oncology drugs, and one, linaclotide, is specific for gastrointestinal disorders. The last drug, peginesatide, was developed for the treatment of anemia during dialysis but was withdrawn soon after its approval due to safety concerns.

Table 1. Cyclic peptide drugs approved in the last ten years by the FDA and/or EMA.

Year[a]	Generic name	Indication	Mode of action	MW (Da)	Route of administration[b]	Company
2006	anidulafungin	fungal infections	fungal 1,3-β-D-glucan synthase inhibitor	1140	i.v. infusion	Vicuron / Pfizer
2007	lanreotide	acromegaly and neuroendocrine tumors	growth hormone release inhibitor	1156	s.c., i.m.	Ipsen
2009	telavancin	complicated skin and skin structure infections (CSSSIs) and nosocomial pneumonia	bacterial cell-wall synthesis inhibitor	1756	i.v. infusion	Theravance
2009	romidepsin	cutaneous T-cell lymphoma (CTCL) and peripheral T-cell lymphomas (PTCLs)	histone deacetylase inhibitor	541	i.v. infusion	Gloucester Pharmaceuticals / Celgene
2012	peginesatide	anemia associated with chronic kidney disease	erythropoiesis stimulating agent	4415	i.v., s.c.	Affymax / Takeda
2012	linaclotide	constipation-predominant irritable bowel syndrome (IBS-C) and chronic idiopathic constipation (CIC)	guanylate cyclase 2C receptor activator	1527	or	Forest Labs / Ironwood Pharmaceuticals
2012	pasireotide	Cushing's disease, acromegaly and neuroendocrine tumors	growth hormone release inhibitor	1047	s.c., i.m.	Novartis
2014	dalbavancin	complicated skin and skin structure infections (CSSSIs)	bacterial cell-wall synthesis inhibitor	1817	i.v. infusion	Durata Therapeutics / Teva
2014	oritavancin	complicated skin and skin structure infections (CSSSIs)	bacterial cell-wall synthesis inhibitor	1793	i.v. infusion	The Medicines Company

(a) Year of first approval by FDA or EMA for at least one of the indicated diseases. (b) Administration route: i.v., intravenous; s.c., subcutaneous; i.m., intramuscular; or, oral.

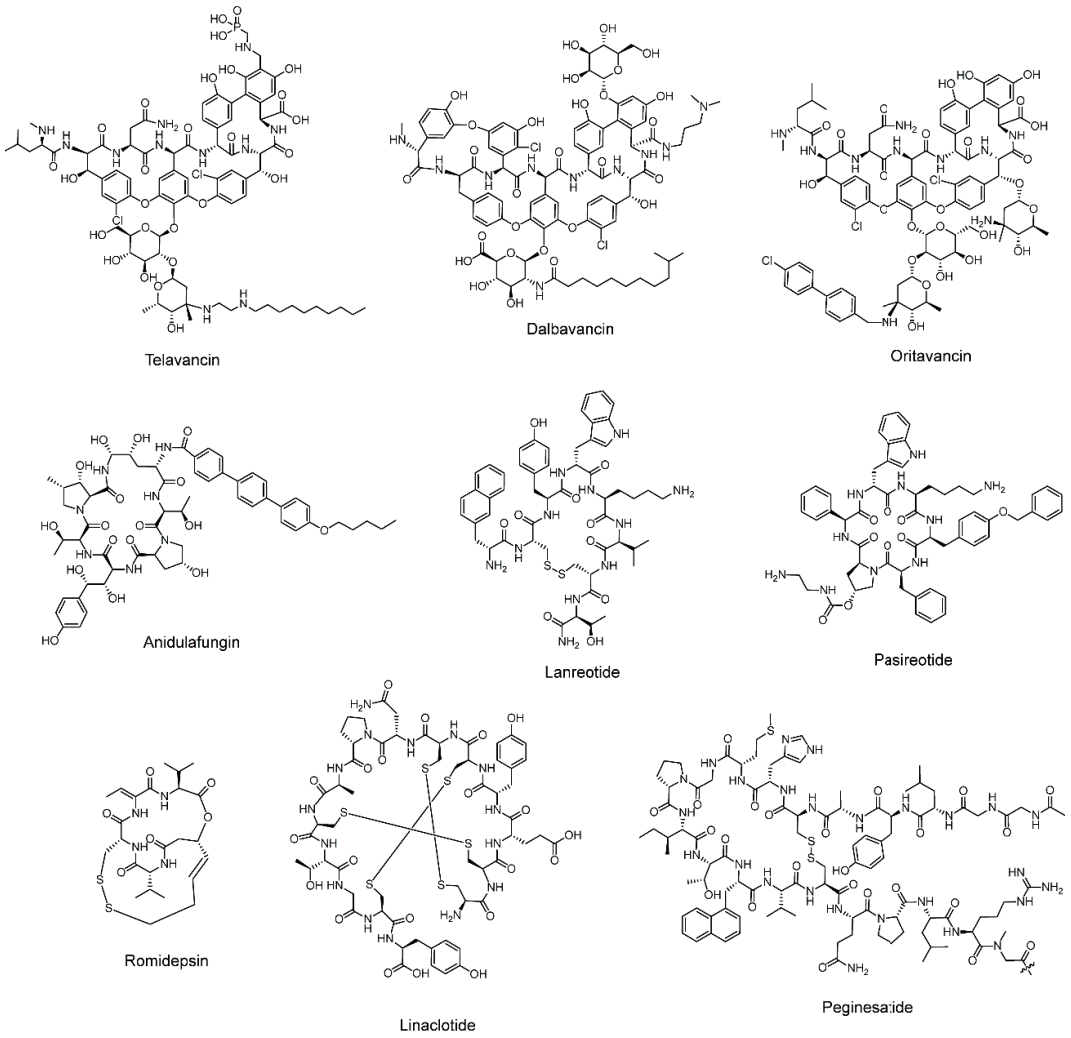

Figure 3. Cyclic peptide drugs approved in the last ten years by the FDA and/or EMA. For peginesatide, the 40 kDa PEG is not shown.

The three antibacterials on this list, telavancin, dalbavancin and oritavancin, are semi-synthetic cyclic lipoglycopeptides.[24] They belong to the same drug class as the established antibiotics vancomycin and teicoplanin, which all contain a common heptapeptidic core with five fixed residues that serves as the main binding site for the D-Ala-D-Ala target. Binding of these drugs to their target blocks the transpeptidation of peptidoglycan precursors in the bacterial cell wall.[25] These three new antibiotics all contain a lipophilic side chain that is thought to increase the dwell time near the target by anchoring them to the cell membrane and/or destabilize the bacterial membrane. Interactions of the hydrophobic tails with cell membranes and plasma proteins also prolong the plasma half-life. These three drugs are used for the treatment of complicated skin and skin structure infections and nosocomial pneumonia. Small variations in their structures cause

subtle differences in their pharmacological effects by fine-tuning their activities towards different bacterial strains or differing pharmacokinetic properties.

The cyclic peptide anidulafungin is a member of the class of echinocandin antifungals to which caspofungin and micafungin, approved in 2001 and 2005, also belong.[26] All three drugs share a similar peptide core formed by six amino acids, two of which are Pro derivatives and two are Thr or Thr derivatives. Anidulafungin, derived from echinocandin B, is a natural fermentation product of *Aspergillus nidulans* wherein the lineoyl side-chain tail is replaced by a lipophilic alkoxytriphenyl group. Like caspofungin and micafungin, anidulafungin inhibits the 1,3-β-D-glucan synthase responsible for fungal cell wall synthesis. Anidulafungin has a high affinity for human plasma proteins and a slow degradation time, giving it a half-life in the body of around 24 hours, doubling that of caspofungin and micafungin.

The oncology drugs lanreotide and pasireotide are analogues of the successful cyclic peptide drug octreotide, which itself is an analogue of the endogenous cyclic peptide hormone somatostatin.[27] Somatostatin blocks the release of hormones such as the growth hormone by inhibiting G-protein-coupled somatostatin receptors. These new mimetics, which have a substantially longer plasma half-life than somatostatin, are used to treat acromegaly and endocrine tumors. Lanreotide, like octreotide, is a disulfide cyclized octapeptide wherein four amino acids are identical and the other four are closely related. The two drugs also have similar pharmacologic properties. Pasireotide's structure was reduced to a hexapeptide cyclized through an amide bond and its sequence conserves only the D-Trp-Lys core of somatostatin.[28] Pasireotide differs from octreotide and lanreotide in its substantially higher affinity for certain receptor subtypes, making it more suitable for treating Cushing's disease and acromegaly in patients unresponsive to the other agents.

The third oncology drug, romidepsin is a natural product isolated from gram-negative *Chromabacterium violaceum,* approved for the treatment of T-cell lymphomas.[29] It is a depsipeptide composed of five backbone-cyclized residues and a disulfide bond that creates a bicyclic structure. The disulfide-cyclized romidepsin is a pro-drug that is significantly more stable in plasma than the active drug. Once inside the cell, it is reduced to its active form wherein a free thiol group chelates the zinc ion in the active site of intracellular histone deacetylase (HDAC) enzymes. The drug inhibits the removal of acetyl groups from Lys residues of N-terminal histone tails, maintaining a more open and transcriptionally active chromatin state which alters gene expression. Romidepsin is the second HDAC inhibitor that entered the market after the small molecule drug vorinostat.

Linaclotide is a 14-amino acid cyclic peptide derived from heat-stable enterotoxins, cyclic peptides produced by various *E.coli* strains which are a frequent cause of diarrhea.[30] The drug provides well-tolerated relief in patients with chronic constipation and irritable bowel syndrome. Linaclotide contains three disulfide bonds that constrain the conformation of the peptide, providing high proteolytic stability. The drug acts by binding to guanylate cyclase C on the surface of intestinal epithelial cells.[31] Activation of the cyclase triggers a signaling pathway that leads to chloride and fluid secretions into the lumen, increasing colonic transit. The location of this target in the intestine allows for linaclotide to be orally administered while not orally available, as the drug does not have to pass through the gastrointestinal lining.[32]

The final cyclic peptide approved in the last ten years is peginesatide, an agonist of the erythropoietin receptor developed for severe anemia in which erythropoietin cannot be used.[33] This cyclic peptide was discovered through phage display panning against the erythropoietin receptor.[34,35] It was then chemically dimerized with a polyethylene glycol (PEG), increasing the affinity, potency and circulation time in blood. It was voluntarily withdrawn from the market, however, one year after its approval due to safety concerns not experienced during the clinical trials. Unlike all the other previously approved cyclic peptide drugs, peginesatide was the first to be developed *de novo*.

Taken together, eight of the newly approved nine drugs have a mechanism of action similar to established drugs and only one, linaclotide, is a first-in-class drug. Besides being highly innovative and serving a large group of patients, linaclotide is also a highlight in terms of sales. It generated revenues of 460 million USD, improving upon the already impressive sales of 140 and 300 million USD in the two first years after approval, and it is likely to become a blockbuster drug within the next five years.[36] Lanreotide and romidepsin are the other two drugs approved in the last ten years to have noteworthy sales, earning 440 and 70 million USD last year, respectively.

1.1.2.2 Peptide macrocycles in clinical development

Our database and literature search has identified over 20 cyclic peptides that are currently undergoing clinical evaluation. These molecules have been developed for a highly diverse set of medical conditions, including several types of cancer, various infectious diseases, endocrine/metabolic disorders, hematological diseases and cardiovascular disorders. The majority of these cyclic peptides, similar to those already approved, are derivatives of natural products from microorganisms or human hormones. Interestingly, several of the cyclic peptides in clinical trials were developed *de novo* using newer

methods based on either rational design strategies or *in vitro* evolution (Tab. 2). We focus in this part on five of these peptides in order to shine a light on the new and innovative techniques for developing cyclic peptide therapeutics.

Table 2. Cyclic peptides developed by *de novo* design or *in vitro* evolution that are currently under clinical evaluation.

Phase[a]	Name	Indication	Mode of action	Discovery platform	Company
2	POL7080	pseudomonas aeruginosa infections, gram-negative infections	LptD protein homolog inhibitor, inhibits outer-membrane biogenesis	iterative modification and screening of peptide libraries using cationic antimicrobial peptide protegrin I as starting point	Polyphor
2	POL6326	metastatic breast cancer, acute myocardial infarction, hematopoietic stem cell mobilization from donors	chemokine receptor CXCR4 antagonist prevents the binding of stromal derived factor-1 (SDF-1) to mobilize stem cells	designed protein epitope mimetic (PEM) based on natural CXCR4 inhibitor T22	Polyphor
2	APL-2	age related macular degeneration, paroxysmal nocturnal hemoglobinuria	complement factor C3 inhibitor, blocks complement activation, PEGylated	phage display screening of cyclic peptide library	Apellis
1/2	ALRN-6924	acute myeloid leukemia, hematological leukemia hematological malignancies, myelodysplastic syndromes, solid tumors	inhibitor of p53-MDM2/MDMX interaction, restores p53-mediated apoptotic activity in tumors	peptide isolated by phage display and modified into stapled peptide	Aileron
1	RA101495	paroxysmal nocturnal hemoglobinuria	complement factor C5 inhibitor, blocks complement induced hemolysis	mRNA display screening of cyclic peptide libraries containing unnatural amino acids	Ra Pharma

(a) For cyclic peptides tested for multiple indications, the most advanced clinical phase is indicated.

POL7080 is a *Pseudomonas aeruginosa*-specific antibacterial cyclic peptide with a new mode of action developed through multiple iterative rounds of peptide library synthesis and screening for enhanced antibacterial activity.[37] The starting point of this evolution process was protegrin I, a β-hairpin peptide having broad antibiotic properties through membrane lytic activity. After stabilizing its secondary structure by a D-Pro-L-Pro β-turn motif, the basis of Polyphor's proprietary PEM technology [38], and several rounds of optimization by amino acid substitution, the new 14-amino acid peptide showed reduced cell lysis but high activity and selectivity towards *Pseudomonas aeruginosa*.

Analysis of the potent antibiotic revealed binding to the membrane protein LptD, involved in membrane biogenesis, and therefore demonstrated a new mode of action from the precursor. A phase 1 trial established the clinical safety and tolerability of POL7080, and this antibiotic is currently under phase 2 trial evaluation for the treatment of *Pseudomonas aeruginosa* infections.

POL6326 is a bicyclic peptide inhibitor of the chemokine receptor CXCR4. Blockage of CXCR4 avoids the interaction with the ligand SDF-1 (stromal cell-derived factor 1), which induces hematopoietic stem cell (HSC) detachment from the bone marrow into the circulating blood.[39] The mobilization of hematopoietic stem cells is of interest for stem cell transplantation, tissue regeneration and chemotherapy. POL6326 was developed using a combination of rational design and iterative optimization by peptide sequence variation and activity testing. In a first step, an analogue of the natural peptide polyphemusin II inhibiting CXCR4 was mounted onto the PEM technology D-Pro-L-Pro template to stabilize its β-strand conformation.[38] In a second step, the potency and various other properties of the receptor antagonist were optimized through several rounds of sequence modification, providing a final amino acid sequence for POL6326 that differs greatly from the starting polyphemusin II. A phase 1 trial for HSC mobilization was completed, and phase 2 trials have been initiated.

APL-2 is a PEGylated cyclic peptide inhibitor of C3, a central protein in the complement cascade. Excessive or uncontrolled activation of the complement system plays a role in a range of autoimmune and inflammatory diseases. APL-2 binds to a site on C3 that prevents binding of convertases and thus conversion to C3b. It is based on compstatin, a disulfide cyclized 13-amino acid peptide derived from a 27-mer peptide isolated by phage selection against C3b.[40] The addition of a PEG moiety to APL-2 prevents fast renal clearance and enables C3 inhibition for several days per injection. APL-2 is currently in phase 2 trial testing for age-related macular degeneration (AMD) and in phase 1 trial for paroxysmal nocturnal hemoglobinuria (PNH). For these two indications, the drug is applied by intravitreal and subcutaneous administration, respectively. A non-PEGylated form of the peptide, APL-1 is in development for inhalation treatment of chronic obstructive pulmonary disease (COPD).

ALRN-6924 is a dual inhibitor of MDM2 and MDMX based on a stapled peptide that interrupts p53 suppression and restores normal p53-mediated apoptosis activity in tumor cells.[41] Stapled peptides stabilize α-helices through hydrocarbon linkers that bridge two amino acid side chains on the same face of a helix. In addition to forming a stable cyclic peptide, this process can facilitate peptide cell penetration. ALRN-6924 was

developed by optimizing the stapled peptide ATSP-7041 which in turn was obtained by stapling the phage display peptide pDI with an 11 carbon linker through ring-closing metathesis. This final stapled peptide mimics an α-helix of p53 that binds to the same region of MDM2/MDMX. ALRN-6924 is currently undergoing testing in a phase 1/2 trial in patients with advanced solid tumors or lymphomas expressing wild-type p53 protein, and in a phase 1 trial in patients with acute myeloid leukemia or advanced myelodysplastic syndrome.

RA101495 is a cyclic peptide that binds and allosterically inhibits the cleavage of the complement factor C5 into C5a and C5b.[42] The peptide was developed by screening mRNA display combinatorial libraries of cyclic peptides based on a combination of natural and unnatural amino acids.[43] Inhibition of C5 activation is of interest for the treatment of complement disorders such as PNH, refractory generalized myasthenia gravis and lupus nephritis. A C5 inhibitor based on a monoclonal antibody, eculizumab, is successfully used for the treatment of PNH and for atypical hemolytic uremic syndrome (aHUS), though it is administered intravenously. The peptide-based inhibitor RA101495 was developed for subcutaneous injection in order to enable more convenient self-administration. A phase 1 trial with RA101495 has been completed successfully.

A look at the techniques used to develop these clinical candidates shows that all depended heavily on peptide library screening. In the case of the two peptides POL7080 and POL6326, natural peptides served as starting points but were extensively modified over several rounds of amino acid substitution and activity testing. As described above, POL7080 was so changed in its sequence that a new mechanism of action had evolved. The development of ALRN-6924 was encouraged by successes with stapled peptides that were rationally designed from the α-helices of p53 located at the p53-MDM2/MDMX binding interface. The template that was eventually used for the development of ALRN-6924 was derived from a phage display peptide library. Finally, the drug candidates APL-2 and RA101495 were developed by *in vitro* evolution through large random peptide library screening using either phage display or mRNA display. These and other powerful *in vitro* evolution techniques are now being broadly applied to develop ligands for a wide range of targets. It can be expected that many more *de novo* cyclic peptides with activities for interesting or previously unexplored targets will be fished out of random libraries by phage or mRNA display, and will soon be evaluated in clinical studies.

1.1.2.3 Future challenges and potential solutions

Several important challenges remain in the development of cyclic peptide therapeutics, the two most important ones being oral availability and cell permeability. Innovative approaches applied in recent years address one or both of these challenges, including the use of cell penetrating peptides [44], the stabilization of peptides in α-helical conformations with hydrocarbon linkers [45], or the *in vitro* evolution of N-methylated peptides.[46] In order to develop cyclic peptides with a good oral availability and that able to efficiently enter cells by passive diffusion, it might be necessary to consider molecules with smaller molecular weights and fewer peptide bonds. One could imagine that future macrocycles will contain only one or a few amino acids with an additional polyketide type component in the backbone. A good role model is the orally available and cell permeable drug tacrolimus which contains a backbone based on one amino acid and a polyketide chain wherein the amino acid forms key interactions with the target. To develop such chimeric peptide/polyketide macrocycle ligands, it will be crucial to create efficient chemistries and strategies that allow the synthesis and screening of large combinatorial libraries.

1.1.3 *In vitro* evolution of peptides

In vitro evolution methodologies are artificial reproductions of spontaneous genetic mutations and functional natural selection, core of the Darwinian process, accelerated in time and limited in space. These techniques allow the generation and screening of an enormous number of variants, while maintaining the linkage between genotype and phenotype, in order to rapidly evolve them towards the desired applications.[47]

Phage display was the first established technology based on an *in vitro* display system, developed by G.P. Smith in 1985.[48] Briefly, DNA coding for randomized combinatorial libraries of peptides, proteins or antibodies is cloned in the genome of bacteriophages. As result, each phage expresses on its surface a single variant fused to a coat protein (phenotype), while the corresponding nucleic acid sequence is inside the phage particle (genotype). Heterogenous mixtures of phage-encoded libraries are screened in a biopanning process to isolate ligands carrying the desired binding properties. Phage clones are incubated with targets, non-binding sequences are removed by multiple washing steps, while the binders are fished out by various elution methods. This cycle of affinity selection is repeated two to three times, enriching the phage population for binding

variants while eliminating the unspecific background. The specific amino acid sequences are retrievable by sequencing the genome of the isolated phages (Fig. 4).[49]

The most commonly used phage strains are the M13, f1 and fd, characterized by a genome expressing five different virion proteins. Combinatorial libraries are commonly displayed on the five copies of the pIII coat protein.[50] This multivalency introduces an avidity effect that might be suitable for initial screenings, when peptide leads have to be captured from a naïve library. A monovalent display is often preferred in the following steps of affinity maturation since avidity effects could skew the binding results towards less desirable clones.[51]

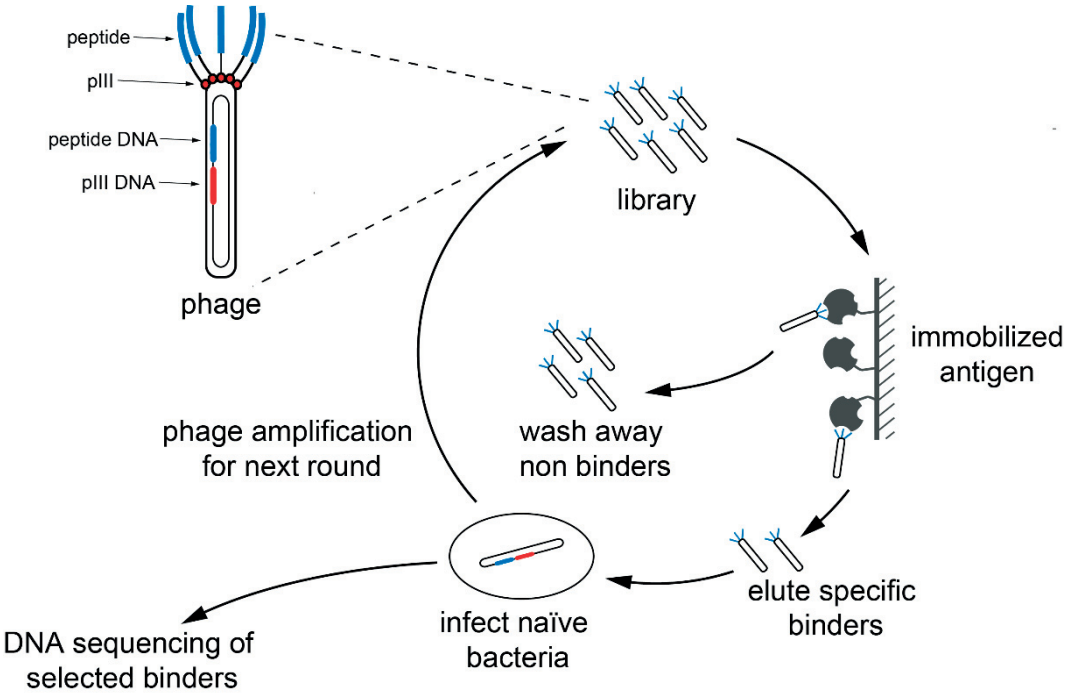

Figure 4. Phage display selection of combinatorial peptide libraries (corresponding DNA and amino acid sequence shown in blue) displayed on the coat protein pIII (corresponding DNA and amino acid sequence shown in red) of a filamentous phage. Libraries are subjected to two or three rounds of incubation with the immobilized target, washing of unspecific binders, elution of specific binders, and reamplification in bacteria for the next round. The amino acid sequences of the peptides are identified by DNA sequencing.

Other display methodologies feasible for *in vitro* evolution of peptides are yeast[52] and bacterial[53] display. Similarly to phage display, they are cell-based techniques that consist in the display of libraries on the cell surface, allowing the direct determination of the binding using cell-flow cytometry. However, they also suffer from reduced library sizes (typically 10^{10} clones) due to a low efficiency of DNA transformation, and from challenging incorporation of unnatural amino acids during the screening.[54] Recently, a new

cell-based system which could introduce unnatural residues in the sequence has been described, however it was limited to a single amino acid addition.[55]

In order to screen larger peptide libraries for *in vitro* evolution, new cell-free systems have been developed and are currently widely applied, such as mRNA[56] and ribosome[57] display. In both methods, screening variants are directly linked to their encoding sequence via puromycin or the ribosome, respectively. Their main advantages over cell-based display are the creation of library consisting of up to 10^{15} variants, and a more efficient inclusion of unnatural residues.[54,58]

So far, two peptides developed by phage display have been approved as drugs, the linear romiplostim (Nplate, Amgen) and the cyclic peginesatide (Hematide, Affimax/Takeda), in addition to several monoclonal antibodies and proteins like the blockbuster adalimumab (Humira, Abbott).[50,59] In contrast, no peptides generated with one of the other mentioned technologies have yet reached the market. This proves that phage display, despite some limitations, is a powerful technique for the generation and screening of large combinatorial libraries, and led to the development of specific ligands.[60] In particular, it allowed for the isolation of bioactive sequences unrelated to the natural binding partner. In future, it might also permit the development of peptides with entirely novel functions, enhancing the hope that new binders can be found for proteins with unknown natural ligands.[50,59] Because of the simplicity of its protocol, the high versatility of applications and manipulations, and the easy generation or commercial availability of different peptide libraries, phage display is still the most common system used for *in vitro* evolution.[61]

1.1.4 Phage selection of cyclic peptides

Since the introduction of phage display for the screening of peptides in the early 1990s, cyclic peptides appear to be the preferred format. Peptides having two Cys residues were often enriched over linear peptides, suggesting their selection as disulfide monocyclized structures.[62] As a consequence, new generations of phage libraries, consisting of two fixed Cys residues flanking a central random sequence, resulted in cyclic peptide binders presenting on average 100 to 1000-fold higher binding affinity respect to linear peptides selected against the same target.[63,64] Better biochemical properties of cyclic peptides stimulated a stronger interest towards the extensive creation of even larger libraries with this format, resulting in the isolation of many cyclic ligands (Fig. 5a).[60,65,66]

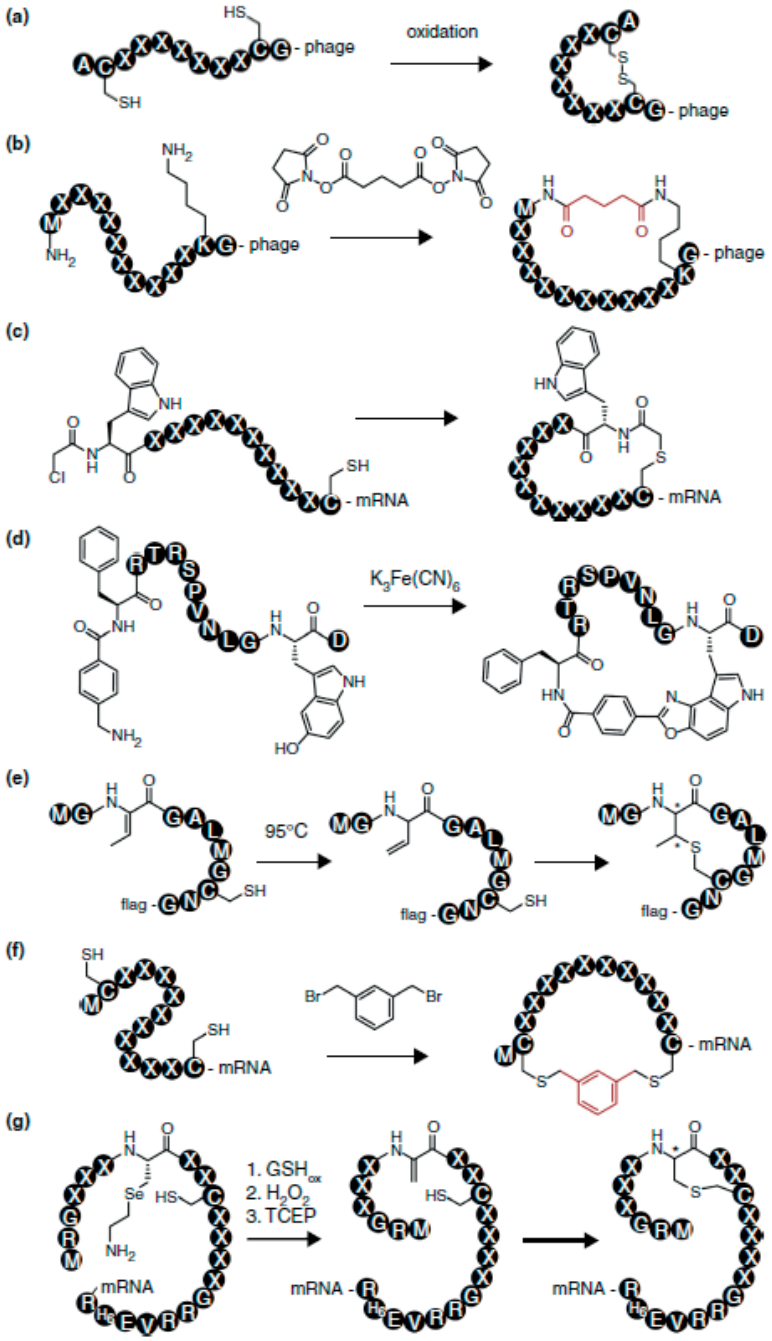

Figure 5. Encoded cyclic peptide libraries. (a) Cyclization of a phage-encoded peptide by oxidation of two Cys to form a disulfide bond. (b) Cyclization of phage-encoded peptides by chemically linking the amino groups of the N-terminus and a Lys residue with disuccinimidyl glutarate. (c) Cyclization of mRNA-encoded peptides by spontaneous reaction of a chloroacetamide group in an unnatural amino acid with a Cys to form a thioether bond. (d) Oxidative cyclization of peptides containing benzylamine and 5-hydroxytryptophane. (e) Peptide cyclization by Michael addition of a Cys side chain to dehydrobutyrine. Dehydrobutyrine is obtained by heat-induced isomerization of vinylglycine. Newly generated stereogenic centers are indicated by asterisks. (f) Cyclization of mRNA-encoded peptides by linking two Cys with the thiol-reactive reagent α,α'-dibromo-m-xylene. (g) Cyclization of an mRNA-encoded peptide library by Michael addition of a Cys residue to dehydroalanine. The latter amino acid is generated by oxidative transformation of 4-selenalysine. The newly generated stereogenic center is indicated by an asterisk. Reprinted with permission from [60], reprinting license nr. 4047111125961, copyright © 2015 Elsevier Ltd.

The only example of an approved peptide drug selected as monocycle is peginesatide, previously introduced in the sub-section 1.1.2. The initial peginesatide precursor was identified after two consecutive phage panels against the human erythropoietin receptor, starting from a peptide library having the CX_8C format. The sequence of the selected peptide was used as template for the generation of two different phagemid libraries: the first one with randomized residues, and the second one with three extra random residues at both termini. The new libraries led to the isolation of a nanomolar peptide binder able to stimulate the erythropoiesis. Further analysis permitted a shortening of the peptide sequence while retaining its activity. The chemical dimerization of two identical peptide molecules achieved an even stronger effect *in vivo*.[34,35] The final structure of peginesatide was based on two identical 21-mer cyclic peptides connected through a linker, which was composed of an iminodiacetic acid and β-Ala, to two 20 kDa PEG units. PEGylation led to three to four weeks of sustained effect in humans, thus making it suitable for monthly dosing.[67] Unfortunately, this drug was recalled from the market due to lethal problems.[33]

Development of non-reducible cyclic bonds have been recently achieved by new chemical cyclization methods applied in different *in vitro* techniques in place of the more traditional disulfide bridges (Fig. 5b-g). Thanks to the different geometries that a peptide can undergo when differently cyclized, the diversity of phage libraries was further enlarged through these methods, thus generating ligands with higher affinity and stability.[60]

1.1.5 Bicyclic peptides

Towards the development of cyclic peptides with even more constrained structures, and thus better affinity, stability and specificity, Heinis *et al.* developed a new methodology for the *in vitro* evolution of bicyclic peptides on phage.[68] As the name suggests, the new molecular format is based on two macrocyclic peptide rings, chemically cyclized around a reactive organic core. In general, bicyclic peptides present all of the properties previously described for cyclic peptides, with some other key advantages.

Unlike monocyclic peptides, both rings of this format can bind the target, partially mimicking the complementary determining regions (CDRs) of antibodies. The wider contact region and a higher number of non-covalent interactions are important for both binding affinity and selectivity.[60] A better specificity could permit the development of drugs with less side effects on paralogous species.[69] The bicyclic format has finally a more compact conformation that shows a much higher potency and stability to proteolytic cleavage compared to the linear and monocyclic counterparts.[68,70,71]

The bicyclic configuration can be obtained by quantitative and selective chemical cyclization of linear peptides containing three Cys residues with a small trivalent thiol-reactive molecule, applying a strategy previously developed to mimic non-linear epitopes of antibodies.[72] Heinis *et al.* efficiently combined the mild reaction required for this peptide cyclization with the enormous variability of phage-encoded combinatorial libraries (up to 10^9 variants). The initial bicyclic format was composed of two rings with six variable positions flanked by Cys residues at both ends and one in the middle (ACX_6CX_6CG, two loops of six residues, named 6x6) modified with a reactive molecule called 1,3,5-tris-(bromomethyl)benzene (TBMB) (Fig. 6). This molecule was chosen since it allowed a symmetric rotational arrangement of the peptide structure and thus the formation of a single product.[68]

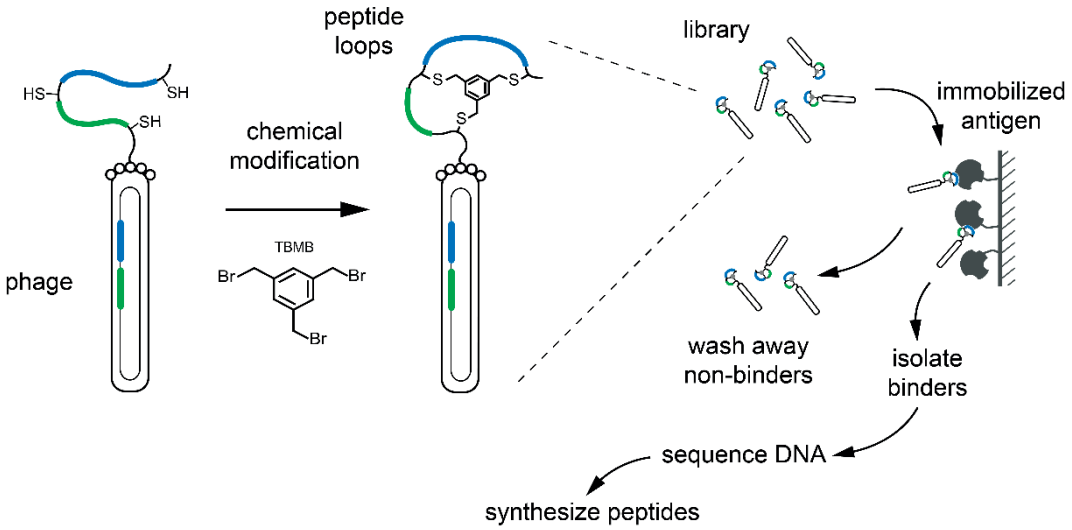

Figure 6. Phage display selection of combinatorial bicyclic peptide libraries (corresponding DNA and amino acid sequence of the N-terminal and C-terminal loops shown in blue and green, respectively) displayed on the coat protein pIII of a filamentous phage. Linear peptide libraries are chemically modified with the cyclization molecule TBMB. Libraries are subjected to two or three rounds of incubation with the immobilized target, washing of unspecific binders, elution of specific binders, and reamplification in bacteria for the next round. The amino acid sequences of the peptides are identified by DNA sequencing.

A high diversity in combinatorial peptide libraries is a critical parameter for the development of ligands. In addition to variation in the amino acid sequence, the diversity of the bicyclic format was further expanded by changing size and geometry of the two loops. This was done varying both the number of amino acids in each ring and the thiol-reactive molecules used for the chemical cyclization.[73]

As a proof of concept, Rentero *et al.* generated fourteen new libraries having different ring size formats (ACX_mCX_nCG, with "m" and "n" representing the number of random amino acids ranging between three and six) (Fig. 7). They screened them against

the same target and showed consensus sequences specific for each new combination, quite different from those previously isolated with the initial 6x6 format.[74] This demonstrated that bicyclic peptides with variable ring sizes could allocate in different manners into protein binding pockets, and this advantage was later efficiently exploited for the selection of ligands against orthologous targets.[69]

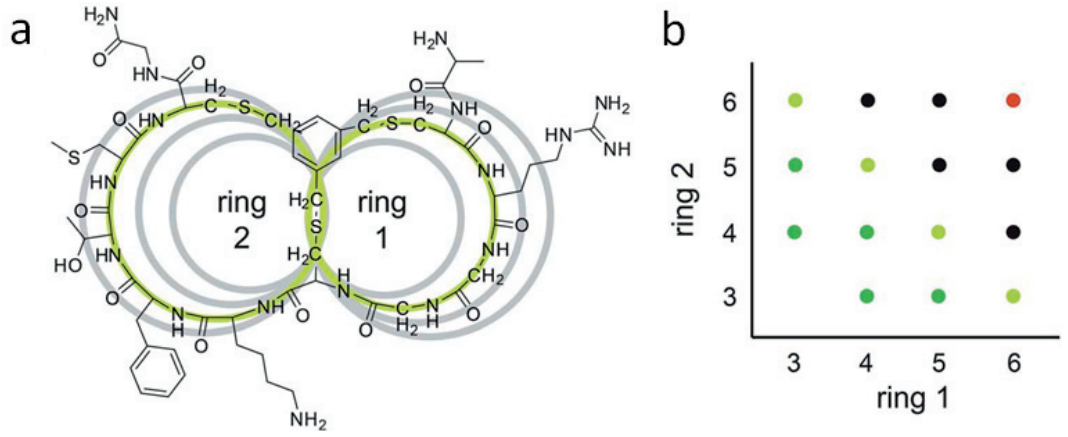

Figure 7. Bicyclic peptide phage libraries with different ring sizes. (a) Chemical structure of a representative bicyclic peptide with green rings of 3 and 4 amino acids. For size comparison, the peptide rings with 3, 4, 5 and 6 variable amino acids are shown as grey circles. (b) Overview of the libraries. Indicated on the axes are the number of variable amino acids in the two rings of the bicyclic peptides. Libraries that were cloned in that work are indicated with different colored dots. The 6x6 library indicated with a red dot was cloned previously. Reprinted with permission from [74], reprinting license nr. 4047120151435, copyright © 2012 Royal Society of Chemistry.

In parallel, structurally different thiol-reactive molecules were tested for the cyclization of the same peptide format. Since the first molecule used (TBMB) is rather small, hydrophobic, and did not contribute to the binding, two new reagents were developed to obtain different geometrical conformations of bicyclic peptides. These were based on either bromoacetamide (TBAB) or acrylamide (TATA) moieties, and they were compatible with the conditions previously set up for cyclization on phage.[75] In addition, they both contain more sophisticated chemical structures, which allowed for extra interactions between the molecule and the peptide sequence (Fig. 8). Both NMR and crystal structure experiments confirmed that the new reagents brought about conformational changes in the peptide and participated in the binding interactions with the target.[75] When applied on phage, they led to the isolation of specific consensus motives, further increasing the number of possible bicyclic formats.[76,77] Combination of these new molecules with different chemical structures triplicated the diversity of each phage library. Recently the library variability was further expanded using sequences carrying four Cys residues, each of them being cyclized into three possible isomers by oxidation.[78] Moreover, structural and

in silico analyses of bicyclic peptides demonstrated that this format is suitable for the synthetic incorporation of unnatural amino acids, a different way to increase peptide diversity and affinity after phage selection.[79]

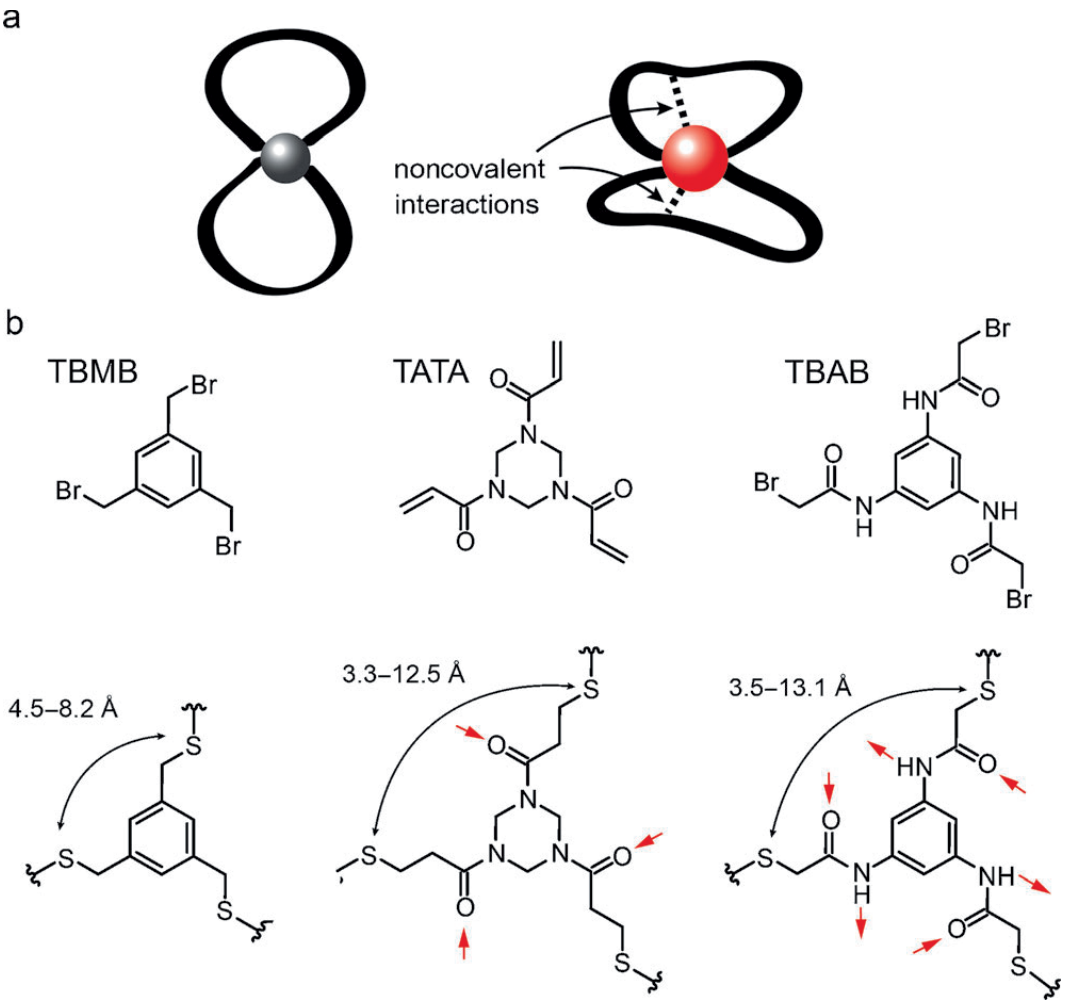

Figure 8. Structurally diverse small molecules for the phage selection of bicyclic peptides. (a) The structures of previously developed and structurally characterized bicyclic peptides were not directed by the central chemical molecule (illustrated by a gray ball; left). Small molecules with polar groups (illustrated as a red ball) form H-bond interactions (black dashed lines) with the peptide loops and serve as nucleating scaffolds (right). (b) Structures of the small molecules, each containing three thiol-reactive groups, before and after reaction. Potential H-bond donors and acceptors are indicated by red arrows. Computed distance ranges between the sulfur atoms of the cyclized peptides are indicated. Reprinted with permission from [76], reprinting license nr. 4047120502109, copyright © 2014 Wiley-VCH Verlag GmbH & Co. KGaA, Weinheim.

1.1.6 Examples of bicyclic peptides

So far, several potent and specific bicyclic peptides with high binding affinity and potency have been isolated against a variety of disease-related protein targets, such as the following human serine proteases plasma kallikrein (PK)[68,69], urokinase-type plasminogen activator (uPA)[70], and coagulation factor XII (FXIIa).[80,81]

1.1.6.1 Plasma kallikrein inhibitor

Human plasma kallikrein (PK) is a serine protease that is involved in several proteolytic cascades such as the intrinsic coagulation pathway and the kallikrein-kininogen system.[82] Its inhibition would be beneficial for different diseases, since an increase in its activity causes an excessive activation of both coagulation factor XII and bradykinin, associated with a higher risk of thrombosis and inflammation, respectively.[82] A PK inhibitor called ecallantide (Kalbitor, Dyax Corporation), a phage selected polypeptide of 60 amino acid, has already been approved for the treatment of a PK-related inflammatory disease called hereditary angioedema (HAE).[83] Since a smaller inhibitor would be preferred, PK immediately emerged as an optimal target for the isolation of bicyclic peptides. The first generation of phage-encoded libraries developed by Heinis *et al.* was subjected to selection and further affinity maturation against immobilized PK, leading to the isolation of a potent 6x6 bicyclic peptide inhibitor, called PK15 (K_i = 1.5 nM) (Fig. 9). This peptide did not show any inhibition of the target activity when not cyclized with TBMB, confirming that the bicyclic structure was critical for the binding. In addition, it was characterized by a high specificity with reduced inhibition of other serine proteases.[68]

However, PK15 was not able to inhibit the orthologous PK from other species such as mouse and rat, preventing the possibility to test its activity *in vivo*. In order to solve this limitation, Baeriswyl *et al.* performed a new selection using a second generation of peptide libraries with smaller loop sizes (3x3 and 5x5, cyclized with TBMB), and succeeded in isolating several bicyclic peptides with inhibitory activities in the pico- or low nanomolar range for human PK, and in the medium nanomolar range for the orthologous proteins. Among them, the best inhibitor, called PK128, was almost inactive against paralogous proteases while it exhibited high potency against human and orthologous monkey and rat PK (K_i = 0.3, 0.4, and 11 nM, respectively).[69]

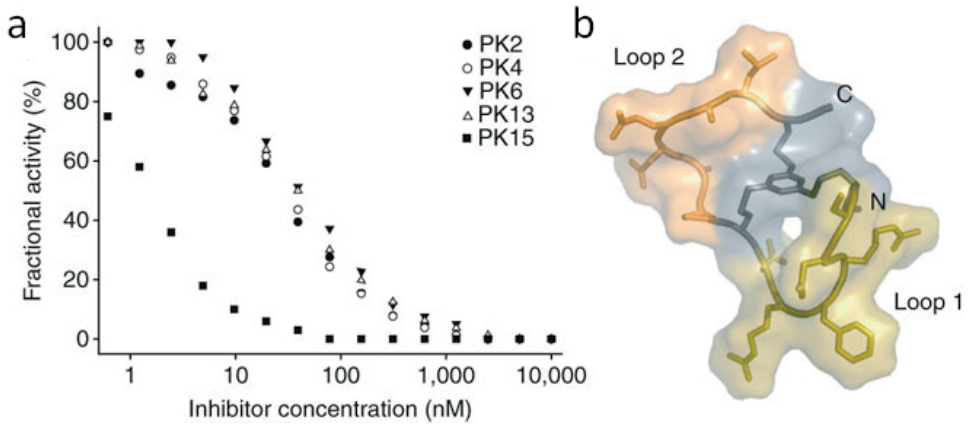

Figure 9. Inhibition of human plasma kallikrein by different bicyclic peptides and NMR solution structure of PK15. (a) The inhibitory activity is expressed as the fractional activity at varying inhibitor concentrations. Clones PK2, PK4, PK6, PK13 and PK15 were isolated in phage selections using two different libraries. (b) The peptide loops of conjugate PK15 are shown in yellow (loop 1) and orange (loop 2). The mesitylene core, the three Cys residues and the terminal Ala (N-terminus) and Gly (C-terminus) are shown in gray. The backbone atoms of the peptide are represented as a cartoon, and the side chains of the amino acids are represented as sticks. Reprinted with permission from [68], reprinting license nr. 4047121037044, copyright © 2009 Nature Publishing Group.

1.1.6.2 Urokinase-type plasminogen activator inhibitor

Human urokinase-type plasminogen activator (uPA) is a serine protease overexpressed in cancer and involved in tumor growth and metastasis. When released from tumor cells, this protease converts the inactive plasminogen to plasmin, which is responsible for the degradation of the extracellular matrix and, as consequence, cancer cell invasion. The inhibition of uPA would be beneficial as initial therapy for limiting metastases.[84] Using the 6x6 phage library and the TBMB cyclization reagent, Angelini *et al.* could isolate a potent and highly specific competitive inhibitor of uPA, called UK18 (K_i = 53 nM). Co-crystallization of UK18 with its target showed a large contact surface and gave extra insights about the binding mechanism of the bicyclic peptide (Fig. 10).[70] In particular, this analysis allowed the specific replacement of a Gly residue with several D-amino acids, which resulted in improvements of peptide's affinity and stability.[79] Angelini *et al.* confirmed what was already observed with PK15: the constrained bicyclic format of UK18 had an advantage in terms of both potency and stability over its monocyclic and linear analogues.[70,71]

The first pharmacokinetic studies with UK18 showed a rapid peptide clearance upon i.v. injection in mice, with a half-life of only 30 minutes.[71] In order to increase the circulation time in blood, UK18 was both recombinantly fused to a Fc region and chemically conjugated to an albumin-binding peptide. These strategies prolonged sensitively

the half-life of the bicyclic peptide to at least one day in mice.[71,85] However, these options were not attractive in terms of production, and their application was thus discontinued.

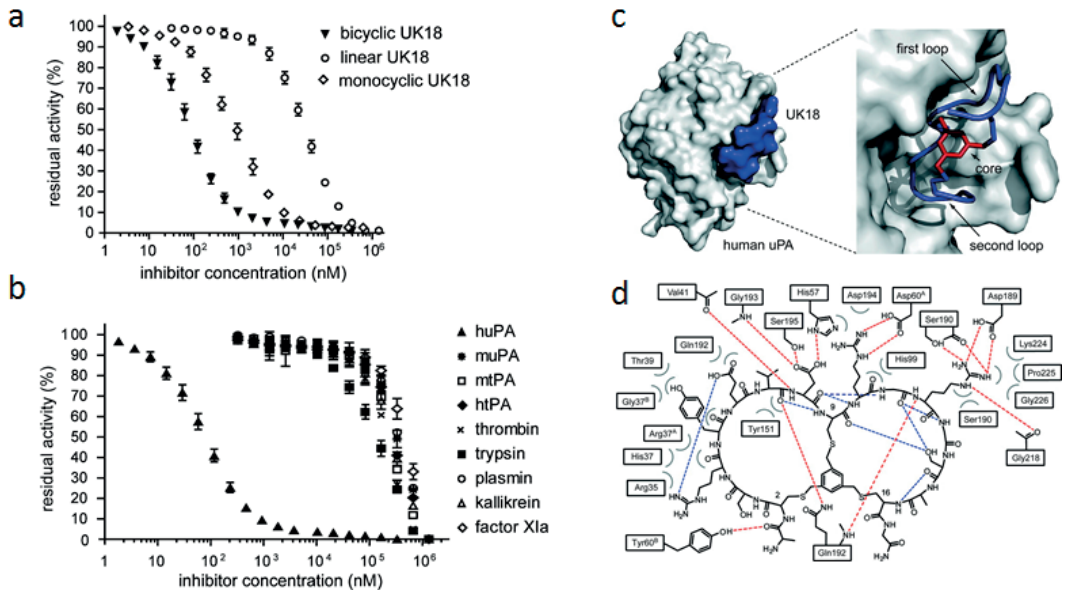

Figure 10. Inhibitory activity and specificity of UK18. Crystal structure of uPA in complex with the bicyclic peptide UK18. (a) Residual activities of uPA incubated with bicyclic UK18 or the linear or monocyclic derivative. (b) The residual activities of uPA and a range of homologous trypsin-like serine proteases were measured at different concentrations of bicyclic peptide UK18. (c) Surface representation of human uPA (gray) in complex with UK18 (peptide ribbon in blue, mesitylene scaffold in red). (d) Schematic representation of molecular interactions between uPA and UK18. Residues of uPA are labeled according to the chymotrypsin numbering system. Potential intermolecular (red) and intramolecular (blue) hydrogen bonds are shown as dashed lines. Bent gray lines indicate residues of UK18 in close contact with uPA (distances shorter than 4.0 Å that are not hydrogen bonds). Adapted with permission from [70], copyright © 2012 American Chemical Society.

1.1.6.3 Coagulation factor XII inhibitor

Activated human coagulation factor XII (FXIIa) is the initial serine protease of a plasma cascade which has several implications in inflammatory, coagulative and immunologic processes.[86] This protease circulates in the blood as inactive zymogen and it is converted to the active form by auto-proteolysis when exposed to negatively charged surfaces. Activated FXIIa cleaves both factor XI, initiating the intrinsic coagulation pathway, and plasma kallikrein, activating the kallikrein-kinin system, which further back-activates FXIIa and amplifies the cascade.[87] Although the physiology of FXIIa has not yet been clarified, its role in coagulation and/or inflammation related diseases, such as thrombosis and hereditary angioedema, has already been extensively documented.[83,88] In addition, surgeries in which the blood makes contacts with medical devices, such as coronary pulmonary bypass (CPB) and extracorporeal membrane oxygenation (ECMO),

can activate FXII and trigger coagulation, with potential life-threating consequences. Currently, heparin is widely used in these situations. However, this drug has itself serious well-known side effects, such as an excessive bleeding, which were stimuli for the discovery of substituents with safer anti-thrombotic effects.[89]

For this reason, FXIIa was considered an important target for the development of new inhibitors. Two phage display screenings were performed against this protein using different libraries of bicyclic peptides. The first selection was performed using a 4x4 library cyclized with TBMB and resulted in weak inhibitors of FXIIa (K_i = 1.2 μM).[80] In the second screening, variations in both peptide library size (3x3, 4x4 and 6x6) and cyclization reagents (TBMB and TATA) were introduced. The phage selection, followed by an affinity maturation step, yielded a medium nanomolar inhibitor, called FXII618. This bicyclic peptide was cyclized with TATA and inhibited FXIIa with a K_i value of 22 nM. Further characterizations showed a much higher selectivity towards the target protease and a better efficiency in the inhibition of the intrinsic coagulation pathway compared to a known FXIIa inhibitor, called corn trypsin inhibitor (CTI) (Fig. 11).[81] However, the bicyclic peptide could be applied exclusively as reagent for coagulation assays in clinical laboratories due to a low stability towards serum proteases and a fast elimination half-life.

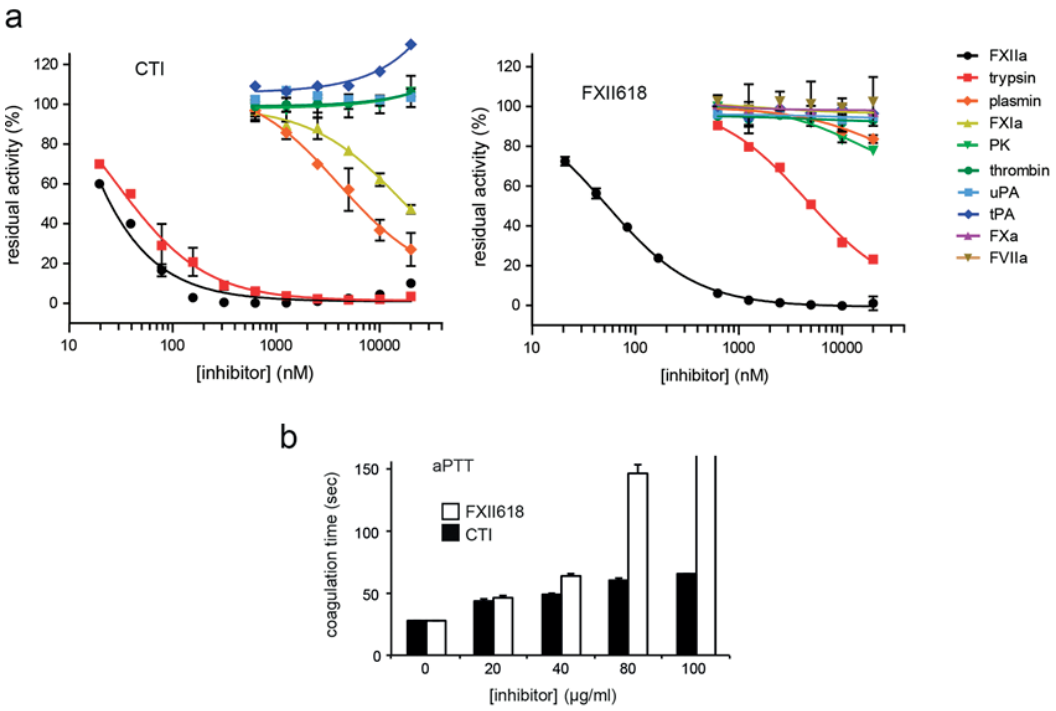

Figure 11. Comparison of FXII618 and CTI. (a) Specificity profile and inhibitory activity of CTI (left panel) and FXII618 (right panel). The residual activity of several trypsin-like serine proteases is shown. (b) Comparison of aPTT in citrated platelet poor plasma in the presence of the same quantities of FXII618 and CTI. Adapted with permission from [81], copyright © 2015 American Chemical Society.

These drawbacks hampered the application of FXII618 in anti-thrombotic therapies where the inhibitor needs to block FXIIa, and prevents the activation of the intrinsic coagulation pathway, over an extended period of time. In order to overcome this limitation, several variants of this bicyclic peptide have been recently developed in our laboratory, introducing D- or unnatural amino acid substitutions. These new bicyclic peptides showed strong improvements in terms of inhibitory activity, target selectivity and plasma stability (Fig. 12).[90,91] The combination of these results and further optimizations led to the design of a potent picomolar FXII inhibitor with even better biochemical properties. However, pharmacokinetic studies in rabbits confirmed that the the plasma half-life of this new inhibitor is still too short to exert efficiently its activity *in vivo* (unpublished data).

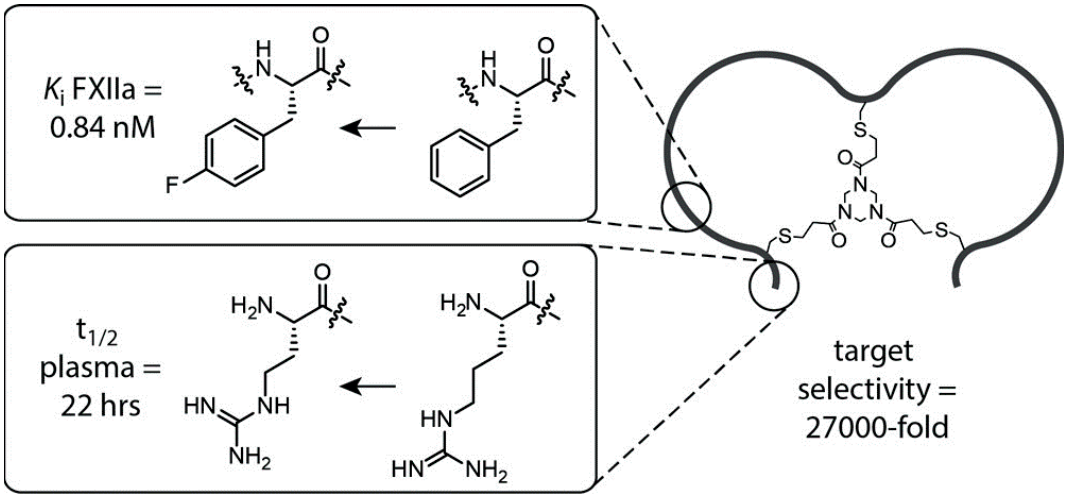

Figure 12. Optimization of FXII618. Adapted with permission from [91], copyright © 2017 American Chemical Society

1.2 - Strategies for prolonging the plasma half-life of peptides

The recent success of peptides as a new class of therapeutics is mainly related to their appealing advantages over other drug formats, as described in the first section. However, this should not hide the limitations which affect peptide ADME (absorption, distribution, metabolism and excretion) profiles. The main drawbacks that impact on their *in vivo* pharmacological efficacy are briefly presented in the following paragraphs.[1,92,93]

First, peptides can undergo enzymatic proteolysis in blood, which is responsible for their short metabolic half-life.[1] Several chemical modifications were efficiently developed to prevent this degradative pathway, such as the previously mentioned cyclization of peptide backbone[11]; the stabilization of α-helical conformation with hydrocarbon linkers[45] or D-Pro-L-Pro β-turn motives[38]; the substitution of natural amino acids and amide bonds susceptible to cleavage by unnatural derivatives and isosteric bonds creating peptidomimetic sequences; and the protective effect of the conjugation to hydrophilic polymers, fatty acids or carbohydrates (Fig. 13).[1,9]

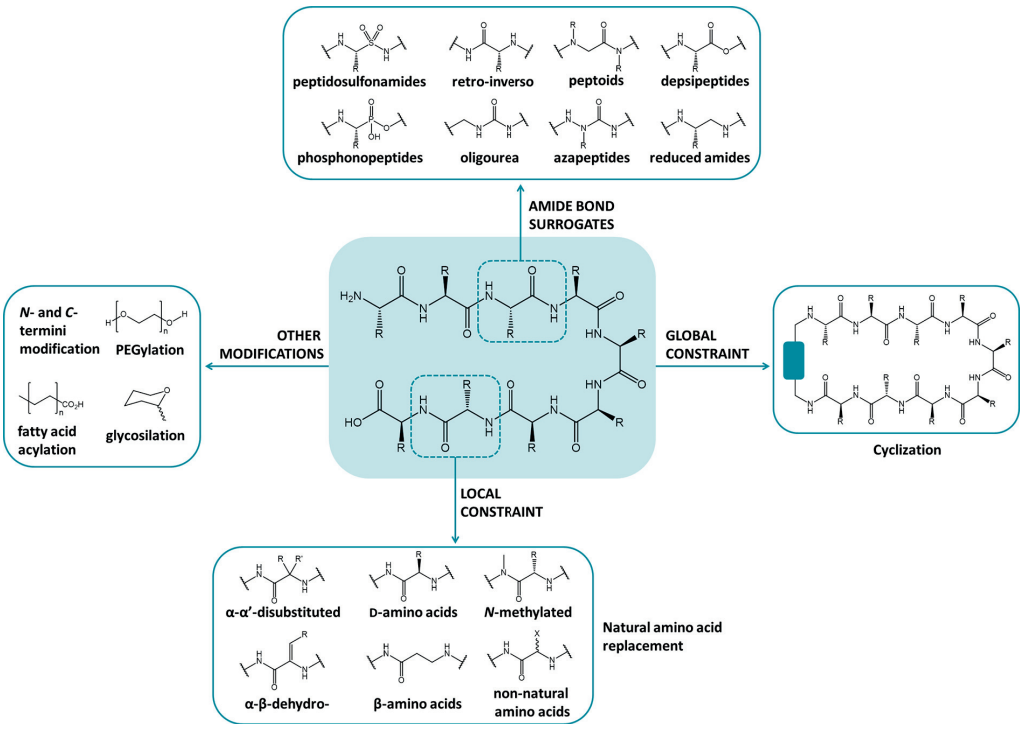

Figure 13. Modification approaches explored for enhancing the pharmacological properties of peptides. Reprinted with permission from [9], copyright © 2014 American Chemical Society.

Second, peptides have limited membrane permeability, and therefore their applicability is restricted to extracellular targets.[92] Innovative solutions were applied to facilitate their entrance into cells, such as conjugation to cell penetrating peptides[44] and stapled formats[45]. Despite these numerous efforts, cyclosporine is the only approved peptide that is cell permeable[46], and few promising candidates are currently in clinical trials.[41,94]

Third, peptides have typically a poor oral availability due to a low stability in the digestive system as well as low absorption by intestinal epithelium.[92] This limitation has been partially challenged through the generation of N-methylated peptides[46,95]. Few peptides are reported as orally available or orally administered, though they exert their activity on a target located in the intestine.[96]

Finally, another shortcoming for peptides to overcome is their negative pharmacokinetic profile generally characterized by short systemic half-lives, and associated with a fast clearance from the circulation by the kidneys.[93] As a direct consequence, peptides that act as antagonists are not available in the body for a period of time sufficient to exert their therapeutic effect. Thus, they require high dosages and frequent injections, affecting the patient's compliance to the treatments.[93] This last criticism is the main problem discussed, addressed and solved in the research project presented in this thesis.

1.2.1 The physiology of renal clearance

Kidneys have an essential physiological role in our body. They are involved in several key processes such as the maintenance of water, acid-base and electrolytes homeostasis; control of blood pressure; production of vitamin D, glucose and erythropoietin; and the removal of metabolic products and chemicals from the blood.[97] Each kidney is divided into approximately one million small units called nephrons, each consisting of a glomerulus that contains a three-layered barrier essential for blood filtration, and a tubule that transforms the filtrate coming out from glomerulus in urine. Glomerular epithelium has pores with a diameter of around 8 nm and cells (podocytes) rich in negatively charged proteoglycans. Thus, the glomerular filtration barrier acts mainly according to size and electrical charge of the molecules entering the kidneys. All the molecules and small proteins below the molecular size and dimension of albumin (66.5 kDa and 8x8x3 nm, respectively) are rapidly cleared.[98] In addition, molecules having a net negative charge are retained in the blood circulation more easily than cationic ones because of a strong repulsion mediated by the negatively charged podocytes in the kidney. As expected, peptides with a molecular weight of 5 kDa are completely filtered out within minutes, showing a filterability value of 1.0, which is the same of water.[97]

Based on this fact, one way to keep peptides in the circulation for a longer time is to hamper the renal filtration by increasing their hydrodynamic volume, without affecting the biological activity. Such an effect can be achieved by covalent genetic fusion or chemical conjugation of peptides to large endogenous or exogenous molecules, and it would be even better if these molecules are negatively charged.[93] Another solution is a non-covalent binding to serum proteins of either peptides themselves or via the linkage to natural ligands or drugs (e.g. fatty acids and ibuprofen) that prolong their half-life by interacting tightly with these proteins (Fig. 14).[93] Strategies developed to counteract the elimination of peptides will be discussed in detail in the following sub-sections.

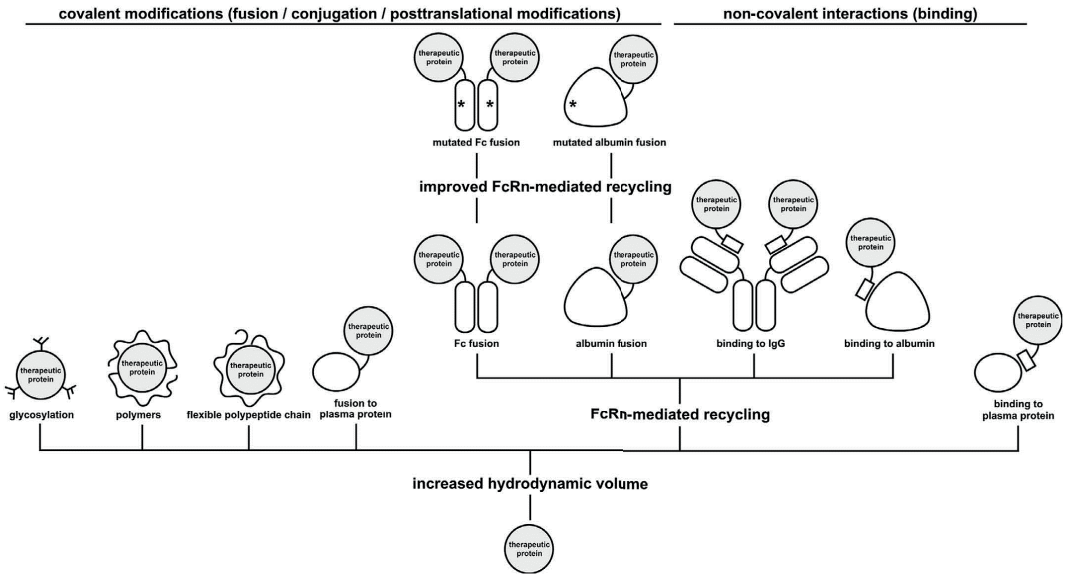

Figure 14. Overview of half-life extension strategies. Reprinted with permission from [93], copyright © 2016 Taylor & Francis.

1.2.2 Attachment to synthetic or natural polymeric units

1.2.2.1 Polyethylene glycol

The hydrodynamic volume of peptides and small proteins can be increased by conjugation to large hydrophilic polymers of natural or chemical derivation (Tab. 3).[93,99] The most common and successful polymer currently used and approved by FDA is the well-known polyethylene glycol [PEG; X-$(CH_2CH_2O)_n$-CH_2CH_2-OH, with X representing either a hydroxy (OH-) or methoxy (CH_3O-) group], based on repeated units of ethylene oxide. The variable number of these units determines the molecular weight and the architecture of the PEG type, and allowed to create a range of polymers with masses from 5 to 50 kDa. Even though the effective size of the conjugates could be smaller than the

clearance threshold, single or multiple PEG monomers attached to a molecule of interest can coordinate several water molecules, thus increasing the overall hydrodynamic volume and avoiding kidney's filtration (Fig. 15).[100] Moreover, PEGylation is a well-established strategy to improve peptides' proteolytic stability as well as their solubility in both aqueous and organic solutions. Finally, PEGylation has been shown to reduce the risk of eliciting protein immunogenicity.[101]

The first PEGylated derivatives were developed in the late 1970s by Davis and coworkers, and according to the chemistry used for the conjugation, they were classified in two generations.[102,103] In the first-generation, the PEG polymers had low molecular weight and this often resulted in diol contamination. Their conjugation suffered from weak bond stability and poor site specificity since it occurred randomly with different reactive groups present in the peptide or protein sequence, mainly N_{ε}-amine of Lys side chains or the N-terminus. Some examples of reactive moieties attached to PEG for conjugation are propionaldehydes and succinimidyl esters, which form imine and amide bond, respectively.[102,103] Despite the difficulty in the characterization of the isomers in the heterogeneous mixtures of products and the low reproducibility of these chemical approaches among different batches, several first-generation PEGylated proteins were approved. These include conjugates of adenosine deaminase (Pegademase, Adagen, Enzon), asparaginase (Pegaspargase, Oncaspar, Enzon) and interferon α2b (Peginterferon, PegIntron, Schering-Plough).[103]

Some of these limitations were overcome in the second-generation of PEG polymers by introducing both chemical groups that react with specific residues and functionalized PEG units that produce larger, degradable, releasable, bifunctional or branched structures.[102,103] One example is represented by PEG units activated with maleimide or haloacetamide moieties that can selectively react with the thiol of a Cys residue.[102,103] Among all the second-generation PEGylated proteins approved using these new chemical options, only two drugs are site-specifically modified. These are the granulocyte colony-stimulating factor (Pegfilgastrim, Neulasta, Amgen), which has a PEG at the N-terminus, and a fragment of anti-tumor necrosis factor (TNF)-α monoclonal antibody (Certolizumab pegol, Cimzia, UCB), which has an added PEG on the thiol group of a C-terminal Cys residue.[104]

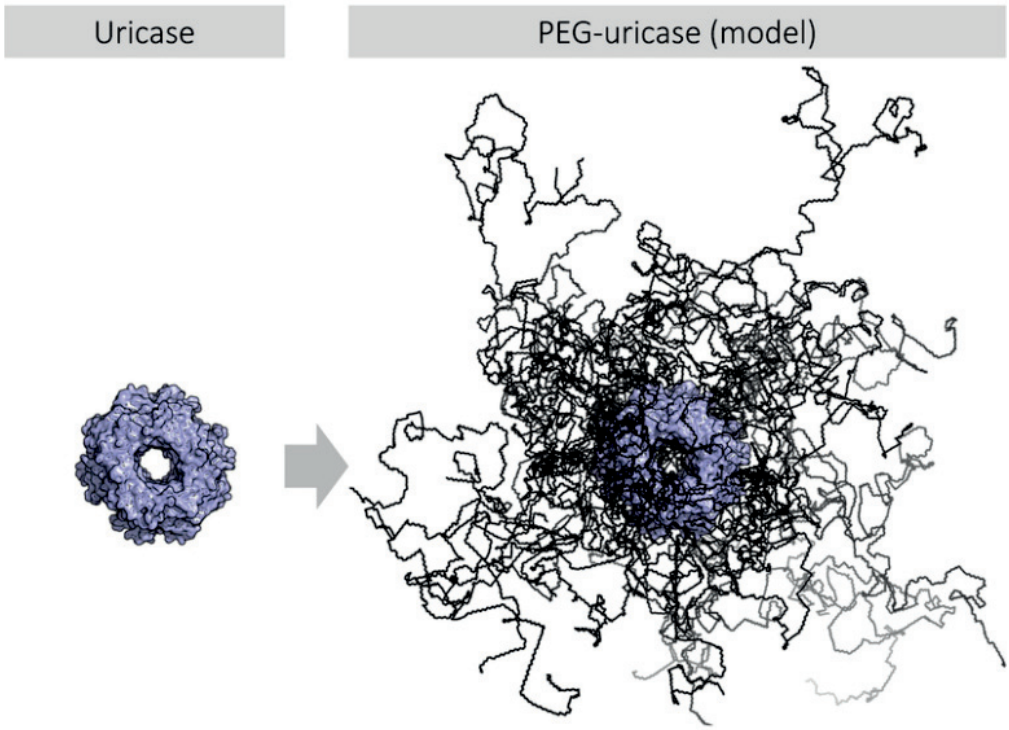

Figure 15. A comparison of uricase and PEG-uricase model adapted from [105]. Reprinted from "Evolution and evolvability" (https://commons.wikimedia.org/wiki/File:PegUricase.png), this figure is available under the terms of CC-BY 4.0 license (https://creativecommons.org/licenses/by/4.0/), via Wikimedia Commons.

Though PEGylation has been widely applied in the last decades and is considered safe, some problems emerged from its use. These include an undesired interaction of PEG with blood components, production of anti-PEG antibodies, allergic reactions and hypersensitivity, cytoplasmic vacuolation in kidneys, concerns about long-term effects of accumulation in the kidney and liver, possible degradation and toxicity of PEG monomers and side-products formed during storage and production.[101,106] In addition, PEG-conjugation reduces the pharmacodynamic properties when compared to the original non-PEGylated proteins, mostly because of the steric hindrance of the large PEG units.[107]

This last point strongly affects the rate of successful attempts to PEGylate peptides due to the few available sites that can be modified without reducing or abolishing peptide's activity. This challenge has limited a number of potential applications, and only one PEGylated peptide has reached the market, most likely due to the distance between the PEGylation site and the pharmacologically active part.[108] In addition to the preiously described peginesatide[33,67] (sub-section 1.1.4), another promising PEGylated peptide was the insulin derivative lispro, modified with a PEG unit on the LysB28 side-chain. The resulting peglispro (Eli Lilly) showed up to 30-fold improved circulating time in a phase 1 trial[109], compared to insulin itself, which has a half-life of few minutes or hours upon i.v.

and s.c. injection, respectively.[110,111] In addition, peglispro showed a preferential hepatic effect, which might result in a better control of glucose release from liver with lower risk of hypoglycemia, thus allowing a safer mode of action.[112] However, the clinical trials also revealed an increase in the concentration of liver enzymes which was asked to be clarified before approvals. Even if the company initially wanted to investigate this side effect, postponing the final submission, the costs of new trials were considered too high and the clinical development discontinued.[112]

Another example is an integrin-binding peptide, called HM-3, modified with different PEG units. The best combination showed a six-fold prolonged half-life in rats and a promising activity in mice, but it has not been tested yet in humans.[113,114] Despite these high number of studies, the development of PEGylated peptides requires further efforts to gain an efficient engineering of the conjugation sites. This is crucial for finding a proper balance between drug properties and cost of productions. New methodologies have already been employed for peptide modification and described in literature.[115] However, any new PEGylated peptide has reached the clinical stage yet.[108]

1.2.2.2 Natural polymers

In order to circumvent the previously mentioned drawbacks of PEGylation, safer and less expensive alternatives for peptide's modification were recently investigated. These substituents are newly designed synthetic PEG analogues and natural polymers made of glycans or polypeptides.[93,99]

Naturally occurring post-translational N- and O-glycosylations usually have a positive impact on the half-life and activity of proteins. Similarly, peptides can be modified with carbohydrates by introducing glycosylation sites in the sequence. N-glycosylation often occurs on Asn residue presented in the motif NXS/TX (with X any amino acid excluded Pro).[93] Addition of two extra glycosylation sites in the sequence of the recombinant human erythropoietin led to Darbepoetin alfa (Aranesp, Amgen), an EPO analogue currently used in patients with anemia caused by renal insufficiency or chemotherapy.[67] Compared to the original protein, Darbopoietin has a half-life in human that is three and five-fold longer when injected i.v. or s.c., respectively.[116]

In contrast, O-glycosylations of Ser or Thr residues are not associated with a specific consensus sequence. This modification is usually introduced by fusing peptides with natural O-glycosylated substrate sites, such as the carboxy-terminal peptide of the chorionic gonadotropin β-chain (CTP).[117] As demonstrated by the approved follicle-stimulating hormone (FSH) conjugated to CTP (corifollitropin-α, Elonova, Merck), the addition of

a O-glycosylated region almost tripled the half-life of the initial protein upon s.c. administration in human.[118,119] Although successful for several protein-based drugs, only few peptides modified with glycans were generated due to difficulties in preparation, and none of them is in clinical use.[120]

Other emerging strategies include conjugation of polypeptides to polysaccharidic polymers such as dextran, polysialic acid (PSA), hyaluronic acid (HA), and hydroxy-ethyl-starch (HES) (Fig 16). All of them have the advantage of being natural or semisynthetic constituents of human metabolic products, and thus have the potential to be poorly immunogenic. Some of them are even already claimed as safe products since they are applied in cosmetics and in hospital as plasma volume expanders or for other applications. Moreover, they have a high hydrodynamic volume and they are often negatively charged, which both are key properties for prolonging the half-life. [99]

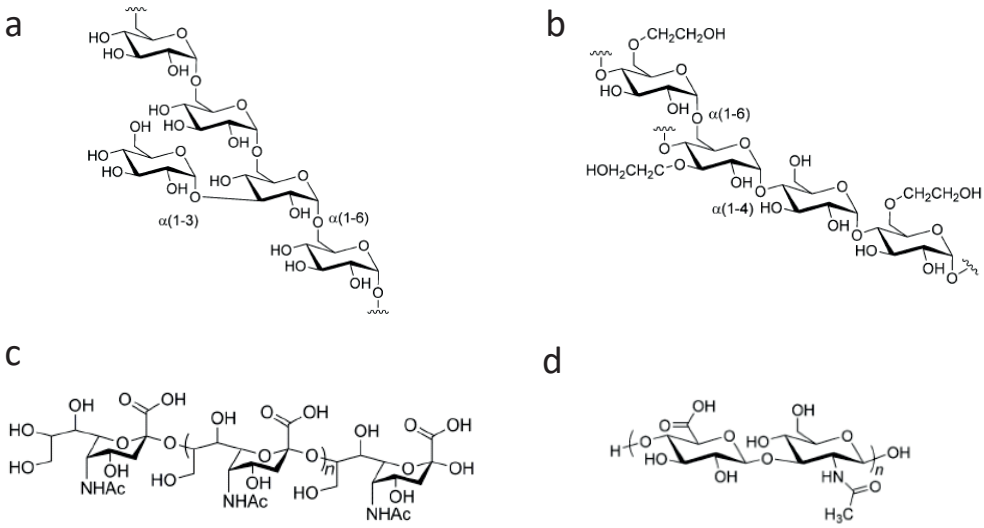

Figure 16. Structures of (a) dextran, (b) HES, (c) PSA and (d) HA. Adapted with permission from [99], reprinting license nr. 4047140757234, copyright © 2016 Wiley-VCH Verlag GmbH & Co. KGaA, Weinheim.

Dextran is a polymer of D-glucose that it is naturally processed by dextranases (Fig. 16a).[99] As an example of its half-life extending ability, the peptide hormone somatostatin conjugated to dextran showed similar activity to the analogue octreotide, but exhibited a 75-fold increased half-life in a phase 1 trial.[121]

Polysialic acid is a group of different polysaccharides, and the most used is the colominic acid (CA) (Fig. 16c). This plays an important role in cell adhesion and synaptic plasticity, and it is fully degraded without toxicity.[99] Several polysialylated proteins, both enzymes and antibody fragments, are currently in pre-clinical and clinical stage, and polysialyated peptides are expected to enter soon. As example, insulin derivatives modified

with two different CA polymers gave a two to three-fold prolonged reduction in glucose levels than the native peptide in mice.[122]

Hyaluronic acid is a linear polymer composed of 20-25 thousand of negatively charged dimeric units of D-glucuronic acid and N-acetyl-D-glucosamine (Fig. 16d).[99] This polymer is widely present in human skin, eyes, and connective tissues. It is highly biocompatible since it is metabolized by enzymes called hyaluronidases. Several peptides modified with HA showed a prolonged half-life and a negligible reduction of their activity. For example, HA was applied to exendin-4 (synthetic form: Exenatide, Byetta, Astrazeneca), which is a peptide analogue of GLP-1 that shares with it activity and 50% sequence identity. Due to a low proteolytic stability towards dipeptidyl peptidase-4 (DPP-4), the half-life of GLP-1 is less than two minutes and 1.5 hours upon i.v. and s.c. injection, respectively.[123] In contrast, the exendin-4 had a corresponding half-life of 30 minutes and 2.5 hours, respectively.[124,125] Several copies of exendin-4 were linked to HA, resulting in a conjugate with a 24-fold higher *in vitro* serum stability and relevant glucose lowering-effect in mice.[126]

Finally, hydroxy-ethyl-starch is a semisynthetic derivative resulting from the hydroxyethylation of the vegetal compound amylopectin (Fig. 16b).[99] Used as plasma volume substituent, it is degraded by α-amylase without any reported immunogenic effect. However, some drawbacks already experienced with PEG conjugation were observed.[99] A promising example of HESylated peptide is a dimeric erythropoietin mimetic peptide, named AGEM400, which displayed an *in vitro* activity superior or equal to EPO and related drugs, and is expected to have a longer half-life when tested *in vivo*.[127]

Peptides can be also recombinantly fused to long unstructured amino acid specific sequences. These hybrid systems, called recombinant PEG mimetics, have the same properties as both polymers and fusion proteins. Non repeated series of amino acids form a fully biodegradable and defined platform that increases peptides' solubility, stability and hydrodynamic volume.[117] The most innovative technology, with a couple of products in clinical trials, is XTENylation. XTEN is a polypeptide sequence up to 864 amino acids composed of only six specific residues (Ala, Asp, Gly, Pro, Ser, and Thr).[128] The first XTEN product was developed by Schellenberger *et al.* and it consisted in the genetic fusion of exendin-4 at the C-terminus of the XTEN polypeptide (VRS-859). Preclinical studies in mice, rats and monkeys, showed a 65 to 125-fold increase of exendin-4 half-life (Fig. 17a).[129] This XTENylated version of exendin-4 just finished a phase 1 trial for type 2 diabetes, resulting in high safety and tolerability, and a 50-fold extended half-life.[128] At a first glance, the XTEN system could appear limited to peptides composed of

only natural amino acids, without allowing multiple copies and chemical modifications of the peptide of interest. However, the introduction of specific reactive moieties on the XTEN sequence, like Cys or alkyne residues, overcomes this limitation and offers new options for site-directed conjugation of peptides and small molecules (Fig. 17b).[130] Moreover, this approach requires few to no modification and purification steps, overcoming some of the disadvantages of PEGylation such as cost and time of production.[117] Since its first application, several other peptides were linked to XTEN showing improvements in plasma half-life.[128]

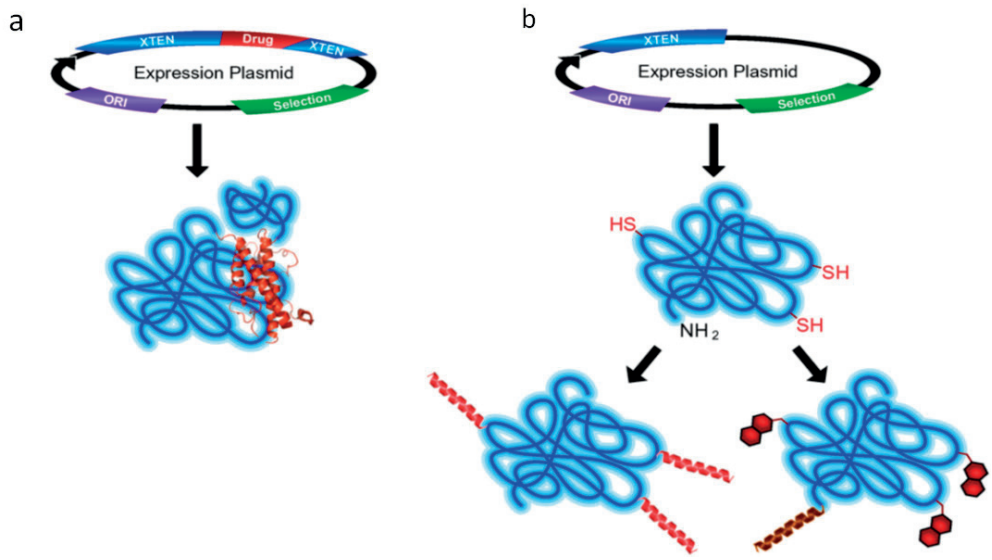

Figure 17. XTENylation of biologically active molecules. (a) Genetic fusion: a single polypeptide includes both the therapeutic and bulking moieties. (b) Chemical conjugation: XTEN is first expressed and purified as an intermediate and then conjugated to biologically active payloads. Reprinted (open access) from [128], this article is available under the terms of CC-BY 4.0 license (https://creativecommons.org/licenses/by/4.0/).

Another recombinant PEG mimetic strategy is ELPylation that exploits the repeated sequence VPGXP (with X any amino acid excluded Pro), found in human elastin and degraded by elastases. Examples of three ELPylated peptides are GLP-1 (Glymera, PB1023), insulin (Insumera, PE0139), and vasoactive intestinal peptide (Vasomera, PB1046) derivatives. All of them are in phase 2 trial and required one injection per week. More similar to XTENylation is PASylation, a strategy developed by Skerra and co-workers. The PAS polypeptide contains only three amino acids (Pro, Ala, Ser) and exhibits a strong positive effect on the half-life. Minor applications include HAPylation, consisting of repeated Gly_4-Ser units, and gelatin-like-protein (GLP) polymers. Several PAS, HAP and GLP derivatives are currently in pre-clinical stage with promising results.[117]

Table 3. Peptide conjugation to polymers.

Cargo		Polymeric conjugate		Factor	Ref.
Type	**$t_{1/2}$**	**Type**	**$t_{1/2}$**		
erythopoethin mimetic peptide (peginesatide)	n.a.	two PEG units of 20 kDa	19-30 hrs (i.v.)[a] 35-68 hrs (s.c.)[a]	- [a]	33 67
insulin (peglispro)	4-6 min (i.v.)[a] 2.3 hrs (s.c.)[a]	one PEG unit of 20 kDa	2.3 hrs (i.v.)[a] 24-46 hrs (s.c.)[a]	28[a] 10-20[a]	109 110 111
integrin-binding peptide (HM-3)	28 min (i.v.)[b]	one PEG unit of 10 kDa	162 min (i.v.)[b]	6[b]	113
somatostatin (sms-D70)	1.5 hrs (s.c.)[a] for octreotide	70 kDa of dextran	112 hrs (s.c.)[a]	75[a]	121
insulin (-)	3 hrs (s.c.)*[c]	22 and 39 kDa of colominic acid	6-9 hrs (s.c.)*[c]	2-3*[c]	122
exendin-4 (-)	1 d (s.c.)*[c]	100 kDa of hyaluronic acid	3 d (s.c.)*[c]	3*[c]	126
erythopoethin mimetic peptide (AGEM400)	n.a.	130 kDa of hydroxy-ethyl-starch	n.a.	-	127
exendin-4 (VRS-859)	2.5 hrs (s.c.)[a]	864 amino acids for XTEN	128 hrs (s.c.)[a]	51[a]	125 128

Half-life (or activity when marked with an asterisk) and factor of improvement were measured for human (a), rat (b) and mouse (c) species. n.a. = not available.

1.2.3 Fusion or conjugation to serum proteins

Blood is composed of blood cells (45%) and plasma (55%). Plasma is an aqueous solution containing 92% water, 7% blood plasma proteins and 1% of other small molecules, such as glucose, amino acids, fatty acids, and waste products. Plasma depleted of clotting proteins is called serum. Plasma proteins have several different functions, including the transport of lipids, hormones, vitamins and minerals in the circulatory system as well as the regulation of cellular activity and the immune system. The three most abundant plasma proteins are albumin (54-60%), globulins (35-38%) and fibrinogen (4-7%). The remaining proteins act as enzymes, complement components, protease inhibitors or kinin precursors. All plasma proteins are synthesized in the liver except for the gamma immunoglobulins (IgGs).[131]

Albumin and IgGs are characterized by a nominal plasma half-life of 19 and 21 days in humans, respectively.[117] The long circulating time in the blood is related to their molecular weight, which prevents fast renal clearance. In addition to this, their half-life is much longer than other plasma proteins thanks to a recycling process mediated by binding to the neonatal Fc receptor (FcRn).[117] In transgenic mice without FcRn, IgG and albumin have a half-life similar to other non filtered proteins with the same or even higher

molecular weight, suggesting a similar degradative pathway.[132] The FcRn is a major histocompatibility complex (MHC) class I-related receptor, widely expressed in the body, and it exerts its function mainly during pregnancy translocating IgGs from the mother to the fetus. However, it also binds IgGs and albumin in a pH-dependent manner as soon as these proteins are internalized by pinocytosis into vesicles. In acidic condition (pH < 6.5), IgGs and albumin bind strongly to the FcRn receptor, while all the other free proteins are directed to lysosomal degradation. Once the receptor is recycled back to the cell surface, the external neutral pH (pH > 7) causes the release of these proteins in the bloodstream (Fig. 18). This mechanism of recycling is valid only for IgG isotypes 1, 2 and 4, and albumin.[132] The FcRn receptor is characterized by two different regions for the binding of these two proteins, and this allows for an efficient recycle with a specific ratio albumin : IgG = 700 : 1.[117]

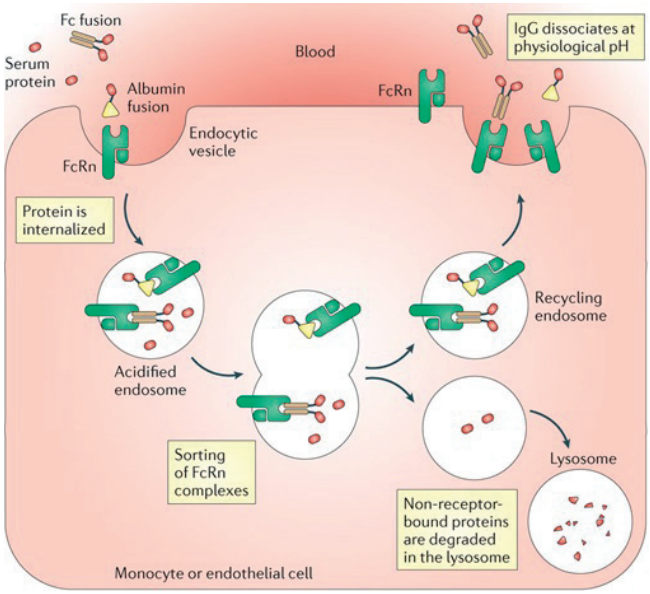

Figure 18. FcRn recycling mechanism. Fc-fusion protein drugs or albumin-fusion protein drugs bind to FcRn on the endothelium. Receptor-bound proteins are internalized into endocytic vesicles. Endosomes are acidified and undergo sorting of FcRn. Non-receptor-bound proteins are degraded in the lysosomal compartment and receptor-bound proteins are recycled back to the cell membrane. The protein therapeutic is subsequently released back into the blood. Reprinted with permission from [133], reprinting license nr. 4047141451047, copyright © 2014 Nature Publishing Group.

Because of their long half-life, both IgGs and albumin have been extensively used in the last decades to improve the pharmacokinetics of peptides and small proteins through a covalent linkage. Moreover, recent analyses proved that IgG and albumin mutants with improved binding affinity for the FcRn receptor are characterized by further prolonged half-life compared to their native counterparts.[134] These optimizations have

already been proven on therapeutic IgGs and recombinant variants of albumin, translating into potential benefits also for the molecules covalently bound to them.[135–137]

The following parts will present some applications of two covalent half-life extension platforms for peptides and small proteins, namely IgGs and transferrin (Tab. 4). Properties of albumin as covalently bound carrier will be detailed in a dedicated section.

1.2.3.1 Gamma immunoglobulin

Gamma immunoglobulins are the most represented type of antibodies in the plasma. Three out of four subclasses have a half-life of around 21 days in humans thanks to their size and FcRn-mediated recycling.[138] The IgG sites responsible for the binding to the receptor are the CH2 and CH3 domains of the 50 kDa Fc region. As consequence, several Fc fusion proteins have been developed since 1980s for half-life extension using this region as platform for the incorporation of proteins and peptides.[117] Several studies demonostrated that the biological activity of the Fc fusion proteins can be modulated i) dimerizing the sequence or the Fc region for avidity effects, ii) inserting specific linker sequences, or iii) changing the orientation of the fused molecules.[139] The first Fc-fusion protein to enter in the market was etanercept (Embrel, Amgen), used for the treatment of rheumatoid arthritis. Etanercept is composed of the extracellular region of the TNF receptor 2 fused to a Fc domain. This molecule binds with high affinity the natural ligand, TNF-α, blocking the activation of its receptor in chronic inflammatory diseases.[117]

In the following decades, at least ten other Fc-fusion proteins were approved by the FDA, and many others are in clinical trials, showing half-lives ranging from five to 13 days.[139] Among them, only two are peptide-Fc proteins (“peptibodies”) (Fig. 19): romiplostim (Nplate, Amgen) and dulaglutide (Trulicity, Eli Lilly), approved for the treatment of immune chronic thrombocytopenia and type 2 diabetes, respectively.[93,117] Romiplostim is composed of two tandem copies of a linear thrombopoietin mimetic peptide recombinantly fused to the C-terminus of an IgG1 Fc fragment using a Gly linker. This peptide was initially developed and further optimized by phage display selection, and it showed an IC_{50} value of 500 pM when tested as dimer.[140,141] Dulaglutide is an optimized analogue of GLP-1 expressed to the N-terminus an IgG4 Fc region. The peptide has been engineered to improve the stability against DPP-4. Further modifications were introduced on the Fc region to reduce its affinity for the FcRn and module the effector properties.[142] Both peptibodies have half-lives of approximately three to five days when s.c. injected in human, allowing a single administration per week.

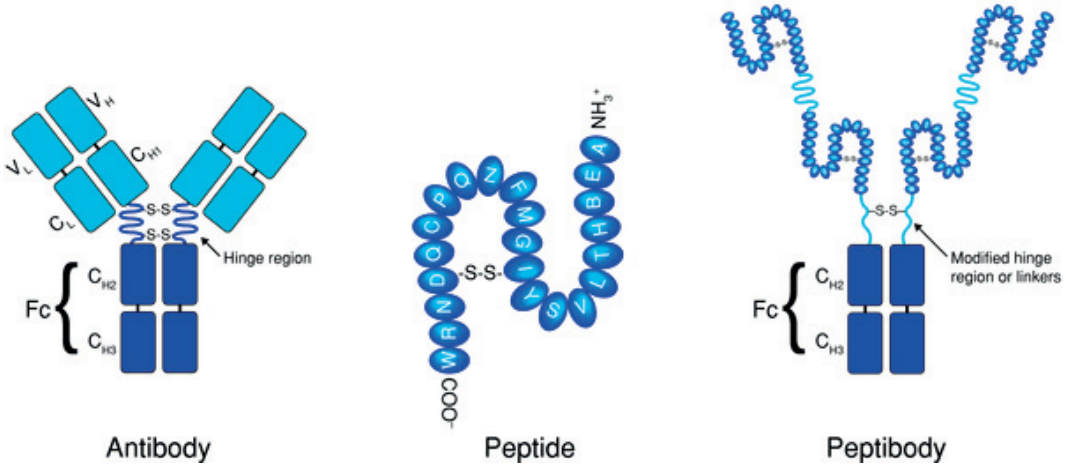

Figure 19. Comparison of the structure of (left) IgG antibodies, (center) a small therapeutic peptide, and (right) a peptibody. Reprinted (open access) from [139], copyright © 2013 Wiley Periodicals, Inc. and the American Pharmacists Association.

Other peptibodies have reached different preclinical and clinical stages with opposing results.[139] The most advanced is blisibimod (AMG-623), a B cell-activating factor (BAFF) antagonist in phase 3 trial for the treatment of systemic lupus erymatosus.[143] It is composed of two equally active parts, each carrying four BAFF-binding peptides, fused to an IgG1 Fc fragment. The BAFF-binding peptide was selected by phage display and cross reacts with both soluble and cell surface BAFF with extremely high affinity (1 pM), interrupting its interaction with the three natural receptors.[144] The BAFF-peptibody has a half-life in human of eight to ten days, shorter than the other anti-BAFF antibodies, but in contrast it can be efficiently expressed in bacteria.[145]

Another peptibody is trebananib (AMG-386), in which the active peptide was isolated by phage display as inhibitor of angiopoietin-1 and -2, and it blocks their interactions with the natural receptor Tie2.[146,147] As romiplostim, trebananib presents two tandem copies of the peptide fused to an IgG1 Fc fragment and showed a half-life of three to six days in human.[148] Because of its potent anticancer activity it reached phase 3 trial. However, these studies were discontinued in 2014 from Amgen without further information.[149]

Two other promising peptibodies were developed and entered in clinical trials, but no data has recently been reported. The first product was a GLP-1 analogue, named CNTO-736, with a significantly prolonged half-life and *in vivo* efficacy in mice.[150,151] The second peptibody was CNTO-528, an erythropoietin mimetic peptide discovered from phage peptide libraries.[152] The peptide was again fused to an IgG1 Fc fragment as either a single or a double copy (CNTO-528 and CNTO-530, respectively), and displayed a much better activity and half-life than erythropoietin.[153,154] In a phase 1 trial, CNTO-528

showed a dose-dependent half-life ranging from 1.5 to 7.5 days.[153] Preclinical studies with CNTO-530 gave similar results in mice.[154]

In our laboratory, Angelini *et al.* developed a peptibody composed of the bicyclic peptide UK18 fused to a Fc fragment in the linear format and the cyclized *in situ*, skipping the individual steps of peptide production, cyclization, purification, activation and chemical conjugation.[85] They initially fused UK18 on both Fc monomers, replacing the hinge region with a short Gly-Ser linker, and they cyclized the peptide with TBMB (Fig. 20a). However, they experienced the formation of different dimers due to a cross-reaction between the two displayed peptides, and this resulted in a 60-fold reduction in the inhibitory activity. Thus, they extended the short Gly-Ser linker testing hinge regions of different lengths and they expressed UK18 only on one of the Fc monomers (Fig. 20b). This new format proved that the inhibition potency was strictly related to the linker size since longer hinge regions had K_i values in the same order of magnitude as the peptide alone.[85] The half-life of the best heterodimeric peptibody was tested in mice upon intravenous injection and resulted to be approximately 1.5 days, 72-fold longer than the bicyclic peptide alone.[71,85] The ELISA assay used for the quantification demonstrated that the peptide was fully stable. These results proved that Fc fusion of peptides that need to be chemically cyclized can be efficiently achieved if appropriate optimizations are introduced in the system.[85]

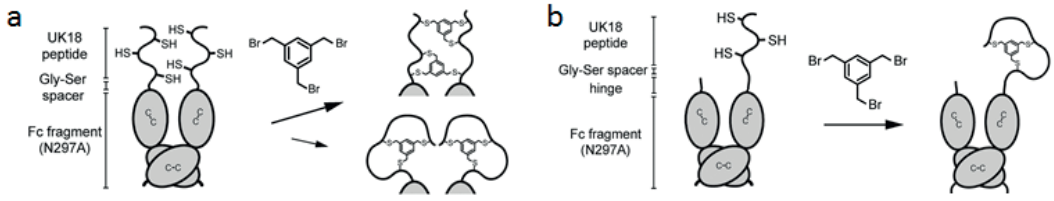

Figure 20. Chemical macrocyclization of UK18-Fc fusion protein. (a) Schematic representation of UK18-Fc homodimer and cyclization reaction of the peptide with TBMB. Two of the nine possible regioisomers are shown, including the desired one (lower drawing). (b) Schematic representation of UK18-Fc heterodimer and cyclization reaction based of the peptide with TBMB. Only the desired isomer can be obtained. Linkers with different lengths were inserted between the peptide and the Fc fragment, using the amino acid sequence of the human IgG1 hinge region wherein Cys were replaced by Ser. Adapted with permission from [85], copyright © 2012 American Chemical Society.

In addition to recombinant expression, peptibodies can be created through a chemical conjugation of peptides to both Lys and Cys residues present or recombinantly added in the hinge part of the Fc region.[139] Mezo *et al.* demonstrated the feasibility of this approach with the atrial natriuretic peptide (ANP). ANP is a natural peptide hormone involved in the control of pressure and fluid in the body, characterized by a short half-life. The peptide was modified with terminal thioester moieties and coupled by native

chemical ligation to an IgG1 Fc fragment bearing two free N-terminal Cys residues (Fig. 21). Similar to other peptibodies previously reviewed, the variation of linker length between peptide and Fc region resulted in molecules with altered *in vitro* activity. The developed monomeric and dimeric conjugates improved the half-life of ANP more than 30-fold in rats. Nevertheless, the degradation of the linear peptide was much faster than the effective half-life of the Fc fragment to which it was conjugated, confirming the superior stability of cyclic peptides over linear ones.[155]

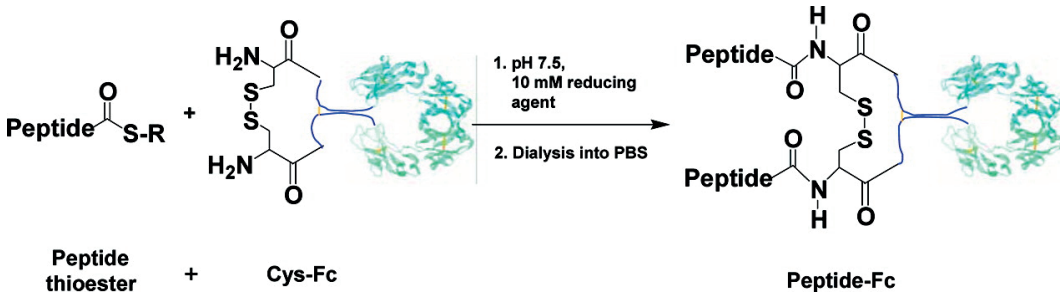

Figure 21. Schematic representation of the semisynthetic method used to generate the ANP-Fc fusion proteins. Reprinted with permission from [155], copyright © 2012 American Chemical Society.

Despite the high success, the Fc fusion protein strategy still has several limitations which makes it less attractive[117,138], such as:

i) difficulties in recombinantly introducing multiple unnatural amino acids in peptide active moieties or for site specific conjugation;
ii) low protein yield due to the complex production and purification steps, further reduced with homo or bispecific dimers, as shown in one of the reported examples (few milligrams of pure heterodimer product before cyclization)[85];
iii) low tissue penetration for targeting solid tumors due to a relatively large size;
iv) high cost of production and issues in storage and/or handling;
v) recombinant engineering often required to remove unwanted ancillary activations of the immune system when targeting soluble proteins, or to restore the proper sites of glycosylation.

1.2.3.2 Transferrin

In addition to IgGs and albumin, transferrin has also been exploited as carrier protein, sharing with them many of the properties and problems. Transferrin is an iron transporter with a molecular weight of 80 kDa that is present in the serum at a relatively high concentration. Transferrin has a half-life of between 14-17 days for the aglycosylated

form, and 7-10 days for the glycosylated one. Similarly to the two other long-lived serum proteins, its half-life is related to a specific receptor-mediated mechanism.[93]

As model peptides widely used in almost all of the half-life extension platforms, the previously described GLP-1 and exendin-4 were fused to transferrin, leading to the generation of different conjugates with retained *in vivo* activity as well as much longer half-lives in different animal models.[156,157] Insulin was also recently fused to transferrin as pro-drug and it showed a 15-fold longer half-life in mice and a better activity than the approved insulin glargine.[158] In addition, transferrin was investigated for its efficient targeting of tumor cells, its potential drug delivery through the blood–brain barrier of chemotherapeutics, and potential oral delivery of biologicals.[159] The last application has a particular interest and it has been already investigated. A still functional and intact transferrin-insulin conjugate was detected in rat serum four hours after its oral administration, demonstrating the ability of transferrin to pass through the gastrointestinal tract.[158]

Table 4. Peptide fusion or conjugation to serum proteins.

Cargo		Serum protein		Factor	Ref.
Type	$\tau_{1/2}$	Type	$\tau_{1/2}$		
thrombopoietin mimetic peptide (romiplostin)	n.a.	Fc fusion	3.5 d (s.c.)[a]	- [a]	140
GLP-1 analogue (dulaglutide)	1-1.5 hrs (s.c.)[a]		4.7 d (s.c.)[a]	75-113[a]	123 142
BAFF-binding peptide (AMG-623)	n.a.		8-10 d (s.c.)[a]	- [a]	145
angiopoietin1- and -2 binding peptide (AMG-623)	n.a.		3-6 d (i.v.)[a]	- [a]	148
GLP-1 analogue (CNTO-736)	n.a.		15-20 hrs (i.v.)[b]	- [b]	151
erythopoethin mimetic peptide (CNTO-528)	n.a.		1.5-7.5 d (i.v.)[a]	- [a]	153
erythopoethin mimetic peptide (CNTO-530)	n.a.		40 hrs (s.c.)[b]	- [b]	154
bicyclic peptide (UK18)	30 min (i.v.)[b]		1.5 d (i.v.)[b]	72[b]	85 71
atrial natriuretic peptide (ANP)	5 min (i.v.)[c]	Fc conjugation	2.8-5.5 hrs (i.v.)[c]	34-66[c]	155
GLP-1 (GLP-1-Tf)	n.a.	transferrin	2 d (i.v., s.c.)[d]	- [d]	156
	n.a.		27 hrs (i.v.)[e]	- [e]	157

Half-life and factor of improvement were measured for human (a), mouse (b), rat (c), monkey (d) and rabbit (e) species. n.a. = not available.

1.2.4 Non-covalent binding to serum proteins

The half-life of peptides can also be prolonged by binding non-covalently to long-lived serum proteins. Peptides are directly conjugated to high affinity binding moieties, such as small molecules or peptides, that tether them to serum proteins after injection, thus impairing their renal filtration. The affinity of the reversible ligands determines the percentage of free and bound bioactive peptides, balancing the fraction available at the target site, non influential if the target is in the plasma, with the fraction saved from clearance.[160] This half-life extension platform offers the following advantages over the other strategies:

i) an easier and less expensive chemical synthesis of peptide conjugates compared to the time- and cost-consuming production, purification and modification of large polymers or proteins;
ii) a conserved small molecular weight (< 5-10 kDa) which preserves the tissue penetration profile of the free fraction of peptide;
iii) a site-specific coupling of the ligands with a reduced impact on the activity of the bioactive peptides;
iv) a higher stability in the formulation (storage and handling);
v) more options as application routes (e.g. oral or nasal administration).

Numerous types of albumin-binding moieties have been characterized and used as ligands, and they will be later described in a dedicated section. In the following paragraphs I presented several non-covalent binding moieties which bind in the blood other plasma proteins than albumin (Tab. 5).

Peptide binders of IgGs were developed by phage display or mRNA display with on average weak affinities, and they were mainly used for purification purposes.[161–163] Delano *et al.* could isolate a 13-mer cyclic peptide which bound to IgG1 with a K_d of 25 nM, and partially overlapped with the IgG binding site for the FcRn receptor.[161] Since no evidence of its use for half-life extension was reported in literature, Sockolosky *et al.* recently tested its genetic fusion to a protein. The resulting IgG-binding peptide conjugate could bind only to human antibodies with high affinity, and this required the pre- or co-administration of hIgGs in mice for the *in vivo* experiments. Compared to the protein alone, the conjugate showed a 70-fold improved half-life.[164]

Different bacterial IgG-binding domains (IgBDs) were recently exploited by Kontermann and co-workers as half-life extension strategy. They demonstrated that the binding domain with the highest affinity for IgG (SpG_{C3}, 56 amino acid, 6151 Da) could efficiently

prolong the half-life of a scDb fusion protein around 18-fold in mice.[165] This specific IgBD was later modified in order to modulate its binding towards the Fab fragment, avoiding any interaction with the Fc region responsible for the FcRn-mediated recycling. Site-directed mutagenesis and phage display resulted in a new variant (SpG_{C3Fab}RR, 56 amino acid, 6062 Da) with the desired selective binding and further improved half-life in mice.[166]

New ligands were developed for a non-covalent binding of the neonatal Fc receptor involved in prolonging the half-life of albumin and IgGs. A new class of affinity protein based on staphylococcal protein A, called affibody[167], was recently screened against human FcRn by performing phage display at acidic pH.[168] Characterization of the isolated affibodies demonstrated a nanomolar affinity at pH 6, while a much weaker binding was measured at pH 7.4, as desired. Preparation of a fusion protein composed of an affibody linked to an albumin-binding construct showed a half-life in mice two to three-fold longer than the construct alone. Most likely the half-life of the albumin-binding construct was limited by the intrinsic half-life of mouse albumin, while the affibody conjugate overcame this bottleneck due to the presence of the double binding partners, confirming the crucial role of the FcRn as well.[168] In addition to affibodies, phage selected peptides have been developed against this specific receptor. A cyclic peptide could efficiently block the interaction between FcRn and IgG, bind to the receptor at an acidic pH, and allow the recycling of a fused protein. However, no half-life related applications were reported.[169,170]

A few other human serum proteins were or could be exploited for non-covalent binding half-life extension. Transthyretin, with a half-life in humans of two days, was used for tethering peptides through a reversible small molecule binder (K_d AG10 = 4.8 nM). Conjugation of AG10 to a native and proteolytic stable gonadotropin-releasing hormone showed a 13- and three-fold longer half-life, respectively, upon i.v. dosing in rats. The greater impact on the native form strongly highlights the positive effect of non-covalent binding in both peptide half-life and stability.[171]

A glycosaminoglycan anticoagulant derivative, which binds the plasma protein antithrombin III with high affinity (K_d idraparinux = 1 nM), was chemically conjugated to insulin. Preclinical studies in rats showed a strong improvement in the circulating half-life of insulin and no side effects on the coagulation system.[172] This insulin conjugate recently entered into a phase 1 trial, showing a half-life of three to five hours.[173] Since the clinical trials of the original binding moiety idraparinux were discontinued due to some long-term side effects, potential risks related to this new strategy must be monitored carefully over the time.[93] Finally, transferrin and its receptor were also targeted by *in vitro* selections resulting in peptides and affibodies with nanomolar affinities. However, none of them has

yet been used for potential half-life extension, but only for cell internalization and cancer targeting.[174–176]

Table 5. Conjugation to plasma protein-binding molecules.

Cargo		Serum protein-binding molecule (target)	Conjugate		Factor	Ref.
Type	**$\tau_{1/2}$**		**Affinity**	**$\tau_{1/2}$**		
mKate (protein)	5-10 min (i.v.)[b]	peptide (IgG)	20-40 nM[a]	8 hrs (i.v.)[b]	≈ 70[a]	164
scDb (protein)	1.3 hrs (i.v.)[b]	SpG_{C3} (IgG)	5-6 nM[a] 46-67 nM[b]	23.3 (i.v.)[b]	18[c]	165
	1.3 hrs (i.v.)[b]	$SpG_{C3Fab}RR$ (IgG)	29-167 nM[a] 19-55 nM[b]	47.8 (i.v.)[b]	37[c]	166
albumin binding construct (protein)	33 hrs (i.v.)[b]	affibody (FcRn)	12-50 nM[a] 90-350 nM[b]	61-91 (i.v.)[b]	2-3[c]	168
mKate (protein)	n.a.	peptide (FcRn)	1-5 μM	n.a.	-	169 170
GnRH (peptide)	3.5 min (i.v.)[c]	AG10 (transthyretin)	200-400 nM[a]	46 min (i.v.)[c]	13[c]	171
GnRH-A (peptide)	58 min (i.v.)[c]			180 min (i.v.)[c]	3[c]	
insulin (peptide)	10 min (i.v.)[c] 2.3 hrs (s.c.)[a]	idraparinux (antithrombin III)	6-96 nM[a]	11 hrs (i.v.)[c] 3-5 hrs (s.c.)[a]	66[c] 1.5-2.5[a]	111 172 173
-	-	peptide (transferrin receptor)	15 nM[a]	-	-	174
-	-	affibody (transferrin)	400 nM[a]	-	-	175
-	-	peptide (transferrin)	70-120 nM[a]	-	-	176

Half-life, affinity and factor of improvement were measured for human (a), mouse (b), and rat (c) species. n.a. = not available.

1.3 - Albumin as platform for half-life extension

Peptides have tipically short plasma half-life and several extension technologies have been developed so far to solve this limitation, as previously illustrated in the second section. Among them, there has been a lot of interest lately in exploiting serum albumin to modulate the pharmacokinetic properties of a variety of peptides and small molecules.[177] Albumin is an interesting protein candidate since it possesses intrinsic biochemical and biophysical properties that make it perfectly suitable for new clinical and pharmaceutical applications.[178] This third section will highlight the main features of albumin, including its exquisite drug carrier properties for the half-life extension of peptides, which is the main goal of the research project presented in this thesis.

1.3.1 Structural properties

Albumin is the most abundant protein in plasma (40 $g \cdot l^{-1}$, 600 μM) with a molecular weight of 66.5 kDa. It is a non-glycosylated single polypeptide chain comprising 585 amino acids in the mature form. It contains 17 disulfide bridges that contribute to its stability and a single odd Cys residue in position 34, which alone makes up 80% of the free thiols in plasma. Its amino acid composition is characterized by a high percentage of ionic amino acids, with 83 and 98 positively and negatively charged residues, respectively (UniProtKB - P02768). The resulting negative net charge highly increases its solubility in aqueous solution.[178]

The secondary structure of albumin is composed of 67% α-helix without any β-sheet element. The tertiary structure is organized as a monomer with a globular heart-shape and dimensions of 80 x 80 x 30 Å. Albumin is ordered in three homologous domains, named I (1-195), II (196-383) and III (384-585), with similar amino acid sequences and structures.[179] Despite these similarities, each domain has peculiar interactions with the others and the relative orientations create an asymmetric module that allocates several ligand binding sites (Fig. 22).

Each domain contains two subdomains, denominated A and B, with four and six α-helices, respectively. The overall structure is extremely stable over a wide range of pH from 4.0 to 9.0,[179] though its fold and shape are pH dependent.[180] In the pH range 4.3-

8.0 albumin conserves its neutral (N) heart-shaped form. Below pH 4.3, albumin undergoes a transition to a fast-migrating (F) form that has a lower helical content and decreased solubility. Further reducing the pH to values lower than 2.7 causes a transition to the extended (E) form, which seems to resemble a molten globule state. Above pH 8.0, a transition to the basic (B) form displays, again, a lower helical content but, in contrast, higher binding affinity for some molecules. A full denaturation of albumin can occur only through the application of very harsh conditions related to dramatic changes in pH and temperature, or through prolonged incubation with chaotropic agents.[180]

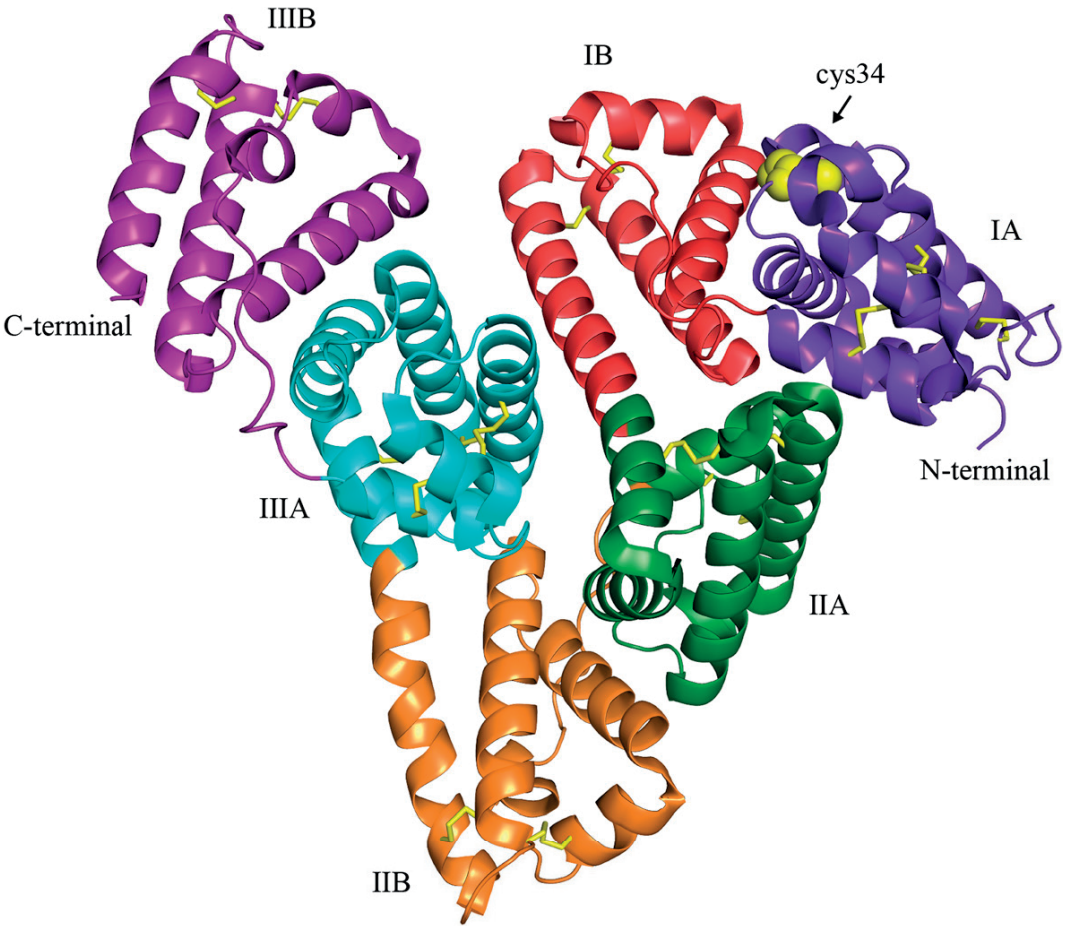

Figure 22. Crystal structure of human albumin. The illustration shows the tertiary structure of human albumin in complex with stearic acid (PDB: 1e7e). The three domains of albumin are shown in purple (IA), red (IB), green (IIA), orange (IIB), blue (IIIA), and violet (IIIB). Yellow sticks depicture disulfide bridges, and yellow spheres highlight the available Cys 34 in domain IA. Reprinted (open access) from [181], this article is available under the terms of CC-BY 4.0 license (https://creativecommons.org/licenses/by/4.0/).

1.3.2 Metabolism and receptors

The plasma concentration of albumin is the result of a sophisticated equilibrium among different synthesis, degradation and distribution mechanisms in the body. Albumin is produced in the liver in an amount of around 10-15 grams per day. A healthy person of 70 kilograms has approximately 360 grams of albumin, one third of which is located in the blood and the remaining is in the extravascular compartment. 80% of this second protein pool is distributed between muscles and skin. Several tissues daily catabolize an amount of albumin that is comparable to the produced one, and this leaves a maximum circulatory half-life of 19 days.[177,178,182]

The long half-life of albumin is mainly related to its structural properties and the ability to binding the neonatal Fc receptor. Molecular weight and net negative charge are the key properties that limit albumin renal elimination, while the pH-dependent recycling process mediated by the receptor avoids intracellular lysosomal degradation.[132] Mutagenesis and co-crystallization studies revealed that the binding site for FcRn is localized on domain III, and it does not overlap with the IgG binding site on the receptor. The residues important for the interaction with FcRn are four His, one in the FcRn (H166) and three on albumin (H464, H510 and H535), and four Trp in the FcRn (W51, W53, W59 and W61), revealing that the binding is both pH and hydrophobically driven.[183,184]

Interestingly, the FcRn receptor is also involved in the rescue of albumin from the glomerular filtration.[132,177] Every day, several kilograms of albumin passes through the kidney, but only three to six grams are filtered out in the glomerulus, with less than 1% that actually enters into the urine. Nearly all of this filtered fraction is recovered by the FcRn, which acts in the kidneys by a transcytosis process that transports albumin through the cytoplasm of the cells and releases it back into the blood.[132,177] In addition to FcRn, the megalin/cubilin complex is also involved in albumin reabsorption from renal excretion. Cubilin is a glycoprotein anchored to the membrane that lacks its own intracellular domains for endocytosis, which are added through an interaction with megalin. The resulting complex has high affinity for albumin and it is capable of performing the desired transcytosis process.[177,181]

In addition to these receptors, albumin can bind to three glycoprotein receptors (gp18, gp30 and gp60) also responsible for its recycling, degradation and intracellular transport.[177,181] Gp18 and gp30 are two receptors that display high affinity for the non-native or modified albumin, which is in this way internalized and degraded in the lyso-

somes. This suggests a specific role of these receptors as scavengers for old, denaturated and non-functional albumin and other proteins.[177,181] In contrast, gp60/albondin is a receptor that binds only the native albumin. It is mainly present in the vascular endothelium and takes part in the transcytosis process of albumin. Upon binding, the albumin-gp60 complex interacts with caveolin-1 and together they form vesicles assigned for the transport of albumin to the other side of the endothelial cells.[177,181]

All of these receptors contribute to albumin homeostasis and long half-life in humans, allowing it to take part in numerous physiological activities. The multitasking properties of albumin, in this way, are directly contrasted with other plasma proteins, which tend to exert a single specific function.[179]

1.3.3 Physiological functions

The main physiological role of albumin in the blood is to preserve the colloid osmotic pressure (COP). Molecular weight, high concentration and overall negative charge are critical for conserving and attracting water into the bloodstream, maintaining blood volume and pressure.[179,182] The presence of almost 200 charged residues in its sequence also determines its role as a pH plasma buffer, while the sulfhydryl group of Cys34 acts as antioxidant scavenger for several radicals. Other effects on the vascular structure and dilatation as well as on blood coagulation are documented.[179,182]

Another important function of albumin is its capacity of binding, and transporting, a broad range of endogenous and exogenous compounds in a covalent and non-covalent manner.[179] These compounds include therapeutic drugs, fatty acids, bilirubin, hemin, hormones, peptides, protein domains, metal ions, divalent cations, nitric oxide and many others.[178,179] Their ability to bind to albumin is often univocal and characterized by high affinity and binding site selectivity at low concentrations. Nevertheless, secondary unspecific binding sites are also present. All together, they modulate the solubility, metabolism and distribution of these ligands, affecting their pharmacokinetic profiles.[177,179]

Both covalent and non-covalent binding to albumin are nowadays widely exploited and they make it a suitable carrier for several different therapeutics. In particular, the capacity of albumin to extravasate from the bloodstream, reaching the lymphatic system and accumulating in cancerous or inflamed areas, arose a strong clinical interest for extending the half-life of peptides and oncology drugs using albumin as platform.[185]

1.3.4 Fusion or conjugation to albumin

Compared to PEGylation and Fc conjugation extension strategies, fusion to albumin (Fig. 23) gained a certain interest only in the 1990s, and so far a single drug based on this format reached the market.[117] Albiglutide (formely Albugon, Tanzeum (US) or Eperzam (EU), GSK) is composed of two copies of a DPP-4-resistant GLP-1 analogue genetically fused to human albumin, and is used to treat type 2 diabetes. The dimer was introduced to reduce the negative impact of the fusion on peptide's potency, and this dimeric format displayed the same effects as the native peptide in animal models. The conjugate has a half-life of five to seven days in human, which doubles that of the GLP-1 peptibody dulaglutide, allowing for once a week s.c. injection.[186]

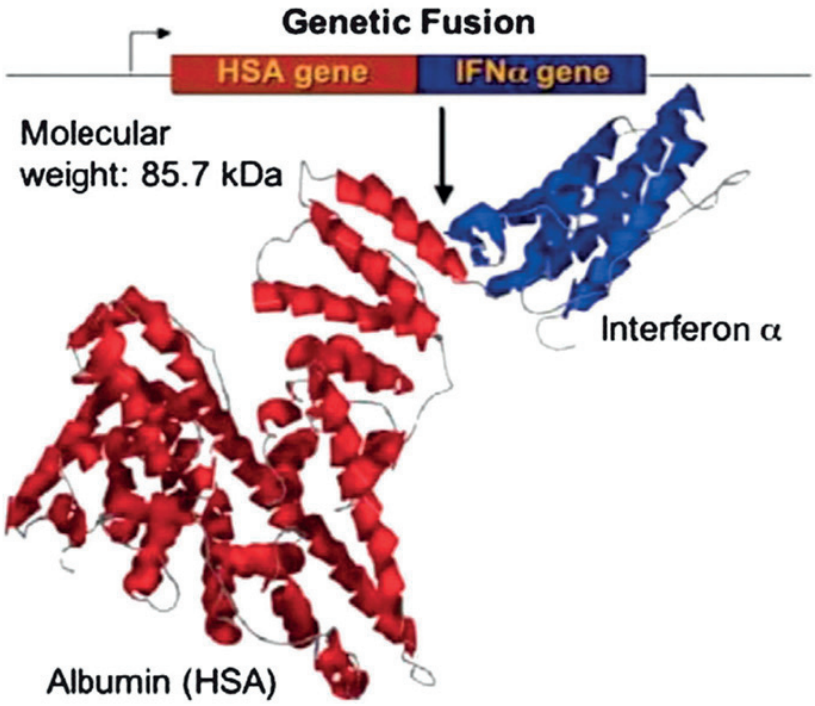

Figure 23. Genetic fusion to albumin. Schematic structure of a representative albumin fusion protein Albuferon. Adapted with permission from [187], reprinting license nr. 4047510754542, copyright © 2016 Royal Society of Chemistry.

There are currently several examples of peptides fused to the N- and C- termini of albumin (Tab. 6). However, the majority of fused products are still proteins, such as cytokines, coagulation factors and antibody fragments.[117] Among peptides, one interesting example consists on the genetic fusion to albumin of the B-type natriuretic peptide (BNP). The peptide was fused as a single copy at the N-terminus of human albumin, showing a strong loss in potency. Therefore, it was prepared as dimer to compensate the reduced activity. The final BNP construct showed a retained activity and an increased half-life in

mice, and improvements up to 200 to 400-fold were seen, depending on the route of administration.[188]

Insulin was also genetically fused to albumin. The two A and B chains of insulin, linked naturally by two disulfide bonds, were instead connected by a short linker and fused to the N-terminus of albumin as single-chain analogue. The resulting conjugate retained insulin activity and had an increased half-life of up to seven hours in mice.[189] Recently, a tandem copy of exendin-4 fused to albumin displayed a 90-fold longer half-life in monkeys compared to its native counterpart.[190]

When recombinant fusion is not possible, peptides can be covalently attached to albumin through chemical conjugation (Fig. 24). This technique mainly exploits either the free thiol group of Cys34 through maleimide coupling or non-specific modifications of the Lys residues present on the surface of albumin. Kratz and co-workers developed a new strategy for albumin conjugation either directly *in vivo*, called the Drug Affinity Complex (DAC™), or just before injection, known as Preformed Conjugate-Drug Affinity Complex (PC-DAC™). The rational behind this strategy was the linkage of drugs with reactive moieties that can covalently bind albumin in a site-specific manner.[185] This technique was successfully applied to numerous peptides. The most advanced drug is an exendin-4 maleimide derivative that was conjugated to albumin (CJC-1134-PC), and showed an increased half-life to approximately eight days in human upon s.c. administration.[191] Another group conjugated an analogue of enfuvirtide, a 36 amino acids linear peptide inhibitor of HIV-1 fusion, to albumin, exploiting maleimide as thiol reactive group. The final albumin conjugate had a half-life between nine to 15-fold longer in monkeys and rats, respectively.[192]

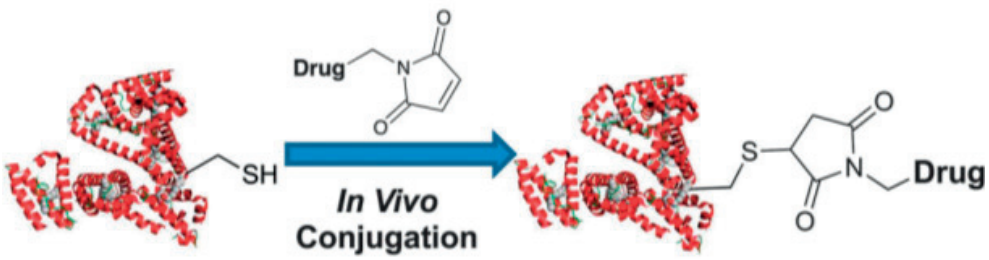

Figure 24. Chemical conjugation to albumin. Schematic description of *in vivo* thiol–maleimide conjugation. Adapted with permission from [187], reprinting license nr. 4047510754542, copyright © 2016 Royal Society of Chemistry.

Different criteria are used to determine the most suitable strategy to apply for peptides between fusion and conjugation to albumin, such as applicability to drug pipeline, site of modification, expression system and other manufacturing considerations.

However, both options are more versatile than Fc fusion proteins and solve some of their previously discussed limitations (sub-section 1.2.3). The monomeric structure of albumin and the absence of glycosylation sites facilitate the recombinant production in non-mammalian cells, provide an easier purification, and ensure the homogeneity of the products.[93] More accessible modification sites, usually far from each other in the sequence, allow for an easier creation of bispecific conjugates with reduced risks of cross-reactivity.[193–195] The absence of effector functions reduces unwanted activation of the immune system, while the smaller size allows for a higher tissue penetration.[185] Nevertheless, these covalent strategies with both IgGs and albumin still share some critical problems[117,133] that include:

i) limited parenteral routes of administration, mainly i.v. and s.c.;
ii) loss of activity of fusion partners due to steric hindrance, not always rescued using different linker length, flexibility/rigidity, and positioning;
iii) preparation of new therapeutic entities and drug formulations that could introduce immune responses against the native protein;
iv) candidates with low solubility and stability, and a high risk of aggregations, which are all potentially concomitant causes of immunogenicity,
v) lack of novelty and relatively difficult to covering with a patent.

The main disadvantages here underlined can be solved with smaller half-life extension platforms, as described in sub-sections 1.2.4 and 1.3.5.

Table 6. Peptide fusion or conjugation to albumin.

Cargo		Albumin		Factor	Ref.
Type	**$\tau_{1/2}$**	**Type**	**$\tau_{1/2}$**		
GLP-1 analogue (albiglutide)	1-1.5 hrs (s.c.)[a]	albumin fusion	5-7 d (s.c.)[a]	80-120[a]	123 186
B-type natriuretic peptide (BNP)	3 min (n.a.)[b]		11 hrs (i.v.)[b] 19 hrs (i.v.)[b]	220-380[b]	188
insulin (albulin)	n.a.		7 hrs (i.v., s.c.)[b]	- [b]	189
exendin-4 (E2HSA)	0.6 hrs (s.c.)[c]		53.4 (s.c.)[c]	89[c]	190
exendin-4 (CJC-1134-PC)	2.5 hrs (s.c.)[a]	albumin conjugation	8 d (s.c.)[a]	77[a]	125 191
enfuvirtide analogue (C34)	1.7 hrs (i.v.)[d] ≈11 hrs (i.v.)[c]		25.8 hrs (i.v.)[d] 102.4 hrs (i.v.)[c]	15[d] 9[c]	192

Half-life and factor of improvement were measured for human (a), mouse (b), monkey (c) and rat (d) species. n.a. = not available.

1.3.5 Non-covalent binding to albumin

As discussed in sub-section 1.2.4, the half-life of peptides in blood can also be prolonged by tethering them non-covalently to long-lived serum proteins, such as albumin. From a therapeutic point of view, the capacity of albumin to act as a non-covalent "taxi" for a huge plethora of exogenous and endogenous molecules can be exploited for prolonging the half-life of peptides.[93,160] The choice of a reversible binding strategy should allow an easy and efficient control of the fraction of active drug that still conserves a reasonable clearance time.[160] Characterization of the binding pockets of these molecules distributed in the three domains of albumin provides a solid base for the development of newly designed albumin-binding ligands to use as extension tags (Tab. 7).[177]

1.3.5.1 Albumin binding sites

In the 1970s, Sudlow and co-workers characterized the two most significant binding sites of albumin that are available for the interaction with a high number of compounds.[98,196] The Sudlow's site I, named warfarin-azapropazone binding site, is a pocket composed of the six helices of subdomain IIA. This binding site generally accomodates dicarboxilic acids and/or bulky heterocyclics carrying a central negative charge. It contains the only Trp residue of albumin (W214) and it is characterized by two clusters of polar residues, located at the bottom (Y150, H242 and R257) and at the entrance (K195, K199, R218 and R222) of the pocket. All ligands of the site I interact with the hydroxyl group of Y150, and they can potentially make two other hydrogen bonds with H242 and either K199 or R222 (Fig. 25a).[98,196]

The Sudlow's site II, also known as the benzodiazepine binding site, is similar to site I and it is composed of six helices of subdomain IIIA. It is smaller and less flexible than site I, and can discriminate ligands based on their size and stereoselectivity. Site II generally accommodates aromatic carboxylic acids with a peripheric negative charge that is located distantly from the hydrophobic center of the molecule. The pocket is again apolar with a single polar cluster located near the entrance (Y411, R410, K414 and S489). Ibuprofen and diazepam, the two main ligands of site II, recognize the hydroxyl group of Y411 while the other residues contribute to the formation of salt-bridges and hydrogen-bond interactions (Figure 25b).[98,196]

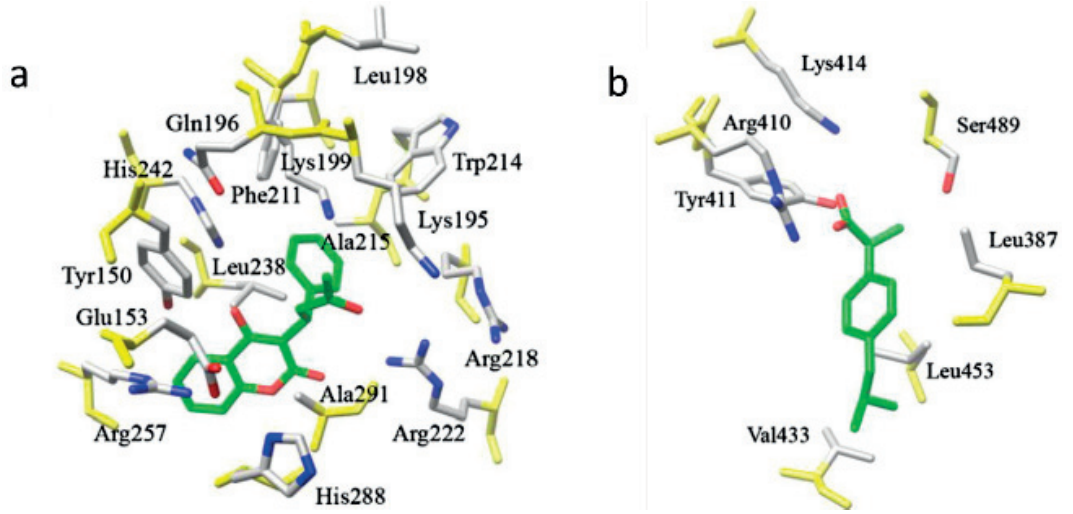

Figure 25. Schematic representation of (a) warfarin bound to Sudlow's site I, and (b) ibuprofen bound to-Sudlow's site II. Drug carbon atoms are colored in green and backbone atoms of the residues building up the sites are colored in yellow. Adapted with permission from [196], reprinting license nr. 4047530294372, copyright © 2010 Elsevier B.V. All rights reserved.

The two Sudlow's sites partially overlap with the binding pockets of the best known albumin ligand, namely fatty acids.[197] Fatty acids act in numerous metabolic processes, such as in the synthesis of cellular membranes, they function as hormones and secondary messengers, and they serve as a reservoir of energy. Fatty acids are composed of a medium-long carbon chain with a negatively charged carboxylic head at one end.[198] Flexible and straight fatty acids lacking carbon-carbon double bonds are defined as saturated. In contrast, the presence of one or multiple double bonds makes unsaturated fatty acids, which are further divided into cis or trans configurations. The double bond positions are indicated as ω (from methyl end) or Δ (from carboxylic end). Saturated myristic, palmitic and stearic acids with 14, 16 and 18 carbons, respectively, are the most common fatty acids found in animals and they are daily introduced with the diet.[198]

One mole of albumin usually transports up to two moles of fatty acids, shielding their hydrophobic character and strongly increasing their sub-micromolar solubility in plasma.[197] The fatty acid-binding properties of albumin were analyzed in the mid-1970s by Spector. With relatively limited information, he could review the presence of five binding sites for saturated and unsaturated fatty acids containing 6 to 18 carbons.[199] Each fatty acid binds the five sites with a different association constant (K_a), and a clear correlation between the length of the side chain and the affinity was reported. Short-medium fatty acids (6 to 12 carbons) bound albumin with K_d values between 60 and 0.5 μM, while the longest ones (14 to 18 carbons) had ten-fold higher affinities for albumin (K_d values

below 50 nM).[199] The high binding affinity of the myristic acid (C14) for human albumin was recently confirmed by Kragh-Hansen *et al.*.[200]

The position of these binding sites was revealed by Curry and co-workers who crystalized albumin in complex with five saturated fatty acids containing 10 to 18 carbons. They showed that fatty acids can bind up to seven different binding sites on albumin, and the shortest one with 10 carbons had two additional binding pockets (Fig. 26).[197] The common binding sites are distributed in the three domains as follows: site 1 in subdomain IB, site 2 at the interface between subdomains IA and IIA, site 3 and 4 in subdomain IIIA (Sudlow's drug-binding site II), site 5 in subdomain IIIB, site 6 at the interface between subdomains IIA and IIB, and site 7 in subdomain IIA (Sudlow's drug-binding site I). Equal mechanisms of binding were observed for the first five sites, with the carboxylic acid interacting with basic and polar residues independently from the length of the chain and the size of the hydrophobic cavities. In contrast, the acid moiety does not play a role in the binding sites 6 and 7, which then consist solely of a hydrophobic binding pocket.[197]

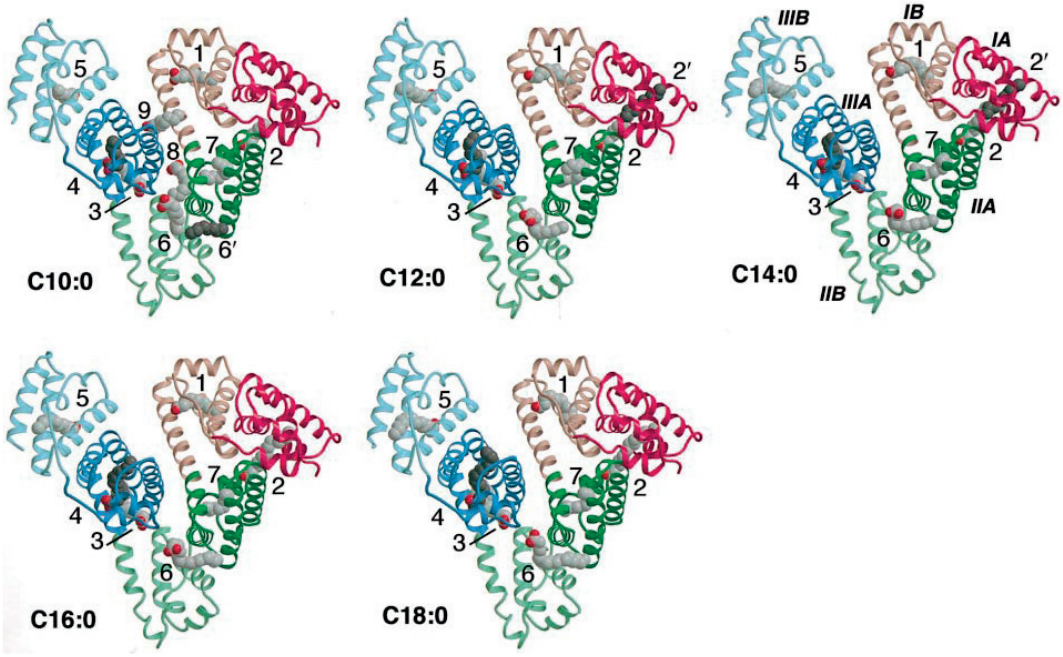

Figure 26. Structures of albumin complexed with five different fatty acids. The protein secondary structure is shown schematically and the domains are color-coded as follows: I, red; II, green, III, blue. The A and B sub-domains are depicted in dark and light shades, respectively. Bound fatty acids are shown in a space-filling representation and colored by atom type (carbon, grey; oxygen, red). Reprinted with permission from [197], reprinting license nr. 4047530712891, copyright © 2000 Academic Press. All rights reserved.

1.3.5.2 Albumin-binding ligands

Fatty acids are the most exploited endogenous ligand of albumin used for half-life extension. So far, the lipidation of peptides was the only non-covalent strategy that has led to the development of three approved drugs. These peptide drugs are insulin and GLP-1 derivatives currently on the market for the treatment of type 1 or 2 diabetes and obesity: insulin detemir (Levemir, Novo Nordisk), liraglutide (Victoza, Novo Nordisk) and insulin deglutec (Tresiba, Novo Nordisk).[99] Lipidated peptides approved or under investigation and relative limitations will be described in the sub-sections 1.3.6 and 1.3.8.

Other endogenous molecules used as albumin binders are bile acids. When conjugated to insulin, they showed a certain degree of affinity for albumin and formed s.c. deposits that were gradually released in the blood, displaying a glucose-control activity longer than 24 hours in pigs.[201] However, both fatty acids and bile acids show relative weak affinities for albumin and low solubilities that severely limited their application to several peptide drugs.[99,202]

Organic binding moieties structurally similar to exogenous drugs (e.g. warfarin, ibruprofen and diazepam) have been also generated for non-covalent interactions with albumin. Genentech coupled several organic compounds, based on sulfonamide or phosphate ester moieties, to a peptide inhibitor of the coagulation factor VIIa.[202,203] The best conjugate could tightly bind albumin and improved the *in vivo* half-life up to 46-fold in rabbits.[203]

Other albumin ligands resembling the structures of fatty acids or small molecules have been identified by Neri and co-workers from the screening of DNA encoded chemical libraries.[204,205] Even though sub-nanomolar albumin binders have been recently isolated from these libraries, only a few 4-(p-iodophenyl) butyric acid derivatives were so far characterized *in vivo*.[204] The best molecule had a high nanomolar affinity for human albumin, and could efficiently prolong the half-life of small molecules or recombinant proteins.[204,206,207] The attachment of this molecule to two contrast agents increased their half-life of approximately 50 to 100-fold in mice.[204] This compound was also conjugated to a tumor-targeting ligand, composed of folic acid and DOTA chelator, and to an engineered scFv antibody fragment, translating into longer half-lives and higher tumor uptake in mice models.[206,207]

Alternatively to small molecules, an increasing number of peptides and protein domains have been used as albumin-binding molecules. A few peptides were isolated from phage selection against albumin, but only one of them exhibited a binding affinity suitable

for *in vivo* experiments.[208,209] Dennis *et al.* developed a cyclic peptide, named SA21, which was fused to a Fab fragment and prolonged its half-life more than 25 times in rabbits and mice.[208] The peptide was later applied to other small proteins and it showed promising preclinical results.[210,211] The development of SA21, its conjugation to a bicyclic peptide and the related issues experienced in our laboratory will be further discussed in the sub-sections 1.3.7 and 1.3.8.

Several albumin-binding domains (ABDs) were discovered in bacterial proteins. So far, the best characterized ABD derives from the streptococcal G protein G148-GA3, which is actually composed of three IgG and three albumin binding domains.[212] The affinity for albumin of one of the three ABDs was strongly improved by phage display and rational design, reaching K_d values in the femtomolar range for human albumin.[213] Despite a relatively small size (46 amino acid, 5110 Da), this high-affinity ABD variant (ABD035) positively impacted on the pharmacokinetics of various proteins at which it was recombinantly fused.[214–217] In contrast with the results obtained using fatty acids or albumin-binding peptides[218,219], the capacity of ABD of prolonging the half-life of conjugates does not correlate with increased binding affinities for albumin, suggesting an intrinsic limit connected to either the FcRn-mediated recycling or albumin half-life.[220]

In a recent study, Levy *et al.* compared two exendin-4 conjugates obtained by appending to its C-terminus either the optimized ABD035 (46 residues) or a shorter version of the peptide SA21 (11 residues).[221] Exendin-4 modified with SA21 had a ten-fold higher potency than the ABD variant, probably related to a different steric hindrance that played a bigger role in the ABD conjugate with the highest affinity for albumin. In contrast, a much weaker binding affinity of SA21 for albumin strongly impacted on conjugates' pharmacokinetics in monkeys, and gave half-lives of two and 14 days for SA21 and ABD variants, respectively, counterbalancing the reduction in activity.[221]

A more recent trend is the development of albumin-binding antibodies. Phage display selections against albumin led to the isolation of fully human domain antibodies (AlbudAbs) with a high binding affinity for albumin and half-lives similar to that of albumin itself ($\tau_{1/2}$ = 24 vs. 35 hrs of mouse albumin; $\tau_{1/2}$ = 43-53 vs. 53 hrs of rat albumin).[222] This platform was already applied to exendin-4, creating a molecule (GSK2374697) that had a half-life from six to ten days in a phase 1 trial in human.[223] Similarly, scFvs and nanobodies (fragments based on the variable domains of camelid heavy chain antibodies) were also developed as albumin binders with promising results.[224–226]

Table 7. Conjugation to albumin-binding molecules.

Cargo		Albumin-binding molecule	Conjugate		Factor	Ref.
Type	**$\tau_{1/2}$**		**Affinity**	**$\tau_{1/2}$**		
insulin (peptide)	2.3 hrs (s.c.)[a]	myristic acid	4.2 μM[a]	5-7 hrs (s.c.)[a]	2-3[a]	99 111 227 228
		γ glu-hexadecenoic diacid	1.8 μM[a]	25 hrs (s.c.)[a]	11[a]	
GLP-1 (peptide)	1-1.5 hrs (s.c.)[a]	γ glu-palmitic acid	n.a.	11-15 hrs (s.c.)[a]	7-15[a]	99 123
insulin (peptide)	n.a.	cholic acid derivatives	13 μM[a]	n.a.	-	201
fVIIa inhibitor (peptide)	7.6 min (i.v.)[b]	naphthalene acyl-sulfonamide	n.a.	30 min (i.v.)[b]	4[b]	202
	4.8 min (i.v.)[b]	diphenylcyclo-hexa-nol phosphate ester	n.a.	222 min (i.v.)[b]	46[b]	203
fluorescein (chemical)	4.6 min (i.v.)[c]	6-(4-(p-iodophenyl) butanamido) hexanoate	108-330 nM[a]	495 min (i.v.)[c]	108[c]	204
Gd-DTPA (chemical)	8.6 min (i.v.)[c]		3.3 μM[a]	408 min (i.v.)[c]	47[c]	
scFv (protein)	20-30 min (i.v.)[c]		3.2, 3.6 μM[a,c]	16.6 hrs (i.v.)[c]	33-50[c]	206
Fab (protein)	53 min (i.v.)[b]	SA21 467, 320, 7, 266 nM[a,b,c,d]	Similar to SA21[b]	32.4 hrs (i.v.)[b]	37[b]	208
	24 min (i.v.)[c]			10.4 hrs (i.v.)[c]	26[c]	
UK18 (peptide)	30 min (i.v.)[c]		321-354 nM[a] 14-24 nM[c]	24-27 hrs (i.v.)[c]	48-54[c]	71
exendin-4 (peptide)	30 min (i.v.)[d]		1560, 210, 610 nM[a,d,e]	11 hrs (i.v.)[d] 2 d (i.v.)[e]	22[d] - [e]	221
		ABD035 16, 18, 123 pM[a,d,e]	5, 8, 40 pM[a,d,e]	16 hrs (i.v.)[d] 14 d (i.v.)[e]	32[d] - [e]	
	2.5 hrs (s.c.)[a]	AlbudAbs	34-600 nM[a,c,d]	6-10 d (s.c.)[a]	58-96[a]	222 223
anti-IL-6R (nanobody)	4.3 hrs (i.v.)[e]	nanobody	22 nM[a]	5-6.6 d (i.v.)[e]	28-37[e]	224
Fab (protein)	0.5 hrs (i.v.)[c]	scFv	5, 162, 7, 3, 54 nM[a,b,c,d,e]	84.2 hrs (i.v.)[c]	168[c]	225
Fab (protein)	1.8-4 hrs (i.v.)[c] n.a.	scFv	3, 4, 3 nM[a,c,e]	62 hrs (i.v.)[c] 8 d (i.v.)[e]	16-34[c] - [e]	226

Half-life, affinity and factor of improvement were measured for human (a), rabbit (b), mouse (c), rat (d) and monkey (e) species. n.a. = not available.

1.3.6 Lipidation of peptides

The physiological metabolism of fatty acids as well as their ability to bind albumin with a high affinity inspired the use of post-translational acylation as a safe and natural platform for prolonging the half-life and the mode of action of peptides and small proteins. So far, this strategy was successfully exploited by the Danish pharma company Novo Nordisk that launched three acylated peptide drugs on the market for the treatment of diabetes and obesity.[99]

Kurtzhals *et al.* pioneered the development of the first clinically available acylated insulin analogue in 1995.[227] Lys29 in the B chain of insulin was conjugated to different saturated fatty acids (10-16 carbons), and Thr30 was removed. The insulin analogue carrying the C14 myristic acid [Lys^{B29}-tetradecanoyl des(B30) insulin] bound albumin with K_d values of 4.2 and 10 μM at 25°C and 37°C, respectively, which was two to three orders of magnitude lower than free fatty acids (Fig. 27a). Subcutaneous injection of this C14 conjugate in rabbits resulted in a prolonged effect on blood-glucose levels.[227] Similar results were confirmed in pig experiments and showed an important correlation between binding affinity for albumin and *in vivo* half-life.[218] In addition, its binding affinity was unaffected by the co-presence of potential competitors, such as free fatty acids and several well-known albumin-binding drugs.[229] This myristoylated insulin analogue was approved in 2004 as insulin detemir (Levemir) for the treatment of type 1 diabetes. The drug has a half-life of five to seven hours upon s.c. injection in human, which is 50 to 100-fold longer than insulin alone in blood (four to six minutes, i.v.; 2.3 hours, s.c.)[110,111], allowing either once or twice-daily dosing.[230] The half-life prolongation is not exclusively related to its ability to bind albumin in blood circulation, but is also associated with the route of administration and the formulation. In presence of phenol and Zn^{2+}, insulin detemir self-assembles into hexameric–dihexameric units, protracting its blood absorption from the subcutaneous deposit site.[231]

Ten years later, Jonassen *et al.* developed a longer-acting acylated insulin for once-daily injection.[228] The new insulin analogue, approved as insulin degludec (Tresiba), conjugated a longer 16 carbons dicarboxylic fatty acid to the LysB29 through a γ-Glu linker, thus introducing two net negative charges (Fig. 27c) that led to improved affinity and solubility. Insulin deglutec has a 2.4-fold stronger affinity for albumin than insulin detemir at 25°C, and a much larger oligomerization upon s.c. injection thanks to the terminal carboxylic acid.[228] These changes resulted in a half-life of 25 hours in humans and a glucose-lowering effect that persisted for more than 42 hours, giving one the

best pharmacokinetic and pharmacodynamic profiles among the currently approved insulin formulations.[232]

As broadly reported in the previous section, the improvement of the GLP-1 half-life is of great interest and several extension platforms have been successfully applied. Acylation also led to the approval of liraglutide (Victoza) in 2009, a once-daily GLP-1 analogue used in the treatment of type 2 diabetes and later obesity.[123] Knudsen *et al.* performed a structure-activity relationship (SAR) study of 36 acylated analogues of GLP-1, varying i) peptide sequence, ii) site of modification, iii) fatty acid, and iv) linker. Several derivatives were equipotent or better than GLP-1, and showed a more than ten-fold prolonged half-life in pigs upon s.c. injection.[123] Among them, the future liraglutide retained the potency of GLP-1 and resulted in promising pre-clinical studies in animals. The final structure is composed of GLP-1 conjugated to Lys26 with a 16-carbon palmitic acid via a γ-Glu linker, and with the Lys34 replaced by Arg (Fig. 27b).[233] A direct measurement of its affinity has not been performed, but dialysis studies confirmed a strong albumin binding.[234] The half-life in human has been calculated as eight hours and 11-15 hours upon i.v. and s.c. injection, respectively, a remarkable improvement compared to the native GLP-1 (1.5 minutes, i.v.; 1-1.5 hours, s.c.).[123,235] As with insulin analogues, the long half-life of liraglutide is also related to self-association with a slow release from the site of injection. In addition to this, a reduced susceptibility to enzyme degradation was noted, probably due to an albumin protective effect upon binding.[235]

These positive results stimulated research into new variants of insulin and GLP-1, and expanded the acylation strategy towards other peptides. Recently, Novo Nordisk developed a new analogue of GLP-1, semaglutide, and the documents for its approval have been recently submitted to the FDA.[236] Starting from the sequence of liraglutide and applying the same criteria of optimization, Lau *et al.* synthesized 45 new variants. They tested i) longer fatty acids or diacids, as done with insulin deglutec, ii) different linkers between Lys26 and fatty acids, and iii) new amino acid substitutions for increasing the enzymatic stability against DDP-4.[237] The selected candidate semaglutide was modified at Lys26 with a octadecanoic diacid (18 carbons and two carboxylic acids) through a long linker composed of two 8-amino-3,6-dioxaoctanoic acid (O2Oc) units and a γ-Glu (Fig. 27d). It also has Ala8 substituted by the unnatural amino acid 2-aminoisobutyric acid. By applying only these few modifications, semaglutide displayed much better properties than liraglutide, similarly to what has been already observed with insulin detemir and insulin deglutec. Despite a lower binding for the receptor, the potency of semaglutide was still equivalent to GLP-1 and liraglutide. Its binding affinity for albumin was six-fold

stronger than liraglutide providing semaglutide with a four-fold longer half-life in pigs upon i.v. injection, and a 48 hour lowering-effect on blood glucose in mice after s.c administration.[237] In humans semaglutide showed a half-life of 155-185 hours, ten and 100-fold longer than liraglutide and GLP-1, respectively, allowing once weekly s.c. dosing.[238]

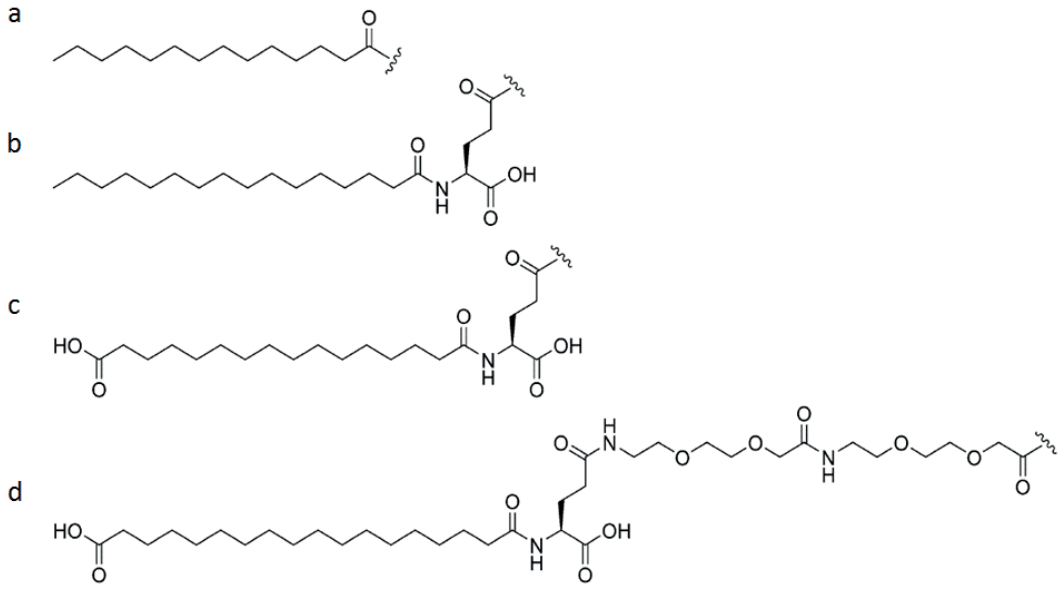

Figure 27. Examples of lipid moieties used for half-life extension of biopharmaceuticals. (a) Myristic acid (insulin detemir). (b) Palmitic acid linked to a γ-Glu linker (liraglutide). (c) Hexadecanoic diacid with a γ-Glu linker (insulin degludec). (d) Octadecanoic diacid coupled to a linker consisting of γ-Glu and two 8-amino-3,6-dioxaoctanoic acid units (semaglutide). Reprinted with permission from [99], reprinting license nr. 4047140757234, copyright © 2016 Wiley-VCH Verlag GmbH & Co. KGaA, Weinheim.

Several other peptides were modified with acylated moieties and showed promising pre-clinical results. A pancreatic polypeptide was modified with the γ-glu-C16 fatty acid moiety used in liraglutide. It exhibited retained *in vitro* stability and affinity for the receptor, and a seven-fold longer half-life in rats upon i.v. injection.[239] Insulin end exendin-4 were modified with a 16-carbon hexadecanoic acid terminating in a sulfonate anion. The derivatives had better affinity for albumin and much higher solubility than insulin detemir. This translated into five to ten-fold prolonged glucose-lowering effects in mice after both i.v. and s.c. administration.[240] The same acylated motif used for semaglutide was also applied to insulin on Lys22, increasing the number of fatty acid carbons to 22. The resulting conjugate, called insulin-327, showed interesting liver-specific effects in dogs and a prolonged half-life.[241] Several other lipidated peptides and small proteins were differently acylated, such as neuromedin U, a GLP-1/GIP co-agonist, calcitonin, oxyntomodulin, human growth hormone and others, providing derivatives with enhanced pharmacokinetic profiles.[99]

Finally, an innovative combination of fatty acids and glyco moieties was recently proposed by Jensen and co-workers for extending the half-life of GLP-1.[242] The improved backbone of liraglutide was conserved and Lys26 was modified with one or two units of mucic acid, a galactose derivative, linked to three different fatty acids via a γ-Glu linker. All of the new conjugates had activity and solubility in the same range of GLP-1 and liraglutide, and could form oligomers as well. The apparent binding affinities for albumin were approximately 1-2.5 μM for all of the glycolipidated peptides, equivalent to what they measured for liraglutide, and this translated into comparable *in vivo* pharmacological effects after s.c. dosing in mice.[242]

1.3.7 Albumin-binding peptides

Albumin is known to bind not only low molecular weight molecules but also peptides and proteins, such as insulin, bradykinin and interferons, and several hundreds of other binders were identified or predicted.[243,244] This observation suggested the application of *in vitro* techniques for the screening of peptides that can bind albumin with a high affinity and can be used as carriers for half-life extension.[208,209] Differently from chemical small moieties, albumin-binding peptides can be easily fused to any protein or peptide, either recombinantly or chemically during solid-phase synthesis.[160]

Towards this goal, in 2002 Dennis *et al.* used phage display to isolate peptides, with two fixed Cys residues and varying loop sizes, that bind albumin with high affinity.[208] They selected several disulfide cyclized binders for rabbit, rat and human albumin, and a clone sharing a high binding for all of the three species was further subjected to affinity maturation. The best albumin binder was an 18 amino acid peptide called SA21 (Ac-RLIEDI<u>C</u>LPRWG<u>C</u>LWEDD-NH_2). The selected peptide bound albumin from different species with affinities of 7 ± 2 nM (mouse), 266 ± 8 nM (rat), 320 ± 22 nM (rabbit), and 467 ± 47 nM (human). The pharmacokinetics of SA21 alone was tested in rabbits upon i.v. injection, and showed an 18-fold prolonged half-life compared to an unrelated control peptide. The fusion of SA21 to the C-terminus of a Fab antibody fragment efficiently prolonged the half-life of the protein up to 37-fold in rabbits and 26-fold in mice after i.v. administration.[208] The importance of developing high-affinity peptide binders was confirmed in a following study where SA21 variants with weaker binding for albumin were prepared and fused to a Fab fragment.[219] The different conjugates showed a five to ten-fold reduced binding affinity for albumin and this correlated with two to three times shorter half-lives, confirming the results obtained in previous studies with different fatty acid-modified insulin analogues.[218,219]

The capacity of SA21 to improve the half-life of bicyclic peptides was recently investigated in our laboratory. Through the chemical conjugation of SA21 to UK18, Heinis and co-workers proved that a non-covalent binding to albumin could improve both pharmacokinetic and metabolic characteristics of peptide conjugates without affecting their activity (Fig. 28).[71] They demonstrated that the chemical conjugation did not interfere with the binding towards the corresponding protein targets, retained for both SA21 and UK18. Experiments in mice showed a prolonged circulation time of the bicyclic peptide from 30 minutes to 24 hours after i.v. dosing, and the conjugate remained fully intact and functional for more than 48 hours.[71] In a second study, they showed that the same conjugate distributed into tumor tissues in high concentrations, not limited by the high affinity of SA21 for the endogenous murine albumin.[245]

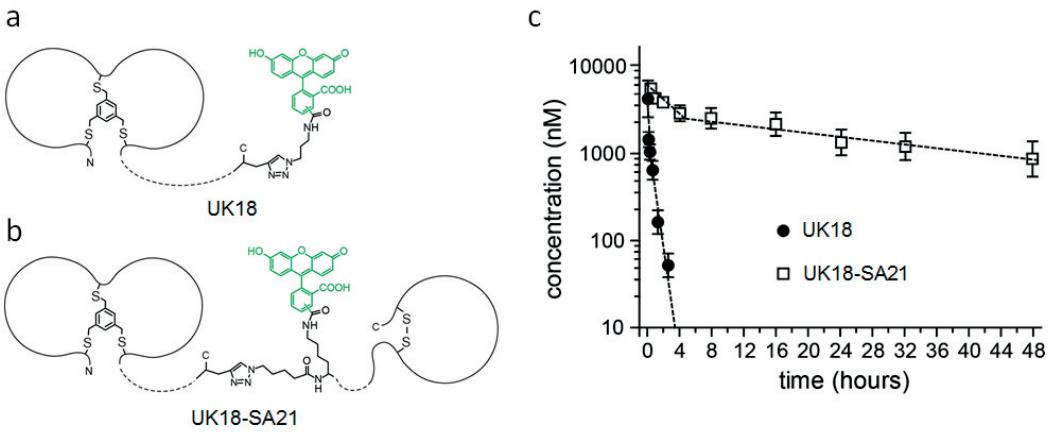

Figure 28. Schematic drawing of (a) UK18 and (b) UK18-SA21. Key chemical structures such as the mesitylene molecule TBMB in the bicyclic peptide, the disulfide bridge in the albumin binding peptide, the triazole linker, and the fluorescein (highlighted in green) are shown. (c) Concentration of UK18 and UK18-SA21 in murine blood upon i.v. injection. Compounds were applied intravenously, blood samples were taken at the indicated time points, and the concentration of conjugate was measured by UFLC and/or ELISA. Adapted with permission from [71], copyright © 2012 American Chemical Society.

1.3.8 Limitations of albumin-binding ligands

The use of non-covalent albumin-binding ligands based on fatty acids or peptides is a great technique for extending the half-life of peptides.[93,99,160] However, previously reported examples reveal some serious limitations, concerning their binding properties, solubility, and ease of synthesis, that must be taken into consideration for future applications. In order to give these techniques mainstream relevance, insights into the development of newly improved albumin-binding ligands should be envisioned to maximize

their biochemical properties and minimize the production steps. All of the current investigations into this area indicate that researchers are aware of this, and strong improvements are needed for competing with high affinity protein-based albumin binders.[213,222]

First, both albumin-binding ligands based on fatty acids or peptides have a relatively low affinity for human albumin that does not allow a full exploitation of these techniques. Fatty acids, upon coupling to peptides, bind to albumin with an approximately 100- to 1000-fold weaker affinity compared to their free forms.[200,227] There is also a problem that can occur with testing albumin binders in species other than humans, such as for the cyclic peptide SA21. This compound has a lower affinity for human albumin compared to other species, which will result in a shorter half-life of the conjugates in human plasma compared to the measured values in rat and mouse.[208,221] A few minor modifications to either fatty acids or peptides could have a strong positive impact on their binding affinity and, thus, pharmacokinetics profiles. For example, these effects could be achieved for i) fatty acids, by introducing negative moieties close to the hydrophobic chain to replace the carboxylic acid lost in the coupling,[99,228,237,242] and for ii) peptides, by applying *in vitro* evolution screenings with either innovative combinatorial libraries or molecule formats based on known albumin ligands.[54,58,60]

Second, these conjugates often show a low solubility that limits the final concentration that can be applied in patients. The high lipophilicity of fatty acids is known to negatively affect the solubility of acylated derivatives.[202] The cyclic peptide SA21 also has a poor solubility in physiological buffers caused by the presence of many hydrophobic amino acids.[208] Its conjugation to several bicyclic peptides resulted in final products with strongly impaired solubility (unpublished data). However, recent successful examples reported in literature of acylated peptides variants with one or more negative charges as enhancers (e.g. diacids or hydrophilic linkers) display an improved aqueous solubility.[99] A higher peptide solubility can also be achieved by shortening the sequence and replacing hydrophobic residues not involved in the binding.

Third, the preparation of these conjugates often involves difficult synthetic processes. The syntheses of either very long conjugates (> 30-40 coupling reactions)[221] or separated bioactive components[71,245], which often require orthogonal protecting groups, need sequential steps of purification and coupling, therefore making this conjugation time consuming and very expensive. For example, the acylation of peptides is typically performed by fatty acid modification of the Nε-amine of Lys side chains or the N-terminus, and this modification can take place either in solution or on resin.[99] When done on resin, acylation is quite straightforward and the fatty acid can be coupled selectively during

SPPS. Usually, a single step of purification is enough to get the desired product. In contrast, acylation in solution is more demanding. It often results in heterogenous mixtures and requires multiple purification steps which affect the overall yield.[99] Similarly to this second aspect, modification of peptides with complex albumin-binding molecules, such as SA21, introduces some synthetic issues. For example, SA21 has a long sequence with a disulfide bridge that complicates the direct conjugation to peptides on resin and greatly reduces the yield due to the multiple steps of purification needed (Fig. 29).[208] Easier synthesis of the conjugates can be achieved by shortening the peptide for simpler attachment during SPPS, removing unwanted disulfide bridges, and/or using specific residues carrying orthogonal protecting groups when modifications on resin are required.

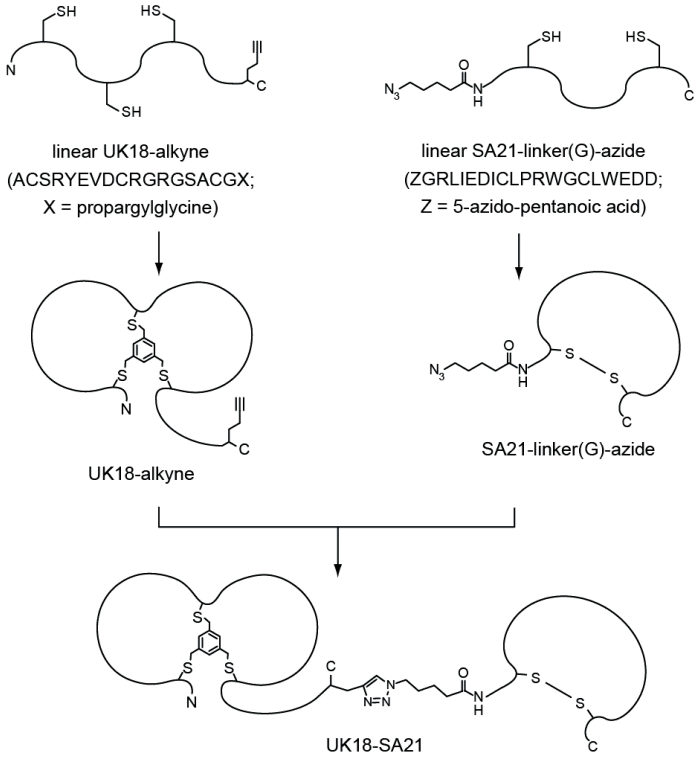

Figure 29. Synthesis of UK18-SA21. UK18 was synthesized with a C-terminal alkyne group (propargylglycine linked to UK18). SA21 was synthesized with an N-terminal azide group (5-azido-pentanoic acid linked via a Gly linker to SA21). The UK18 derivative was cyclized by reaction with TBMB and the SA21 derivative was cyclized by oxidation. The two fragments were linked together by Huisgen cycloaddition. Reprinted with permission from [245], reprinting license nr. 4052131274235, copyright © 2015 American Association for Cancer Research.

As a solution to these problems of currently existing albumin binding ligands, the research project presented in this thesis combines the excellent albumin binding properties of fatty acids and our expertise in the rational evolution of peptide affinities. The goal is to solve the problems discussed for both acylation and peptide-based extension strategies through a fusion of the two techniques.

2. Aim of the project

Peptides applied intravenously suffer from a rapid clearance from the blood circulation by renal filtration. Their exceptionally short half-life prevents the application to diseases that require prolonged drug exposure.[93] Several strategies have been applied to extend the *in vivo* half-life of peptides, including fusion to long-lived serum proteins, PEGylation and conjugation to albumin-binding molecules.[93,99,117] The latest strategy is particularly attractive as it does not significantly increase the size of peptides. However, existing molecules or peptides binding to albumin present relatively weak affinities, low solubility in physiological buffers, and difficult synthesis of the conjugates.[202,204,208,227]

The first goal of this research project was the development of an albumin-binding tag more in line with our needs, taking into consideration the previously mentioned limitations. Specifically, I aimed to engineering a ligand that presents:

i) high affinity for human albumin in the low-medium nanomolar range (< 50 nM);
ii) small format for an easy and economic synthesis of therapeutic conjugates;
iii) high solubility of resulting conjugates in physiologic solutions (> 1 mg·ml^{-1}).

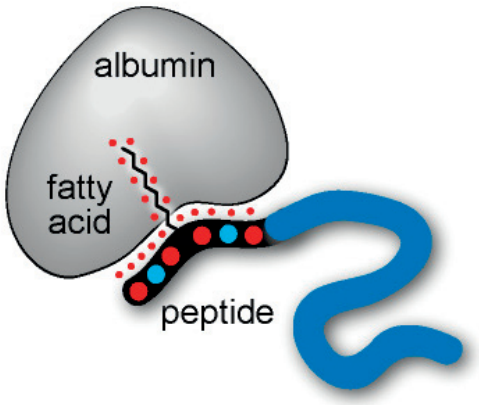

Figure 30. Schematic representation of a bioactive peptide (in blue) modified with a peptide-fatty acid chimera. Interactions involved in the binding from both fatty acid and peptide are shown as red dots.

Towards this end, I conceived the ligand design shown in Figure 30 in which a fatty acid is conjugated to a short peptide, both parts interacting with human albumin. While fatty acids are reported to bind albumin with a certain affinity (K_d values between 2 to 5 μM upon conjugation to peptides)[227,228], a random peptide does not. Therefore, a suitable amino acid sequence needs to be evolved in order to form additional contacts and thus increase the binding affinity of the chimera for albumin.

Since a high affinity was expected to translate into a prolonged half-life [218,219], as secondary goal I conjugated the developed albumin-binding tag to three bioactive bicyclic peptides and checked their pharmacokinetic profiles in different animal models.

3. Results and discussion

3.1 - Development of a high affinity albumin-binding tag

Towards the development of a high affinity peptide-fatty acid tag, in a first step I established an efficient synthetic strategy for the preparation of this molecule format by automated solid-phase peptide synthesis (SPPS). An optimized procedure was required for the straightforward and economic synthesis of several peptide-fatty acid variants that were later screened for albumin binding. Another aim of this step was the identification of a fatty acid that could efficiently bind albumin in the context of the new format. In a second step, I tested the solubility in aqueous solution of the peptide-fatty acid tag coupled to two different bicyclic peptides. In a third step, I evolved the sequence of the peptide through iterative rounds of synthesis and affinity testing by applying as screening methodology a fluorescence polarization assay against human albumin. Fourth, I characterized the binding of the optimized tag for rat albumin and in human serum. Finally, I confirmed its binding affinity for albumin by isothermal titration calorimetry.

3.1.1 Synthesis and albumin binding of a peptide modified with different fatty acids

A strategy was developed for the automated synthesis of linear peptides carrying a fatty acid modification at an amino acid side chain. The selected peptide format had a 7-mer sequence H-XXXKXXX-NH_2, with the amine side chain of Lys (K) orthogonally protected with a Dde (1-(4,4-dimethyl-2,6-dioxycyclohex-1-ylidene)ethyl) group, and X was any possible amino acid. A short PEG_2 linker was added at the N-terminus and coupled with fluorescein (F) to enable the measurement of the binding affinity for albumin by fluorescence polarization. The central Lys(Dde) residue was selectively deprotected with 2% hydrazine, and the free amine was reacted with the carboxylic head of a fatty acid to form an amide bond (Fig. 31). The described procedure was fully automated for the synthesis of peptide-fatty acid variants on a standard peptide synthesizer.

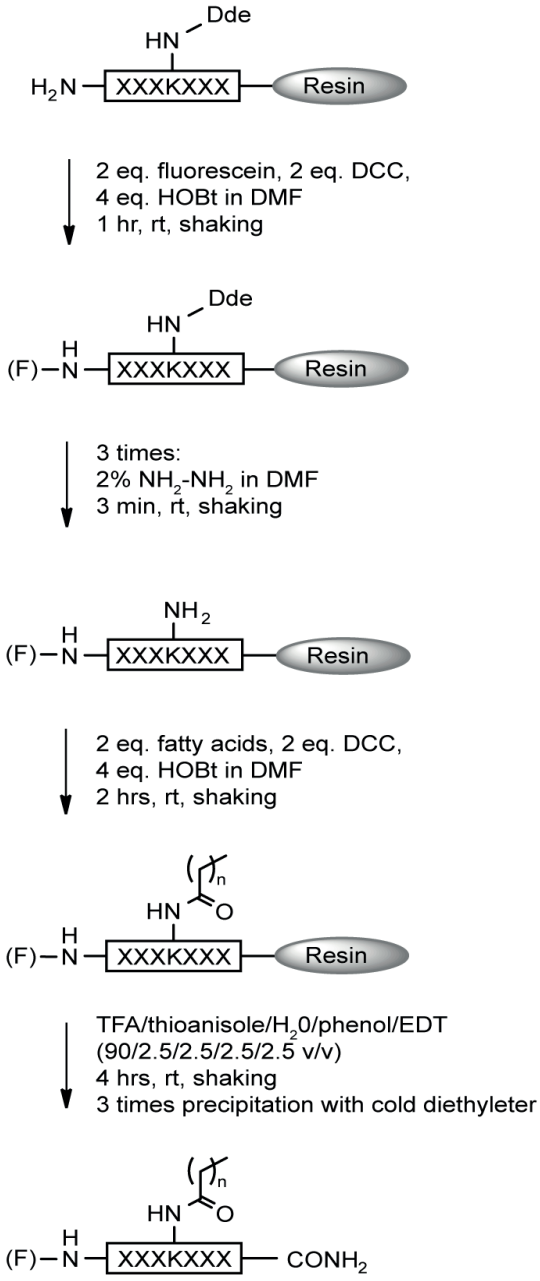

Figure 31. General scheme for the synthesis of a peptide-fatty acid tag. X represents any amino acid; (F) is fluorescein, ▬ (dash) between (F) and N-terminus is PEG_2.

Peptide cleavage from the resin and side chain deprotection were carried out in standard acidic conditions, and the crude products purified by HPLC. The short length of the linear peptides allowed for syntheses with minimal side products and efficient purifications, as confirmed by mass spectrometry and analytical HPLC (Fig. 32). A typical yield for a small-scale synthesis (0.03 mmol) was approximately 60-70% of the expected amount that was calculated considering a maximal efficiency for each coupling step, fluorescein and fatty acids included.

Once established the synthesis, the binding affinity of the peptide-fatty acid tag for human albumin was tested using the sequence (F)-PEG_2-SSSKSSS-NH_2 (Fig. 32a) modified at the Lys side chain with either one of the three most abundant fatty acids present in human blood (myristic, palmitic or stearic; Fig. 32b-d, respectively).[198] The initial sequence was based on six hydrophilic Ser residues mainly for solubility purposes.

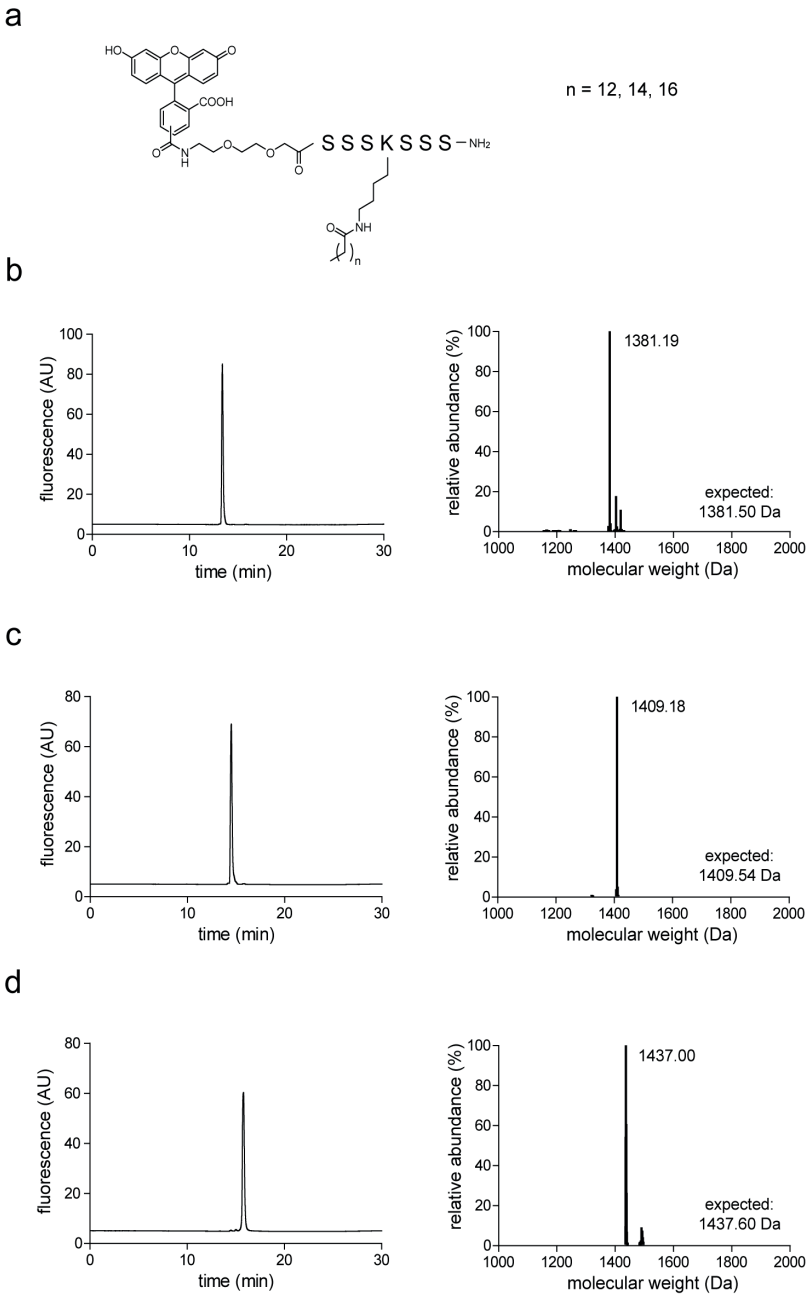

Figure 32. Characterization of three different peptide-fatty acid tags. (a) Structure of the peptides. RP-HPLC chromatograms (left panel) and deconvoluted mass spectra (right panel) of (b) myristoylated, (c) palmitoylated, and (d) stearoylated peptides. Amino acids shown as single letter code; fluorescein, PEG_2 and fatty acid tail shown as structural formula.

Peptides carrying myristic, palmitic or stearic acid bound human albumin with K_d values of 1900 ± 200, 1080 ± 120 and 1480 ± 150 nM (Fig. 33a), respectively, with affinities comparable to the approved acylated insulins.[227,228] The results showed that an affinity maturation of the Ser-based sequence was required to approach the desired low-medium nanomolar binding affinity for albumin. The affinity for albumin was also determined in human serum in the presence of all of the other blood components, which can either nonspecifically bind the peptide-fatty acid tag or compete for the same albumin binding sites (e.g. free fatty acids). Dilutions of serum were performed considering the average concentration of albumin in the blood (600 μM).[178] The peptide modified with the palmitic acid showed a binding affinity for albumin in human serum of approximately a factor two better respect to the two other peptide-fatty acid tags (Fig. 33b). Therefore, palmitic acid was chosen as albumin ligand for peptide maturation, and named K_{palm} when conjugated to Lys in the peptide sequence.

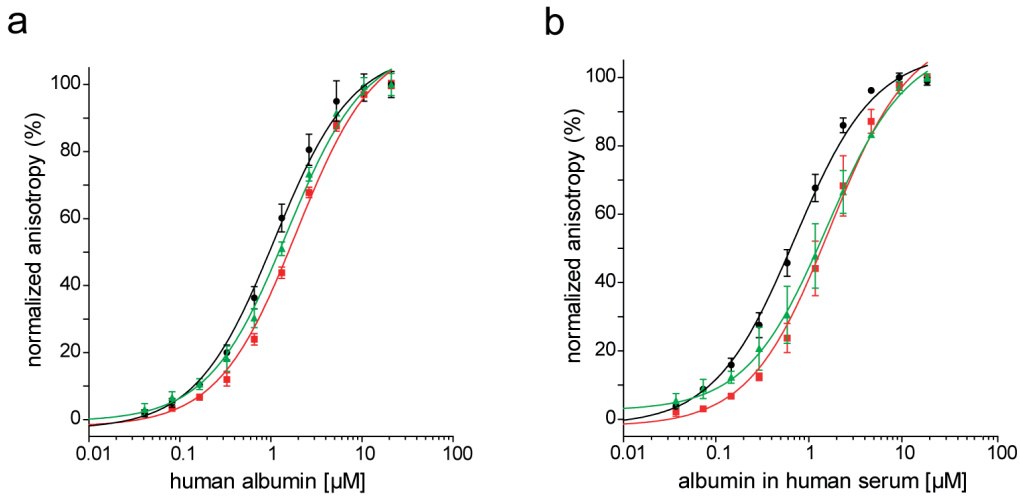

c

(F)-SSSKSSS

HN

O

myristic acid (n = 12)

palmitic acid (n = 14)

stearic acid (n = 16)

	albumin binding (K_d) [nM]	
	human albumin	human serum
(F)-SSSK$_{myr}$SSS	1900 ± 200	1680 ± 190
(F)-SSSK$_{palm}$SSS	1080 ± 120	690 ± 70
(F)-SSSK$_{ste}$SSS	1480 ± 150	1560 ± 100

Figure 33. Binding of the three peptide-fatty acid tags. Fluorescence polarization isotherms with (a) human albumin and (b) human serum. (c) Structure of the peptides and dissociation constants. Amino acids shown as single letter code; (F) is fluorescein; myr is myristic acid, palm is palmitic acid; ste is stearic acid; ▬ (dash) between (F) and Ser-based tag is PEG_2.

3.1.2 Solubility of bicyclic peptides conjugated to different albumin-binding tags

The strategy described above was applied for the synthesis of four tagged bicyclic peptides in order to determine the impact of the peptide-fatty acid tag on the conjugates' solubility in physiological buffer (Fig. 34). The peptide-fatty acid tag was appended to the peptides' C-termini during SPPS, spaced by a short PEG_2 linker. The N-terminus of bicyclic peptides was kept inaccessible to fatty acid modification using a Boc-protected amino acid. Lys(Dde) residue was deprotected and the free amine was conjugated with palmitic acid. After cleveage from the resin, the cyclization of the bicyclic peptides with the thiol-reactive molecule TBMB was carried out in a mixture of MeCN and aqueous buffer, pH 8.0, 30°C for 1h, and then the reaction mixture was purified.

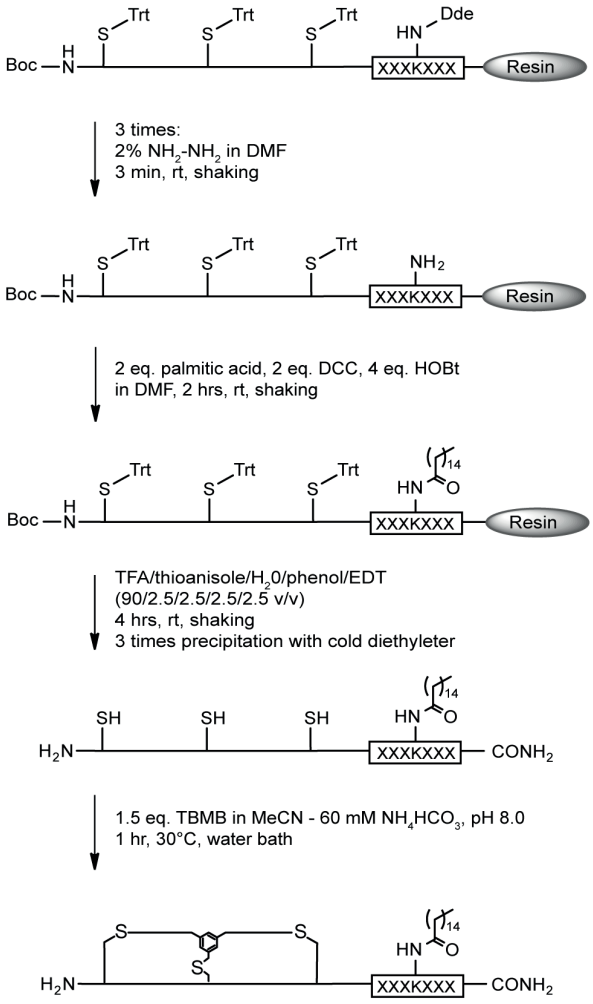

Figure 34. Synthesis of a bicyclic peptide conjugated to a peptide-fatty acid tag. X represents either Ser or Gly residues.

A single step of purification gave on average 30% yield of tagged bicyclic peptides with 90% purity (Fig. 35). The four conjugates were prepared using as model two well-characterized phage display selected bicyclic peptides, UK18[70] and PK15[68], that were conjugated with two peptide-fatty acid tags, $GGGK_{palm}GGG$ (Fig. 35a, UK18-GKG; 35b, PK15-GKG) or $SSSK_{palm}SSS$ (Fig. 35c, UK18-SKS; 35d, PK15-SKS).

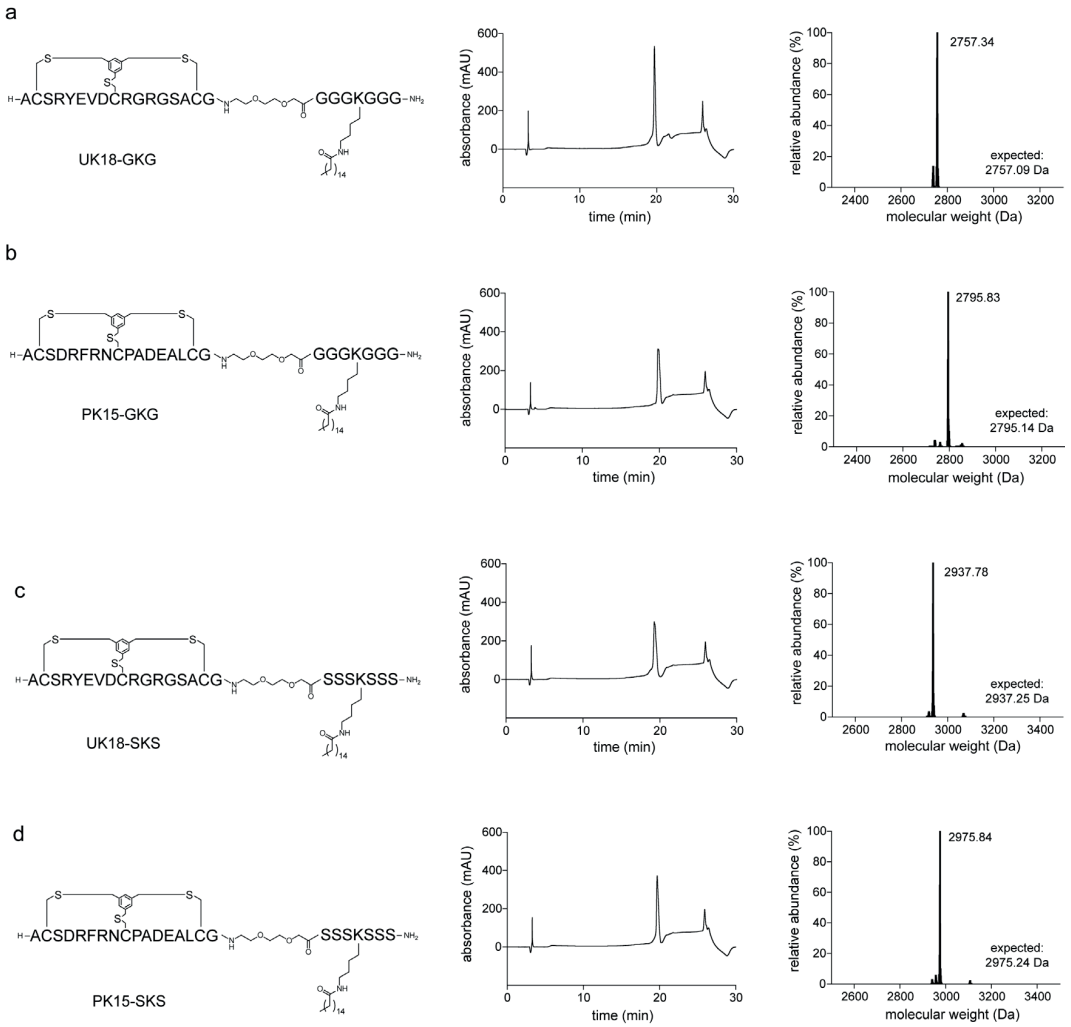

Figure 35. Characterization of the four conjugates used in solubility assay. Structure (left panel), RP-HPLC chromatograms (central panel) and deconvoluted mass spectra (right panel) of (a) UK18-GKG, (b) PK15-GKG, (c) UK18-SKS, and (d) PK15-SKS. Amino acids shown as single letter code; TBMB, PEG_2 and palmitic acid shown as structural formula.

The idea was to determine the maximum solubility of the conjugates by measuring the absorbance of saturated solutions in PBS. However, one of the chosen bicyclic peptides did not contain aromatic residues, not allowing direct measurements of absorbance at 280 nm. Therefore, the molar extinction coefficients at wavelengths where peptide bond usually absorbs light, which is in the UV range 190-230 nm[246], were calculated for

all constructs. Even if proteins and peptides show a λ_{max} at around 190 nm, the absorbance at 205 nm is usually preferred to avoid instrument-related technical limitations, and problems with intensities that are too high to be accurately measured.[246] To maximize the reproducibility of the assay and reduce the risk of external influences, measurements at 210 and 220 nm were performed as well. The choice of the solvent was also crucial since several physiological buffers exert a certain degree of absorbance.[247] Both milliQ water and PBS were tested and did not give absorbance in the selected range.

The molar extinction coefficients (ε_{nm}) in milliQ water were calculated by preparing serial dilutions of conjugates, initially fully dissolved at a concentration of one mg·ml^{-1}. Absorbances were registered and plotted against peptide concentrations, allowing the creation of "wavelength-specific calibration curves", in which the slope of the linear regression indicates the molar extinction coefficient (Fig. 36).

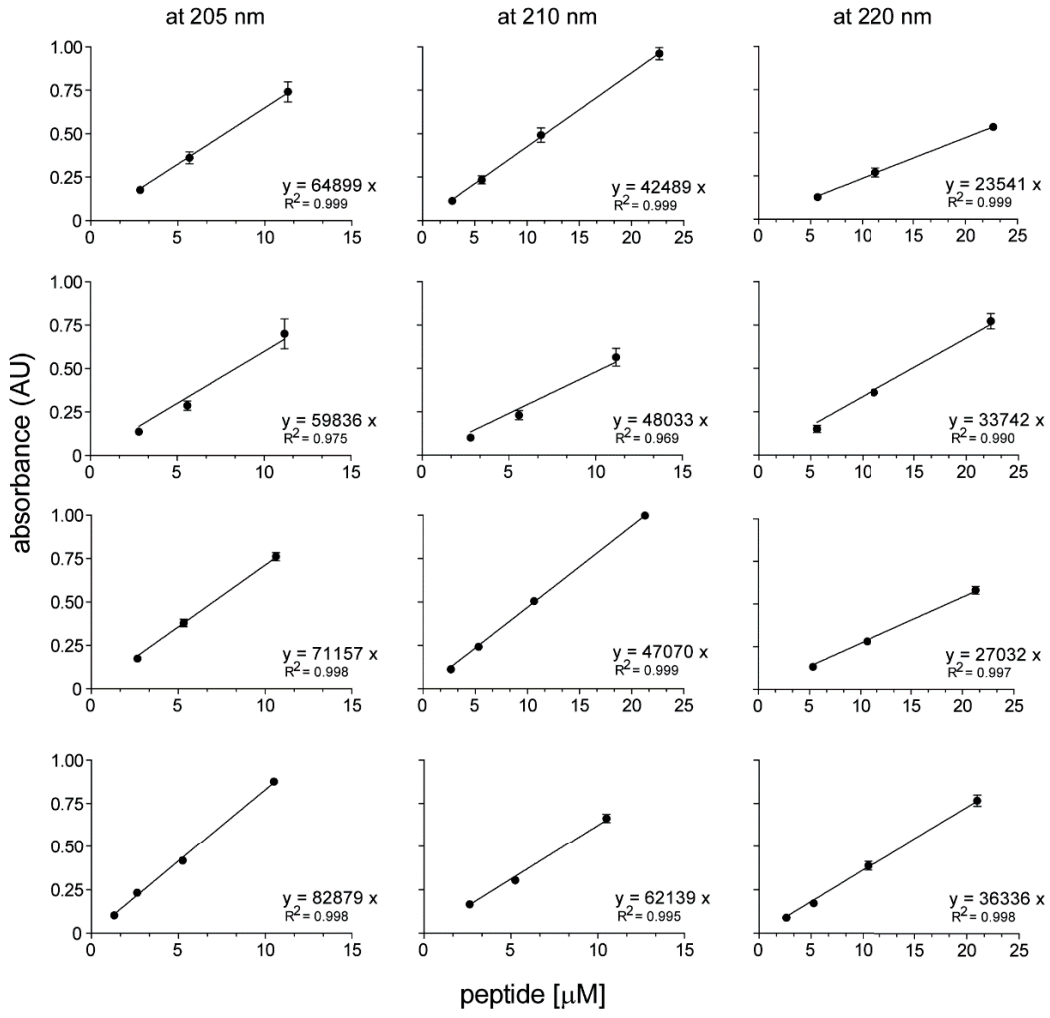

Figure 36. Calibration curves of the four conjugates. Conjugates UK18-GKG (first line), PK15-GKG (second line), UK18-SKS (third line) and PK15-SKS (fourth line).

In literature, extinction coefficients at 205 nm can be estimated by multiplying the molecular weight of a protein by a fixed absorptivity equal to 31 ml·mg^{-1}·cm^{-1}.[248] A more precise equation, called Scopes method, considers the absorbance of the aromatic side chains introducing a value related to an Abs_{280}/Abs_{205} ratio.[247] However, both equations did not consider the individual participation of the other amino acid side chains. A new method which overcomes this limitation was recently proposed, and a related website is available for calculating the molar extinction coefficients (http://spin.niddk.nih.gov/clore) starting from peptide sequences.[248]

Since the four conjugates analyzed contained two extra amide bonds from the PEG_2 linker and the coupled palmitic acid, I included them in the calculation as two Gly residues. In this model, Gly and Ser contribute equally, thus the different peptide-fatty acid tags were non-influential, and the two resulting ε_{205} coefficients were:

- 81700 M^{-1} cm^{-1} for tagged UK18;
- 83270 M^{-1} cm^{-1} for tagged PK15.

These calculated ε_{205} coefficients were compared to the experimental ones (Fig. 37), showing a difference lower than 10% for both derivatives with the Ser-based tag, while the discrepancy was much higher with the Gly-based one (20-30%). These results gave already a first indication about the peptide solubility, since a better approximation was obtained with the Ser-based tag. It is possible that the Gly derivatives were not fully dissolved, thus lowering the effective measured concentration. In addition, the extinction coefficients measured at 210 and 220 nm were lower, as expected.[246]

		molar absorption coefficient (ε_λ) [M^{-1} cm^{-1}]		
		at λ = 205 nm	at λ = 210 nm	at λ = 220 nm
UK18-GKG	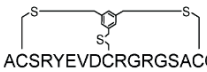 ACSRYEVDCRGRGSACG-GGGK$_{palm}$GGG	64899 ± 5198	42489 ± 1823	23541 ± 915
PK15-GKG	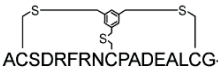 ACSDRFRNCPADEALCG-GGGK$_{palm}$GGG	59836 ± 7015	48033 ± 4569	33742 ± 1940
UK18-SKS	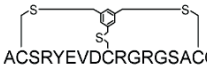 ACSRYEVDCRGRGSACG-SSSK$_{palm}$SSS	71157 ± 2617	47070 ± 770	27032 ± 1179
PK15-SKS	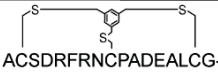 ACSDRFRNCPADEALCG-SSSK$_{palm}$SSS	82879 ± 2083	62139 ± 2412	36336 ± 1592

Figure 37. Molar extinction coefficients of the four conjugates. Amino acids shown as single letter code; palm is palmitic acid; λ is wavelength; **—** (dash) between Gly- or Ser-based tags is PEG_2.

The solubility in PBS was determined by preparing saturated solutions of conjugates at a theoretical concentration of ten mg·ml^{-1}, let them equilibrate at room temperature and centrifuged twice, before performing several serial dilutions and recording absorbances at the three different wavelengths (Fig. 38a). Conjugates' concentrations were calculated by applying the Lambert-Beer equation counting the experimental ε_{nm} coefficients, dilution factors and molecular weights.

a

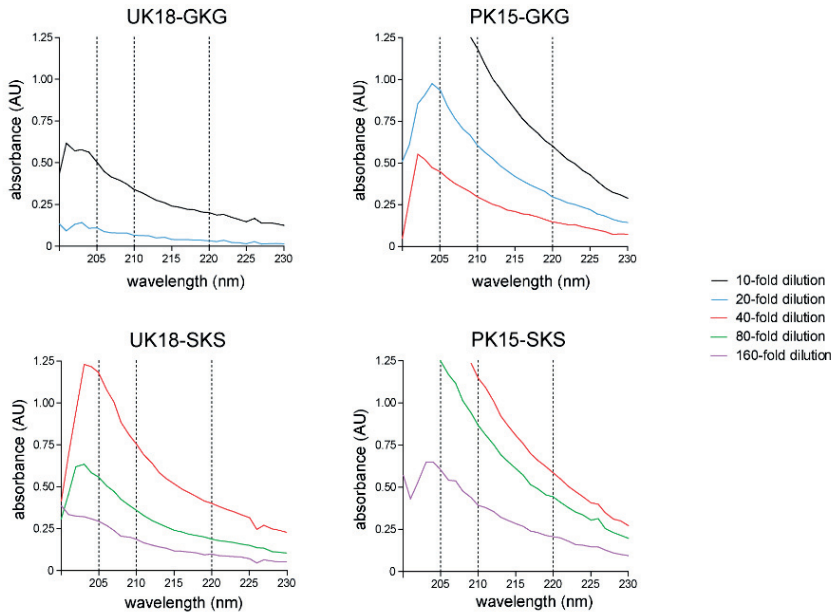

b

		peptide concentration [mg·ml^{-1}]			
		at λ = 205 nm	at λ = 210 nm	at λ = 220 nm	average
UK18-GKG	ACSRYEVDCRGRGSACG-GGGK$_{palm}$GGG	0.21*	0.22*	0.23*	0.22 ± 0.01
PK15-GKG	ACSDRFRNCPADEALCG-GGGK$_{palm}$GGG	0.85 ± 0.09	0.70 ± 0.05	0.49 ± 0.04	0.68 ± 0.18
UK18-SKS	ACSRYEVDCRGRGSACG-SSSK$_{palm}$SSS	1.92 ± 0.21	1.85 ± 0.08	1.73 ± 0.15	1.83 ± 0.09
PK15-SKS	ACSDRFRNCPADEALCG-SSSK$_{palm}$SSS	3.54 ± 0.08	2.84 ± 0.54	2.51 ± 0.52	2.96 ± 0.53

Figure 38. Solubility of the four conjugates. (a) Spectra of absorbance of the four different conjugates. (b) Solubility of the four different conjugates at three different wavelengths and their average. Amino acids shown as single letter code; palm is palmitic acid; λ is wavelengths; **—** (dash) between Gly and Ser is PEG_2.

The maximal solubility was reduced from more than ten mg·ml^{-1} (UK18 and PK15, data not shown) to approximately 0.2-0.7 mg·ml^{-1} if the tag was GGGK$_{palm}$GGG, and to 1.8-3.0 mg·ml^{-1} if the tag was SSSK$_{palm}$SSS (Fig. 38b). Tagged PK15 derivatives were two times more soluble than the corresponding UK18 ones, indicating different intrinsic

solubility of the bicyclic peptides. Comparison between the different tagged formats showed that the Ser-based tag was four to eight times more soluble than the Gly-based one, demonstrating that the solubility can be modulated by the amino acid sequence of the peptide and possibly be further enhanced with suitable substitutions. Since the desired solubility higher than one $mg \cdot ml^{-1}$ was reached for the palmitoylated Ser-based tag, I thus continued the development of the high affinity albumin-binding tag with this sequence as starting point.

3.1.3 Affinity maturation of the albumin-binding tag

The peptide-fatty acid (F)-PEG_2-$SSSK_{palm}SSS$-NH_2 tag, with a K_d value of 1080 ± 120 nM, was subjected to iterative cycles of synthesis and affinity testing in order to improve the binding affinity for albumin. Towards this goal, variants of the peptide-fatty acid tag were synthesized substituting one of the six Ser residues at a time to either Trp (W), Tyr (Y), Leu (L), Asp (D), Glu (E) or Gly (G) (Fig. 39). Amino acids presenting hydrophobic and negatively charged side chains were preferably screened since it is well known how these moieties are the structural requirements for the binding to human albumin.[178] Aromatic residues Trp and Tyr were chosen as capable of establishing hydrophobic interactions and hydrogen bonds, and together with Asp and Glu were considered the most promising residues for the affinity maturation. Leu was selected among all of the hydrophobic amino acids due to its longer branched side chain. Due to the presence of Ser in the starting sequence, no other polar residues were screened. Gly was included to check if a higher degree of flexibility would favor certain binding conformations.

The synthetic strategy shown in sub-section 3.1.1 (Fig. 31) was applied for the automated synthesis of all of the peptide variants carrying the palmitic acid. The binding affinity for human albumin was measured by fluorescence polarization. The standard deviations were lower than the 15% of the K_d values and facilitated the detection of relatively small affinity differences among variants. In each maturation cycle, the peptide-fatty acid variant with the best affinity was selected for the next step, the amino acid substitution fixed and the process repeated. If different amino acid substitutions were showing similar improvements: i) the negatively charged residues Asp and Glu were selected as they normally enhance the solubility, with Glu preferred for stability reason due to the propensity of Asp to isomerize into iso-Asp, racemize into D-Asp or hydrolyze [249]; ii) the hydroxylic Tyr was preferred over Trp. If different amino acid positions inside the sequence led to similar affinities, the substitution closest to the central palmitoylation was fixed to firstly evolve the peptide from this anchor towards the two peptide ends.

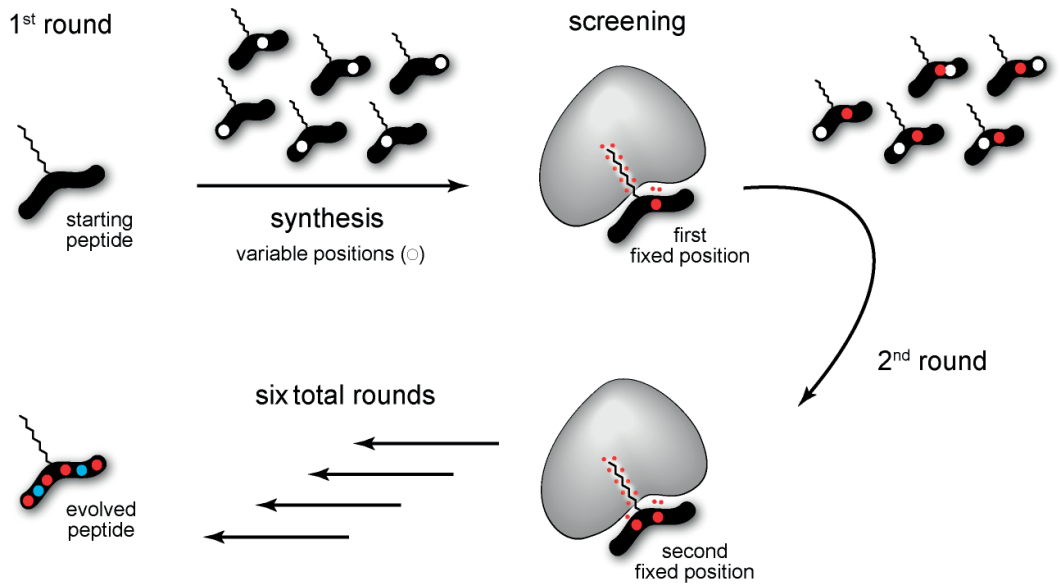

Figure 39. Schematic representation of the strategy applied for the evolution of the peptide moiety. Libraries of peptide-fatty acid variants were synthesized by individually replacing each variable position with six specific amino acids. These variants were then screened against human albumin. The substitution showing the best improvement was fixed and a new round of selection started, replacing the remaining variable positions.

In the first cycle (Fig. 40), 36 variants were synthesized and all the peptides modified with Asp and Glu showed strong improvements, independently from the position. Six of them showed around two-fold increase in binding affinity. This might be related to the restoring of the negative charge of the fatty acid, which was lost due to the coupling with Lys. Hydrophobic residues were not well tolerated, except for the second position. Trp reduced the affinity of the starting peptide more than a factor three. Gly acted as neutral residue without affecting the affinity. Following the criteria previously defined, the first selected variant had a Glu fixed in position five (K_d = 520 ± 50 nM).

In the second cycle (Fig. 41), 30 variants of (F)-PEG_2-$SSSK_{palm}$ESS-NH_2 were synthetized and again Asp or Glu peptides showed an improvement in binding affinity. Six of them had a two-fold better K_d value. The substitutions placed after the fixed Glu had a slightly lower impact, suggesting a potential incompatibility. Observations made in the first cycle about hydrophobic residues and Gly were confirmed. A negative charged core around the palmitoylation was created fixing a Glu in position three (K_d = 250 ± 30 nM).

In the third cycle (Fig. 42), substituents of the remaining four Ser positions determined the synthesis of 24 variants of (F)-PEG_2-$SSEK_{palm}$ESS-NH_2. A two-fold improved binding affinity was found among peptides substituted in position two for both hydrophobic and negatively charged residues. The result was not unexpected due to a better tol-

erability previously observed for the aromatic residues in that specific position. The maturation continued via two different paths, both with a fixed residue in position two, which was either Glu (K_d = 140 ± 15 nM, cycle 4a; Fig. 43) or Tyr (K_d = 123 ± 9 nM, cycle 4b; Fig. 44).

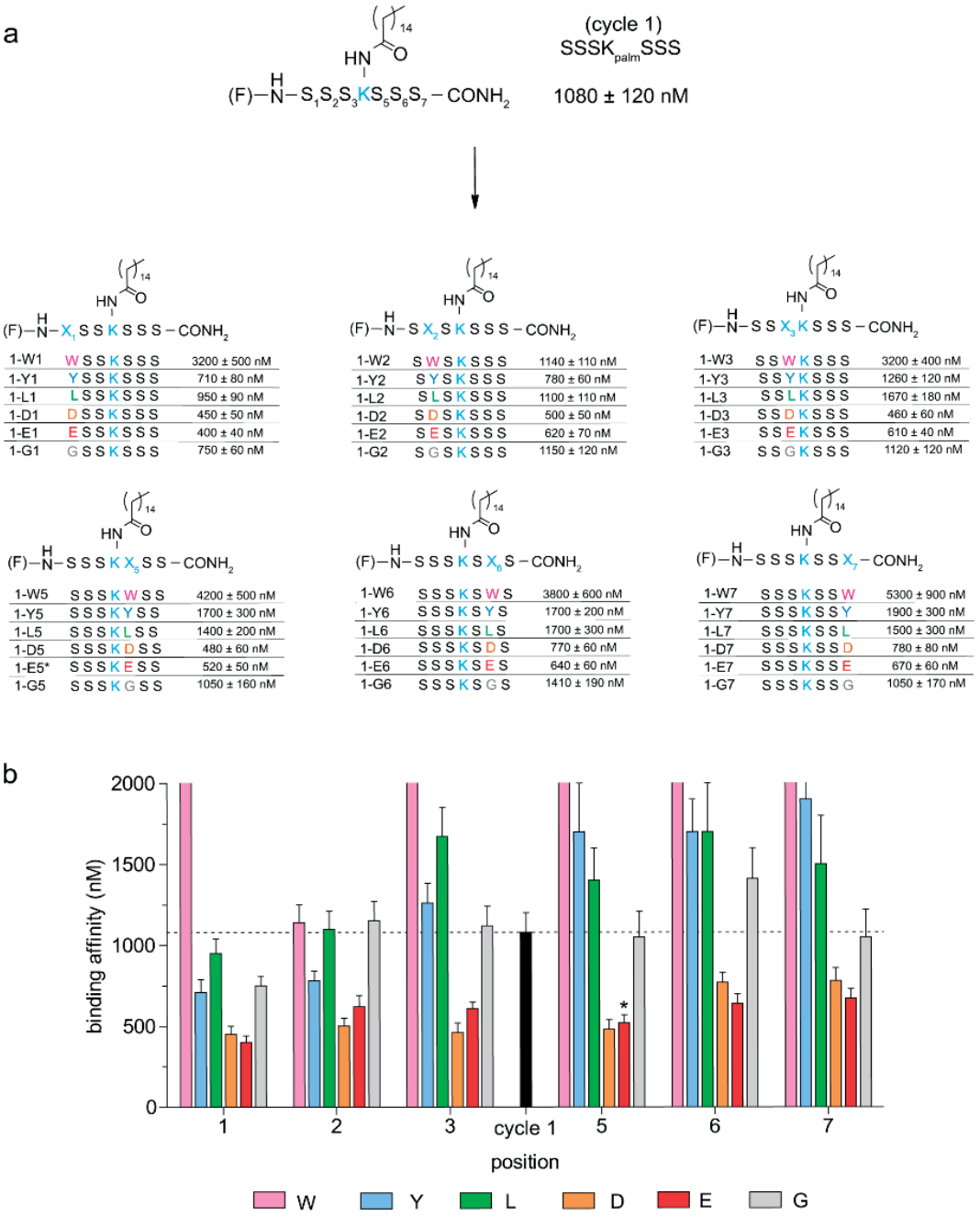

Figure 40. Binding affinity of the 1st cycle tag variants. (a) Sequences and dissociation constants, and (b) binding signature plot. Peptide marked with asterisk was fixed for the next round; dotted line indicates the binding affinity of the starting peptide; amino acids shown as single letter code; (F) is fluorescein; palm is palmitic acid; ▬ (dash) between (F) and N-terminus is PEG2.

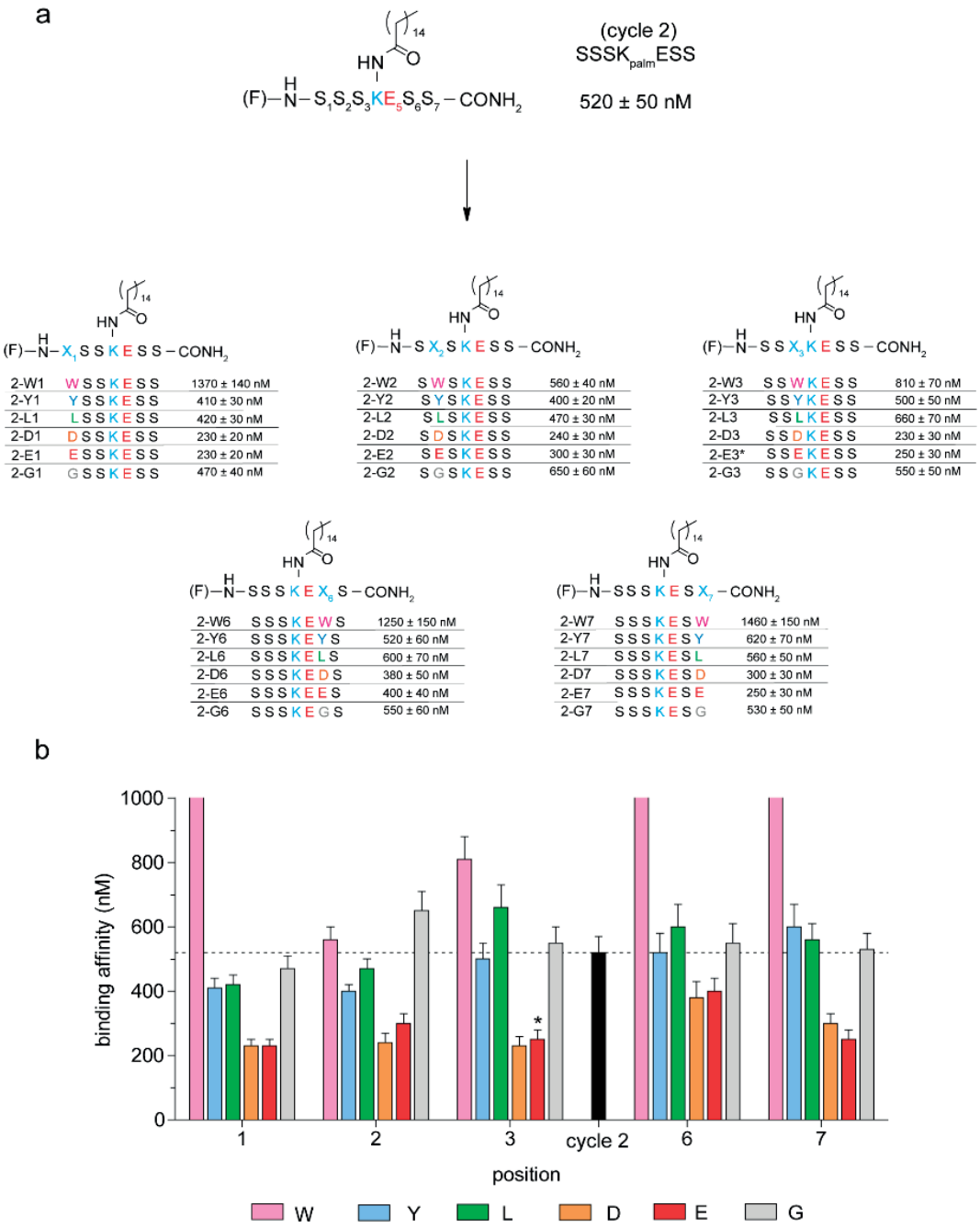

Figure 41. Binding affinity of the 2nd cycle tag variants. (a) Sequences and dissociation constants, and (b) binding signature plot. Peptide marked with asterisk was fixed for the next round; dotted line indicates the binding affinity of the starting peptide; amino acids shown as single letter code; (F) is fluorescein; palm is palmitic acid; — (dash) between (F) and N-terminus is PEG2.

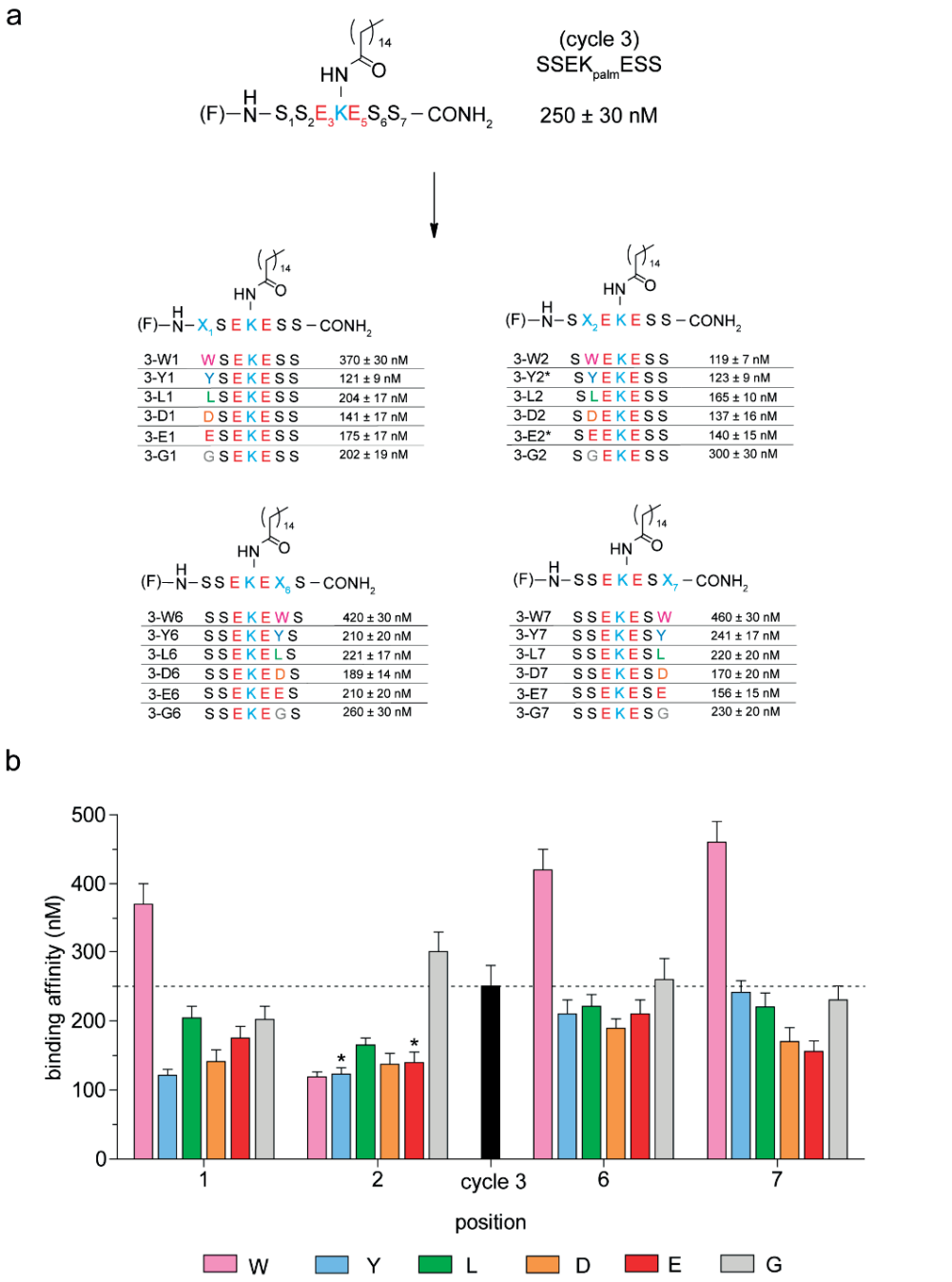

Figure 42. Binding affinity of the 3rd cycle tag variants. (a) Sequences and dissociation constants, and (b) binding signature plot. Peptides marked with asterisk were fixed for the next round; dotted line indicates the binding affinity of the starting peptide; amino acids shown as single letter code; (F) is fluorescein; palm is palmitic acid; ▬ (dash) between (F) and N-terminus is PEG_2.

Starting from the fourth cycle, variants with Asp and Gly were not synthetized anymore. Asp substitutions did not give any advantage over Glu, while binding affinities of Gly peptides were always neutral compared to the Ser counterparts. In the 4a path arising from (F)-PEG$_2$-SEEK$_{palm}$ESS-NH$_2$ (Fig. 43), no significant improvements were measured among the 12 variants analyzed. Only a couple of them showed a small increase in the binding affinity, suggesting that the fixed Glu in position two forced the peptide in a conformation which did not allow other stronger interactions.

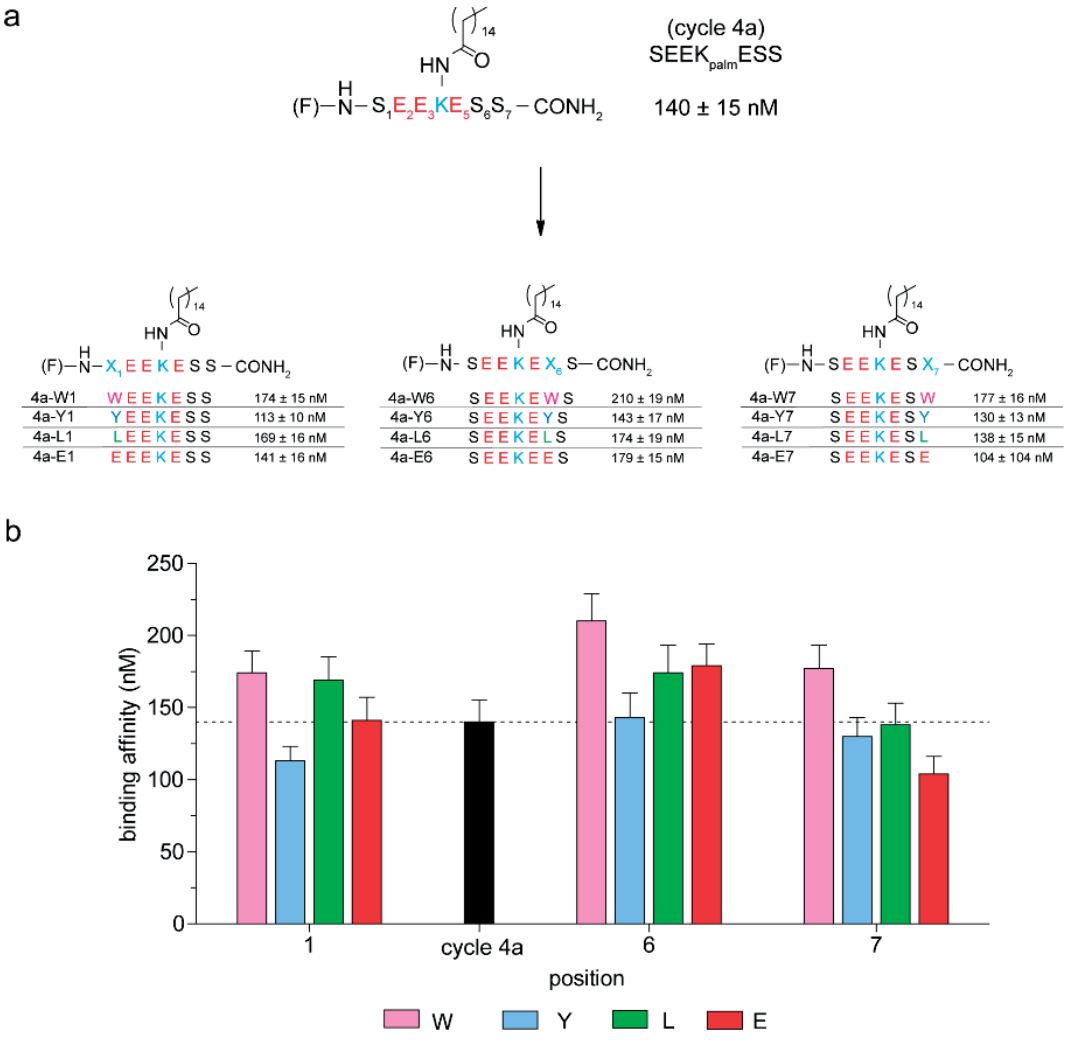

Figure 43. Binding affinity of the 4ath cycle tag variants. (a) Sequences and dissociation constants, and (b) binding signature plot. Dotted line indicates the binding affinity of the starting peptide; amino acids shown as single letter code; (F) is fluorescein; palm is palmitic acid; **—** (dash) between (F) and N-terminus is PEG$_2$..

In contrast, the second path 4b gave much better results. Three variants out of the 12 based on (F)-PEG$_2$-SYEK$_{palm}$ESS-NH$_2$ (Fig. 44) exhibited nearly a factor two improvement in the binding affinity when Ser were replaced with Glu, independently from the position. Trp dramatically reduced the affinity, while Tyr and Leu had basically a neutral behavior.

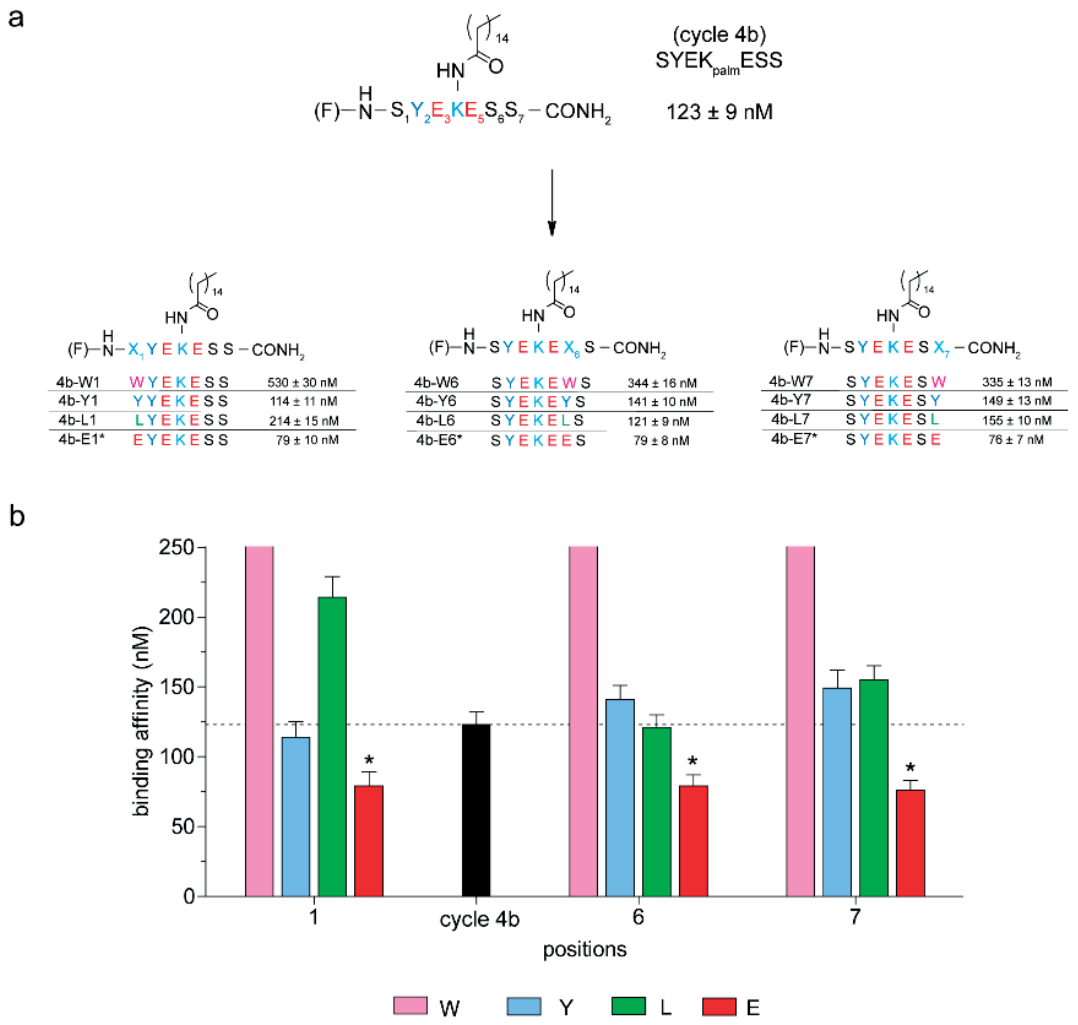

Figure 44. Binding affinity of the 4b[th] cycle tag variants. (a) Sequences and dissociation constants, and (b) binding signature plot. Peptides marked with asterisk were fixed for the next round; dotted line indicates the binding affinity of the starting peptide; amino acids shown as single letter code; (F) is fluorescein; palm is palmitic acid; **—** (dash) between (F) and N-terminus is PEG$_2$.

Since the K_d values of the three best variants were identical (K_d Glu-1 = 79 ± 10 nM; K_d Glu-6 = 79 ± 8 nM; K_d Glu-7 = 76 ± 7 nM), I decided to keep the three sequences as templates and change the two remaining positions with either Tyr or Glu, since these amino acids resulted to be the most promising for further binding affinity improvements. This strategy led to the synthesis of nine variants (Fig. 45) with three Glu peptides in common among the different paths. Two of them converged to the same best peptide-fatty acid tag, that was (F)-PEG_2-EYEK$_{palm}$ESE-NH_2 (K_d = 46 ± 4 nM).

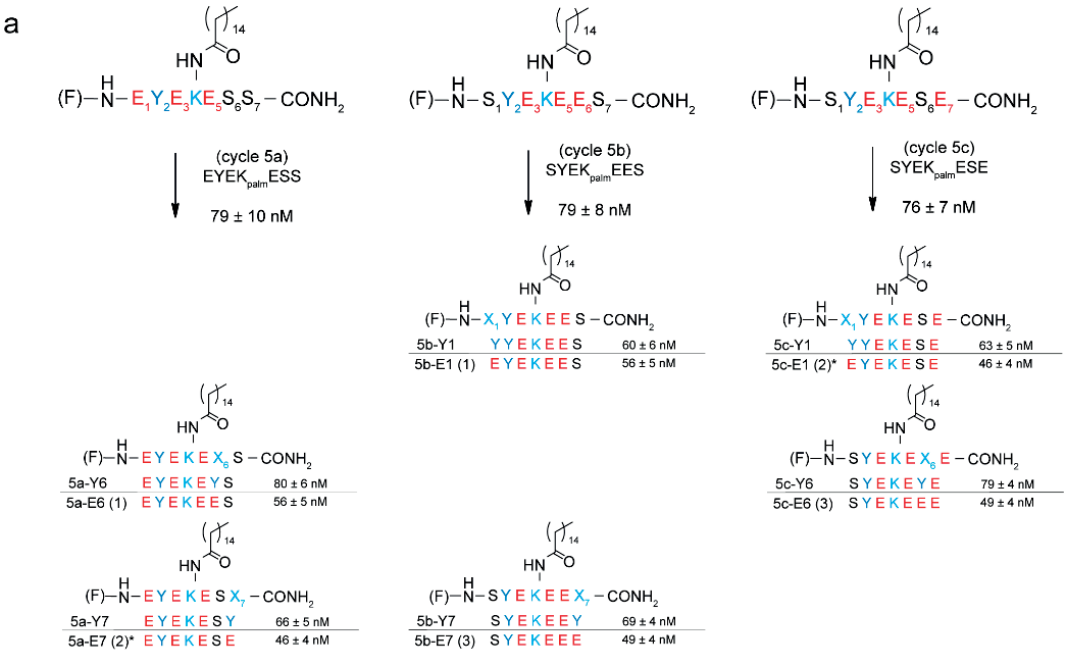

Figure 45. Binding affinity of the 5th cycle tag variants. (a) Sequences and dissociation constants, and (b) binding signature plot. Peptide marked with asterisk was fixed for the next round; dotted line indicates the binding affinity of the starting peptide; amino acids shown as single letter code; (F) is fluorescein; palm is palmitic acid, **—** (dash) between (F) and N-terminus is PEG_2.

Finally, in order to complete the selection and replace all of the different Ser residues, two last variants were prepared (Fig. 46a). Tyr substitution gave a slightly better affinity (39 ± 3 nM), leading to the final sequence of the evolved peptide-fatty acid tag (F)-PEG$_2$-EYEK$_{palm}$EYE-NH$_2$, later abbreviated as (F)-tag (Fig. 46b). Its affinity was 27-fold improved respect to the starting point and satisfied the need of generating a high-affinity albumin-binding tag with a K_d value in the low-medium nanomolar range.

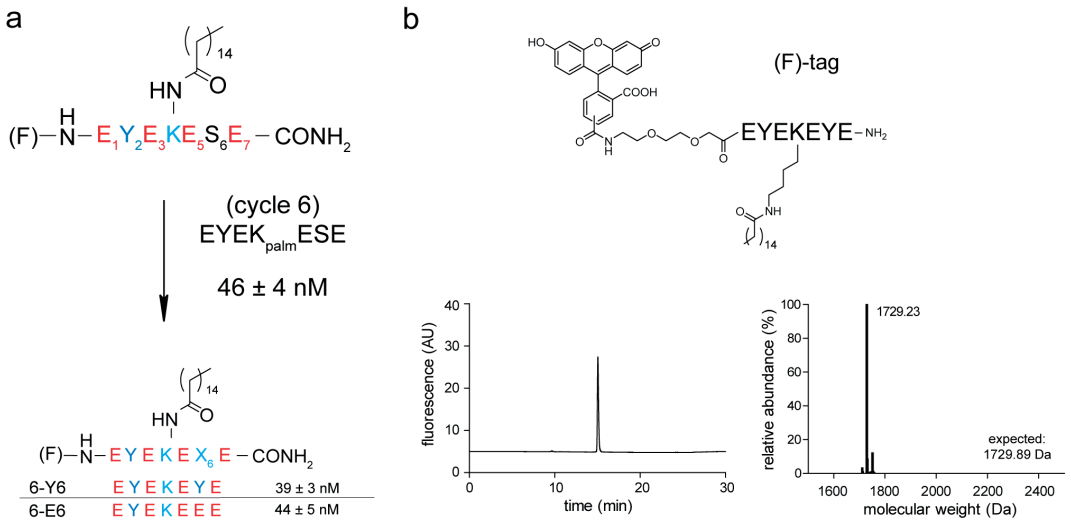

Figure 46. Binding affinity of the 6th cycle tag variants and characterization of the evolved tag. (a) Sequences and dissociation constants. (b) Structure (upper panel), RP-HPLC chromatogram (lower panel, left) and deconvoluted mass spectrum (lower panel, right) of the (F)-tag. Amino acids shown as single letter code; (F) is fluorescein, palm is palmitic acid; ▬ (dash) between (F) and N-terminus is PEG$_2$; fluorescein, PEG$_2$ and palmitic acid shown as structural formula.

The binding affinity of the (F)-tag was compared to those ones reported for the albumin-binding peptide SA21 and the approved acylated insulins (Fig. 47).[71,208,227,228] The evolved tag showed an affinity for human albumin ten- and more than 50-fold higher, and this should translate into a much more prolonged half-life extension in human.

	albumin binding (K_d) [nM]	factor of improvement
(F)-tag: (F)-EYEK$_{palm}$EYE	39 ± 3[a]	-
SA21: Ac-RLIEDICLPRWGCLWEDD-NH$_2$	467 ± 47[b] 321 ± 27[a]	8-12
Insulin detemir - Insulin deglutec	4200-1800[c]	50-100

Figure 47. Binding affinity of evolved tag, SA21 and acylated insulins. Amino acids shown as single letter code; (F) is fluorescein; palm is palmitic acid; Cys residues involved in the disulfide bridge are underlined. In the table: K_ds measured by a) fluorescence polarization, b) surface plasmon resonance, and c) albumin immobilized on agarose.

The best tag variants selected in each cycle were compared in the same plate and the resulting binding curves are shown in Figure 48. The graphic clearly shows that the binding was improved by a factor two in the first four rounds of evolution, and finally the affinity slowly reached the targeted range in the last cycles.

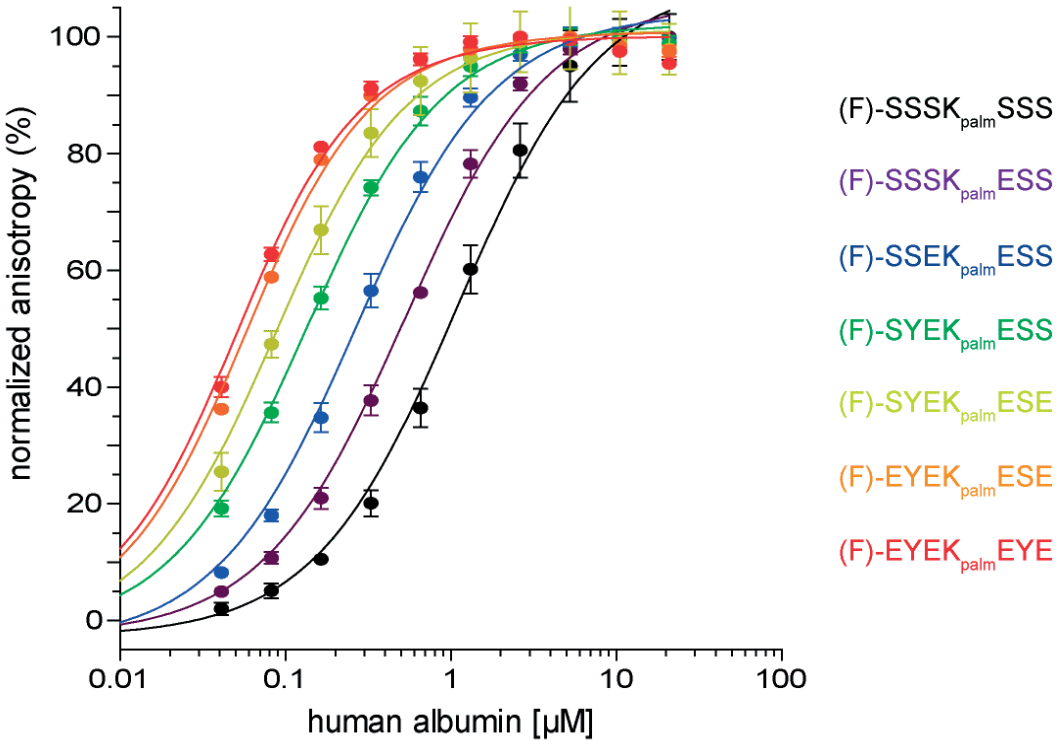

Figure 48. Binding isotherms of the evolved tag and precursors with human albumin. Amino acids shown as single letter code; (F) is fluorescein; palm is palmitic acid; ▬ (dash) between (F) and tag variants is PEG_2.

3.1.4 Binding to rat albumin and human albumin in serum

The binding affinity of the best tag variants was also determined in human serum and for rat albumin (Fig. 49). Rat albumin was tested to understand if rats were suitable as animal model for *in vivo* pharmacokinetic studies. Fluorescence polarization with human serum showed affinities comparable to that determined with pure human albumin, confirming a specific binding of the tag variants to the protein even in presence of fatty acids and other blood components (Fig. 49b). Experiments with rat albumin showed that the final (F)-tag binds the orthologous protein with a K_d value of 220 ± 30 nM, six-fold weaker than that for human albumin, but still in a range of affinity suitable for the desired *in vivo* experiments in rats (Fig. 49a).

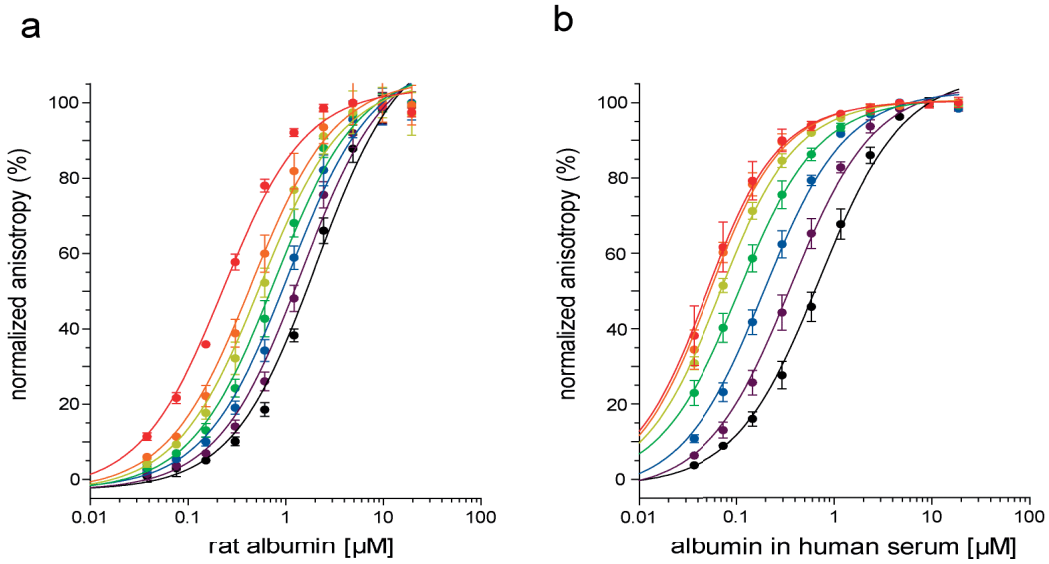

c

		albumin binding (K_d) [nM]		
		human albumin	rat albumin	human serum
cycle 0	(F)-SSSK$_{palm}$SSS	1080 ± 120	2000 ± 300	690 ± 70
cycle 1	(F)-SSSK$_{palm}$ESS	520 ± 50	1500 ± 200	350 ± 30
cycle 2	(F)-SSEK$_{palm}$ESS	250 ± 30	1050 ± 150	180 ± 16
cycle 3	(F)-SYEK$_{palm}$ESS	123 ± 9	770 ± 110	95 ± 3
cycle 4b	(F)-SYEK$_{palm}$ESE	76 ± 7	540 ± 70	57 ± 2
cycle 5a, 5c	(F)-EYEK$_{palm}$ESE	46 ± 4	430 ± 50	41 ± 3
cycle 6	(F)-EYEK$_{palm}$EYE	39 ± 3	220 ± 30	37 ± 2

Figure 49. Binding of the evolved tag and precursors with different albumins. Fluorescence polarization isotherms with (a) rat albumin and (b) human serum. (c) Dissociation constants. Amino acids shown as single letter code; (F) is fluorescein; palm is palmitic acid; ▬ (dash) between (F) and tag variants is PEG_2.

In addition to the best tag variants, all the peptides from the last three cycles were tested with human serum and rat albumin (Fig. 50). The results with human serum confirmed the binding trend about high affinity and specifity for human albumin. In contrast, affinities for rat albumin showed that the selected tag variants were not always corresponding to the best binders, except for the evolved (F)-tag, suggesting a different pattern of interactions in the binding site.

		albumin binding (K_d) [nM]		
		human albumin	rat albumin	human serum
cycle 4b	(F)-EYEK$_{palm}$ESS	79 ± 10	520 ± 70	61 ± 4
cycle 4b	(F)-SYEK$_{palm}$EES	79 ± 8	650 ± 90	63 ± 3
cycle 4b	(F)-SYEK$_{palm}$ESE	76 ± 7	540 ± 70	57 ± 2
cycle 5a	(F)-EYEK$_{palm}$EYS	80 ± 6	450 ± 60	67 ± 3
cycle 5a	(F)-EYEK$_{palm}$ESY	66 ± 5	400 ± 50	52 ± 1
cycle 5a, 5b	(F)-EYEK$_{palm}$EES	56 ± 5	510 ± 60	52 ± 4
cycle 5a, 5c	(F)-EYEK$_{palm}$ESE	46 ± 4	430 ± 50	41 ± 3
cycle 5b	(F)-YYEK$_{palm}$EES	60 ± 5	540 ± 70	68 ± 4
cycle 5b	(F)-SYEK$_{palm}$EEY	69 ± 4	460 ± 60	68 ± 2
cycle 5b, 5c	(F)-SYEK$_{palm}$EEE	49 ± 4	490 ± 60	45 ± 1
cycle 5c	(F)-YYEK$_{palm}$ESE	63 ± 5	490 ± 60	48 ± 2
cycle 5c	(F)-SYEK$_{palm}$EYE	79 ± 4	510 ± 60	78 ± 2
cycle 6	(F)-EYEK$_{palm}$EYE	39 ± 3	220 ± 30	37 ± 2
cycle 6	(F)-EYEK$_{palm}$EEE	44 ± 5	380 ± 50	37 ± 2

Figure 50. Binding of the evolved tag and last variants with different albumins. Dissociation constants. Amino acids shown as single letter code; (F) is fluorescein; palm is palmitic acid; — (dash) between (F) and tag variants is PEG_2.

3.1.5 Isothermal titration calorimetry

The binding affinity of the evolved (F)-tag (Fig. 46) was further studied by isothermal titration calorimetry (ITC) in order to validate the results obtained in the fluorescence polarization screening. ITC was also used to investigate the number of binding sites on albumin and the enthalpic and entropic thermodynamic parameters.

ITC experiments were carried out in duplicate using a concentration of (F)-tag in the syringe (40 μL at 500 μM) ten-fold higher than the concentration of albumin in the cell (300 μL at 50 μM). Number and volume of injections were varied to get a sufficient release of heat for peak integration as well as a clear picture of the binding events (Fig. 51a, 51d). Peptide titrated into buffer showed a certain degree of heat release related to either nonspecific interactions or buffer mismatch. However, heat changes were always lower than the experimental ones and thus subtractable from these data (Fig. 51b, 51e).

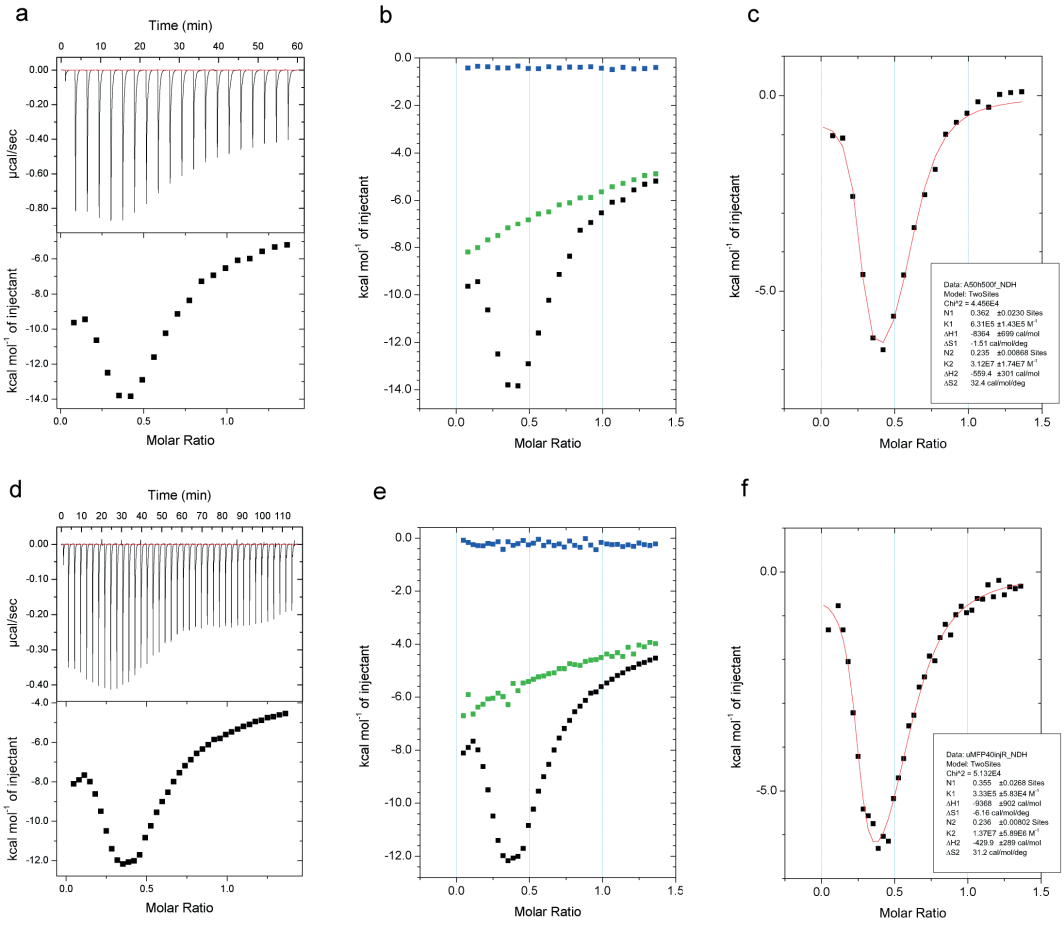

Figure 51. ITC profile of (F)-tag binding to human albumin. Raw data and binding isotherms obtained by integrating the titration of peptide into protein with (a) 19 (2 μL each) or (d) 38 (1 μL each) injections. Binding isotherms obtained by integrating the titrations of peptide into protein (black), peptide into buffer (green) and buffer into protein (blue) with (b) 19 or (e) 38 injections (same experimental conditions). Two-sites binding model fitting of titration of peptide into protein with (c) 19 or (f) 38 injections after blanking them.

The isotherms (Fig. 51c, 51f) were fitted with a two-sites binding model. They showed the same curve shape reported for one of the three theoretical ITC isotherms observed for a ligand that binds to two independent binding sites on a protein (Fig. 52).[250] If the ligand binds with similar affinity and enthalpy change on both binding sites, the two

events are close enough to be thermodynamically indistinguishable and a single curve is obtained (Fig. 52a). If the ligand binds with different affinities, the shape of the curve is strickly related to enthalpy changes. Figure 52b shows a situation in which the binding site with the highest affinity has the strongest enthalpy change. In contrast, in Figure 52c the same high-affinity binding site demonstrates the weakest enthalpy change.

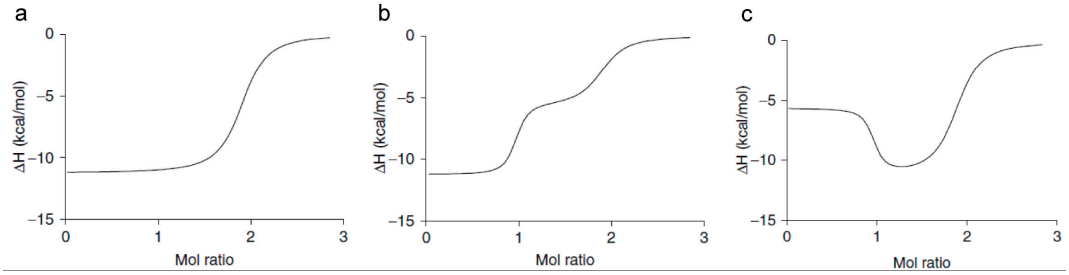

Figure 52. Possible experimental isotherms in a two-sites binding model. (a) A system where affinity and enthalpy are indistinguishable. Systems where higher affinity correlates with either a (b) stronger or a (c) weaker exothermic enthalpy change. Adapted with permission from [250], reprinting license nr. 4047541382989, copyright © 2007 Elsevier Inc. All rights reserved.

In both experiments (Fig. 51c, 51f) the curves were similar to the isotherm shown in Figure 52c and differences in binding affinities and enthalpy changes were measured. Applying this model, the binding site with the highest affinity had the weakest enthalpy change (K2: K_d = 53 ± 29 nM, $\Delta H \approx$ -0.5 kcal·mol^{-1}), while the binding site with reduced affinity showed a stronger enthalpy change (K1: K_d = 2.3 ± 1.0 µM, $\Delta H \approx$ -8.5 kcal·mol^{-1}) (Fig. 53a). This K_d value for the K2 binding site confirmed the nanomolar affinity of the (F)-tag measured by fluorescence polarization, thus recommending the use of this technique for a faster and easier calculation of the binding strength of acylated peptides. In addition, the presence of more than one binding sites on albumin was consistent with data reported in literature for fatty acids.[197]

Thermodynamic parameters were further analyzed and gave some insights into the potential binding mechanism of the (F)-tag (Fig. 53b). Both binding events were thermodynamically favorable since the values of Gibbs free energy (ΔG) were negative. However, the binding was guided in a different manner. As expected in this model, the binding site with the highest affinity (K2) correlated with a weaker enthalpy change. As consequence, this first event was mainly entropy-driven ($-T\Delta S \approx$ -9.5 kcal·mol^{-1}·K^{-1}), with hydrophobic interactions as well as conformational changes playing a crucial role in the overall affinity. On the other hand, the second event took place in a binding site where the (F)-tag had a 40-fold weaker affinity (K1) and it was strongly enthalpy-driven ($\Delta H \approx$ -

8.5 kcal·mol^{-1}), suggesting a major involvement of hydrogen and van der Waals bonds, with in contrast unfavorable conformational changes, as confirmed by the loss of entropy.

a

experimental settings	binding site	K_a (M^{-1})	K_d (M)[a]	ΔG (kcal·mol^{-1})[b]	ΔH (kcal·mol^{-1})	–TΔS (kcal·mol^{-1} K^{-1})[c]
19 injections 2 μL each	K1	6.31 x 10^5	1.6 x 10^{-6}	- 7.91	- 8.36	0.45
	K2	3.12 x 10^7	32 x 10^{-9}	- 10.22	- 0.56	- 9.66
38 injections 1 μL each	K1	3.33 x 10^5	3.0 x 10^{-6}	- 7.53	- 8.87	1.14
	K2	1.37 x 10^7	73 x 10^{-9}	- 9.73	- 0.49	- 9.48

b

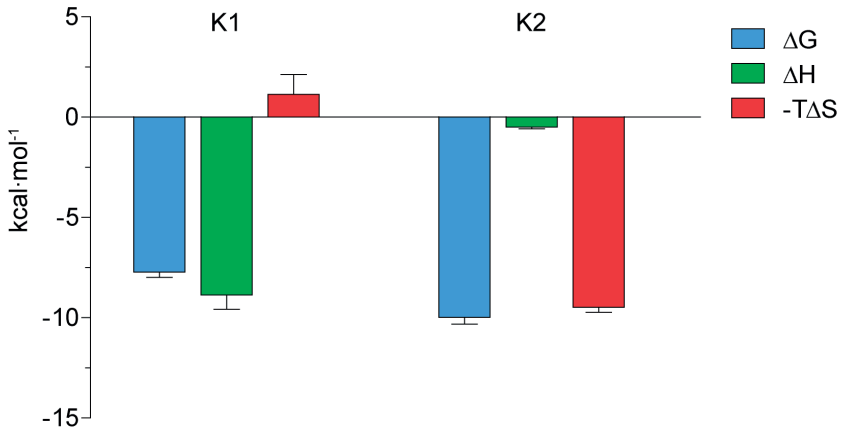

Figure 53. Thermodynamic parameters calculated using a two-sites binding model. (a) Table with corresponding values, and (b) signature plot of average values. In the table: a) K_d calculated as reciprocal of the K_a, b) ΔG = ΔH - TΔS, and c) Temperature at 25°C = 298.15 K.

According to these data, I could hypothesize that all of the moieties on the (F)-tag were important for binding to K2 site on albumin with high affinity, in particular the hydrophobic parts (ΔS). After the saturation of this site, (F)-tag also took part in a second binding event on site K1, where hydrogen bonds (ΔH) prevailed on the hydrophobic interactions. Therefore, I might speculate that the hydrophobic parts did not fit properly in the second site, and in consequence they were not able to find a "partner ligand" on albumin, thus not contributing actively to the binding.

3.1.6 Role of fluorescein in albumin binding

I finally tested if the hydrophobic N-terminal fluorescein contributed to the albumin binding of the tag since it has already been reported that it has a certain affinity for this serum protein (K_d ≈ 70 μM).[204] A second tag format was synthetized by coupling the

fluorescein to the C-terminus through a click chemistry reaction (Fig. 54a). An alkyne residue was placed at the C-terminal end, separated from the sequence by a short PEG_2 linker. The N-terminus was acetylated with acetic anhydride, the Lys(Dde) selectively deprotected and the free amino group modified with palmitic acid. The purified peptide was finally subjected to a click chemistry reaction[71] and re-purified, resulting in a 95% pure fluorescein labeled tag-(F) (Fig. 54b).

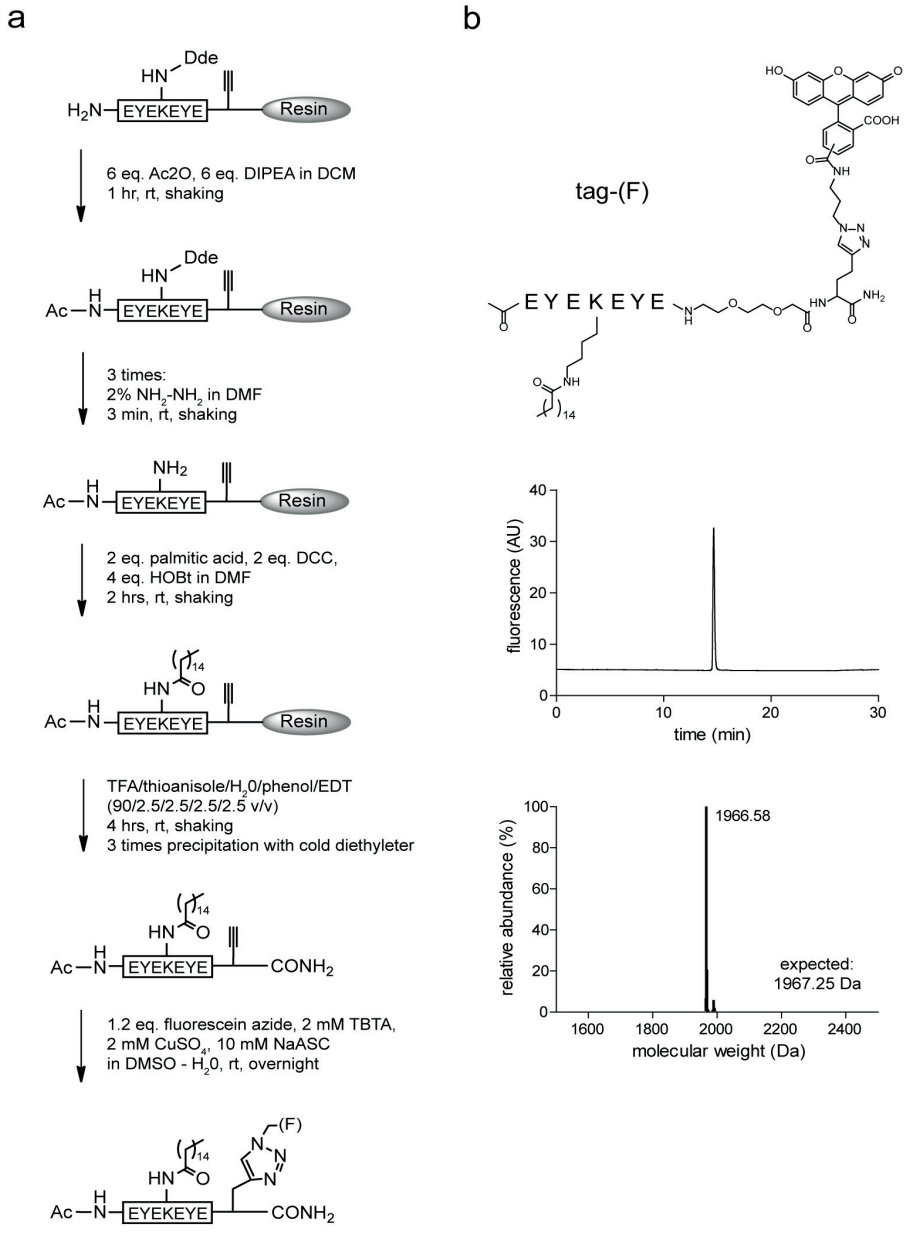

Figure 54. Synthesis and characterization of the tag fluorescein labeled at the C-terminus. (a) Synthesis, (b) structure (upper panel), RP-HPLC chromatogram (middle panel) and deconvoluted mass spectrum (lower panel) of the tag-(F). Ac is acetyl group; (F) is fluorescein. Amino acids shown as single letter code; fluorescein, triazole ring, PEG_2 and palmitic acid shown as structural formula.

Fluorescence polarization assays were performed with human albumin, human serum, and rat albumin. The C-terminal labeled tag-(F) bound human albumin with K_d values of 1-1.5 μM, which were 30 to 40-fold weaker than the affinity measured for the N-terminal labeled (F)-tag. This result pointed out that fluorescein labeling had an impact on the binding of the tag for human albumin. Most probably this moiety acted as an eighth amino acid and, in combination with the palmitic acid, placed the peptide in a precise pocket on albumin surface, inducing a site-specific evolution. Thus, the tag format designed without the N-terminal fluorescein lost these crucial interactions and its binding affinity dropped to 1 μM. In contrast, only a factor two decrease in affinity was observed for tag-(F) with rat albumin, confirming a different binding specificity of the tag between the two species (Fig. 55).

a

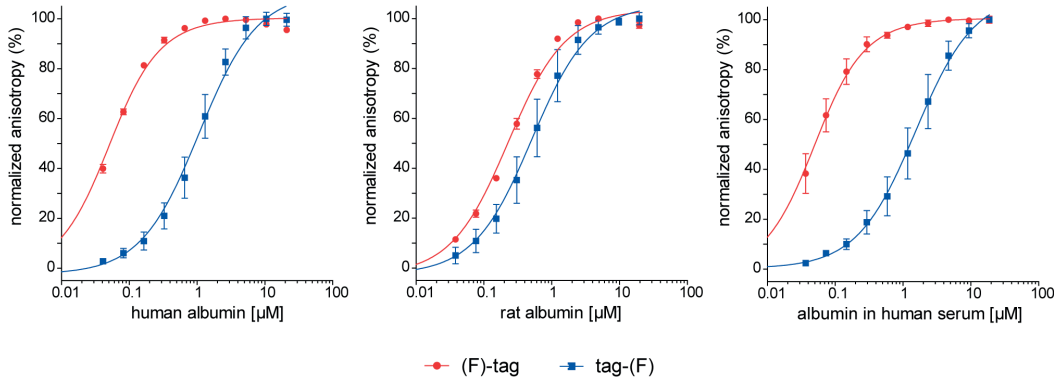

b

		albumin binding (K_d) [nM]		
		human albumin	rat albumin	human serum
(F)-tag	(F)-EYEK$_{palm}$EYE	39 ± 3	220 ± 30	37 ± 2
tag-(F)	EYEK$_{palm}$EYE-(F)	1060 ± 140	500 ± 50	1520 ± 80

Figure 55. Binding of the N- and C-fluorescein labeled tag with different albumins. (a) Fluorescence polarization isotherms with human albumin (left panel), rat albumin (middle panel) and human serum (right panel). (b) Dissociation constants. Amino acids shown as single letter code; (F) is fluorescein; palm is palmitic acid, ▬ (dash) between tag and (F) at both peptide ends is PEG_2.

To confirm this observation, a competitive assay was performed using the non-labeled tag as competitor (Fig. 56a). Fixed concentrations of (F)-tag and albumin were incubated with an increasing amount of competitor, and the displacement quantified by fluorescence polarization. IC_{50} values were graphically determined (Fig. 56b) and analyzed by applying the equation developed by Rossi and Taylor.[251] The calculated K_d value of 720 ± 100 nM was 20-fold weaker than the affinity measured for the N-terminal labeled

(F)-tag. The affinity of the non-labeled tag was consistent with the value found for tag-(F) (Fig. 55), and confirmed the role of fluorescein in the binding.

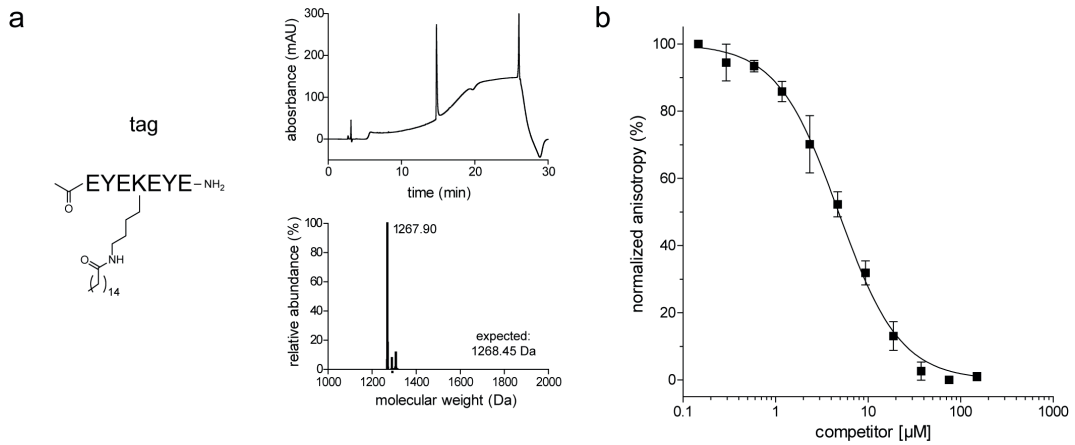

Figure 56. Characterization and competitive assay of the non-labeled tag. (a) Structure (left panel), RP-HPLC chromatogram (upper right panel) and deconvoluted mass spectrum (lower right panel) of the tag. (b) Fluorescence polarization isotherm with (F)-tag, human albumin and increasing concentration of tag. Amino acids shown as single letter code; palmitic acid shown as structural formula.

These data were compared to ITC experiments and implemented the analysis. The low affinity of (F)-tag in the K1 binding site correlated with the value obtained for the non-labeled tag in fluorescence polarization. The K1 binding event showed a weak entropic contribution, suggesting that the hydrophobic structures were not efficiently involved in the binding, even if they were physically present. Most likely, the binding mechanism of the tag lacking the N-terminal fluorescein was also enthalpy-driven, independently from the site of interaction, due to the absence of this hydrophobic moiety. These results reciprocally confirmed that fluorescein conjugation had a positive impact on the binding affinity, but only when it is placed in a precise position in the sequence.

ITC experiments with non-labeled tag and co-crystallization of (F)-tag with albumin would have given a stronger support to this hypothesis. A colleague tried to crystalize (F)-tag with albumin by applying conditions established in literature.[197] Small crystals of either albumin with only fatty acids, used as stabilizing agents, or with fatty acids and (F)-tag were obtained. The yellow color observed in the crystal confirmed the presence of (F)-tag (data not shown). However, it was not possible to determine the electron density of the tag itself, probably due to the negative influence of multiple low affinity binding sites and/or the flexibility of the tag. Crystallization trials were not further investigated.

3.2 - Application of the albumin-binding tag to two bioactive peptides

Having generated a high affinity peptide-fatty acid tag, I applied it to two bicyclic peptides that were previously developed in our laboratory. In a first step, I synthesized four conjugates connecting the two bicyclic peptides to the tag at either one of the two ends. In a second step, I tested the effect of bicyclic peptides on the tag affinity for albumin and, at the same time, the impact of the tag on bicyclic peptides' inhibitory activity against the relative targets. In a third step, I assessed the plasma stability of the conjugates in human plasma. Finally, I performed pharmacokinetic studies in rats of the N-terminal tagged bicyclic peptides, the tag itself and one of the bicyclic peptide alone.

3.2.1 Synthesis of tagged bicyclic peptides

The two bioactive bicyclic peptides used as models were PK128 and UK18 (subsection 1.1.6).[69,70] UK18 was previously tested *in vivo* and it suffered from a fast renal clearance, with a half-life of 30 minutes upon i.v. injection in mice.[71] The conjugates were synthesized by appending the tag to both N- and C-peptides' termini, spaced by a short PEG_2 linker, directly during SPPS. The synthetic strategies that were applied are described in sections 3.1, and they are here schematically represented (Fig. 57). Lys(Dde) residue was deprotected on resin and the free amine acylated with palmitic acid. After cleveage, both peptides were cyclized with TBMB in a mixture of MeCN and aqueous buffer, and then the reaction mixture was purified.

The tagged bicyclic peptides were differently modified according to the experiments that had to be carried out. The formats to be tested in fluorescence polarization assays were labeled with fluorescein, either directly at the N-terminus (Fig. 57a), which was also the format selected for pharmacokinetic studies, or by click chemistry at a C-terminal alkyne residue (Fig. 57b). The formats destined for inhibition assays were not labeled, due to the potential interference that fluorescein might have with the fluorogenic substrate used in these tests. In this case, the N-terminal format was acetylated with fluorescein replaced by an acetyl group (caption of Fig. 57 for details), while the C-terminal one was kept unmodified at the alkyne residue.

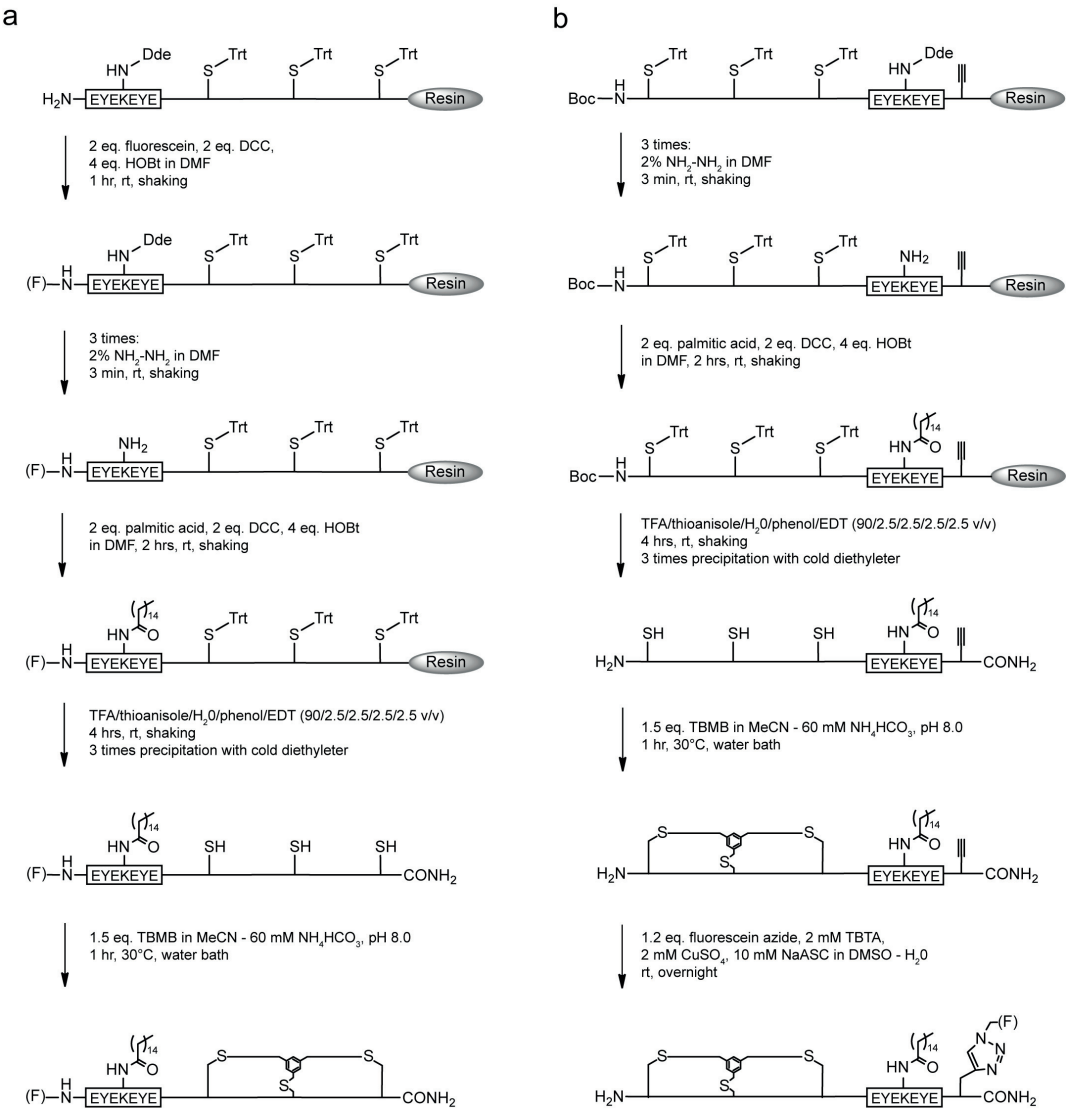

Figure 57. Synthesis of bicyclic peptides conjugated to the evolved peptide-fatty acid tag. Synthesis of (a) N-terminal and (b) C-terminal formats. (F) is fluorescein. Acetylation of the N-terminal tagged format was carried out using 6 equiv. of Ac2O and 6 equiv. of DIPEA in DCM, 1 hr at room temperature under shaking.

3.2.2 Albumin binding and solubility

After a single step of cyclization and HPLC purification, all the fluorescein labeled peptides had purity greater than 95% and around 40% yield (Fig. 58b-e). As control, the bicyclic peptide UK18 alone was synthesized and labeled at the N-terminus with fluorescein (Fig. 58a).

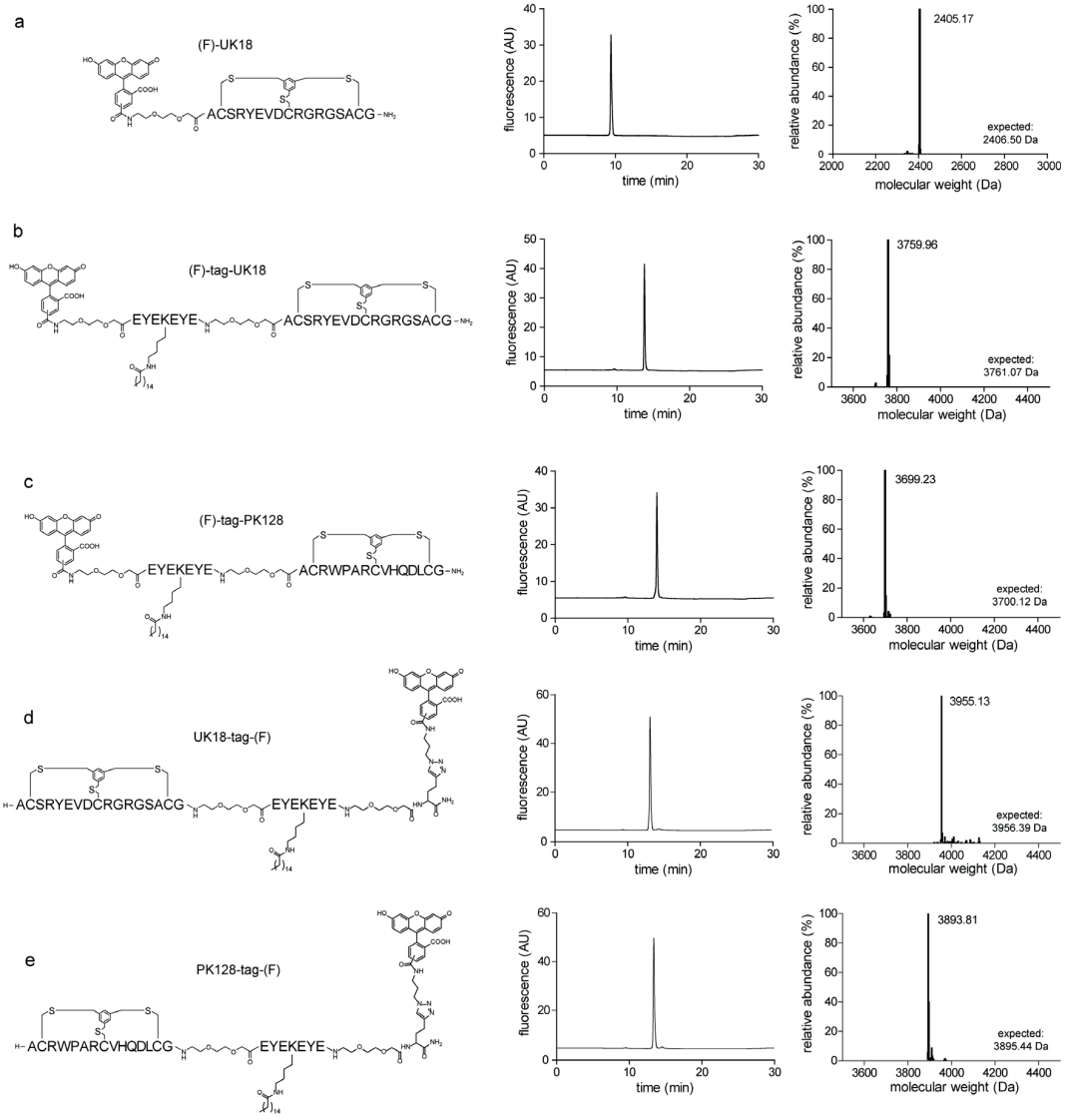

Figure 58. Characterization of UK18 and the four fluorescein labeled conjugates. Structure of the peptides (left panel), RP-HPLC chromatograms (central panel) and deconvoluted mass spectra (right panel) of (a) (F)-UK18, (b) (F)-tag-UK18, (c) (F)-tag-PK128, (d) UK18-tag-(F), and (e) PK128-tag-(F). Amino acids shown as single letter code; fluorescein, TBMB, PEG_2 and palmitic acid shown as structural formula. ▬ (dash) between (F), tag and bicyclic peptide is PEG_2.

The binding affinity of the fluorescein labeled conjugates was measured for human albumin, human serum, and rat albumin (Fig. 59). Compared to the (F)-tag alone, the N-tagged bicyclic peptides (Fig. 58b-c) bound human albumin with K_d values in the high nanomolar range (K_d of (F)-tag = 39 nM vs. K_ds of conjugates ≈ 150-200 nM), with a three to five-fold weaker binding affinity. The same extent of reduction was found for rat albumin (K_d of (F)-tag = 220 nM vs. K_d of conjugates ≈ 700-800 nM). The fluorescein labeled bicyclic peptide (F)-UK18 did not bind to albumin at all, and the same result can be expected for peptide (F)-PK128.

a

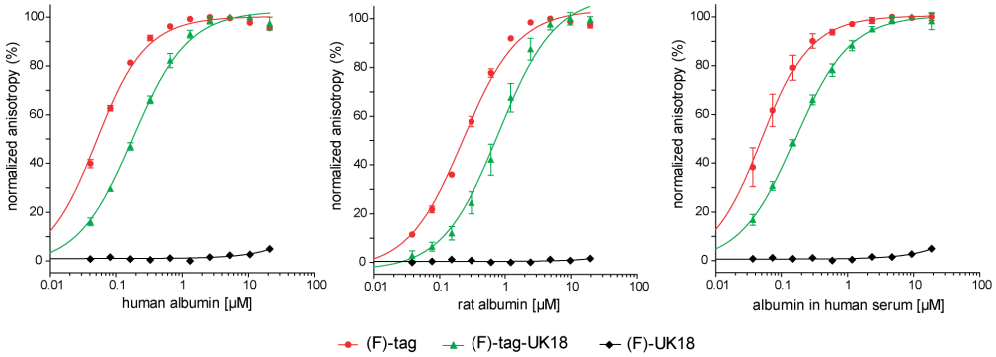

b

		albumin binding (K_d) [nM]		
		human albumin	rat albumin	human serum
(F)-tag	(F)-EYEK$_{palm}$EYE	39 ± 3	220 ± 30	37 ± 2
(F)-UK18	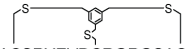 (F)-ACSRYEVDCRGRGSACG	> 100,000	> 100,000	> 100,000
(F)-tag-UK18	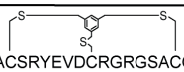 (F)-EYEK$_{palm}$EYE-ACSRYEVDCRGRGSACG	168 ± 13	780 ± 110	149 ± 6

c

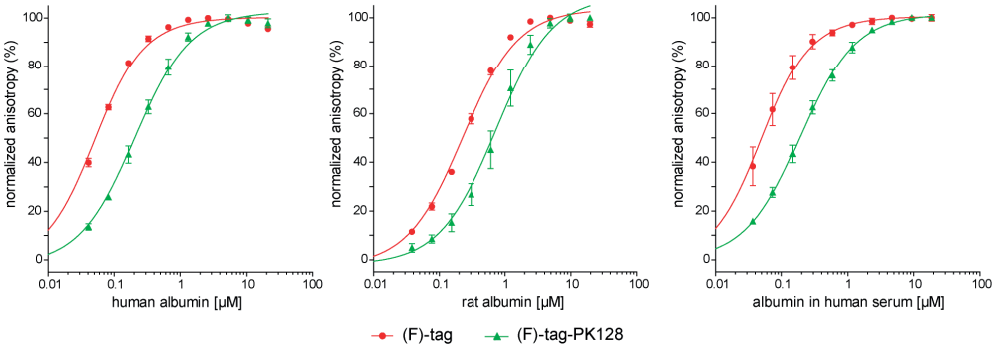

d

		albumin binding (K_d) [nM]		
		human albumin	rat albumin	human serum
(F)-tag	(F)-EYEK$_{palm}$EYE	39 ± 3	220 ± 30	37 ± 2
(F)-PK128	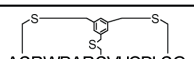 (F)-ACRWPARCVHQDLCG	n.d.	n.d.	n.d.
(F)-tag-PK128	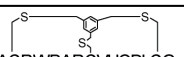 (F)-EYEK$_{palm}$EYE-ACRWPARCVHQDLCG	194 ± 16	720 ± 90	181 ± 5

Figure 59. Binding of (F)-tag, bicyclic peptides and N-tagged bicyclic peptides with different albumins. Fluorescence polarization isotherms with human albumin (left panel), rat albumin (middle panel) and human serum (right panel) of (a) UK18 and (c) PK128 conjugates. (b and d) Dissociation constants. Amino acids shown as single letter code; n.d. is not determined; (F) is fluorescein; palm is palmitic acid; ▬ (dash) between (F), tag and bicyclic peptide is PEG_2.

The solubility of the N-tagged bicyclic peptides chosen for pharmacokinetic studies was investigated in the physiological buffer PBS as described in sub-section 3.1.2. The presence of fluorescein allowed to determine peptide's concentration by measuring the absorbance at 495 nm, using a molar extinction coefficient equal to 68,000 $M^{-1} \cdot cm^{-1}$ (Thermo Scientific). The two conjugates (F)-tag-UK18 and (F)-tag-PK128 showed a good solubility of 1.23 ± 0.35 $mg \cdot ml^{-1}$ and 1.18 ± 0.18 $mg \cdot ml^{-1}$, respectively, which satisfied our needs, being higher than one $mg \cdot ml^{-1}$ (Fig. 60). Compared to the previous results (solubility of 1.8-3.0 $mg \cdot ml^{-1}$, sub-section 3.1.2), the slightly lower solubility can be explained with the introduction of fluorescein, which at the same time removed the N-terminal positive charge and introduced a hydrophobic moiety.

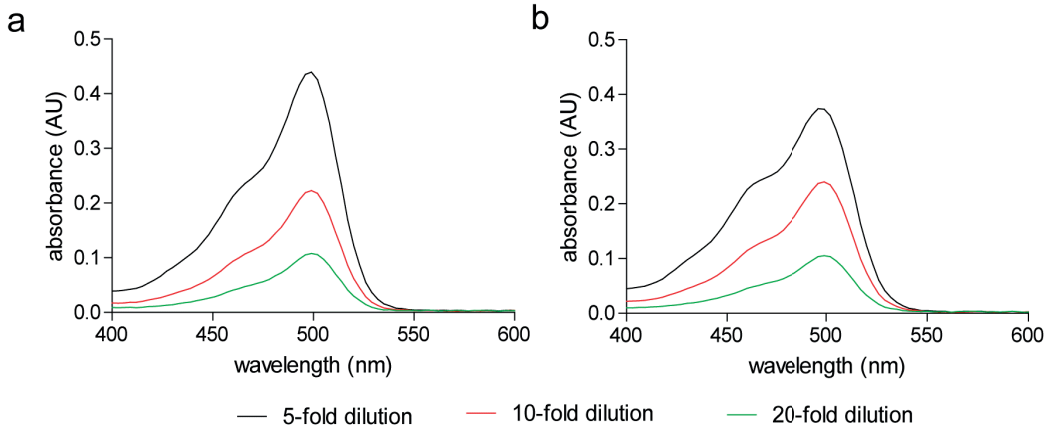

Figure 60. Solubility calculation of the N-tagged bicyclic peptides. Spectra of absorbance of (a) (F)-tag-UK18 and (b) (F)-tag-PK128. Average values of four measurements are indicated.

Fluorescence polarization assays of the C-tagged bicyclic peptides (Fig. 58d-e) showed a three to five-fold reduction of the binding affinities, similar to what previously measured for the N-tagged ones (Fig. 61). Thus, considering the higher K_d value of the tag-(F) peptide alone, the C-tagged bicyclic peptides bound albumin in the low micromolar range (K_d of tag-(F) = 1060 nM vs. K_d of conjugates ≈ 3-5 μM). As previously observed, this second format had a lower impact on the decrease of binding affinity for rat albumin.

These results underlined that the bicyclic peptides influenced the binding affinity of the tag for albumin to the same extent, independently from the site of conjugation. The best tag format labeled with fluorescein at the N-terminus, namely (F)-tag, did not show a dramatic loss in binding efficacy for albumin, giving an affinity still three and more than ten-fold better than albumin-binding peptide SA21 and acylated insulin analogues, respectively (sub-section 3.1.3). The main difference in affinity between the N- and C-tagged formats arose only from the position of fluorescein in the peptide sequence.

a

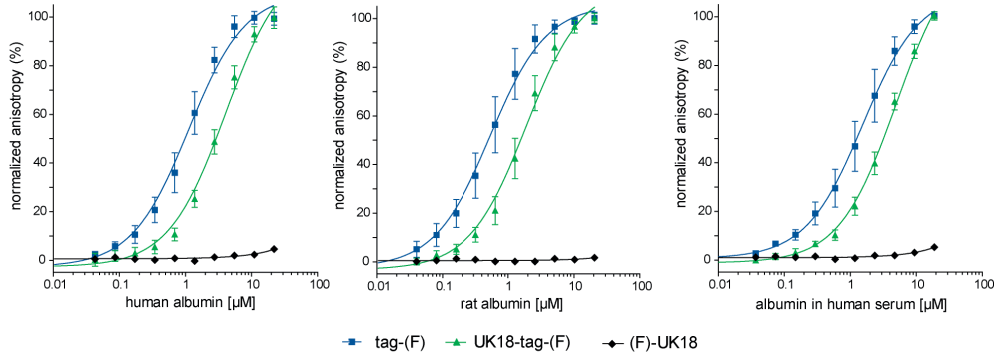

b

		albumin binding (K_d) [nM]		
		human albumin	rat albumin	human serum
tag-(F)	EYEK$_{palm}$EYE-(F)	1060 ± 140	500 ± 50	1520 ± 80
(F)-UK18	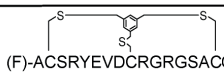 (F)-ACSRYEVDCRGRGSACG	> 100,000	> 100,000	> 100,000
UK18-tag-(F)	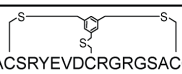 ACSRYEVDCRGRGSACG-EYEK$_{palm}$EYE-(F)	3900 ± 600	1800 ± 300	4900 ± 400

c

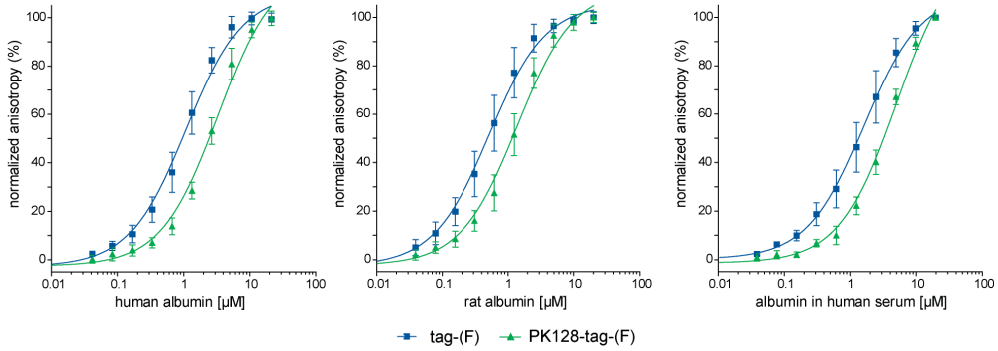

d

		albumin binding (K_d) [nM]		
		human albumin	rat albumin	human serum
tag-(F)	EYEK$_{palm}$EYE-(F)	1060 ± 140	500 ± 50	1520 ± 80
(F)-PK128	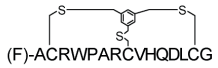 (F)-ACRWPARCVHQDLCG	n.d.	n.d.	n.d.
PK128-tag-(F)	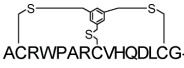 ACRWPARCVHQDLCG-EYEK$_{palm}$EYE-(F)	3200 ± 500	1330 ± 190	4700 ± 500

Figure 61. Binding of tag-(F), bicyclic peptides and C-tagged bicyclic peptides to different albumins. Fluorescence polarization isotherms with human albumin (left panel), rat albumin (middle panel) and human serum (right panel) of (a) UK18 and (c) PK128 conjugates. (b and d) Dissociation constants. Amino acids shown as single letter code; n.d. is not determined; (F) is fluorescein; palm is palmitic acid, ▬ (dash) between (F), tag and bicyclic peptide is PEG_2.

3.2.3 Inhibition of proteases

Acetylated tagged bicyclic peptides modified and purified once by HPLC gave conjugates with purity greater than 95% and again around 40% yield (Fig. 62c-f). The bicyclic peptides UK18 and PK128 were still available in the laboratory and used as references, after checking their purity and stability (Fig. 62a-b).

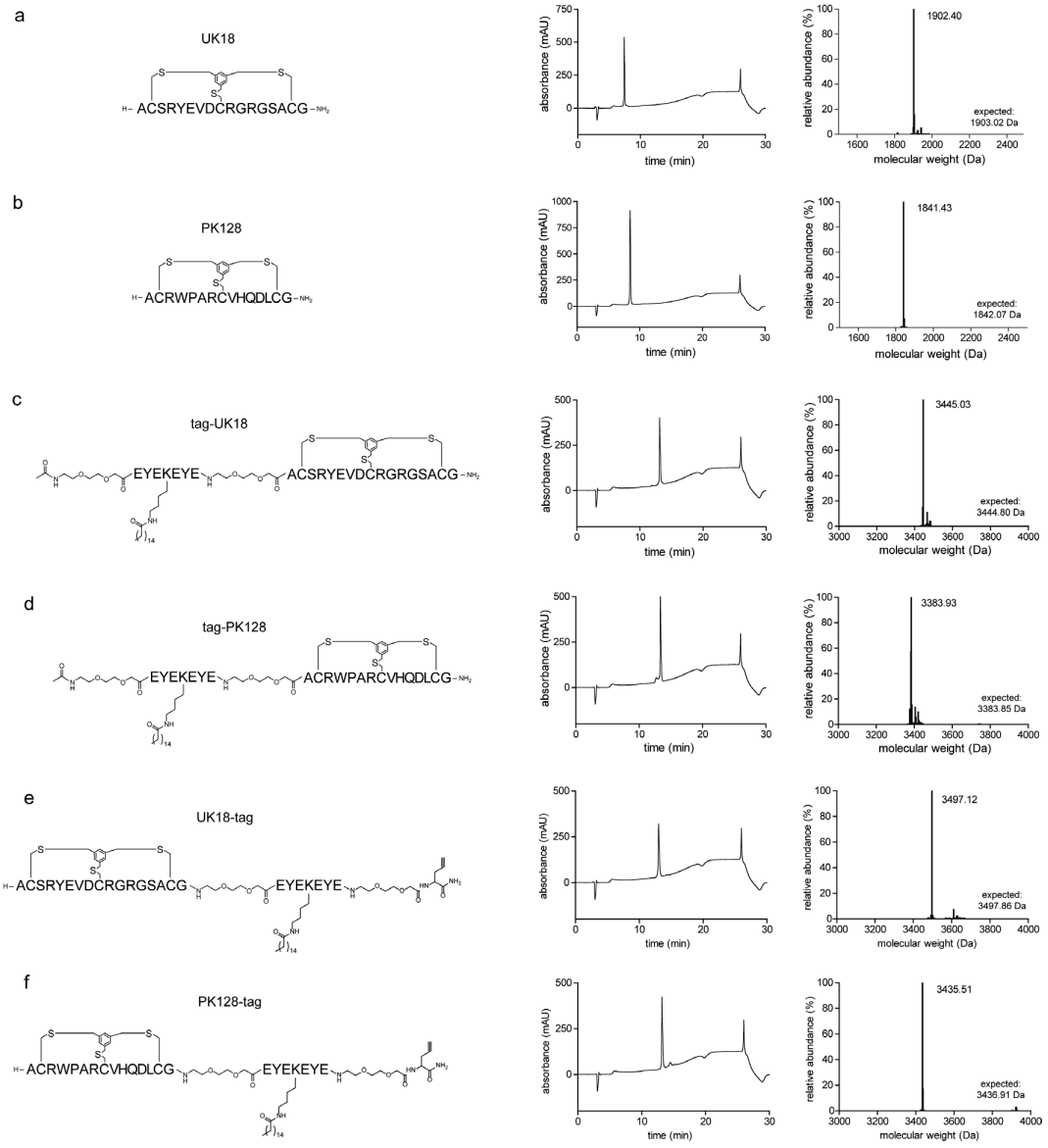

Figure 62. Characterization of UK18, PK128 and the four non-labeled conjugates. Structure of the peptides (left panel), RP-HPLC chromatograms (central panel) and deconvoluted mass spectra (right panel) of (a) UK18, (b) PK128, (c) tag-UK18, (d) tag-PK128, (e) UK18-tag and (f) PK128-tag. Amino acids shown as single letter code; propargylglycine, TBMB, PEG_2 and palmitic acid shown as structural formula.

The capacity of these four conjugates to inhibit their protease targets was assessed in inhibition assays. These assays were carried out by incubating the target proteases with different concentration of conjugates, and adding a fluorogenic substrate that is cleaved and emits accordingly to the percentage of enzyme not inhibited. IC_{50} values were graphically determined and, applying the Chang-Prusoff equation, the inhibition constants were calculated. In order to simulate the physiological situation in the plasma, where the tagged bicyclic peptides are supposed to inhibit their targets in presence of high concentrations of albumin, the assay was also performed in a buffer containing highly pure human albumin.[71]

a

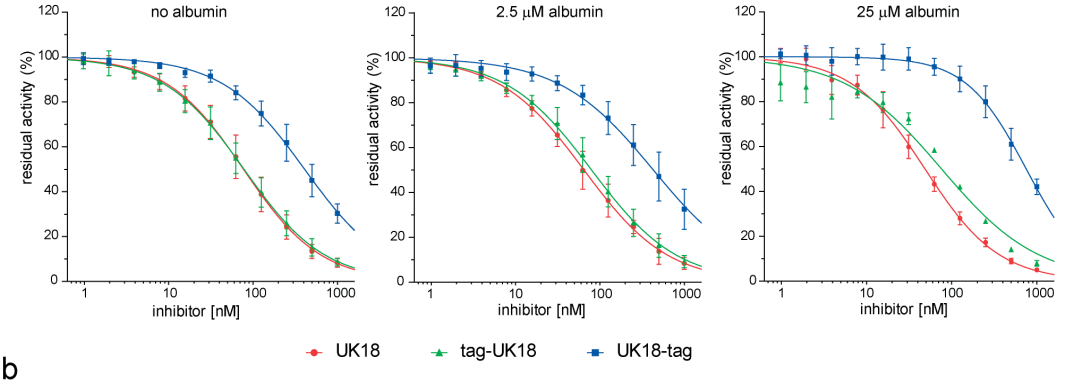

b

		inhibition of huPA (K_i) [nM]		
		in absence of albumin	in presence of albumin 2.5 μM	25 μM
UK18	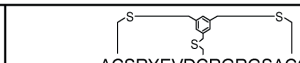 ACSRYEVDCRGRGSACG	55 ± 9	46 ± 14	34 ± 7
tag-UK18	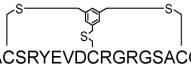 $EYEK_{palm}$EYE-ACSRYEVDCRGRGSACG	56 ± 15	57 ± 19	52 ± 7
UK18-tag	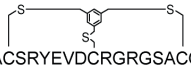 ACSRYEVDCRGRGSACG-$EYEK_{palm}$EYE	290 ± 50	320 ± 140	520 ± 80

Figure 63. Inhibition of UK18 and conjugates against uPA. (a) Graphs of enzymatic activity tested without albumin (left panel) or in presence of two different concentrations (2.5 μM, middle panel, and 25 μM, right panel). (b) Inhibition constants. Amino acids shown as single letter; palm is palmitic acid; **—** (dash) between tag and bicyclic peptide is PEG_2.

UK18 alone exhibited a K_i of 55 ± 9 nM against its target uPA (urokinase-type plasminogen activator), confirming the values already published (Fig. 63).[70] The N-tagged UK18 inhibited uPA with unchanged potency independently from the concentration of albumin. On the other hand, the C-tagged UK18 showed a five to ten-fold worse K_i values compared to the peptide alone (Fig. 63). Most likely, the presence of the tag reduced the accessibility of the second ring of the bicyclic peptide to the catalytic site,

and the effect was even amplified by albumin binding hindrance. These results confirmed the previous structural X-ray analysis that evidenced the involvement of the residues around the second ring, mainly Glu-8, Arg-10 and Arg-12, in making interactions with the target.[70]

a

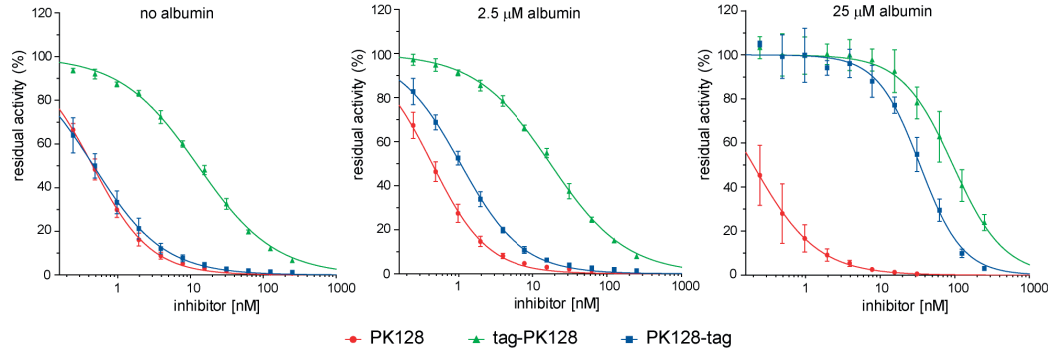

b

		inhibition of hPK (K_i) [nM]		
		in absence of albumin	in presence of albumin 2.5 μM	25 μM
PK128	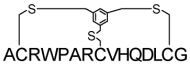 ACRWPARCVHQDLCG	0.35 ± 0.04	0.34 ± 0.08	0.18 ± 0.11
tag-PK128	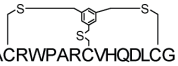 $EYEK_{palm}$EYE-ACRWPARCVHQDLCG	10 ± 1	13 ± 1	79 ± 18
PK128-tag	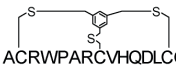 ACRWPARCVHQDLCG-$EYEK_{palm}$EYE	0.37 ± 0.11	0.81 ± 0.12	27 ± 5

Figure 64. Inhibition of PK128 and conjugates against PK. (a) Graphs of enzymatic activity tested without albumin (left panel) or in presence of two different concentrations (2.5 μM, middle panel, and 25 μM, right panel). (b) Inhibition constants. Amino acids shown as single letter; palm is palmitic acid; ▬ (dash) between tag and bicyclic peptide is PEG_2.

PK128 alone had the same K_i of 350 ± 40 pM reported in literature for its target PK (plasma kallikrein) (Fig. 64).[69] In contrast with UK18 conjugates, the N-tagged PK128 inhibited PK with a K_i value 30-fold weaker than the peptide alone, while the C-tagged PK128 had K_i value almost unchanged, suggesting that the N-terminal region of the bicyclic peptide is involved in the interactions with the binding pocket of the target. These results were not unexpected, since PK128 belongs to a consensus which was mainly conserved in the first peptide loop.[69] Both PK128 conjugates showed an increase in the K_i values when tested in presence of albumin (2.5 or 25 μM). With the highest albumin concentration used, the reduction in the activity was around 200-fold for the N-tagged bicyclic peptide, and 80-fold for the C-tagged one (Fig. 64). These results confirmed that the introduction of the tag at the N-terminus sterically hindered the inhibition of plasma

kallikrein more than in the C-terminal format, and this effect was further enhanced when the tag was bound to albumin.

In conclusion, the tag differently influenced peptide activity according to the position in which it was appended. Only for UK18, the N-terminal tagged format presented unchanged potency in all of the experimental conditions tested. This specific case was quite promising since that conjugate had also the best albumin binding format with the N-terminus labeled with fluorescein. In contrast, PK128 showed a more significant decrease in its activity in the same N-terminal format, underlying how the effects of the tag positioning are peptide-dependent and cannot be easily predicted.

3.2.4 Inhibition of the intrinsic coagulation pathway

The potency of PK128 and its conjugates was further assessed by measuring their capacity to prolong the activated partial thromboplastin time (aPTT), which is the time required for plasma to coagulate upon external activation of the intrinsic coagulation pathway.[80] Plasma kallikrein plays an important role in this pathway, and its blocking might be used as enhancer in the treatment of thrombosis and related diseases.[82] The aPTT of the tagged bicyclic peptides was determined *ex vivo* by incubating different concentrations of conjugates in plasma and triggering the coagulation with $CaCl_2$ (Fig. 65).

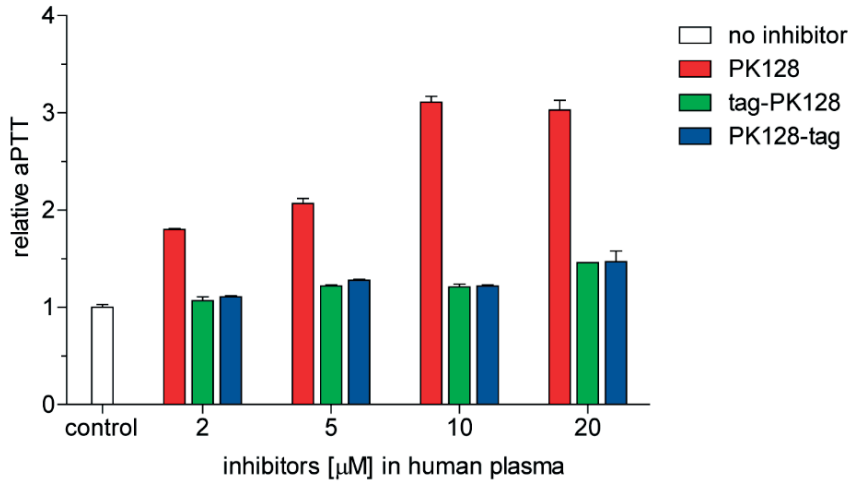

Figure 65. Coagulation parameter aPTT for PK128 and conjugates in human plasma. Peptide's activity was measured upon incubation at 37°C with human plasma and pathromtin; coagulation was triggered by $CaCl_2$.

The bicyclic peptide alone prolonged the aPTT in a concentration dependent manner, and the concentration needed to get a doubling of the coagulation time (EC_{2x}) was equal to 5 μM. In contrast, the two conjugates did not strongly prolong the coagulation

time and the estimated EC_{2x} was much higher than 20 μM. The reduced effect on the coagulation pathway correlated with the lower inhibitory activity measured for both conjugates in presence of albumin. Because of these negative results, aPTT tests were not performed with rat plasma, which I initially wanted to use as animal model in a PK-related inflammatory study of carrageenan-induced paw edema.[252] PK128 conjugates were kept, together with the UK18 ones, as models for pharmacokinetic studies in rats.

3.2.5 Plasma stability of tagged bicyclic peptides

The stability of the tagged bicyclic peptides UK18 and PK128 in blood plasma was assessed with an assay previously developed in our laboratory, in which peptides are firstly incubated in plasma, and then their residual activity is quantified by inhibition assays.[91] The test has the aim to reveal the fraction of peptide and/or its metabolic derivatives that are still functional and could efficiently inhibit the target, independently from the proteolytic events that might have already occurred (e.g. removal of terminal amino acids or ring opening). Tagged bicyclic peptides were incubated for two days in human plasma at 37°C and samples were collected at eight different time points. Before analyzing the samples, plasma was diluted in assay buffer and heat-inactivated to avoid nonspecific cleavage activity of other blood proteases on the fluorogenic substrate. The inhibition constant measured for the first time point was considered as reference for the maximum percentage of residual activity, and all of the other values were calculated accordingly.

The unmodified bicyclic peptides showed strong differences in their stability. Half of the bicyclic peptide UK18 was still active after one day ($t_{1/2}$ = 34.9 ± 9.8 hrs) (Fig. 66a), while PK128 was completely inactivated in few hours ($t_{1/2}$ = 1.8 ± 0.3 hrs) (Fig. 66b). The relatively good plasma stability of UK18 confirmed previous observations according to which the fraction of intact peptide after 24 hours was still a 40% of the starting amount.[71] In contrast, all of the tagged bicyclic peptides were fully functional and resistant to proteases for more than two days. The improvement in terms of stability was more pronounced for PK128 (> 25-fold), and the strong protective effect on its degradative pattern was most likely associated to the binding to albumin, as already well documented for the GLP-1 analogue Liraglutide.[253]

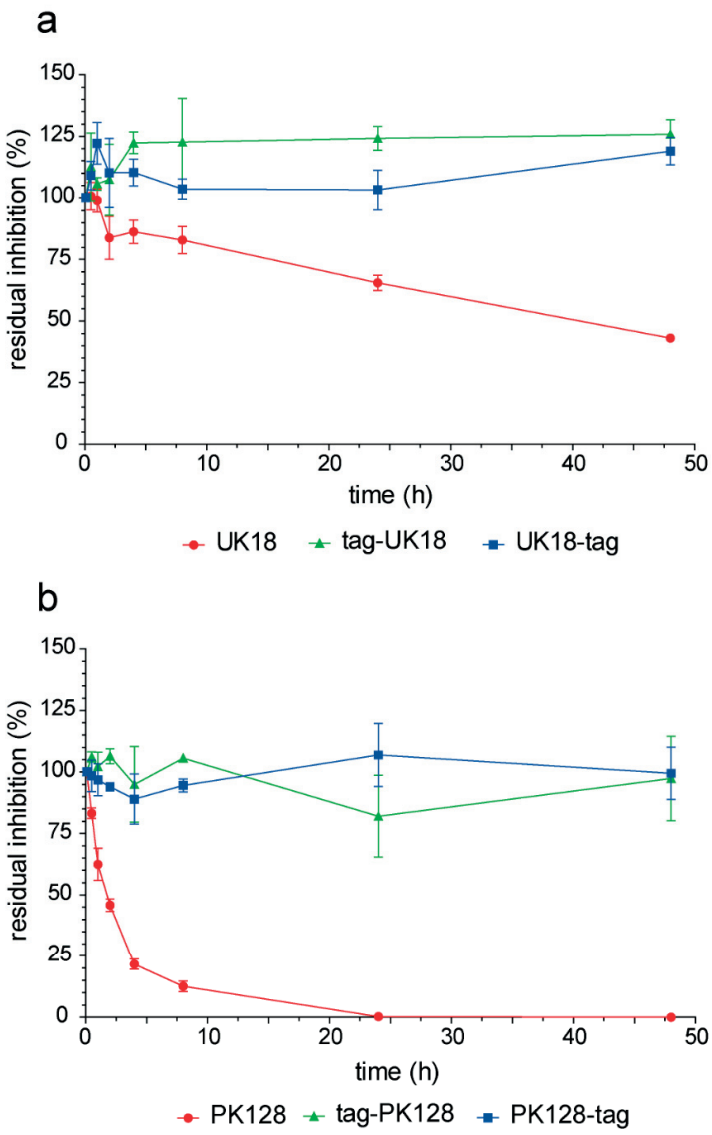

Figure 66. Stability of bicyclic peptides and conjugates in human plasma. The percentage of peptide still active at the different time points determined as ratio with the initial inhibition constant (K_i(t=5min)/K_i(t=Xmin)*100) for (a) UK18 and conjugates and (b) PK128 and conjugates.

3.2.6 Pharmacokinetics in rats

Pharmacokinetic experiments were carried out in rats to test the elimination half-life of the two N-terminal tagged bicyclic peptides PK128 and UK18, tag and UK18 alone. The *in vivo* studies (injection and blood collection) were performed by the American company Washington Biotechnology, Inc. (Baltimore, MD, USA). Peptides had purity higher than 95% and they were prepared as 10 mM stocks in DMSO. Intravenous administrations (200 μl) were performed after dilution of the peptide stocks in PBS, pH 7.4, 0.01% SDS to a final concentration of 130 μM. The relative doses were 0.5 mg·kg^{-1} for tagged

bicyclic peptides, 0.3 mg·kg^{-1} for UK18 and 0.25 mg·kg^{-1} for tag. Three rats for each peptide were used, blood samples collected at eight different time points, processed to plasma and sent to us for further analyses.

3.2.6.1 Detection and quantification of peptides in plasma

Peptide quantification in plasma samples was performed using a HPLC system coupled to a fluorescence detector, after applying an optimized protein precipitation protocol. These experiments required the setting of the proper excitation wavelength for fluorescein, which was different in the acidic condition used in HPLC, and the investigation of the detection limit of the instrument.

Fluorescein has four different ionic forms according to the pH of the solution in which it is dissolved, and each of them presents a pH-dependent spectrum of absorption. At physiological pH, the main form is the di-anionic fluorescein, with quantum yield of 0.93 and the strongest maximum absorbance at 490 nm. Solvents used in HPLC are commonly prepared at acidic pH adding trifluoroacetic acid. At this pH, fluorescein is either in its neutral or cationic format, with lower quantum yield (0.31 and 0.17, respectively) and maximum absorbance at around 440 nm.[254] In contrast, fluorescein emission spectra are pH-independent with a maximum between 520-530 nm, and only the signal intensity varies as function of the excitation wavelength used.[255] These results were experimentally confirmed by measuring absorption and emission spectra of fluorescein in different conditions (Fig. 67).

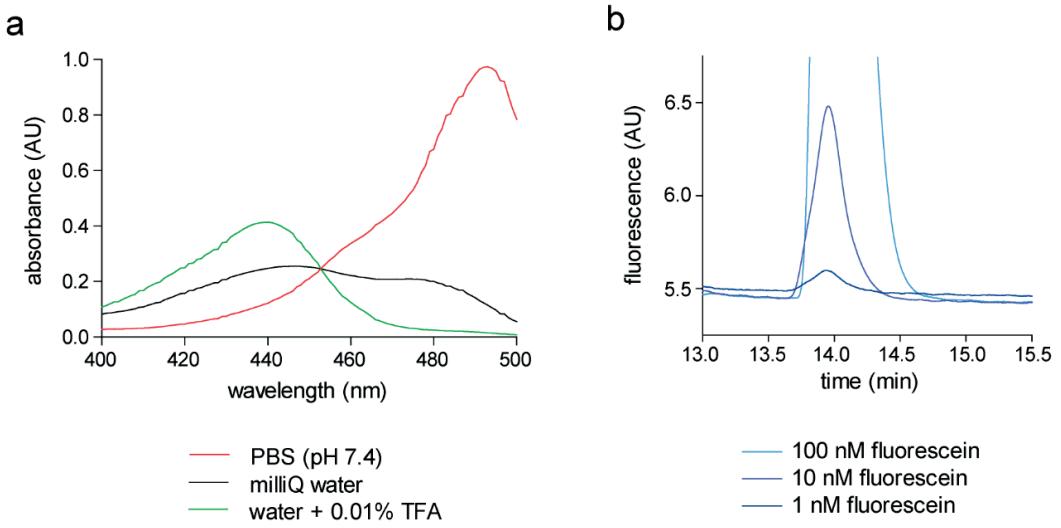

Figure 67. Absorption and HPLC detection limits of fluorescein. (a) Absorbance of a fixed concentration of fluorescein prepared in three solvents with different pH. (b) Chromatograms of different concentrations of fluorescein run RP-HPLC buffer (water + 0.01% TFA) with excitation at 445 nm and emission at 535 nm.

At pH 7.4 fluorescein confirmed its maximum absorbance at 490 nm. In contrast, this parameter was lower and shifted to 440-450 nm when fluorescein was diluted in HPLC solvent (pH 2.0) or milliQ water (pH 5.0). At nearly 460 nm fluorescein presented its characteristic isosbestic point, with an equal absorption for all of the pH values (Fig. 67a).[255] The maximum emission was in the expected range at around 535 nm for all the conditions tested (data not shown). The sensitivity in HPLC was checked running a fluorescein dilution series up to 1 nM and setting the detector at 445 and 535 nm as excitation and emission wavelengths, respectively. In this condition, a clear area under the curve (AUC) was visible also for the lowest concentration used, indicating a detection limit sufficient for evaluating concentrations in the single digit nanomolar range (Fig. 67b). All the following HPLC experiments were run by applying this optimized setting.

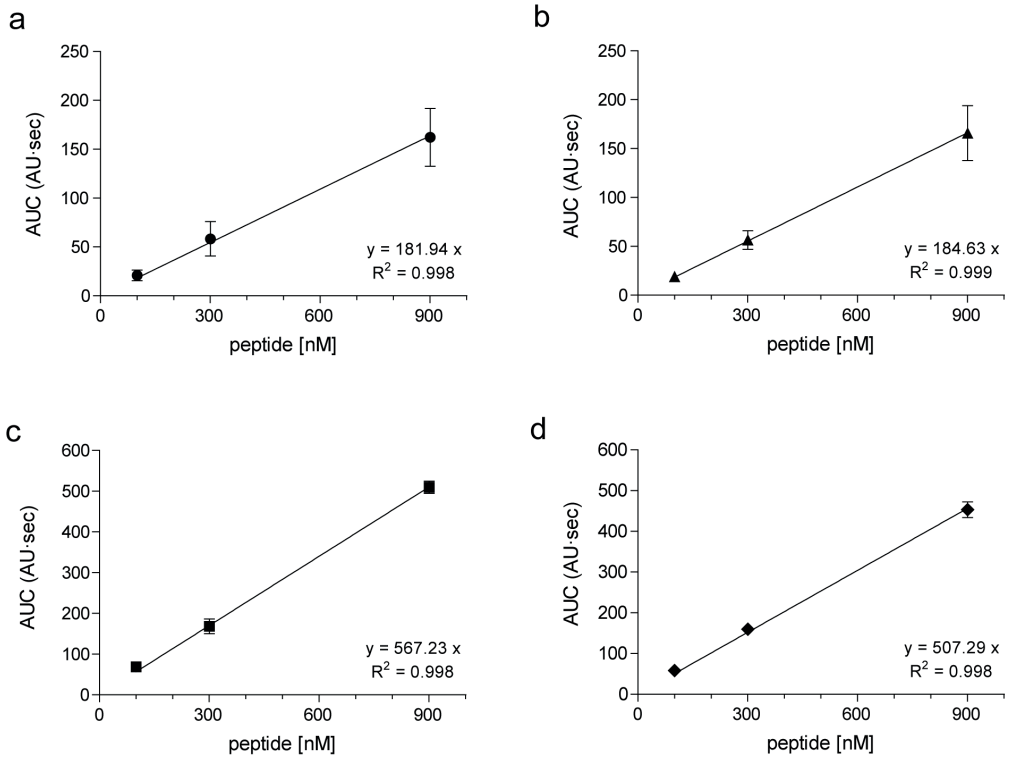

Figure 68. Calibration curves for pharmacokinetic studies. Linear regression calculation of the four peptides (a) (F)-tag-UK18 (a), (b) (F)-tag-PK128, (c) (F)-tag and (d) (F)-UK18.

A new protocol of protein precipitation was developed for detecting fluorescein labeled peptides in plasma. Plasma proteins had to be first denatured using the chaotropic agent guanidinium hydrochloride, able to disrupt the structure of proteins and to enhance consequently the release of the tag bound to albumin. Proteins were then precipitated with cold ethanol and removed by centrifugation. The supernatant containing the peptide was dried under vacuum and then dissolved for HPLC analysis. Before the precipitation

step, a fixed concentration of fluorescein as internal standard had been added in each sample in order to adjust later the AUCs of the peptides. Quantification of the peptides after each precipitation protocol showed an average recovery higher than 90% compared to the same peptide concentrations freshly prepared in buffer. Following this procedure, calibration curves were prepared using serial dilutions of each fluorescein labeled peptides in rat plasma and later used for peptide quantification (Fig. 68).

3.2.6.2 Plasma half-life in rats

The zoomed chromatograms of the four peptide formats tested in each rat are here reported (Fig. 69 and 70), while whole HPLC runs are shown in the supporting information (Fig. S1-S4). The conjugate (F)-tag-UK18 showed a single peak in all the samples, and it was visible in plasma for more than 24 hours (Fig. 69a). The absence of degradation products proved the protective effect of the conjugation. In contrast, the conjugate (F)-tag-PK128 had a faster clearance from the blood, with the last detectable peak at eight hours (Fig. 69b). Starting from the one hour time point, a small peak eluting before the intact peptide was observed, probably due to a proteolytic event. However, the fraction was not taken into account for peptide quantification due to its negligible size.

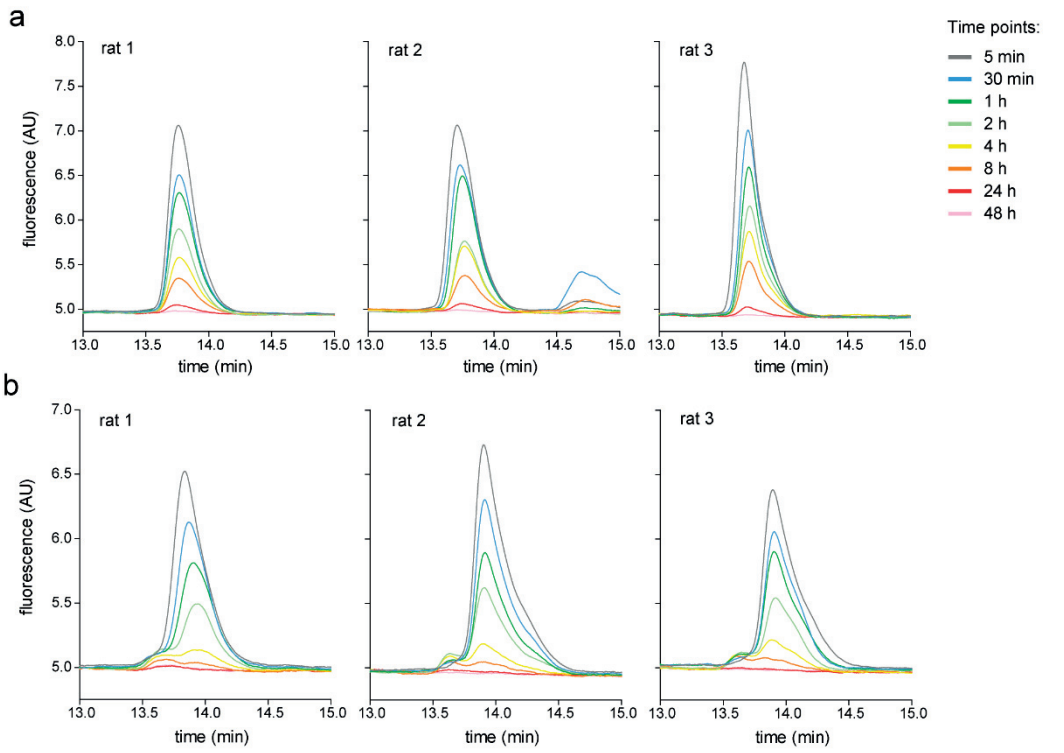

Figure 69. RP-HPLC chromatograms of N-tagged bicyclic peptides. Chromatograms of plasma samples for (a) (F)-tag-UK18 and (b) (F)-tag-PK128. An extra peak observed for (F)-tag-UK18 in the central panel was coming from plasma and suggested an incomplete protein precipitation step.

The (F)-tag alone was clearly present in rat plasma up to 48 hours and, despite its linear format, it was fully intact thanks to the high affinity for albumin that hindered it from proteases (Fig. 70a). In addition, the branched fatty acid in the middle of the sequence probably offered an extra protection, as already observed for peptides synthesized in dendrimeric formats.[256] In contrast, the bicyclic peptide (F)-UK18 was fully cleared from the blood circulation in less than one hour, and 80% was partially degraded within four minutes (Fig. 70b). However, the residual inhibitory activity of UK18 in plasma had a much longer duration ($\tau_{1/2}$ = 34.9 ± 9.8 hrs) than its clearance time *in vivo*. Therefore, the whole peak was used for the quantification, considering the peptide, even if partially degraded, still functional.

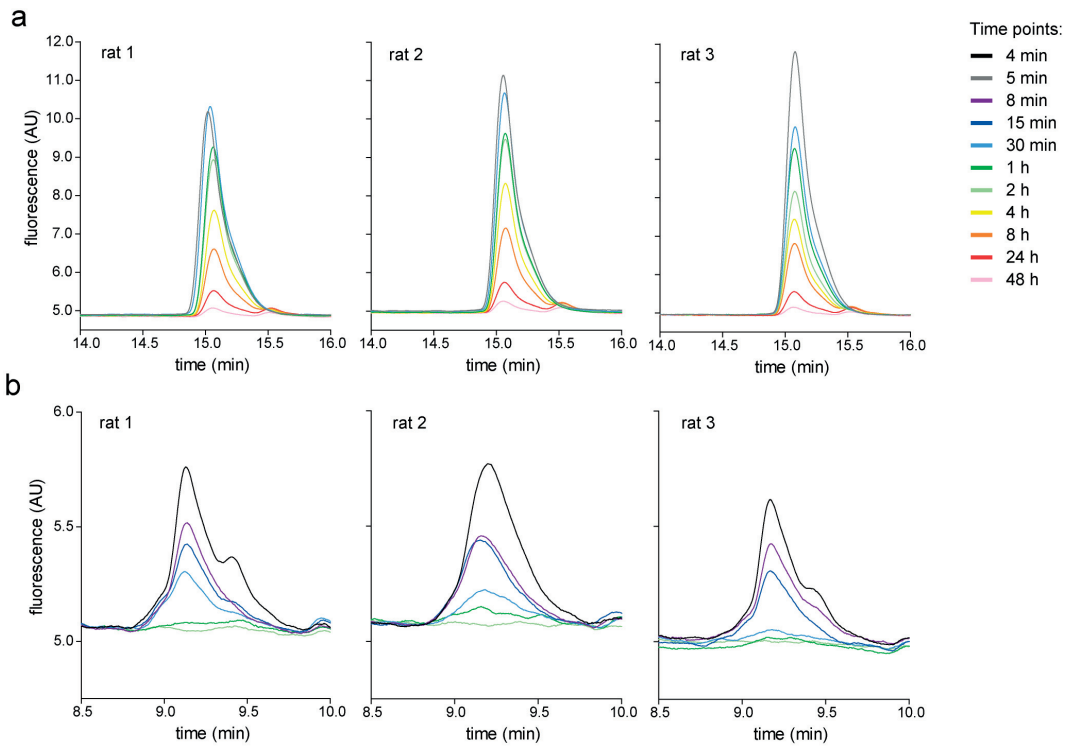

Figure 70. RP-HPLC chromatograms of tag and bicyclic peptide UK18. Chromatograms of plasma samples for (a) (F)-tag (a) and (b) (F)-UK18.

The metabolic stability of the bicyclic peptide UK18 was further investigated *ex vivo* in rat plasma to understand its pattern of degradation. The peptide was incubated at 37°C for 72 hours, the plasma proteins were precipitated and the peptide analyzed by HPLC and LC-MS (Fig. 71a-b). Both chromatograms had the same pattern of the *in vivo* samples, with a peak eluting before the intact peptide. Mass analyses revealed that this first peak contained two UK18 fragments with either hydrolysis or loss of a Gly residue. Considering the degradation pattern already studied for UK18 when incubated in human

plasma[71], I speculated that the second ring opened between Arg12 and Gly13 and, afterward, the Gly residue was cleaved (Fig. 71c).

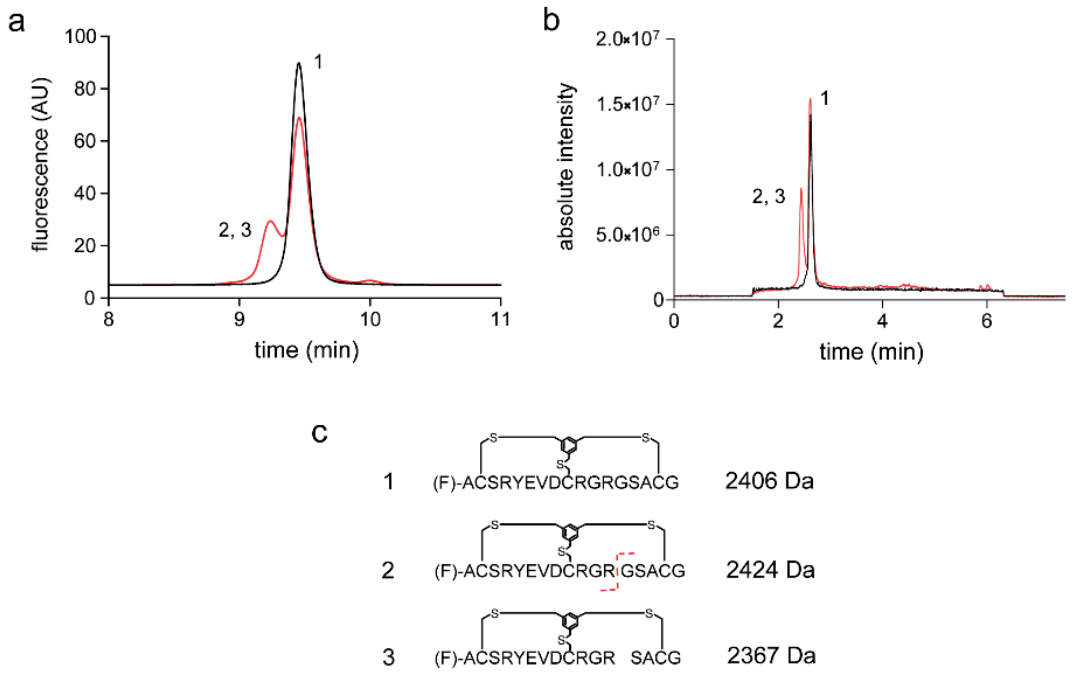

Figure 71. Plasma stability of (F)-UK18. Chromatograms of intact (black) and incubated (red) peptide in rat plasma analyzed by (a) RP-HPLC and (b) LC-MS chromatograms. (c) Masses detected in the indicated peaks and potential structures of peptide fragments corresponding to the masses. Amino acids shown as single letter code; (F) is fluorescein; ▬ (dash) between (F) and bicyclic peptide is PEG_2.

Using the calibration curves previously prepared, the AUCs of each time point were converted in concentrations. Blood processing to plasma after collection halves its volume, thus if a peptide distributes only in plasma should double its concentration. The concentrations of the tag and the N-tagged bicyclic peptides after five minutes were almost the double of the theoretical values in blood upon i.v. injection, suggesting that these peptides stayed mainly in plasma due to their binding to albumin. In addition, this result showed that the recovery of the peptides from plasma in each protein precipitation step was quantitative. In contrast, the bicyclic peptide UK18 showed a six-fold lower plasma concentration, indicating a fast distribution and/or elimination. The concentrations were plotted versus time and analyzed with a two-compartment model (biexponential equation: $C_p = A \cdot e^{-\alpha \cdot t} + B \cdot e^{-\beta \cdot t}$). Pharmacokinetic parameters were determined as reported in literature (Fig. 72), and a table with the equations used is reported in the supporting information (Tab. S1). [257]

a

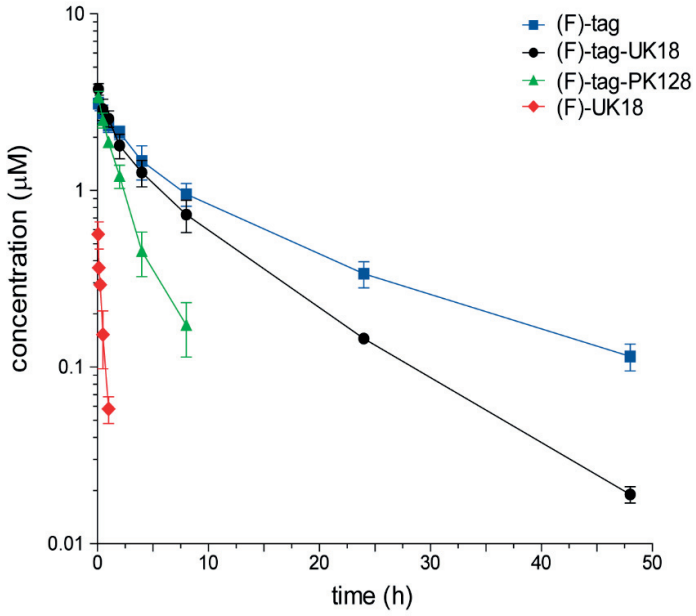

b

PARAMETERS (unit)	(F)-tag	(F)-UK18	(F)-tag-UK18	(F)-tag-PK128
$\tau_{1/2}\alpha$ (hrs)	1.5 ± 0.4	n.d.	1.0 ± 0.1	0.9 ± 0.2
$\tau_{1/2}\beta$ (hrs)	12.3 ± 0.4	0.30 ± 0.02	7.4 ± 0.2	2.9 ± 0.7
AUC ($mg \cdot min \cdot ml^{-1}$)	3.2 ± 0.5	0.034 ± 0.004	4.6 ± 0.6	1.7 ± 0.3
CL ($ml \cdot hrs^{-1} \cdot kg$)	4 ± 1	500 ± 70	7 ± 1	18 ± 4
V_D ($ml \cdot kg^{-1}$)	74 ± 13	200 ± 40	77 ± 12	76 ± 7

Figure 72. Pharmacokinetic profiles in rats. (a) Plasma concentrations plotted versus time upon i.v. injections. (b) Table with the parameters calculated for each peptide; (F) is fluorescein; ▬ (dash) is PEG_2.

The two tagged bicyclic peptides and the tag alone presented similar distribution half-lives of around one hour, but they were cleared differently. Tagged UK18 showed an elimination half-life of 7.4 ± 0.2 hours, while tagged PK128 had a shorter half-life of 2.9 ± 0.7 hours, that might be partially caused by the small proteolytic process observed (Fig. 69b). Instead, the tag alone had a longer elimination half-life of 12.3 ± 0.4 hours, which is related to its four-fold higher binding affinity for rat albumin (K_d of (F)-tag = 220 nM vs. K_d of conjugates ≈ 700-800 nM). The short half-life of the bicyclic peptide UK18 was approximately 18 ± 1 min, confirming the fast clearance previously observed in mice experiments.[71] This value for UK18 was confirmed comparing the injected dose and the back extrapolated amount of peptide in plasma after i.v. injection (C_{p0}), which resulted to

be again six-fold lower. In contrast, the C_{p0}s of the tagged bicyclic peptides were consistent with the injected doses. In conclusion, the N-terminal tag prolonged the circulation time and preserved the stability of UK18 of around 25-fold to over seven hours in rats.

Scientific literature and EMA reported a plasma half-life of only three to four hours for liraglutide and insulin deglutec upon s.c. injection in rats.[253,258,259] Therefore, considering the different route of administration used in our *in vivo* studies and the high protection of the conjugation, the tagged bicyclic peptides resulted more promising in the same animal model, and they might translate in a terminal half-life of several days in human.

Other important parameters calculated from the biexponential equation were the area under the curve (AUC), the clearance (CL) and the volume of distribution (V_D) (Fig. 72b). The AUC is used to quantify the fraction of a drug that reaches and stays in the plasma, and thus could exert its biological effect. As expected, it correlated with the half-lives and showed, for example, that the tagged UK18 would be 100-fold more active than the non-tagged bicyclic peptide *in vivo*.

The CL expresses the volume of plasma which is purified from a drug in a certain period: higher values of CL indicates a faster removal and a shorter elimination half-life. The peptide with the shortest half-life, UK18, had a clearance of half-liter per hour, while all the other peptides were cleared only few milliliters in the same unit of time.

Finally, the V_D describes the volume in which a drug distributes in the total body. It is commonly related to the weight, which was on average 200 grams for the rats used in our experiments. Considering this aspect, the V_D of the tag and the tagged bicyclic peptides was approximately 15 ml, consistent with the blood volume of the rats. This definitively proved that the tagged bicyclic peptides distributed mainly in the bloodstream, where they were fully bound to albumin. In contrast, the V_D of UK18 was much higher due to a fast and non-specific tissue distribution.

3.3 – Application of the albumin-binding tag to a FXII inhibitor for therapeutic use

The high affinity peptide-fatty acid tag was finally applied to a promising version of a highly specific inhibitor of FXIIa previously developed in our laboratory (sub-section 1.1.6).[81,90,91] The newly developed FXII inhibitor displayed an excellent inhibitory activity, target selectivity and plasma stability, with a K_i value of around 300-500 pM. However, pharmacokinetic studies in rabbits revealed that its half-life was too short to efficiently exert its pharmacological activity *in vivo* (unpublished data). Therefore, I initially synthesized a few conjugates carrying the tag at the N-terminus, but I observed a strong reduction in the inhibitory activity against FXIIa in both enzymatic and coagulation assays. Subsequently, I tested conjugates with different combinations of linker lengths between the bicyclic peptide and the tag, and I changed the positioning of the tag. The aim was to retain FXIIa inhibitory activity and exploit the tag binding format with the highest affinity for albumin. Among the various combinations, the most active conjugate was i.v. injected in rabbits and it demonstrated that the conjugation prolonged the half-life of the inhibitor and allowed an efficient blocking of the intrinsic coagulation pathway.

3.3.1 First generation: tag at the N-terminus

The first conjugates were synthesized by appending the tag at the N-terminus of the bicyclic peptide FXII inhibitor and varying the length of the linker in between, which was composed of a single Gly or an increasing number of short PEG_2 units up to five copies. The tag was modified at the N-terminus with either fluorescein for the binding assay or an acetyl group for the inhibition assay to avoid interference with the fluorogenic substrate. This step was followed by deprotection of Lys(Dde) and acylation of its free amine with palmitic acid. After cleveage from the resin, the FXII inhibitor was cyclized with TATA in a mixture of MeCN and aqueous buffer, and then purified by HPLC. The presence of the desired conjugates was confirmed by mass spectrometry and the purity assessed by analytical HPLC (Fig. 73 and 75).

3.3.1.1 Albumin binding

Fluorescein labeled conjugates (Fig. 73) were used in fluorescence polarization assays to measure the binding affinity for human albumin in serum and for rabbit albumin

(Fig. 74). Rabbits were chosen for *in vivo* studies due to i) an easier quantification of the intrinsic coagulation time, since the inhibition of FXIIa in rabbit plasma affects the aPTT to a larger extent compared to other animal plasma (unpublished data), and ii) the possibility to collect big volumes of plasma, being rabbit the animal model with the highest blood volume among all the commonly used rodents.

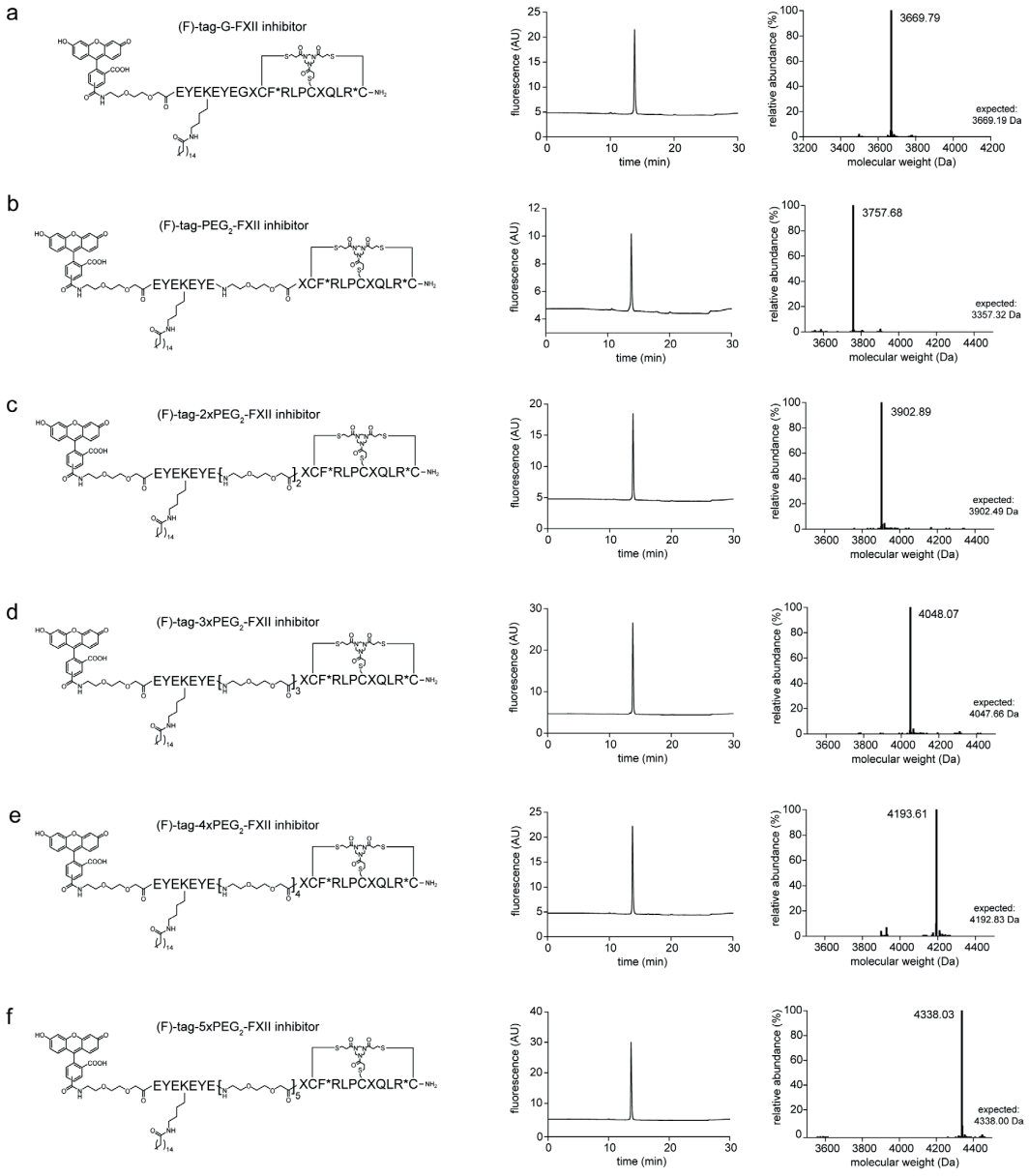

Figure 73. Characterization of the first-generation of fluorescein labeled FXII inhibitor conjugates. Structure of the peptides (left panel), RP-HPLC chromatograms (central panel) and deconvoluted mass spectra (right panel). Amino acids shown as single letter code; F* and R* represent p-fluoro Phe and β-homo Arg, respectively; X represents unnatural amino acid newly substituted; fluorescein, TATA, PEG_2 and palmitic acid shown as structural formula.

a

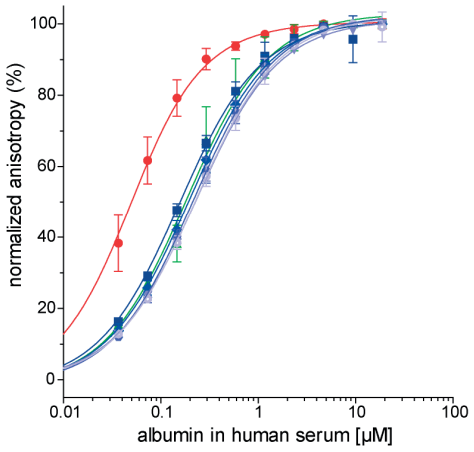

b

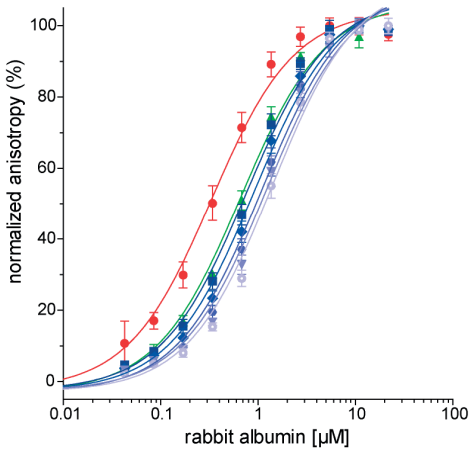

(F)-tag
(F)-tag-G-FXII inhibitor
(F)-tag-2xPEG$_2$-FXII inhibitor
(F)-tag-4xPEG$_2$-FXII inhibitor
(F)-tag-PEG$_2$-FXII inhibitor
(F)-tag-3xPEG$_2$-FXII inhibitor
(F)-tag-5xPEG$_2$-FXII inhibitor

c

		albumin binding (K_d) [nM]	
		human serum	rabbit albumin
(F)-tag	(F)-EYEK$_{palm}$EYE	37 ± 2	320 ± 40
(F)-tag-G-FXII inhibitor	 (F)-EYEK$_{palm}$EYEGXCF*RLPCXQLR*C	173 ± 19	650 ± 80
(F)-tag-PEG$_2$-FXII inhibitor	 (F)-EYEK$_{palm}$EYE-PEG$_2$-XCF*RLPCXQLR*C	145 ± 9	740 ± 100
(F)-tag-2xPEG$_2$-FXII inhibitor	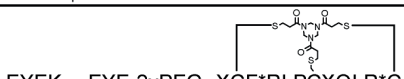 (F)-EYEK$_{palm}$EYE-2xPEG$_2$-XCF*RLPCXQLR*C	185 ± 6	890 ± 120
(F)-tag-3xPEG$_2$-FXII inhibitor	 (F)-EYEK$_{palm}$EYE-3xPEG$_2$-XCF*RLPCXQLR*C	205 ± 8	1080 ± 150
(F)-tag-4xPEG$_2$-FXII inhibitor	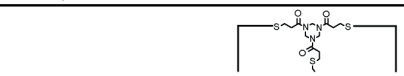 (F)-EYEK$_{palm}$EYE-4xPEG$_2$-XCF*RLPCXQLR*C	218 ± 3	1220 ± 190
(F)-tag-5xPEG$_2$-FXII inhibitor	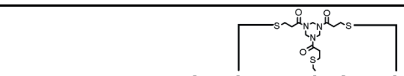 (F)-EYEK$_{palm}$EYE-5xPEG$_2$-XCF*RLPCXQLR*C	219 ± 7	1400 ± 200

Figure 74. Binding of (F)-tag and the first-generation of fluorescein labeled FXII inhibitor conjugates with different albumins. Fluorescence polarization isotherms with (a) human serum and (b) rabbit albumin. (c) Dissociation constants. Amino acids shown as single letter code; F* and R* represent p-fluoro Phe and β-homo Arg, respectively; X represents unnatural amino acid newly substituted; (F) is fluorescein; palm is palmitic acid; ▬ (dash) between (F) and tag is PEG_2.

The first-generation of fluorescein labeled conjugates bound human albumin in serum in the high nanomolar range (K_d of (F)-tag = 37 nM vs. K_ds of conjugates ≈ 150-220 nM), showing a three to five-fold decrease compared to the (F)-tag alone (Fig. 74a). The longer the linker between the tag and the bicyclic peptide, the stronger the negative impact was on albumin binding affinity of the tag. This trend was confirmed with rabbit albumin. The (F)-tag alone showed a K_d of 320 ± 40 nM, around nine-fold weaker than for human albumin. Conjugates with the shortest linkers (Gly and single PEG_2) showed the best binding, with only a factor two decrease in affinity (K_ds of conjugates ≈ 500-750 nM). As the number of PEG_2 units increased, the binding affinity for rabbit albumin dropped to a K_d value of 1.4 μM for the conjugate with the longest linker (Fig. 74b). However, the three to five-fold of affinity reductions were consistent with the results obtained in human serum.

3.3.1.2 Inhibition of FXIIa

The acetylated conjugates (Fig. 75) were tested for inhibitory activity against FXIIa both in presence and absence of human albumin (Fig. 76). While establishing the activity assay conditions, I found out that the fluorogenic substrate used for FXIIa was sensitive to traces of proteases present in the commercially available human albumin. This determined a reduction in the concentration of albumin to add in the buffer from 25 to 10 μM, and an increase in the enzyme concentration in order to ensure a clear signal over the non-specific background. The K_i value of the bicyclic peptide FXII inhibitor measured in absence of albumin was used as reference for comparison with the conjugates.

The FXII inhibitor alone showed the expected high picomolar inhibition constant (K_i = 0.46 ± 0.08 nM) (unpublished data). As observed for PK128 conjugates (sub-section 3.2.3), the K_i value of the FXII inhibitor was reduced when conjugated to the tag. Interestingly, the results showed that the distance between tag and FXII inhibitor played a crucial role, with conjugates having longer linkers that presented better K_i values. In absence of albumin, there was a 14-fold decrease in inhibitory activity for the conjugate with the longest linker (5xPEG_2, K_i = 6.6 ± 1.8 nM) and a 32-fold for that one with the shortest linker (G, K_i = 14.9 ± 0.6 nM) (Fig 76a). The potency was further reduced in presence of albumin, and considering the same two conjugates the K_i values were 28- and 252-fold lower, respectively (5xPEG_2, K_i = 13 ± 1 nM; G, K_i = 116 ± 16 nM) (Fig. 76b).

These results suggested that, first of all, the tag placed at the N-terminus partially hindered the capacity of the FXII inhibitor to efficiently access and inhibit the catalytic

site of the target with its first ring.[81] This lowering effect on the inhibition constants was even more evident in conjugates with short linkers between the tag and the bicyclic peptide, probably due to the steric hindrance of the closer albumin bound to the tag.

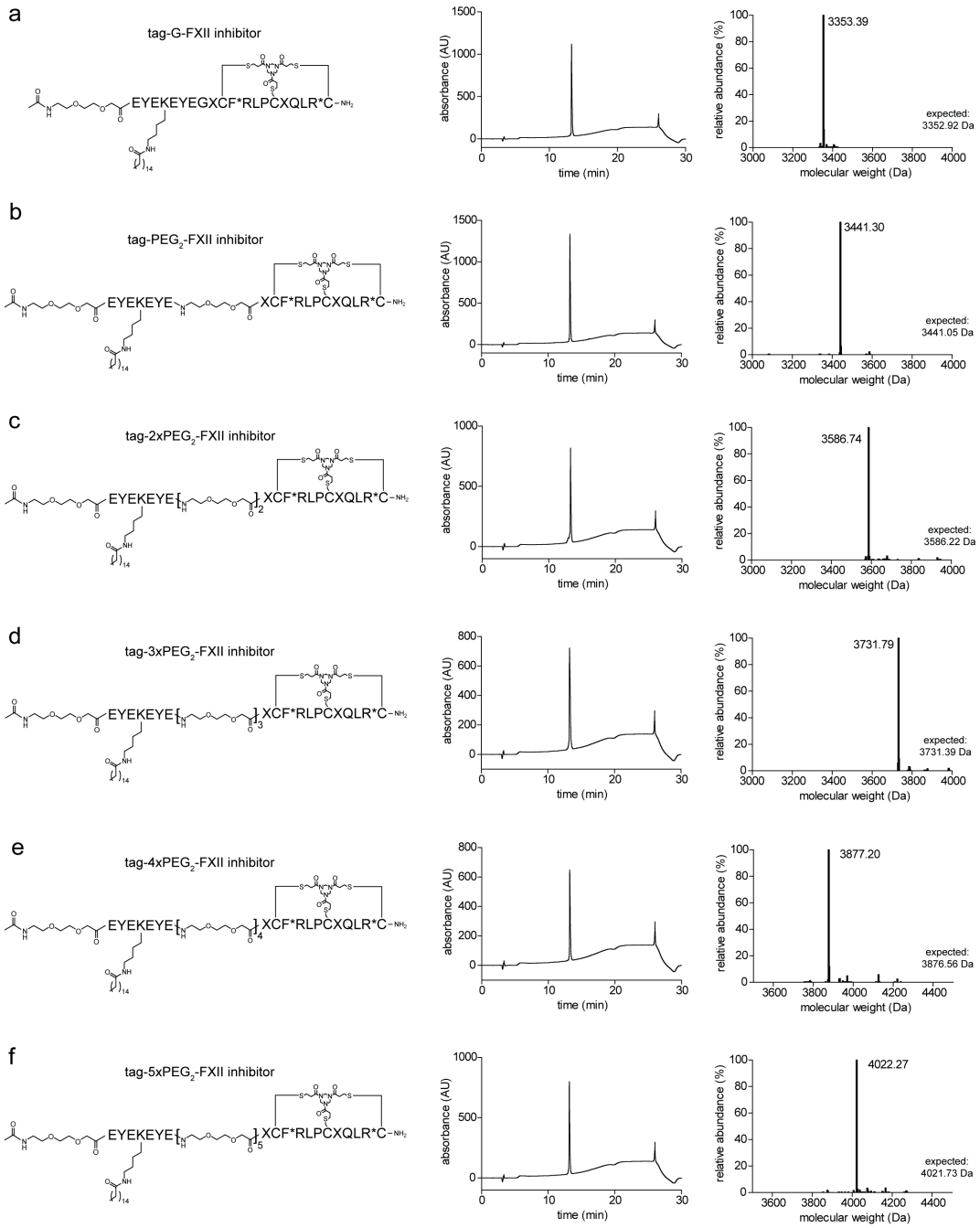

Figure 75. Characterization of the first-generation of acetylated FXII inhibitor conjugates. Structure of the peptides (left panel), RP-HPLC chromatogram (central panel) and deconvoluted mass spectra (right panel). Amino acids shown as single letter code; F* and R* represent p-fluoro Phe and β-homo Arg, respectively; X represents unnatural amino acid newly substituted; TATA, PEG_2 and palmitic acid shown as structural formula.

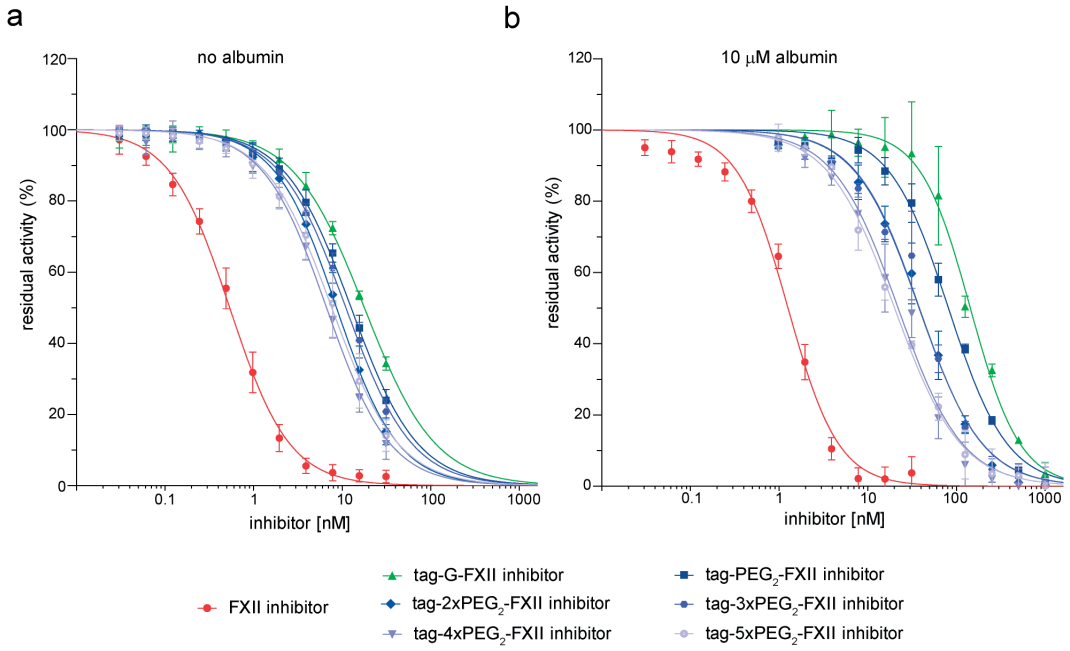

c

		inhibition of β-hFXIIa(K_i) [nM]	
		in absence of albumin	in presence of albumin
FXII inhibitor	XCF*RLPCXQLR*C	0.46 ± 0.08	1.1 ± 0.1
tag-G-FXII inhibitor	$EYEK_{palm}$EYEGXCF*RLPCXQLR*C	14.9 ± 0.6	116 ± 16
tag-PEG_2-FXII inhibitor	$EYEK_{palm}$EYE-PEG_2-XCF*RLPCXQLR*C	10.6 ± 1.2	68 ± 8
tag-2xPEG_2-FXII inhibitor	$EYEK_{palm}$EYE-2xPEG_2-XCF*RLPCXQLR*C	7.3 ± 1.3	32 ± 8
tag-3xPEG_2-FXII inhibitor	$EYEK_{palm}$EYE-3xPEG_2-XCF*RLPCXQLR*C	9.3 ± 1.4	30 ± 4
tag-4xPEG_2-FXII inhibitor	$EYEK_{palm}$EYE-4xPEG_2-XCF*RLPCXQLR*C	5.6 ± 1.4	16 ± 3
tag-5xPEG_2-FXII inhibitor	$EYEK_{palm}$EYE-5xPEG_2-XCF*RLPCXQLR*C	6.6 ± 1.8	13 ± 1

Figure 76. Inhibition of FXII inhibitor and the first-generation of acetylated FXII inhibitor conjugates against FXIIa. Graphs of enzymatic activity tested (a) without or (b) in presence of 10 μM albumin. (a) Inhibition constants. Amino acids shown as single letter code; F* and R* represent p-fluoro Phe and β-homo Arg, respectively; X represents unnatural amino acid newly substituted; palm is palmitic acid.

3.3.1.3 Inhibition of the intrinsic coagulation pathway

The most used test to evaluate the potential therapeutic activity of FXII inhibitors is an *ex vivo* coagulation assay that measures aPTT in plasma. As illustrated in subsection 3.2.4, this test shows the role that a specific protein, in our case FXIIa, plays in the intrinsic coagulation pathway, and the efficiency of its blocking. The activity of the FXII inhibitor and the first-generation of acetylated conjugates was determined by measuring their aPTT in both human and rabbit plasma at a fixed concentration (10 μM) (Fig. 77).

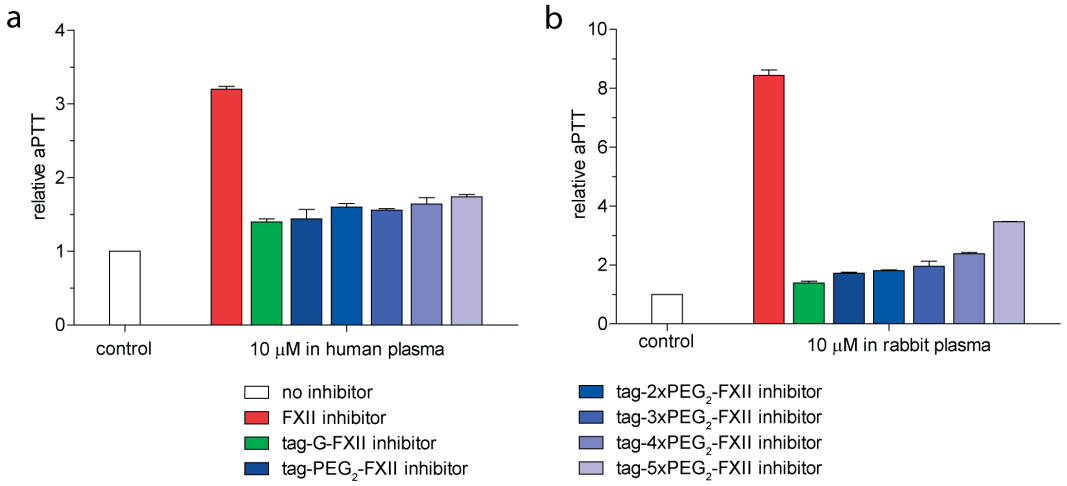

Figure 77. Coagulation parameter aPTT for the first-generation of acetylated FXII inhibitor conjugates in different plasma. The activity of the conjugates was measured upon incubation at 37°C with human (a) or rabbit (b) plasma and pathromtin or actin, respectively; coagulation was triggered by $CaCl_2$.

The FXII inhibitor alone strongly prolonged the aPTT in both plasma types, and the much stronger effect observed with rabbit plasma (eight-fold in rabbit vs. three-fold in human) was related to the intrinsic sensitivity of the assay. In human plasma, all of the conjugates gave a weak effect with an average prolongation factor of only 1.5, and the conjugate carrying the longest linker ($5xPEG_2$) was slightly better than the others. Anyway, its relative coagulation time was half that of the unmodified bicyclic peptide. This same conjugate was still the best in rabbit plasma, as well, but it was almost three times less efficient than the FXII inhibitor. The impacts of each conjugate on the coagulation time nicely correlated with the linker length trend previously observed for the inhibitory activity. In fact, the format with the longest linker showed the best inhibitory results among all the tested conjugates, while also retaining a good affinity for human albumin. However, the negative impact of the tag on the FXII inhibitor activity was still too high. In order to avoid any possible intereference at the N-terminus region of the bicyclic peptide, a second format with the tag appended at peptide's C-terminus was tested.

3.3.2 Second generation: tag at the C-terminus

The second generation of conjugates consisted of a C-terminally branched (F)-tag attached to the FXII inhibitor as follows. Briefly, the bicyclic peptide was synthesized with an N-terminal Boc-protected amino acid and inserting a C-terminal GKG sequence, which presented an orthogonally protected Lys(Dde). After the selective deprotection of this residue, the synthesis of the tag sequence was started on the free amine side chain, spaced by zero to three PEG_2 units. The tag was either fluorescein labeled or acetylated at N-terminus as described above. The Lys(Dde) of the tag was deprotected and its free amine modified with palmitic acid. After cleveage from the resin, the FXII inhibitor was cyclized with TATA in a mixture of MeCN and aqueous buffer, and then purified by HPLC. The desired conjugates were confirmed by mass spectrometry and the purity assessed by analytical HPLC (Fig. 78 and 80).

3.3.2.1 Albumin binding

The binding affinity of fluorescein labeled conjugates (Fig. 78) was again determined for human albumin in serum and for rabbit albumin (Fig. 79).

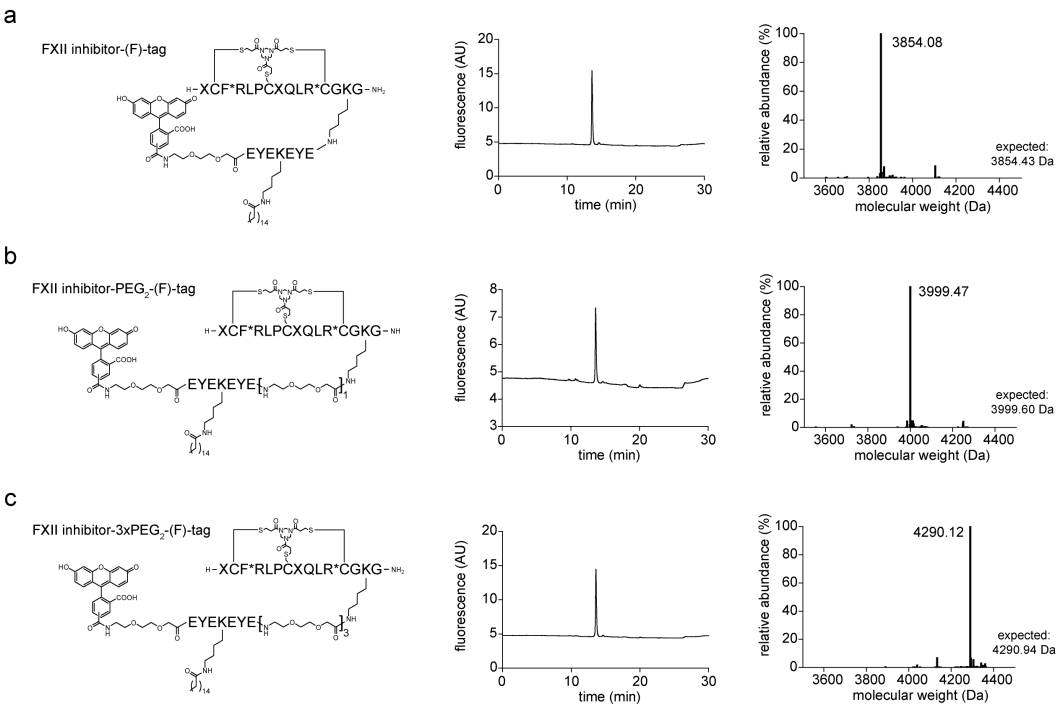

Figure 78. Characterization of the second-generation of fluorescein labeled FXII inhibitor conjugates. Structure of the peptides (left panel), RP-HPLC chromatograms (central panel) and deconvoluted mass spectra (right panel). Amino acids shown as single letter code; F* and R* represent p-fluoro Phe and β-homo Arg, respectively; X represents unnatural amino acid newly substituted; fluorescein, TATA, PEG_2 and palmitic acid shown as structural formula.

The second-generation conjugates bound human albumin in serum in the high nanomolar range (K_d of (F)-tag = 37 nM vs. K_ds of conjugates ≈ 140-180 nM), showing a three to five-fold reduction in binding affinity similar to that measured for all the other N-terminal tagged bicyclic peptides. The previous trend correlating the linker lengths with the K_d of the conjugates for both human and rabbit albumin was also confirmed. The conjugate without the PEG_2 unit showed the best affinity (138 and 510 nM for human and rabbit albumin, respectively), while the other formats spaced by one or three PEG_2 units exhibited a small but clear decrease in binding (Fig. 79).

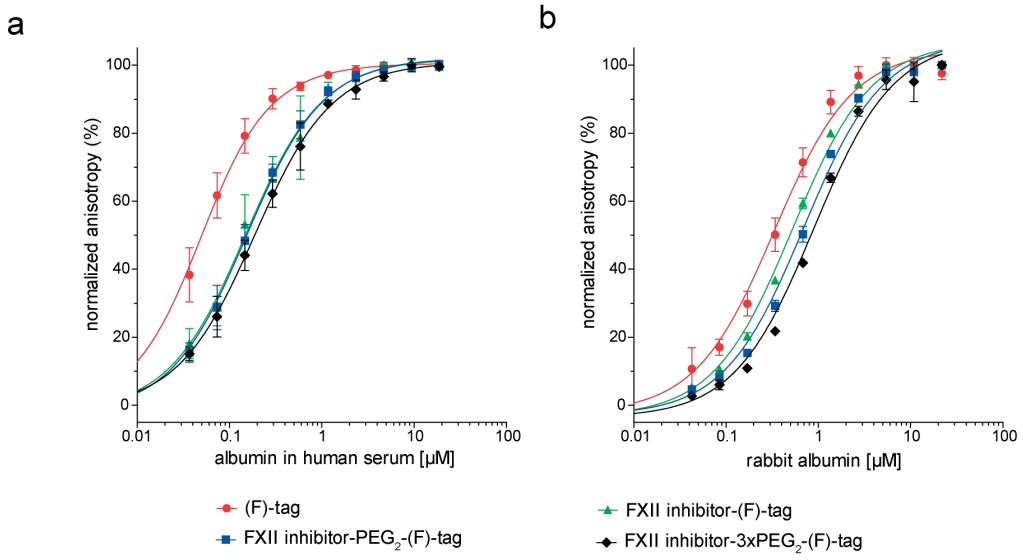

c

		albumin binding (K_d) [nM]	
		human serum	rabbit albumin
(F)-tag	(F)-EYEK$_{palm}$EYE	37 ± 2	320 ± 40
FXII inhibitor-(F)-tag	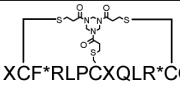 XCF*RLPCXQLR*CGK[(F)-EYEK$_{palm}$EYE]G	138 ± 14	510 ± 60
FXII inhibitor-PEG$_2$-(F)-tag	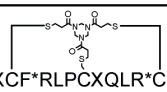 XCF*RLPCXQLR*CGK[PEG$_2$-(F)-EYEK$_{palm}$EYE]G	142 ± 8	680 ± 90
FXII inhibitor-3xPEG$_2$-(F)-tag	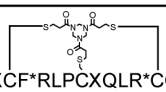 XCF*RLPCXQLR*CGK[3xPEG$_2$-(F)-EYEK$_{palm}$EYE]G	177 ± 7	880 ± 130

Figure 79. Binding of (F)-tag and the second-generation of fluorescein labeled FXII inhibitor conjugates with different albumins. Fluorescence polarization isotherms with (a) human serum and (b) rabbit albumin. (c) Dissociation constants. Amino acids shown as single letter code; F* and R* represent p-fluoro Phe and β-homo Arg, respectively; X represents unnatural amino acid newly substituted; (F) is fluorescein; palm is palmitic acid; ▬ (dash) between (F) and tag is PEG_2.

3.3.2.2 Inhibition of FXIIa

In terms of inhibition, the three second-generation acetylated conjugates (Fig. 80) inhibited the target with on average a K_i value of 2.5 nM without albumin, and 6 nM in presence of albumin, five- and 14-fold weaker compared to FXII inhibitor alone, respectively (Fig. 81). These conjugates all displayed a factor two improvement of K_i over the best first-generation conjugate (5xPEG_2, K_i without albumin = 6.6 nM, K_i with albumin = 13 nM). The homogeneity of the results obtained with the three conjugates suggested that a maximum improvement in the inhibitory activity was probably reached with this kind of format. The position of the tag seemed to play a more important role, since linker differences among conjugates were not longer influencing the K_i values. Even though the loss in inhibitory activity was still high in presence of albumin, aPTT tests were repeated with the hope to confirm the better results obtained with these conjugates.

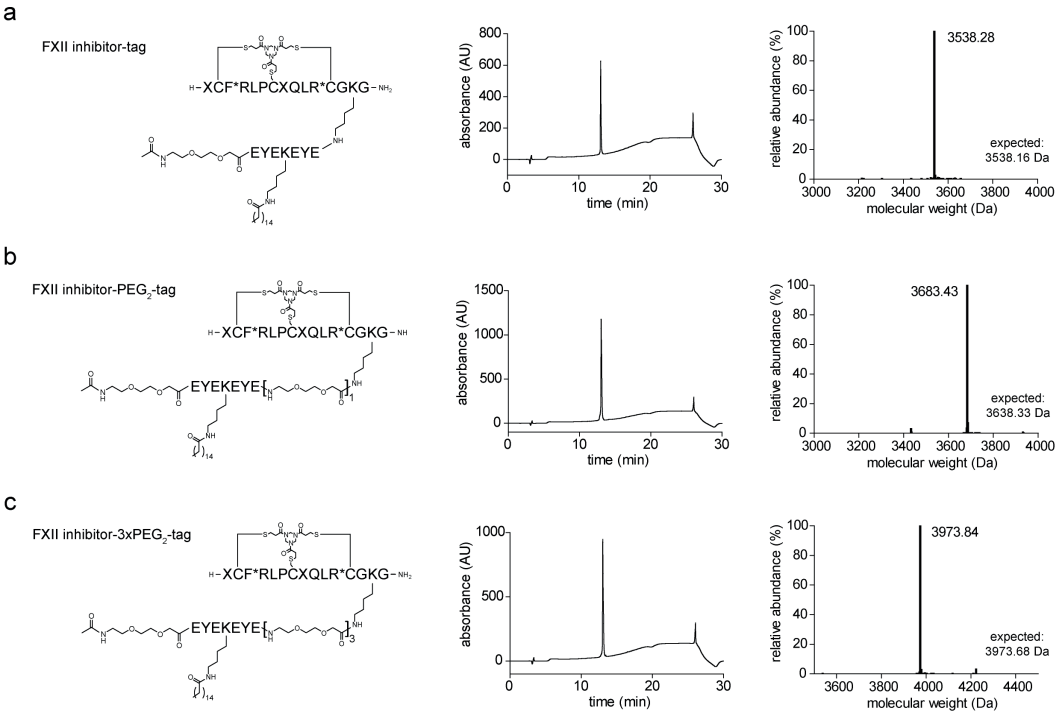

Figure 80. Characterization of the second-generation of acetylated FXII inhibitor conjugates. Structure of the peptides (left panel), RP-HPLC chromatograms (central panel) and deconvoluted mass spectra (right panel). Amino acids shown as single letter code; F* and R* represent p-fluoro Phe and β-homo Arg, respectively; X represents unnatural amino acid newly substituted; TATA, PEG_2 and palmitic acid shown as structural formula.

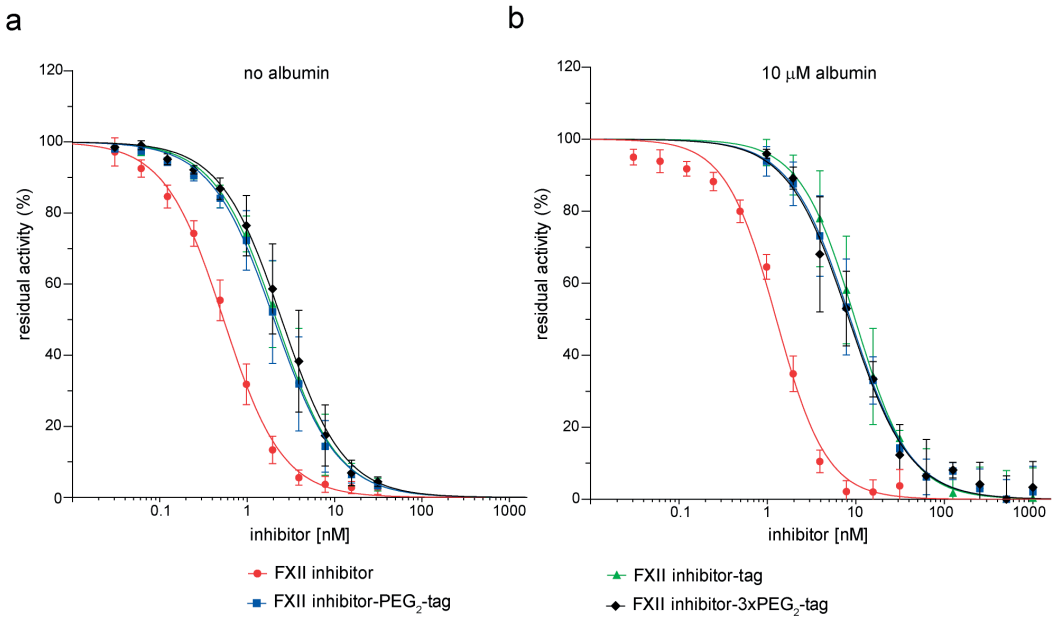

c

		inhibition of β-hFXIIa(K_i) [nM]	
		in absence of albumin	in presence of albumin
FXII inhibitor	XCF*RLPCXQLR*C	0.46 ± 0.08	1.1 ± 0.1
FXII inhibitor-tag	XCF*RLPCXQLR*CGK[EYEK$_{palm}$EYE]G	2.2 ± 0.5	7 ± 3
FXII inhibitor-PEG$_2$-tag	XCF*RLPCXQLR*CGK[PEG$_2$-EYEK$_{palm}$EYE]G	2.1 ± 0.5	5.8 ± 1.9
FXII inhibitor-3xPEG$_2$-tag	XCF*RLPCXQLR*CGK[3xPEG$_2$-EYEK$_{palm}$EYE]G	2.5 ± 0.2	5.8 ± 1.7

Figure 81. Inhibition of FXII inhibitor and the second-generation of acetylated FXII inhibitor conjugates against FXIIa. Graphs of enzymatic activity tested (a) without or (b) in presence of 10 μM albumin. (c) Inhibition constants. Amino acids shown as single letter code; F* and R* represent p-fluoro Phe and β-homo Arg, respectively; X represents unnatural amino acid newly substituted; palm is palmitic acid.

3.3.2.3 Inhibition of the intrinsic coagulation pathway

The aPTT of the second-generation of acetylated conjugates was assessed in both human and rabbit plasma at a fixed inhibitor concentration (10 μM) (Fig. 82). Results in human plasma had the same weak effect previously measured for the first-generation of conjugates, with a prolongation of the coagulation time only equal to a factor 1.5. Actually, a longer prolongation was expected since the K_is values measured for these conjugates were better than those of the first-generation counterparts. Most likely, once the conjugates are incubated in physiological conditions (e.g. human plasma with 600 μM

albumin), binding to albumin and resulting steric hindrance are the main cause of activity reduction, independent of a free or hindered N-terminus. It was expected that the three conjugates would display a similar impact on aPTT prolongation in rabbit plasma because the K_i values were identical. However, one of them, the conjugate with the longest PEG linker, prolonged the coagulation time two-fold better than the others, though its impact was still half of the desired effect shown by the FXII inhibitor alone. The evidence that the conjugate with the longest PEG linker showed again the best result further supported the idea about the negative impact of albumin hindrance on peptide's activity, and directed the choice towards the final format to test.

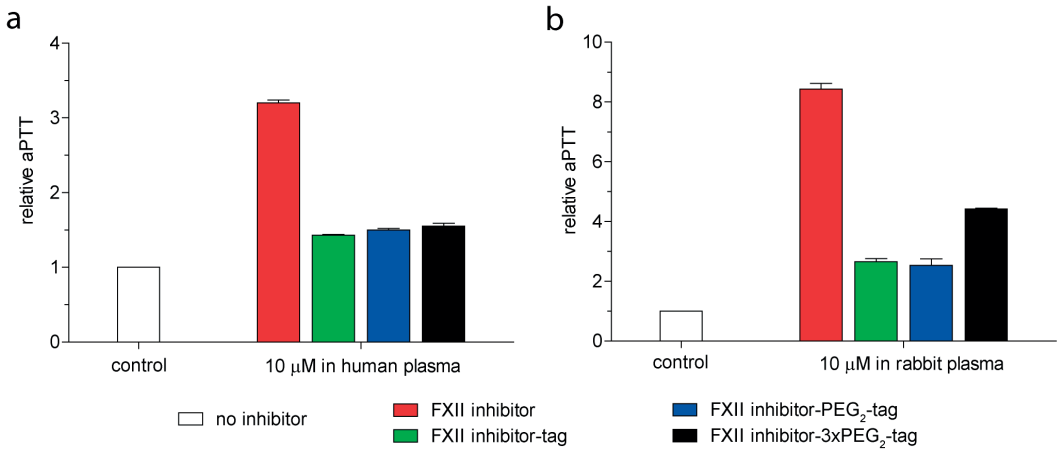

Figure 82. Coagulation parameter aPTT for the second-generation of acetylated FXII inhibitor conjugates in different plasma. The activity of the conjugates was measured upon incubation at 37°C with (a) human or (b) rabbit plasma and pathromtin or actin, respectively; coagulation was triggered by $CaCl_2$.

3.3.3 Third generation: longer N-terminal linker

Since the distance between the albumin-binding tag and the bicyclic peptide appeared to be crucial for its inhibitory activity, the linker length was increased using very long PEG units. In addition, considering the homogeneity of the results exhibited by the C-terminal tagged FXII inhibitors and the complex synthesis they required, it was decided to work again on the N-terminus modified conjugate. Therefore, a single third-generation conjugate composed of a N-tagged bicyclic peptide with three units of a PEG_{24} linker ($3xPEG_{24}$) between the (F)-tag and the FXII inhibitor was produced. In this case, only the fluorescein labeled conjugate was synthetized, prepared and characterized as described above for the first-generation of conjugates (Fig. 83c). In addition, the FXII inhibitor alone was synthesized and labeled at the N-terminus with fluorescein and was used as control in binding assays (Fig. 83a).

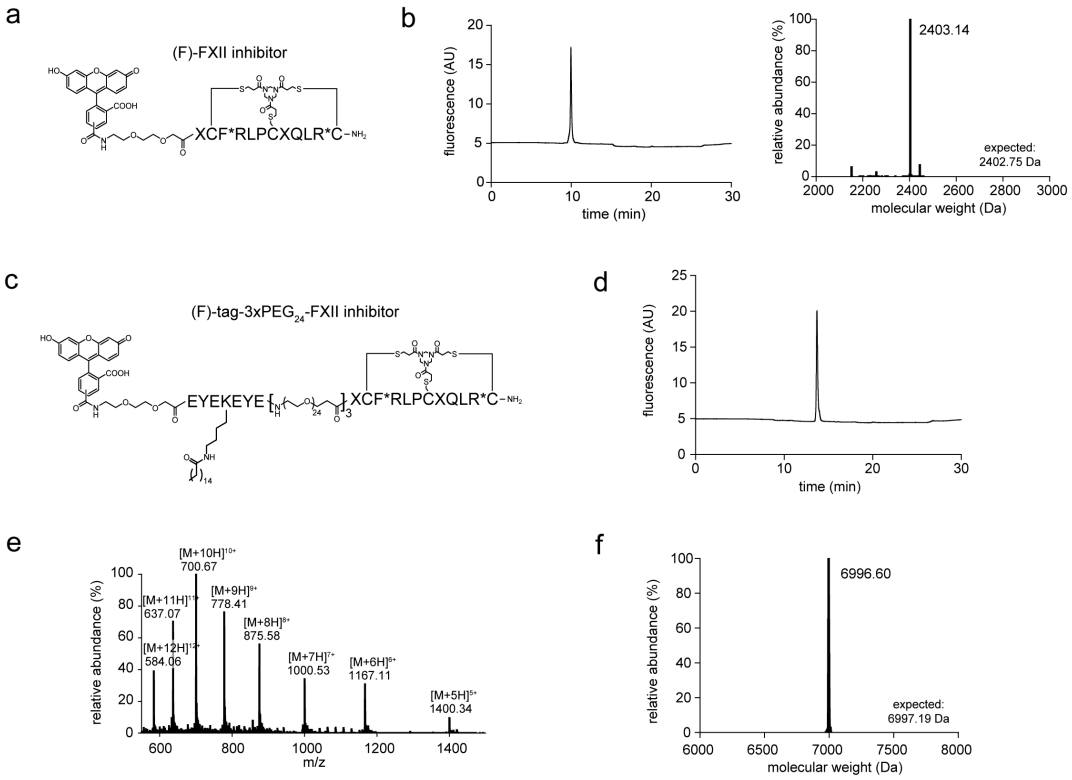

Figure 83. Characterization of the fluorescein labeled FXII inhibitor and (F)-tag-3xPEG$_{24}$-FXII inhibitor. (a) Structure of the FXII inhibitor, (b) RP-HPLC chromatogram (central panel), and deconvoluted mass spectrum (right panel). (c) Structure of (F)-tag-3xPEG$_{24}$-FXII inhibitor, (d) RP-HPLC chromatogram, (e) m/z, and (f) deconvoluted high resolution mass spectra. Amino acids shown as single letter code; F* and R* represent p-fluoro Phe and β-homo Arg, respectively; X represents unnatural amino acid newly substituted; fluorescein, TATA, PEG$_2$ and palmitic acid shown as structural formula.

The (F)-tag-3xPEG$_{24}$-FXII inhibitor showed a K_d of 224 ± 11 nM for human albumin in serum and a K_d of 1600 ± 300 nM for rabbit albumin, both five-fold weaker than the tag alone and consistent with the previous results obtained for the other conjugates (Fig. 84). As already observed for the N-tagged first-generation conjugates, the major length of the linker resulted in a slightly negative impact on the binding affinity (e.g. for rabbit albumin: K_d of tag = 320 nM, K_d of tag-PEG$_2$ conjugate = 650 nM, K_d of tag-5xPEG$_2$ conjugate = 1400 nM). The fluorescein labeled FXII inhibitor did not bind to albumin at all, as expected.

a

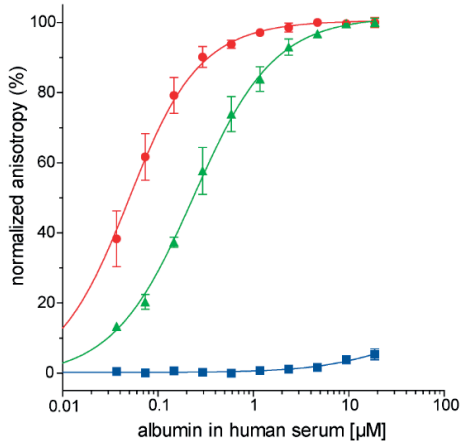

b

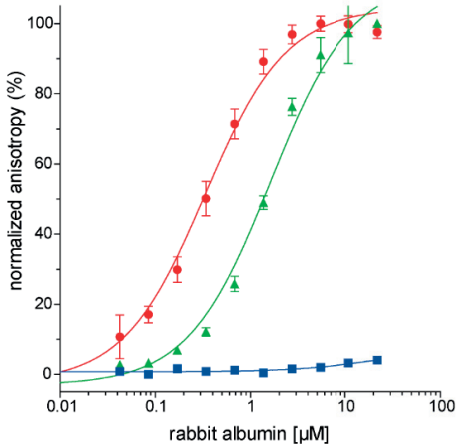

(F)-tag (F)-tag-3xPEG$_{24}$-FXII inhibitor (F)-FXII inhibitor

c

		albumin binding (K_d) [nM]	
		human serum	rabbit albumin
(F)-tag	(F)-EYEK$_{palm}$EYE	37 ± 2	320 ± 40
(F)-FXII inhibitor	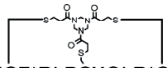 (F)-XCF*RLPCXQLR*C	> 100,000	> 100,000
(F)-tag-3xPEG$_{24}$-FXII inhibitor	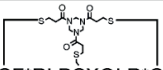 (F)-EYEK$_{palm}$EYE-3xPEG$_{24}$-XCF*RLPCXQLR*C	224 ± 11	1600 ± 300

Figure 84. Binding of (F)-tag and (F)-tag-3xPEG$_{24}$-FXII inhibitor with different albumins. Fluorescence polarization isotherms with (a) human serum and (b) rabbit albumin. (c) Dissociation constants. Amino acids shown as single letter code; F* and R* represent p-fluoro Phe and β-homo Arg, respectively; X represents unnatural amino acid newly substituted; (F) is fluorescein; palm is palmitic acid; ▬ (dash) between (F) and tag is PEG$_2$.

The inhibition assay was performed using the fluorescein labeled third-generation conjugate, instead of the acetylated format previously used. In fact, the fluorescein moiety revealed to not interfere with the assay, probably due to the low concentrations of inhibitor tested. The conjugate showed the same single digit nanomolar inhibitory activity (K_i values ≈ 3 nM) with and without albumin in the assay, with a potency only six-fold weaker than the FXII inhibitor alone (Fig. 85). Compared to the two best conjugates, in presence of albumin this conjugate inhibited FXIIa two to four-fold better (second-generation, K_i = 5.8 ± 1.7 nM; first-generation, K_i = 13 ± 1 nM). This promising result clearly confirmed the negative impact of albumin hindrance, which thus could be strongly reduced with an even longer linker.

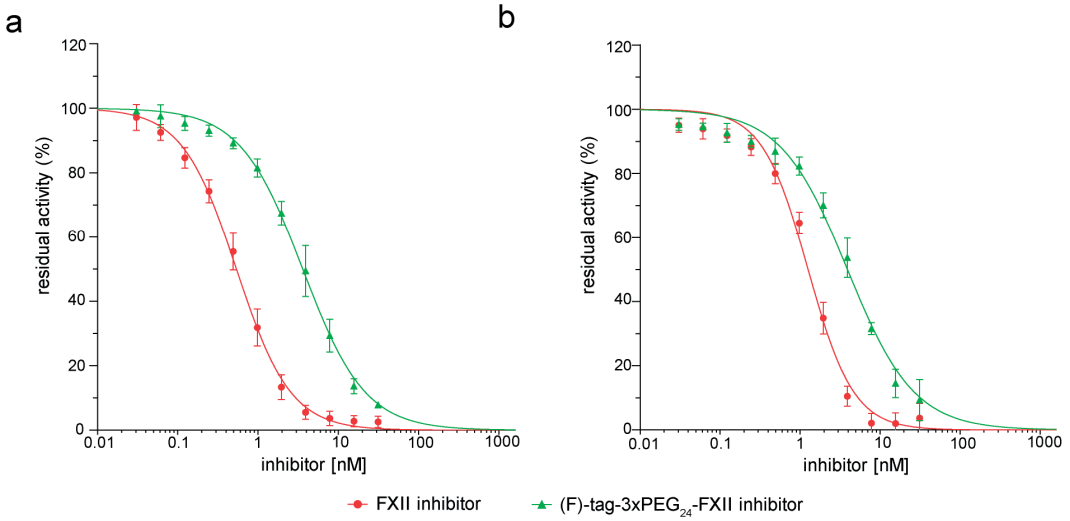

c

		inhibition of β-hFXIIa(K_i) [nM]	
		in absence of albumin	in presence of albumin
FXII inhibitor	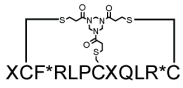 XCF*RLPCXQLR*C	0.46 ± 0.08	1.1 ± 0.1
(F)-tag-3xPEG$_{24}$-FXII inhibitor	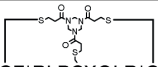 (F)-EYEK$_{palm}$EYE-3xPEG$_{24}$-XCF*RLPCXQLR*C	3.1 ± 0.6	3.3 ± 0.4

Figure 85. Inhibition of FXII inhibitor and (F)-tag-3xPEG$_{24}$-FXII inhibitor against FXIIa. Graphs of enzymatic activity tested (a) without or (b) in presence of 10 μM albumin. (c) Inhibition constants. Amino acids shown as single letter code; F* and R* represent p-fluoro Phe and β-homo Arg, respectively; X represents unnatural amino acid newly substituted; palm is palmitic acid.

Finally, the aPTT of the (F)-tag-3xPEG$_{24}$-FXII inhibitor was assessed at three different concentrations (10, 5 and 2 μM). The same concentrations were tested for the two most promising conjugates from the first- and second-generation (Fig. 86). The FXII inhibitor confirmed the excellent results obtained previously. At all of the concentrations tested, the bicyclic peptide alone prolonged the aPTT more than a factor two and eight for human and rabbit plasma, respectively (unpublished data). The third-generation conjugate did not give any improvements compared to the previous two formats when incubated with human plasma, still not showing more than a factor 1.5 in the prolongation of the coagulation time. In contrast, it did, however, showed a prolongation time equal to the unmodified FXII inhibitor when tested in rabbit plasma at the highest concentration.

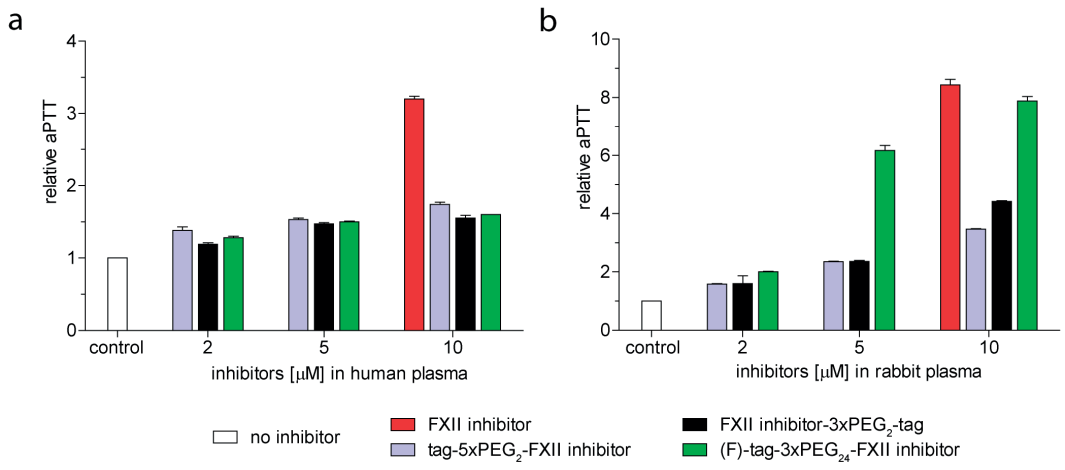

Figure 86. Coagulation parameter aPTT for FXII inhibitor and the best FXII inhibitor conjugates in different plasma. The activity of the conjugates was measured upon incubation at 37°C with (a) human or (b) rabbit plasma and pathromtin or actin, respectively; coagulation was triggered by $CaCl_2$.

At the lower concentration of 5 μM, (F)-tag-3xPEG$_{24}$-FXII inhibitor was still able to prolong the coagulation time by more than six-fold, and its EC_{5x} and EC_{2x} (the concentrations needed to get five- and two-fold longer coagulation times) were calculated to be around 4 and 2 μM in rabbit plasma, respectively. On the other hand, it was only possible to estimate an EC_{2x} of around 4 μM for the other conjugates (Fig. 87). By further analyzing the EC_{2x} and the less used $EC1_{1.5x}$ of the three conjugates and FXII inhibitor alone in both human and rabbit plasma, I noticed that on average the three conjugates had a 30 to 50-fold weaker activity. Since the EC_{2x} of the FXII inhibitor in human plasma is at around 1 μM, the same relative aPTT value with the three conjugates could be obtained only using concentrations higher than 30 μM.

Despite an unsatisfactory prolongation of the coagulation in human plasma, the result obtained in rabbit plasma with the (F)-tag-3xPEG$_{24}$-FXII inhibitor was extremely promising for the *in vivo* animal experiments that we had planned. According to the aPTT, concentrations up to 2 μM of the (F)-tag-3xPEG$_{24}$-FXII inhibitor can be detected and should allow a quantification of its *in vivo* activity over a prolonged period of time, assuming that the tag increases the half-life as it was previously observed in rats.

	$EC_{1.5x}$ aPTT (μM)		EC_{2x} aPTT (μM)		EC_{5x} aPTT (μM)	
	human plasma	rabbit plasma	human plasma	rabbit plasma	human plasma	rabbit plasma
FXII inhibitor	0.18 ± 0.06	0.04 ± 0.01	1.0 ± 0.3	0.07 ± 0.01	n.d.	0.11 ± 0.03
tag-5xPEG$_2$-FXII inhibitor	4.4 ± 0.3	1.7 ± 0.1	n.d.	3.6 ± 0.1	n.d.	n.d.
FXII inhibitor-3xPEG$_2$-tag	6.8 ± 1.8	1.9 ± 0.5	n.d.	3.7 ± 0.5	n.d.	n.d.
(F)-tag-3xPEG$_{24}$-FXII inhibitor	5.1 ± 0.4	0.9 ± 0.1	n.d.	1.9 ± 0.1	n.d.	4.2 ± 0.5

Figure 87. Coagulation parameters aPTT (extrapolated E_C values) for FXII inhibitor and the best FXII inhibitor conjugates in plasma.

Finally, the specificity of the (F)-tag-3xPEG$_{24}$-FXII inhibitor towards its target was assessed against a panel of six structurally related or functionally important proteases (Fig. 88). Five proteases out of six were inhibited less than 30% at the highest inhibitor concentration tested (10 μM). Only trypsin, which is a protease not present in the blood, was inhibited more than 50% with a K_i = 6 ± 1.8 μM, 2,000-fold higher than the K_i for the specific target. The conjugate was almost three times less active than the FXII inhibitor alone over trypsin (unpublished data), showing also a reduction in its activity against unwanted targets.

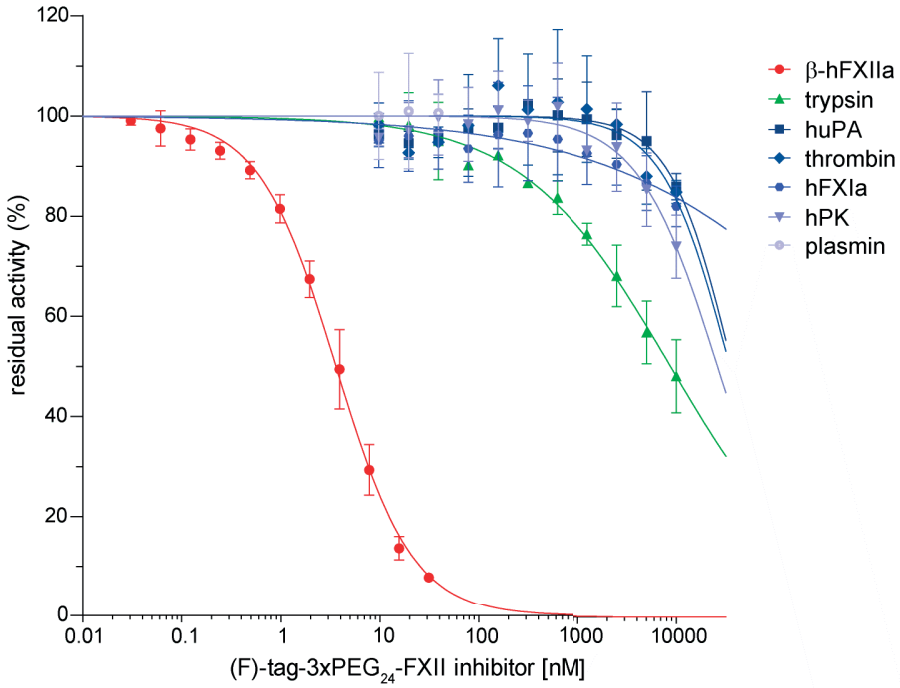

Figure 88. Specificity of the (F)-tag-3xPEG$_{24}$-FXII inhibitor. Residual activities of FXIIa and a range of serine proteases measured at different concentrations of conjugate, using different fluorogenic substrates.

3.3.4 Pharmacokinetics and *in vivo* activity in rabbits

Pharmacokinetic experiments were carried out in rabbits for the third-generation conjugate (F)-tag-3xPEG_{24}-FXII inhibitor (Fig. 83c). The *in vivo* studies (injection and blood collection) were outsourced to the American company Washington Biotechnology, Inc. (Baltimore, MD, USA). Because pharmacokinetic studies of the FXII inhibitor were already performed in rabbits by the colleagues who developed it (unpublished data), a well-defined amount of peptide was prepared in order to get a similar concentration in the animals upon i.v. injection. Some issues were experienced during the synthesis of the conjugate, performed with new batches of Fmoc-PEG_{24}-OH amino acid that were less pure and stable than the first batch. The presence of side products required multiple steps of purification, and a subsequent loss in yield. Initially, the purity was only assessed via LC-MS in order to discriminate between the desired conjugate and the impurities. The overall purity of the final compound as assessed in analytical HPLC was only around 75-80%, with small peaks detected after the final compound (Fig. 89a). These peaks could be later characterized and showed the same mass of the desired product, suggesting that a full cyclization of the bicyclic peptide probably did not occur as desired. There is no mass change upon cyclization with TATA, and thus the mass remains equal and could not be distinguished in LC-MS, which does not run as long of a gradient as the HPLC. Nevertheless, before sending the peptide for pharmacokinetic studies, peptide's activity and binding affinity for albumin were tested by aPTT and fluorescence polarization, respectively. Since all the samples gave the expected results (Fig. 89b-c), the conjugate was considered suitable for the aim of the *in vivo* study.

The final amount of peptide produced was around 42 mg, which was divided equally into three samples, each of them dissolved in 3.5 ml of PBS, pH 7.4, 0.01% SDS. Rabbits were i.v. injected with 3 ml of a 570 μM (F)-tag-3xPEG_{24}-FXII inhibitor (5 $mg \cdot kg^{-1}$ in PBS, pH 7.4, 0.01% SDS) solution, resulting in a final blood concentration of approximately 14 μM. Blood samples were collected at ten different time points and immediately processed to plasma using tubes treated with Na citrate to avoid the coagulation cascade, since the main goal of the test was to see a prolonged *in vivo* effect of the conjugate on the intrinsic coagulation pathway.

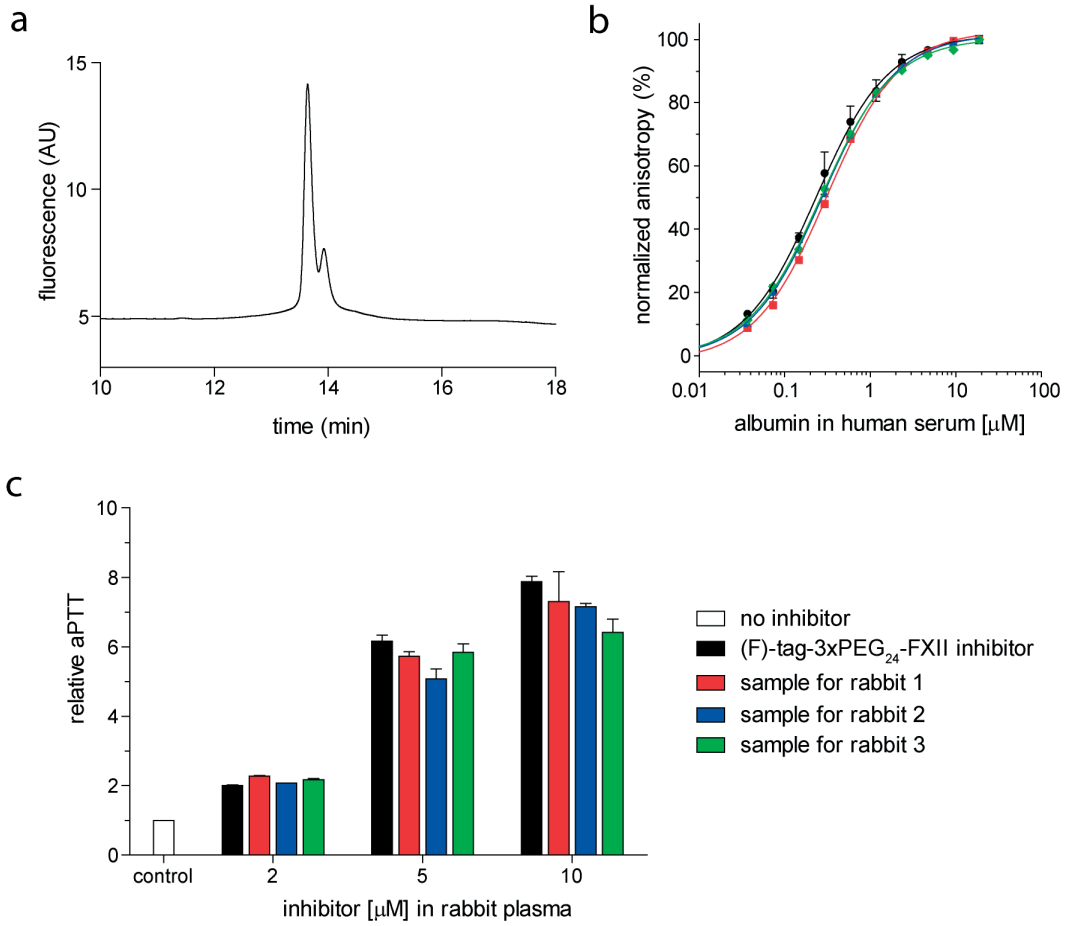

Figure 89. Quality control of the up-scaled produced (F)-tag-3xPEG$_{24}$-FXII inhibitor stock solutions for *in vivo* experiments. (a) RP-HPLC chromatogram, (b) fluorescence polarization isotherms and (c) coagulation parameter aPTT of the three batches sent for pharmacokinetic studies. The color code used for aPTT columns and binding isotherms in the fluorescence polarization graph are the same.

3.3.4.1 Plasma half-life in rabbits

Applying the same protocol of protein precipitation previously described in subsection 3.2.6, plasma samples and calibration curves were prepared and run in HPLC with a fluorescence detector in order to detect the conjugate. For both samples and calibrations, only the AUCs of the main peak were integrated and used for peptide quantification in plasma. Again, a fixed concentration of internal standard was added in each sample as a control to adjust the AUCs of the peptides. The zoomed chromatograms of the peptide tested in three different rabbits are here reported (Fig. 90) while full runs are shown in the supporting info (Fig. S5).

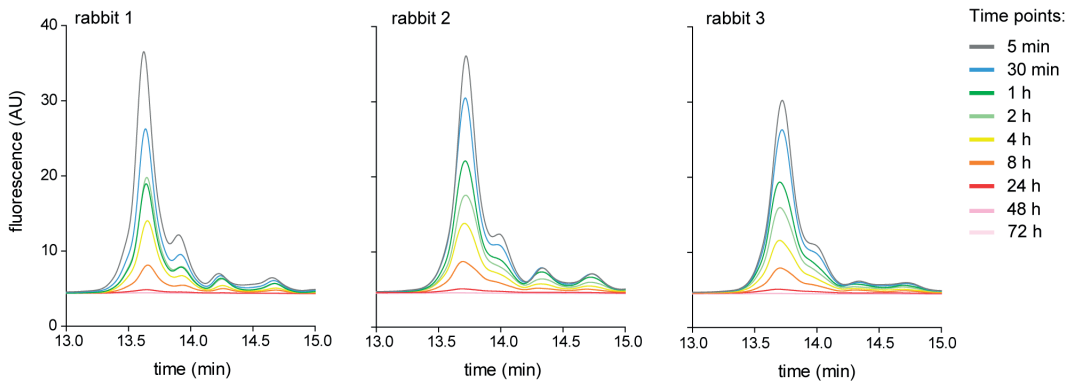

Figure 90. RP-HPLC chromatograms of the (F)-tag-3xPEG$_{24}$-FXII inhibitor. Chromatograms of rabbit plasma samples collected at different time points.

The (F)-tag-3xPEG$_{24}$-FXII inhibitor showed the same peak pattern previously observed in the HPLC. Their ratio and decrease over the time were similar to each other, confirming their behavior as fractions of the correct tagged bicyclic peptide. A completely new small peak appeared after one hour (retention time = 12 min, Fig. S5) and might be a degradation product of the not fully modified peptides. However, the low concentration did not allow its collection and characterization. The main peak of the conjugate was still detectable in plasma after 24 hours and only its AUCs were taken into account for peptide quantification in plasma (Fig 91a). The initial concentration in plasma was calculated considering the relative purity of the sample (75%) and it was doubled to account for the observation that the peptide tagged to albumin will be located mainly in plasma (sub-section 3.2.6). After five minutes, the concentration was exactly in the expected range (19 μM), confirming that tagged bicyclic peptides remain in plasma. The concentrations were plotted versus time, analyzed with a two-compartment model (biexponential equation: $C_p = A \cdot e^{-\alpha \cdot t} + B \cdot e^{-\beta \cdot t}$) and pharmacokinetic parameters determined (Fig. 91d).[257]

The (F)-tag-3xPEG$_{24}$-FXII inhibitor had a half-life in the same range as the previously tested tagged bicyclic peptides in rats. The distribution half-life was around one hour, and the elimination half-life was 5.2 ± 0.4 hours. Compared to the half-life of the FXII inhibitor alone in rabbits (13 ± 2 min), previously determined by LC-MS detection (unpublished data), the tag prolonged its elimination time by around 24-fold in rabbits. The short half-life of the bicyclic peptide was consistent with the fast clearance measured for UK18 in rats (Fig. 72, sub-section 3.2.6).

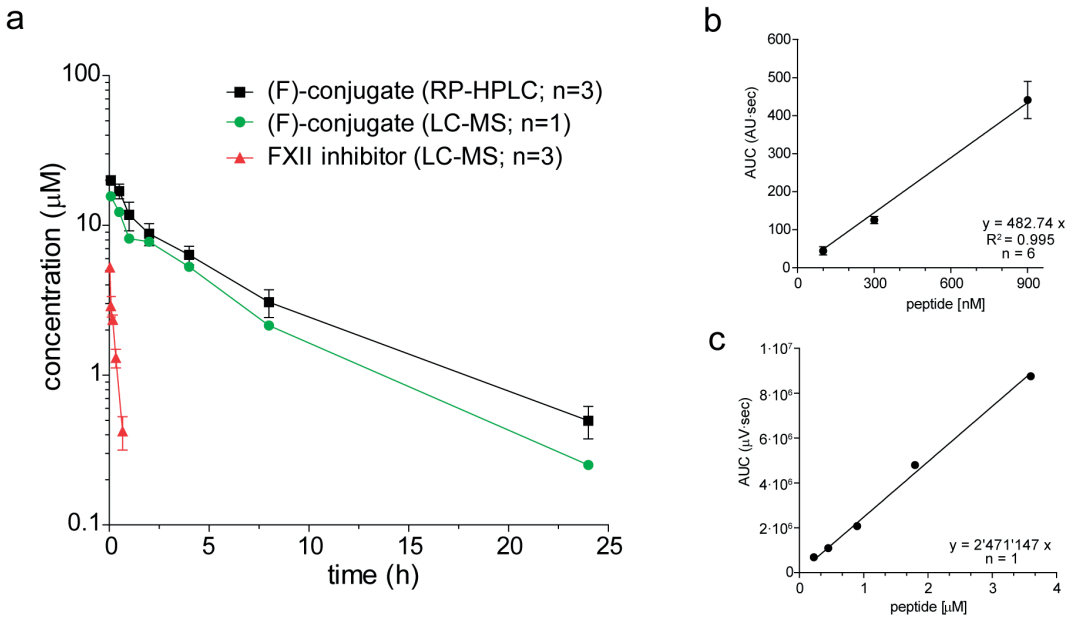

d

PARAMETERS (unit)	(F)-tag-3xPEG$_{24}$ FXII inhibitor		FXII inhibitor
	RP-HPLC (n=3)	LC-MS (n=1)	LC-MS (n=3)
$\tau_{1/2}\,\alpha$ (hrs)	1.0 ± 0.2	0.5	n.d.
$\tau_{1/2}\,\beta$ (hrs)	5.2 ± 0.4	4.5	0.21 ± 0.04
AUC (mg·min·ml^{-1})	41 ± 7	28	0.18 ± 0.01
CL (ml·hrs^{-1}·kg)	6 ± 1	8	1000 ± 40
V_D (ml·kg^{-1})	46 ± 7	50	300 ± 50

Figure 91. Pharmacokinetic profiles in rabbits of the (F)-tag-3xPEG$_{24}$-FXII inhibitor and FXII inhibitor. (a) Plasma concentrations plotted versus time upon i.v. injections in the three rabbits determined for the conjugate by RP-HPLC (black line) and LC-MS (green line) and for FXII inhibitor (red line). Linear regression calculation of the conjugate quantified by (b) RP-HPLC and (c) LC-MS. (d) Pharmacokinetic parameters. (F) is fluorescein; ▬ (dash) between (F) and tag is PEG$_2$

The other pharmacokinetic parameters AUC, CL and V_D were calculated and gave the expected values (Fig. 91d). AUCs correlated with the half-lives and showed that the conjugate would be 200-fold more active than its non-tagged format *in vivo*. Similarly, the clearance of the FXII inhibitor was one liter per hour, while the tagged bicyclic peptide was cleared 100-fold more slowly. Finally, the volume of distribution, calculated considering for rabbits a weight of around 2-2.5 kilograms, gave a value for the (F)-tag-

3xPEG$_{24}$-FXII inhibitor consistent with its distribution mainly in the bloodstream (approximately 120 ml), while the V_D of the bicyclic peptide alone was much higher due to a rapid non-specific tissue distribution.

Since the half-life of the FXII inhibitor alone was previously determined by LC-MS, one of the plasma series was analyzed using this detection strategy for direct comparison. The optimized protocol of plasma protein precipitation was applied for the preparation of calibration curves and peptide quantification by LC-MS, integrating only the AUC of the peak with the correct mass (Fig. 91a and 91c). A fixed concentration of the albumin-binding peptide SA21 was added as an internal standard. Even though the experiment was performed once, the resulting pharmacokinetic parameters were in the same range previously calculated, and confirmed the quality and reliability of the measurements performed with the fluorescence detector (Fig. 91d).

3.3.4.2 Prolonged inhibition of the intrinsic coagulation pathway

Thanks to the prolonged circulation time of the (F)-tag-3xPEG$_{24}$-FXII inhibitor in rabbits, its ability to block the intrinsic coagulation pathway could be tested from *in vivo* samples. The different plasma samples were analyzed by aPTT, adding actin and $CaCl_2$ as previously described. A pre-dosing sample, collected from each rabbit just before injecting the conjugate, was used as blank. The conjugate solutions in PBS were first checked by aPTT to test the stability and activity of the stocks sent for the pharmacokinetics (Fig. 92). Once their quality was verified, they were used as a control at a fixed concentration in parallel with each aPTT experiment performed using plasma samples.

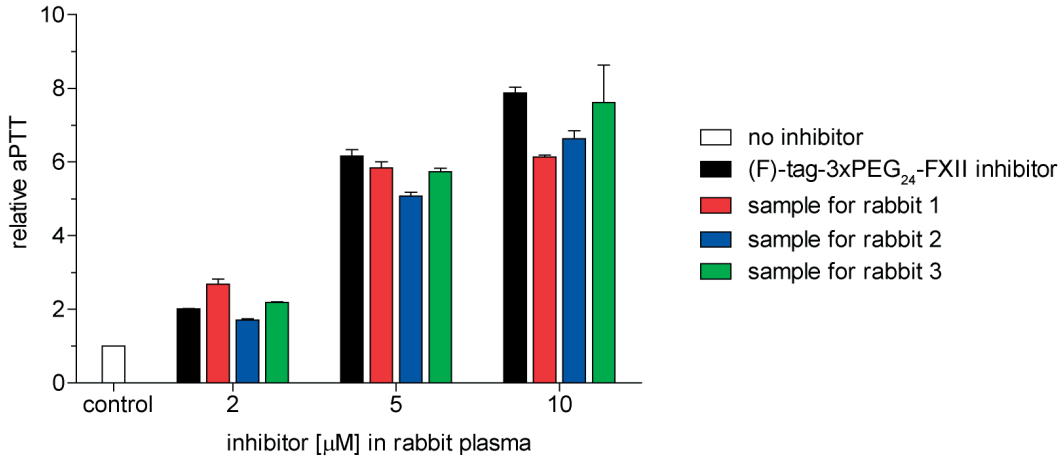

Figure 92. Coagulation parameter aPTT for the (F)-tag-3xPEG$_{24}$-FXII inhibitor stock solutions returned after pharmacokinetic studies. The activity of the conjugate was measured upon incubation at 37°C with rabbit plasma and actin, respectively; coagulation was triggered by $CaCl_2$.

The results from *in vivo* samples showed that the prolonged half-life of the (F)-tag-3xPEG$_{24}$-FXII inhibitor allowed an efficient blockage of the intrinsic coagulation for more than eight hours, the last time point at which a clear EC$_{2x}$ was still detectable, when this pathway was externally triggered (Fig. 93). I observed that, even if the conjugate concentrations measured by HPLC were similar among the three rabbits, samples from rabbit 2 showed a longer coagulation time in the first time points. In addition, the relative prolongation times were slightly lower than expected, even considering the three-fold dilution required to perform the assay. Taken together, these observations indicated an *in vivo* variability that is difficult to predict. However, the results clearly showed that, in case of thrombotic events in blood, the conjugate would be able to efficiently prevent the activation of the cascade for a prolonged period of time. Given the seven-fold higher affinity of the (F)-tag-3xPEG$_{24}$-FXII inhibitor to human albumin and known allometric scaling effects among different species, the weaker impact of the conjugate on aPTT measured in human plasma will be probably compensated by a much longer *in vivo* half-life in humans. Therefore, an expected half-life of more than one day should offer, at the appropriate peptide's plasma concentrations, a solid protection over the time that strongly reduces the risk of thrombosis triggered by pathological or external factors.

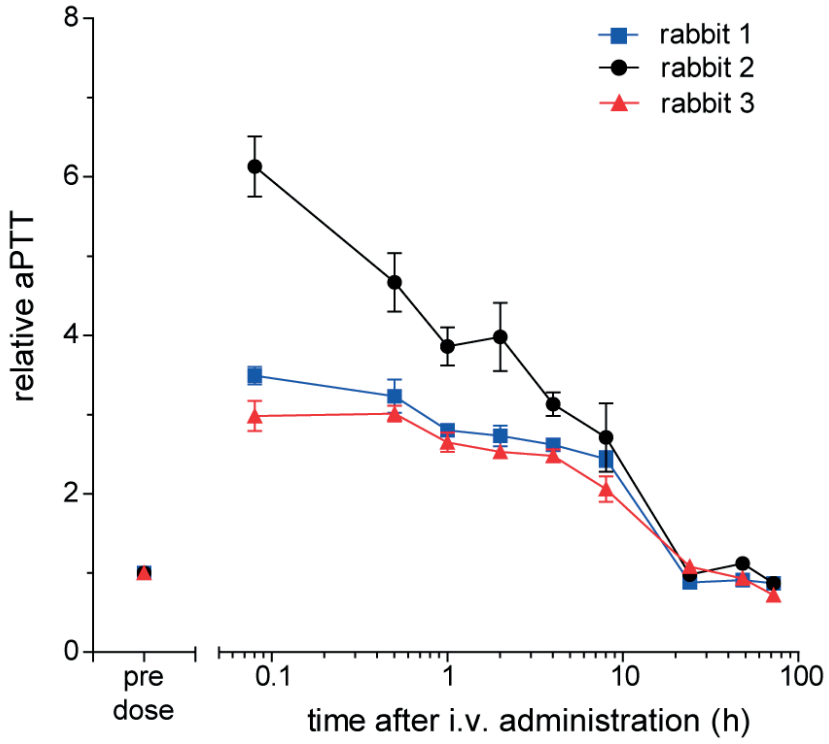

Figure 93. Coagulation parameter aPTT for the (F)-tag-3xPEG$_{24}$-FXII inhibitor in rabbits. The activity of the conjugate on plasma samples collected at different time points was measured upon incubation at 37°C with actin, respectively; coagulation was triggered by $CaCl_2$.

4. Conclusions

Lipidation is an established strategy for extending the circulation time of peptides as showcased by the approved drugs insulin detemir, insulin degludec and liraglutide. In these peptide drugs, fatty acids such as myristic or palmitic acid are appended to an amino acid within the peptide sequence of the drug itself. Peptides bind via the fatty acid to serum albumin, thus delaying their blood clearance.[123,227,228] It is expected that the half-life of these or other peptides can be further prolonged by embedding the fatty acid into a portable peptide sequence that enhances the binding to albumin. In fact, studies on acylated insulin analogues and albumin-binding peptides demonstrated that stronger affinities for albumin correlated with prolonged half-lives.[218,219]

Herein, I conceived a chimeric tag based on a fatty acid coupled to a Lys residue within a short peptide sequence that can be appended directly to bioactive peptides during their synthesis. I optimized the strategy to create this kind of conjugates on resin by automated SPPS, and succeeded in obtaining the desired products with high yield and purity by a single step of purification in a straightforward and economic manner. The solubility of these conjugates in aqueous solution correlated with the polarity of the acylated peptide sequence, showing that amino acid variations can strongly improve this important parameter. Initial albumin binding assays by fluorescence polarization identified a peptide sequence of seven residues modified with a palmitic acid as the best peptide-fatty acid format.

The affinity of this tag was improved by evolving the peptide sequence through six iterative rounds of amino acid substitution and binding assays for more than 150 variants. In addition to the palmitic acid, negatively charged or hydrophobic amino acids, flanking the central acylated Lys, were essential for increasing the affinity, resulting in a specific sequence of four Glu and two Tyr residues. The evolved tag exhibited a K_d of 39 nM for human albumin, improving the binding of the initial format by 27-fold. In addition, this tag was ten to more than 50-fold better than all the peptide- or fatty acid-based albumin binders developed so far.[71,208,227,228] The fluorescein moiety, initially added to the N-terminus of the tag to perform fluorescence polarization assays, revealed to be actually essential for the binding affinity. Another technique named isothermal titration calorimetry confirmed the result obtained by fluorescence polarization. In addition, the tag was able to bind rat and rabbit albumin with K_d values of 220 and 320 nM, respectively. This result proved that rats and rabbits could be valid animal models for *in vivo* pharmacokinetic studies of peptides conjugated to our albumin-binding tag.

The following step was the application of the evolved tag to two bioactive bicyclic peptides, UK18 and PK128, previously developed in our laboratory.[69,70] The tag was appended at either one of the two ends and the biochemical properties of the conjugates were characterized. The tag, when coupled to the N-terminus of the bicyclic peptides, kept the desired nanomolar affinity for human albumin. In contrast, tag conjugation had a different positioning- and peptide-dependent impact on the activity of the bicyclic peptides. For example, the N-terminal tagged UK18 retained its inhibitory activity, while the same conjugate format affected the potency of PK128. In addition, tag conjugation improved the proteolytic stability of bicyclic peptides, since they were intact and still functional upon prolonged incubation in plasma, in contrast to the non-tagged counterparts. Finally, the presence of four negatively charged amino acids in the tag sequence determined a conjugates' solubility higher than one $mg \cdot ml^{-1}$, despite the long hydrophobic tail of palmitic acid. Pharmacokinetic studies in rats of the UK18 conjugate revealed that the tag could prolong the circulation time of the bicyclic peptide 25-fold upon i.v. injection. This conjugate had a half-life of over seven hours, longer than the approved drugs liraglutide and insulin deglutec in rats.[253,258,259] In this sense, it might be conceivable to replace the albumin binding moieties used in those drugs with the tag here described.

All of these observations offered a valuable starting point for the half-life extension of the most advanced bicyclic peptide developed in our laboratory so far, a highly specific antagonist of the activated coagulation factor XII.[81,90,91] The testing of different synthetic structures of conjugates led to an optimized format that conserved both inhibitory activity against FXIIa and high affinity for albumin. *In vivo* experiments showed a 24-fold prolonged half-life in rabbits upon i.v. injection that translated into an efficient blockage of the intrinsic coagulation pathway for up to eight hours.

In conclusion, I developed a chimeric tag that combines the excellent albumin binding properties of fatty acids and the effective rational evolution of peptide affinity. This tag binds human albumin with low-medium nanomolar K_d, while it shows approximately six to nine-fold weaker affinity for rat and rabbit albumin. Tag conjugation to three bioactive peptides improves their pharmacokinetic profiles in these animal models. Considering the different affinity for human albumin as well as the allometric scaling, it is likely that peptide drugs modified with this tag can achieve half-lives of more than one day in humans. If such conjugates are administrated as a depot, an even longer exposure may be reached.

Thus, I hope that the tag presented in this work will be of interest for a large research and business audience in academic and industry labs because it is easily applicable to virtually any peptide moiety, including small proteins. This technology could be also useful for pharmaceutical industry, since with this tag it should be possible to expand the application range of peptide therapeutics from the current mostly short-lived agents that act mainly as receptor agonists to long-acting peptide drugs that can also address targets that require actions over extended time periods, such as the inhibition of enzymes or receptors.

5. Material and methods

Material

Abbreviation or product code	Name	Supplier
-	Fmoc and boc-protected amino acids	GL Biochem (Shanghai, China)
-	Fmoc-rink amide AM resin	
-	N-Fmoc-propargylglycine	
HBTU	O-benzotriazole-N,N,N′,N′-tetramethyl-uronium-hex-afluoro-phosphate	
HOBt	1-hydroxybenzotriazole	
HATU	1-[Bis(dimethylamino)methylene]-1H-1,2,3-triazolo[4,5-b]pyridinium 3-oxid hexafluorophosphate	
DCC	N,N-dicyclohexylcarbodiimide	Sigma-Aldrich (Steinheim, Germany)
5(6)-FAM	5(6)-carboxyfluorescein	
TBMB	1,3,5-tris(bromomethyl)benzene	
TATA	1,3,5-triacryloyl-1,3,5-triazinane	
TFA	trifluoroacetic acid reagent plus 99%	
NaASC	Sodium ascorbate	
TBTA	tris((1-benzyl-1H-1,2,3-triazol-4-yl)methyl) amine	
$CuSO_4$	Copper(II) sulfate	
-	Phenol	
-	Ethanol	
HCOOH	Formic acid	
DMSO	Dimethylsulfoxide	
DCM	Dichlorometane	
A1653 - A4327	Human albumin	
A6272	Rat albumin	
A0639	Rabbit albumin	
H4522	Human serum	
C7078	Casein from bovine milk	
PEG_{24}	Fmoc-NH-$[PEG]_{24}$-CH_2CH_2COOH	PurePEG (San Diego, CA, USA)
PEG_2	Fmoc-NH-$[PEG]_2$-CH_2COOH	Iris Biotech GmbH (Marktredwitz, Germany)
Lys(Dde)	N-alpha-(1-(4, 4-dimethyl-2,6-dioxocyclohex-1-yli-dene)ethyl)-N-epsilon-(9-Fmoc)-L-lysine	
NH_2-NH_2	Hydrazine hydrate (hydrazine 64%)	Acros Organics (Geel, Belgium)
-	Diethyl ether	
-	Piperidine	

Myr (C14)	Myristic acid	TCI (Zwijndrecht, Belgium)
Palm (C16)	Palmitic acid	
Ste (C18)	Stearic acid	
Gnd·HCl	Guanidinium hydrochloride	
EDT	1,2-ethanedithiol	
NH_4HCO_3	Ammonium bicarbonate	Applichem (Darmstadt, Germany)
Na_2HPO_4	Disodium phosphate	
KH_2PO_4	Potassium dihydrogen phosphate	
Tween-20	Polysorbate 20	
SDS	Sodium dodecyl sulfate	
Tris	Tris(hydroxymethyl)aminomethane	
DIPEA	N,N-diisopropylethylamine	Roth (Karlsruhe, Germany)
DMF	Dimethylformamide	
NaCl	Sodium chloride	
KCl	Potassium chloride	
$MgCl_2$	Magnesium chloride	
$CaCl_2$	Calcium chloride	
MeCN	Acetonitrile	Fisher Scientific (Loughborogh, UK)
TFA	Trifluoroacetic HPLC grade	
-	Thioanisole	Alfa Aesar (Karlsruhe, Germany)
-	Acetic anhydride (Ac2O)	Merck (Honenbrunn, Germany)
5(6)-FAM azide	5(6)-carboxyfluorescein azide	Tenova Pharmaceuticals (San Diego, CA, USA)
-	Fluorogenic substrates: Z-Gly-Gly-Arg-AMC, Z-Phe-Arg-AMC, Boc-Gln-Gly-Arg-AMC, H-D-Val-Leu-Lys-AMC	Bachem (Bubendorf, Switzerland)
-	Enzymes: PK, FXIIa, FXIa, trypsin, thrombin, plasmin	Molecular Innovations Innovative Research (Novi, MI, USA)
-	Human, rat and rabbit plasma	
Pathromtin* SL	Silicon dioxide particles, plant phospholipids in HEPES buffer system	Siemens (Erlangen, Germany)
Dade/Actin	Cephalin, extract from dehydrated rabbit brain containing 0.1 mM ellagic acid	
$CaCl_2$ solution	Calcium chloride solution	

All reagents were used as received without further purification.

Peptide synthesis

Peptides were synthesized on an Advanced ChemTech 348Ω parallel peptide synthesizer (AAPPTec) by standard Fmoc solid-phase chemistry on Rink Amide resin (0.26 mmol/g resin, 0.03 mmol scale), using DMF (99.5% pure) as a solvent. The coupling was carried out twice for each natural amino acid (4 equiv.) using HBTU (4 equiv.), HOBt (4 equiv.) and DIPEA (6 equiv.). The coupling of unnatural amino acids (2 equiv.) was performed once using HATU (2 equiv.) and DIPEA (4 equiv.). Fmoc groups were removed using a 20% v/v solution of piperidine in DMF. Washing steps were performed with DMF.

Fluorescein and acetyl modifications at the N-terminus

Peptides were modified with 5(6)-FAM (2 equiv.), DCC (2 equiv.) and HOBt (4 equiv.) in 3 ml DMF and shaken for 1 hr at 400 rpm for N-terminal fluorescein labeling. Peptides were modified with Ac2O (6 equiv.) and DIPEA (6 equiv.) in 3 ml DCM and shaken for 1 hr at 400 rpm for N-terminal acetylation.

Peptide acylation with fatty acids

Lys(Dde) was selectively deprotected by incubating the resin 3 times with 2% hydrazine hydrate in DMF for 3 min at 400 rpm, which also cleaved the Fmoc groups. The N-terminus was protected by Boc in unlabeled peptides not modified with fluorescein or acetyl. Peptides were acylated at the Lys side chain by the addition of free fatty acid (2 equiv.), DCC (2 equiv.) and HOBt (4 equiv.) in 3 ml DMF and shaken for 2 hrs at 400 rpm.

Peptide cleavage and deprotection

Final peptides were deprotected and cleaved from the resin under reducing conditions (90% TFA, 2.5% H_2O, 2.5% thioanisole, 2.5% phenol, 2.5% EDT) for 4 hrs with shaking at room temperature. The resin was removed by vacuum filtration, and the peptides were precipitated with cold diethyl ether (50 ml) and incubation for 30 min at -20°C, and pelleted by centrifugation. The precipitated peptides were washed twice with cold diethyl ether (30 and 20 ml, respectively). Peptides were either lyophilized or directly purified.

Chemical cyclization

Crude peptide (9 ml, 1.2 mM) was dissolved in 40% v/v MeCN and 60% v/v aqueous reaction buffer (60 mM NH_4HCO_3, pH 8.0) and cyclization linker TBMB or TATA was added (1 ml, 15 mM in MeCN). The final reagent and solvent concentrations in the reaction mixture were 1 mM peptide, 1.5 mM cyclization linker, 50% v/v aqueous reaction

buffer, and 50% v/v MeCN. The reaction mixture was incubated at 30°C in a water bath for 1 hr and then lyophilized.

Fluorescein modification at the C-terminus

Peptides were modified on a propargylglycine residue by click chemistry for C-terminal fluorescein labeling. Alkylated peptide (10mM), 5(6)-FAM azide (12 mM) and TBTA (20 mM) in DMSO were mixed with a catalytic mixture composed by CuSO4 (20 mM) and NaASC (100 mM) in H2O, and the volume adjusted with DMSO. The final reagent and solvent concentrations in the reaction mixture were 1 mM peptide, 1.2 mM 5(6)-FAM azide, 2 mM TBTA, 2 mM $CuSO_4$, 10 mM NaASC, 30% v/v H_2O and 70% v/v DMSO. The reaction proceeded at room temperature overnight.

Peptide purification

Short peptides acylated with fatty acid were purified by semi-preparative reversed-phase HPLC (PrepLC 4000-Waters system, Vydac C18 TP1022, 250 × 22 mm, 10 μm) using a flow rate of 20 ml·min^{-1} and a linear gradient of 50-90% v/v solvent B in 15 min. Cyclized peptides acylated with fatty acid were purified by semi-preparative reversed-phase HPLC (PrepLC 4000-Waters system, Vydac C18 TP1022, 250 × 22 mm, 10 μm) using a flow rate of 20 ml·min^{-1} and a linear gradient of 30-80% v/v solvent B in 30 min. Peptides modified by click chemistry were purified by semipreparative reversed-phase HPLC (PrepLC 4000-Waters system, XBridge BEH300 Prep C18 column, 9.4 mm × 250 mm, 10 μm, Waters) using a flow rate of 6 ml·min^{-1} and a linear gradient of 30-80% v/v solvent B in 30 min. Fractions containing the desired peptide were lyophilized.
Solvents: A, 99.9% v/v H_2O and 0.1% v/v TFA; B, 99.9% v/v MeCN and 0.1% v/v TFA.

HPLC and mass spectrometric analysis

The mass of purified peptides was determined by electrospray ionization mass spectrometry (ESI-MS) in positive ion mode on a single quadrupole liquid chromatograph mass spectrometer (LCMS-2020, Shimadzu). The purity was assessed by RP-HPLC (Agilent 1260 HPLC system) using a C18 column (Agilent ZORBAX 300SB-C18, 4.6 mm × 250 mm, 5 μm). Peptides used in the solubility assay were run with a flow rate of 1 ml·min^{-1} in a linear gradient 0-50% v/v solvent B over 15 min, while all the other peptides were run with a linear gradient of 0-100% v/v solvent B over 15 min (A: 94.9% v/v H_2O, 5% v/v MeCN and 0.1% v/v TFA; B: 94.9% v/v MeCN, 5% v/v H_2O and 0.1% v/v TFA).

Fluorescence polarization albumin binding assay

Human albumin (A1653), rat albumin (A6272), rabbit albumin (A0639), and human serum (H4522) were serially diluted (2-fold) in phosphate buffer saline (PBS; 10 mM Na_2HPO_4, 1.8 mM KH_2PO_4, 137 mM NaCl, 2.7 mM KCl,), pH 7.4, 0.01% v/v Tween-20. The highest concentrations were 28 μM for human albumin, 26 μM for rat albumin, 29 μM for rabbit albumin and 25 μM for human albumin from serum (assuming a concentration of albumin equal to 600 μM in serum). 45 μl of the dilutions were added to 15 μl of fluorescent peptide (100 nM) in black 96-well half area microtiter plates. The concentrations of albumin in the assay plate were ranging from 21 μM (human albumin), 19.5 μM (rat albumin), 21.75 μM (rabbit albumin) and 18.75 μM (human albumin in serum) to around 40 nM. The final concentration of fluorescent peptide was 25 nM in all wells. Fluorescence anisotropy was measured with an Infinite M200Pro plate reader (Tecan) using an excitation filter at 485 nm and an emission filter at 535 nm. Dissociation constant of fluorescent peptide (K_d) was determined by nonlinear regression analysis of anisotropy versus the total concentration of proteins $[P]_T$ using the following equation[71] :

$$\mathbf{A} = \mathbf{A_f} + (\mathbf{A_b} - \mathbf{A_f}) \cdot \left\{ \frac{\left[([\mathbf{L}]_\mathbf{T} + \boldsymbol{K}_\mathbf{d} + [\mathbf{P}]_\mathbf{T}) - \sqrt{([\mathbf{L}]_\mathbf{T} + \boldsymbol{K}_\mathbf{d} + [\mathbf{P}]_\mathbf{T})^2 - 4[\mathbf{L}]_\mathbf{T} \cdot [\mathbf{P}]_\mathbf{T}} \right]}{2[\mathbf{P}]_\mathbf{T}} \right\}$$

A is the experimental fluorescence anisotropy. A_f and A_b are the fluorescence anisotropy for free and the fully bound fluorescent peptide, respectively. $[L]_T$ and $[P]_T$ represent total fluorescent peptide and albumin concentration, respectively. Values were calculated with Prism 5 (GraphPad software).

Isothermal titration calorimetry

Fluorescent tag (500 μM) and human albumin (50 μM, A1653) were prepared in PBS, pH 7.4, 0.01% v/v Tween-20. Titrations of fluorescein tag in the syringe (40 μl) into human albumin in the cell (300 μl) were carried at 25°C out with a MicroCal™ iTC200 (MicroCal/GE Healthcare). 20 or 40 injections of a 2 or 1 μl volume, respectively, were performed, lasting 2 sec and spaced 180 sec. The value associated with the first peak was excluded. The background heat of injection, determined by injecting both fluorescent tag into buffer and buffer into human albumin, was measured and subtracted from the heat of binding. Data were analyzed using Origin for ITC software, and fitted with a two-sites binding model. The Gibbs free energy change was calculated using equations $\Delta G = R \cdot T \cdot \ln(K_d) = \Delta H - T \cdot \Delta S$, with R = 1.987 $cal \cdot K^{-1} \cdot mol^{-1}$ and T = 298.15 K.

Competitive fluorescence polarization albumin binding assay

Human albumin and fluorescent tag were diluted to 300 nM and 75 nM, respectively, in PBS, pH 7.4, 0.01% v/v Tween-20. Acetylated tag was serially diluted (2-fold) in PBS, pH 7.4, 0.01% v/v Tween-20 starting from a concentration of 450 μM. 20 μl of each dilution was added into black 96-well half area microtiter plates. The concentrations in the assay plate were 100 nM for human albumin and 25 nM for fluorescent tag in all wells, and ranging from 150 μM to 44 nM for acetylated tag. Fluorescence anisotropy was measured with an Infinite M200Pro plate reader (Tecan) using an excitation filter at 485 nm and an emission filter at 535 nm after 15 min incubation. IC_{50} value was calculated with GraphPad Prism5 software using the log(inhibitor) vs. response variable slope model. Dissociation constant of acetylated tag (K_d^C) was determined applying the following equation[251]:

$$K_{\mathbf{d}}^{C} = \frac{(\mathbf{L}\cdot\mathbf{P})_{\mathbf{50}}\cdot\mathbf{I}_{\mathbf{50}}\cdot K_{\mathbf{d}}}{([\mathbf{L}]_{\mathbf{T}}\cdot[\mathbf{P}]_{\mathbf{T}}) + (\mathbf{L}\cdot\mathbf{P})_{\mathbf{50}}\cdot([\mathbf{P}]_{\mathbf{T}} - [\mathbf{L}]_{\mathbf{T}} + (\mathbf{L}\cdot\mathbf{P})_{\mathbf{50}} - K_{\mathbf{d}})}$$

where:

$$\mathbf{I}_{\mathbf{50}} = \mathbf{IC}_{\mathbf{50}} - \frac{[\mathbf{P}]_{\mathbf{T}}}{\mathbf{2}}$$

and

$$(\mathbf{L}\cdot\mathbf{P})_{\mathbf{50}} = [\mathbf{L}]_{\mathbf{T}}\cdot\frac{\mathbf{A}_{\mathbf{50}} - \mathbf{A}_{f}}{\mathbf{A}_{b} - \mathbf{A}_{f}}$$

IC_{50} represents concentration of unlabeled tag needed to displace 50% of fluorescent tag from albumin. $(L{\cdot}P)_{50}$ represents multiplied value of fluorescent tag and albumin concentration at IC_{50}. A_{50} is the experimental fluorescence anisotropy at IC_{50}. A_f and A_b are the fluorescence anisotropy for free and the fully bound fluorescent tag, respectively. K_d is the dissociation constant for the binding equilibrium of fluorescent tag. $[L]_T$ and $[P]_T$ represent total fluorescent tag and albumin concentration, respectively.

Solubility assay

The molar extinction coefficients of unlabeled UK18 and PK15 conjugates were determined at 205, 210 and 220 nm by measuring the absorption on a GeneQuant 1300 UV-Vis spectrophotometer (GE Healthcare) of serial dilutions in water starting from an initial concentration of one $mg{\cdot}ml^{-1}$. The solubility was measured by dissolving peptides in PBS, pH 7.4 at a theoretical concentration of ten $mg{\cdot}ml^{-1}$. A maximal amount of peptide was

dissolved by inverting the tube at room temperature for 45 min. Non-dissolved peptide was removed by centrifugation for 30 min at 13,000 g and transfer of the supernatant to a new tube. This process was repeated once. The solubility of unlabeled UK18 and PK15 conjugates was determined by measuring the absorption at 205, 210 and 220 nm with a Cary 50 UV-Vis spectrophotometer (Varian) upon serial dilutions in PBS. The solubility of fluorescent UK18 and PK128 conjugates was determined by measuring the absorption at 495 nm and using a molar extinction coefficient of 68,000 $M^{-1}cm^{-1}$ with a NanoDrop 8000 UV-Vis spectrophotometer (Thermo Scientific) upon serial dilutions in PBS.

Protease inhibition assays

K_i values of UK18 and acetylated/unlabeled conjugates were determined by measuring residual activity of recombinant human urokinase[70] (1.5 nM) in the presence of different dilutions of inhibitor (2-fold dilutions, ranging from 1 μM to 0.97 nM final concentration) using the fluorogenic substrate Z-Gly-Gly-Arg-AMC (50 μM final concentration). K_i values of PK128 and acetylated/unlabeled conjugates were determined by measuring residual activity of human plasma kallikrein (0.25 nM) in presence of different dilutions of inhibitor (2-fold dilutions, ranging from 250 nM to 0.24 nM final concentration) using the fluorogenic substrate Z-Phe-Arg-AMC (50 μM final concentration). The enzymatic assays were performed at 25°C in a volume of 150 μl of assay buffer (10 mM Tris-Cl, pH 7.4, 150 mM NaCl, 10 mM $MgCl_2$, 1 mM $CaCl_2$, 0.01% v/v Tween-20, 0.1% (w/v) casein (bovine milk; C7078)) containing 5% v/v DMSO. Activity in presence of human albumin (99% pure, fatty acid free; A4327) was measured at an albumin concentration of 25 μM.

K_i values of FXII inhibitor, acetylated tagged FXII inhibitors and fluorescent tag-3xPEG_{24}-FXII inhibitor were determined by measuring residual activity of human FXIIa (0.4 nM) in the presence of different dilutions of inhibitor (2-fold dilutions, ranging from 31.25 nM to 0.31 nM final concentration) using the fluorogenic substrate Boc-Gln-Gly-Arg-AMC (50 μM final concentration). The enzymatic assay was performed at 25°C in a volume of 150 μl of assay buffer containing 1% v/v DMSO. Activity in presence of human albumin (99% pure, fatty acid free; A4327) was measured at an albumin concentration of 10 μM. Increased concentrations of acetylated tagged FXII inhibitors (2-fold dilutions, ranging from 1 μM to 0.97 nM final concentration; except for FXII inhibitor and (F)-tag-3xPEG_{24}-FXII inhibitor, with final concentrations kept unchanged) and of FXIIa (3 nM) were used as fluorogenic substrate hydrolysis by albumin preparations interfered with the assay.

Fluorescence intensity was measured for 30 min or 1 hr using an Infinite M200Pro plate reader (Tecan; AMC-substrates: excitation at 368 nm, emission at 467 nm) with a read

every minute. Sigmoidal curves were fitted to the data using the following log(inhibitor) vs. response variable slope model equation:

$$\mathbf{y} = \frac{\mathbf{100}}{\mathbf{1} + \mathbf{10}^{(\mathbf{log}IC_{\mathbf{50}} - \mathbf{x})\mathbf{p}}}$$

wherein x is the peptide concentration, y is the residual percentage of protease activity, p is the Hill slope. IC_{50} values were derived from the fitted curve Prism 5 (GraphPad software). The K_i values were calculated based on the IC_{50} values applying the Cheng-Prusoff equation: $K_i = IC_{50}/(1+(S/K_m)$ wherein IC_{50} is the functional strength of the inhibitor, S is the total substrate concentration and K_m is the Michaelis-Menten constant for substrate hydrolysis catalyzed by the enzyme. The following K_m values were used for the calculation: 112 μM for urokinase / Z-Gly-Gly-Arg-AMC [70], 165 μM for plasma kallikrein / Z-Phe-Arg-AMC [69], 256 μM for FXIIa / Boc-Gln-Gly-Arg-AMC [90].

The specificity of fluorescent tag-3xPEG_{24}-FXII inhibitor (2-fold dilutions, ranging from 10 μM to 9.7 nM final concentration) was assessed by measuring the inhibition of the following human serine proteases: urokinase 1.5 nM, factor XIa 0.25 nM, plasma kallikrein 0.25 nM, thrombin 1 nM, plasmin 2.5 nM, trypsin 0.1 nM. The following fluorogenic substrates were used at 50 μM final concentration: Z-Phe-Arg-AMC for plasma kallikrein, Boc-Phe-Ser-Arg-AMC for factor XIa, Z-Gly-Gly-Arg-AMC for urokinase, thrombin and trypsin, and H-D-Val-Leu-Lys-AMC for plasmin.

Plasma stability assay

20 μM of UK18, PK128, and relative acetylated conjugates was incubated in human plasma at 37°C in a water bath. Probes were taken at different time points (5 min, 0.5, 1, 2, 4, 8, 24 and 48 hrs), diluted to 3 μM (urokinase inhibitors) or 0.75 μM (plasma kallikrein inhibitors) with assay buffer, heat inactivated by incubation at 65°C for 20 min, centrifuged at 16,000 g for 5 min and the supernatant transferred to a new tube. The inhibitory activity of each sample was assessed by preparing a series of 2-fold dilutions and measuring residual protease activity for urokinase and plasma kallikrein as described above. Residual inhibition in % was calculated using the equation $IC_{50,0h}/IC_{50,xh}$*100 wherein IC_{50},0h is the functional strength of the inhibitor at time point 0 and $IC_{50,xh}$ the functional strength of inhibitor after one of the different plasma incubation periods mentioned above. The resulting percentages of inhibition were plotted in Prism 5 software (GraphPad software) versus time and analyzed using a one-phase decay model.

Pharmacokinetic study in rats

Female Sprague Dawley rats were injected with 0.5 mg·kg^{-1} fluorescent UK18 and PK128 conjugates, 0.3 mg·kg^{-1} fluorescent UK18, or 0.25 mg·kg^{-1} fluorescent tag, in 200 μl PBS, pH 7.4, 0.01% SDS (130 μM) via the tail vein (3 animals per group). Blood samples (100 μl) were collected at different time points via the orbital sinus into tubes containing EDTA, processed to plasma by centrifugation at 360 g for 15 min at 4°C and stored at −80°C. Peptide injection and blood sample collection was performed by Washington Biotech Inc. following ethical standards for animal studies of the Office for Laboratory Animal Welfare (OLAW), a division of the U.S. Public Health Service as administered by the National Institutes for Health. Samples were analyzed by RP-HPLC (Agilent 1260 HPLC system) equipped with a fluorescence detector (Shimadzu RF-10AXL detector, excitation at 445 nm, emission at 535 nm) using a C18 column (Agilent ZORBAX 300SB-C18, 4.6 mm x 250 mm, 5 μm) and a linear gradient of solvent B 0−100% v/v over 15 min at a flow rate of 1 ml min^{-1} (solvent A: 94.9% v/v H_2O, 5% v/v MeCN and 0.1% v/v TFA; solvent B: 94.9% v/v MeCN, 5% v/v H_2O and 0.1% v/v TFA). Plasma samples were processed before RP-HPLC analysis as follows. 2 μM fluorescein was added as standard to 5 μl plasma sample. 5 μl of 7 M guanidinium hydrochloride solution, pH 2.0 (adjusted with HCl) was added, mixed and incubated for 10 min at room temperature to denature proteins. 200 μl of cold ethanol was added and incubated on ice for 1 hr to precipitate proteins. Samples were centrifuged at 9,000 g for 15 min at 4°C and the supernatant dried by centrifugal evaporation under vacuum. Dried samples were dissolved by stepwise addition of 10 μl DMSO and 90 μl solvent A (99.9% v/v H_2O, 0.1% v/v TFA). 95 μl were analyzed by RP-HPLC. Peptides were quantified by integrating the area under the peaks, and normalization was based on the standard and comparison to standard curves. Standard curves were obtained by analyzing known peptide quantities that were dissolved in plasma and processed as well as analyzed using the same procedure. Pharmacokinetic parameters were calculated using a two-compartment model.[257] Time points: 5 min, 0.5, 1, 2, 4, 8, 24 and 48 hrs for fluorescent tag, fluorescent UK18 and PK128 conjugates; 4, 8, 15 min, 0.5, 1, 2, 4 and 8 hrs for fluorescent UK18.

Coagulation assays

aPTT (activated Partial Thromboplastin Time) was measured on a STart4 coagulation analyzer (Diagnostica Stago). PK128, FXII inhibitor and relative acetylated or fluorescent conjugates were mixed with human and rabbit plasma at known concentrations. 100 μl of human plasma was incubated at 37°C with 100 μl of Pathromtin* SL for 2 min. 100 μl

of rabbit plasma with was incubated at 37°C with 100 µl of Dade/Actin for 3 min. Coagulation was triggered by addition of 100 µl of $CaCl_2$ solution (25 mM). The time to coagulation was assessed by monitoring the movement of a steel ball in the plasma.

Pharmacokinetic study in rabbits

Female New Zealand White rabbits were injected with 3.7 $mg \cdot kg^{-1}$ FXII inhibitor in 1 ml PBS, pH 7.4 (3 mM) or 5 $mg \cdot kg^{-1}$ fluorescent tag-3xPEG_{24}-FXII inhibitor in 3 ml PBS, pH 7.4, 0.01% SDS (570 µM) via the ear vein (3 animals per group). Blood samples (1.8 ml) were collected at different time points via the auricular artery of the opposite ear into tubes containing Na citrate, processed to plasma by centrifugation at 360 g for 15 min at 4°C and stored at −80°C. Peptide injection and blood sample collection were performed by Washington Biotech Inc. following ethical standards for animal studies of the Office for Laboratory Animal Welfare (OLAW), a division of the U.S. Public Health Service as administered by the National Institutes for Health. Plasma samples were treated as the rat plasma samples described above. Samples from rabbits treated with fluorescent tag-3xPEG_{24}-FXII were analyzed by RP-HPLC using fluorescence detection and quantified as in the rat experiment described above. Samples from rabbits treated with FXII inhibitor were analyzed on a single quadrupole liquid chromatography mass spectrometer (LC/MS-2020, Shimadzu), using a C18 column (Phenomenex Kinetex® 2.6 µm C18 100 Å, LC Column 50 x 2.1 mm), a linear gradient of solvent B (5−30%) over 4.5 min at a flow rate of 1 $ml \cdot min^{-1}$ (solvent A: 94.95% v/v H_2O, 5% v/v MeCN and 0.05% v/v HCOOH; solvent B: 94.95% v/v MeCN, 5% v/v H_2O and 0.05% v/v HCOOH) and ESI detection in positive mode. FXII inhibitor analyzed by LC-MS was quantified based on the absolute intensities of the detected mass peaks (M^{3+} and M^{4+}) and adjusted according to the intensity of the mass peaks of the internal standard (fixed concentration of a peptide sequence similar to FXII inhibitor). Peptide concentrations in the plasma samples were calculated according to linear external standard curves obtained from dilution series of the peptide prepared in rabbit plasma. Pharmacokinetic parameters were calculated using a two-compartment model.[257] Time points: 5 min, 0.5, 1, 2, 4, 8, 24 and 48 hrs for fluorescent tag-3xPEG24-FXII inhibitor; 2, 5, 10, 20 and 40 for FXII inhibitor. aPTT of plasma samples collected from rabbits treated with fluorescent tag-3xPEG_{24}-FXII conjugate were determined as described above. Pre-dose samples were used as blank.

6. Supporting information

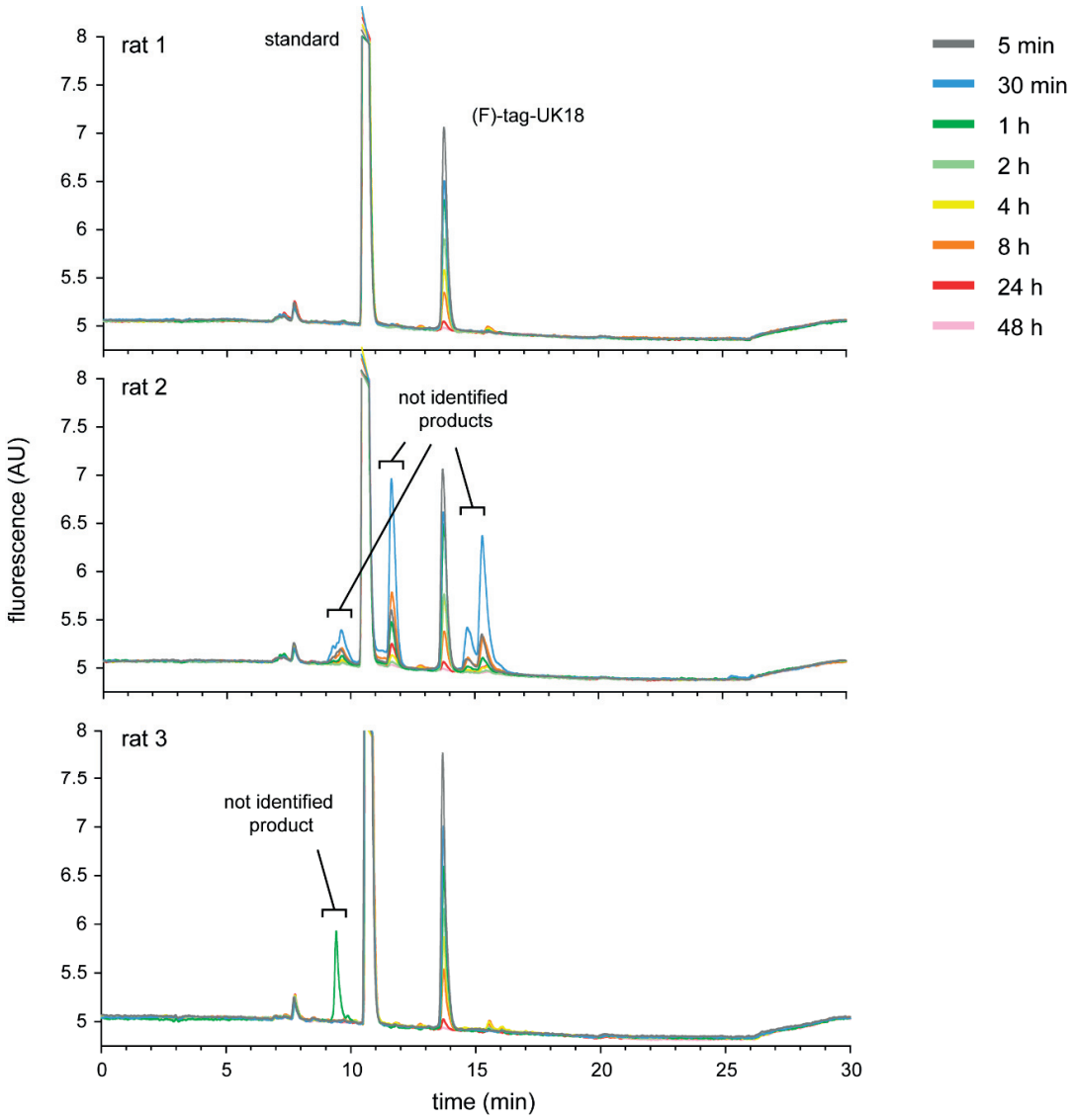

Figure S1. Pharmacokinetic study of fluorescein labeled tag-UK18 in rats. Fluorescent peptide species in blood samples taken from three rats at the indicated time points were analyzed by RP-HPLC and fluorescence detection. The blood samples were spiked with a fluorescent standard.

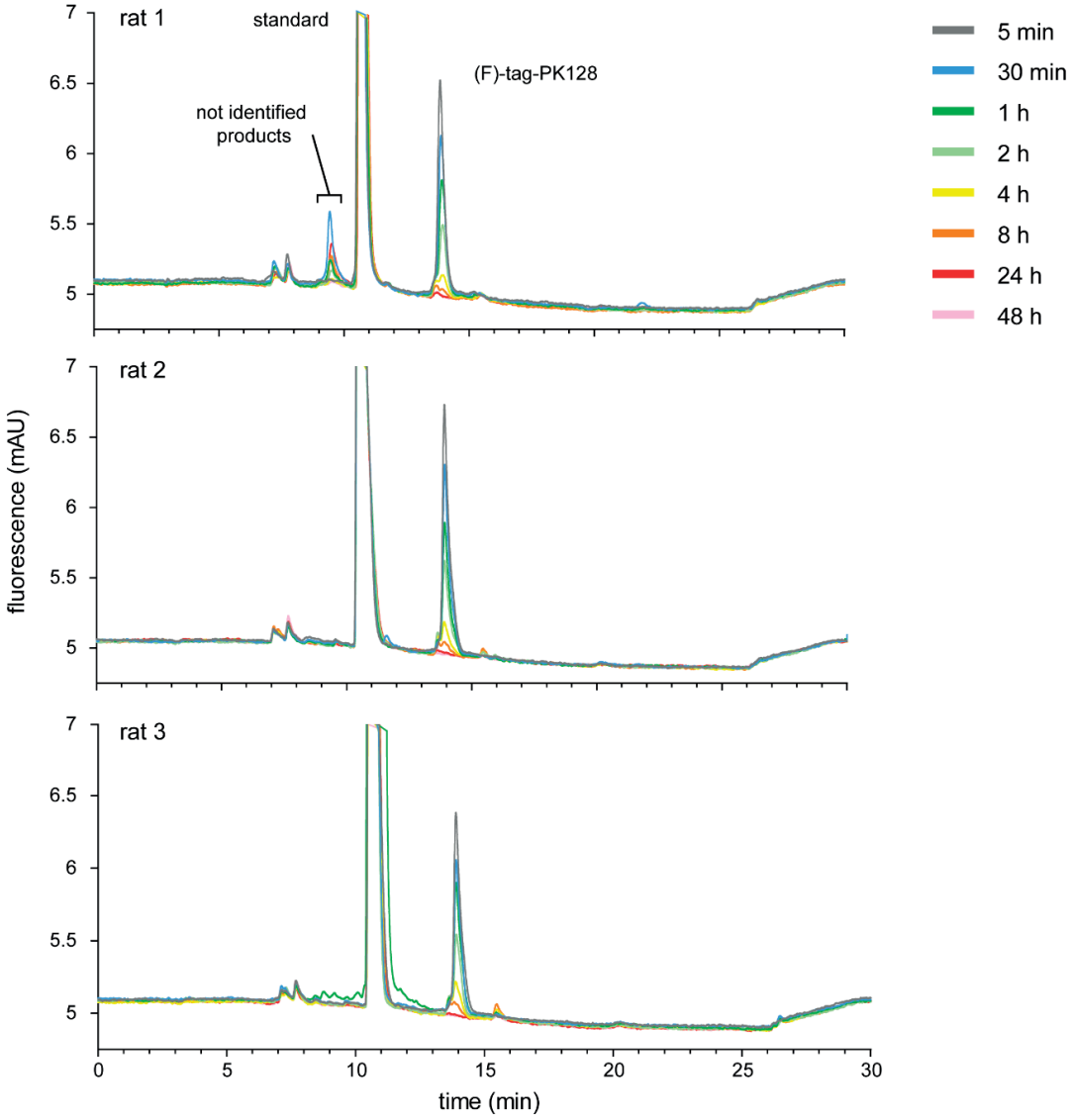

Figure S2. Pharmacokinetic study of fluorescein labeled tag-PK128 in rats. Fluorescent peptide species in blood samples taken from three rats at the indicated time points were analyzed by RP-HPLC and fluorescence detection. The blood samples were spiked with a fluorescent standard.

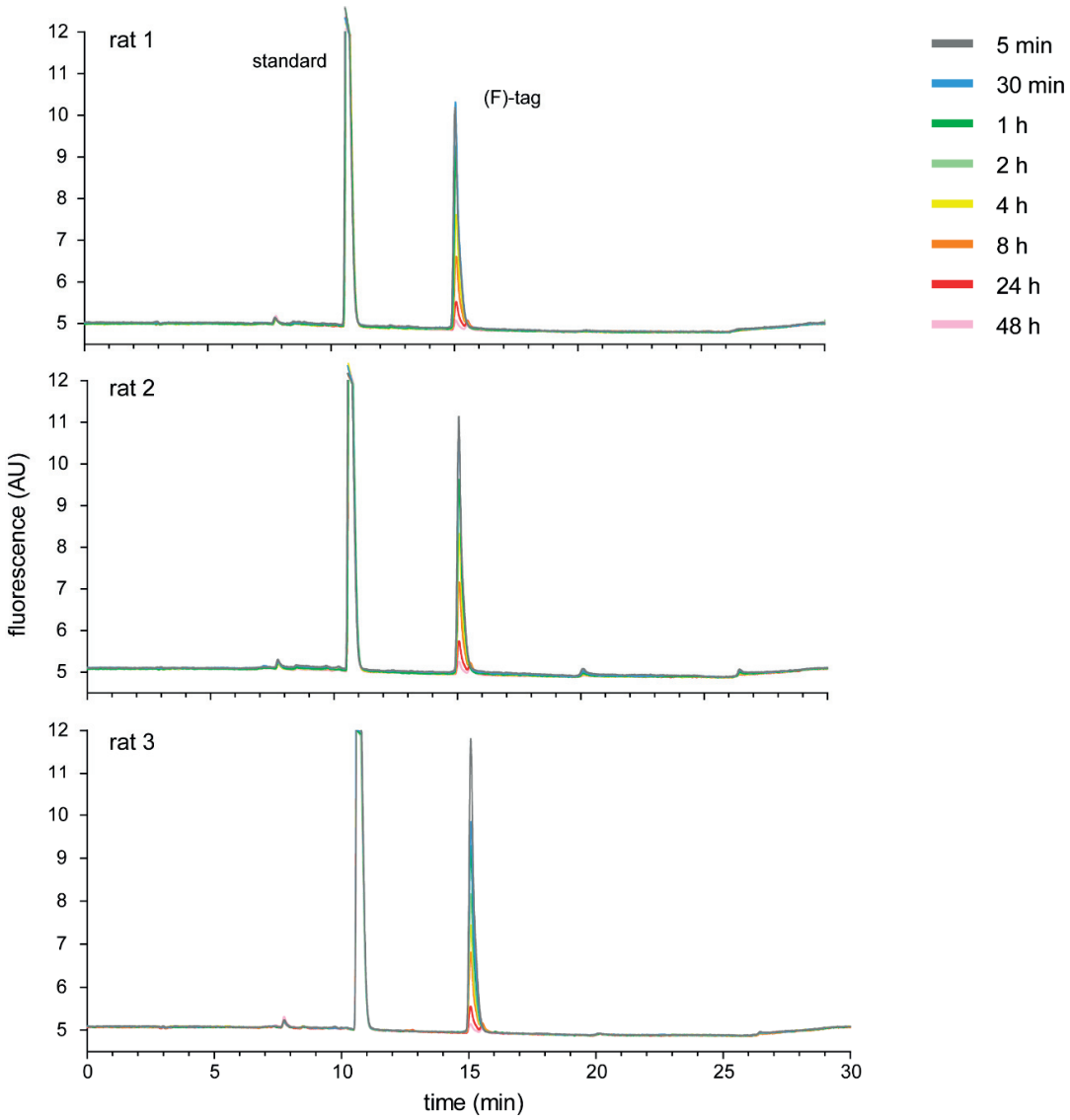

Figure S3. Pharmacokinetic study of fluorescein labeled tag in rats. Fluorescent peptide species in blood samples taken from three rats at the indicated time points were analyzed by RP-HPLC and fluorescence detection. The blood samples were spiked with a fluorescent standard.

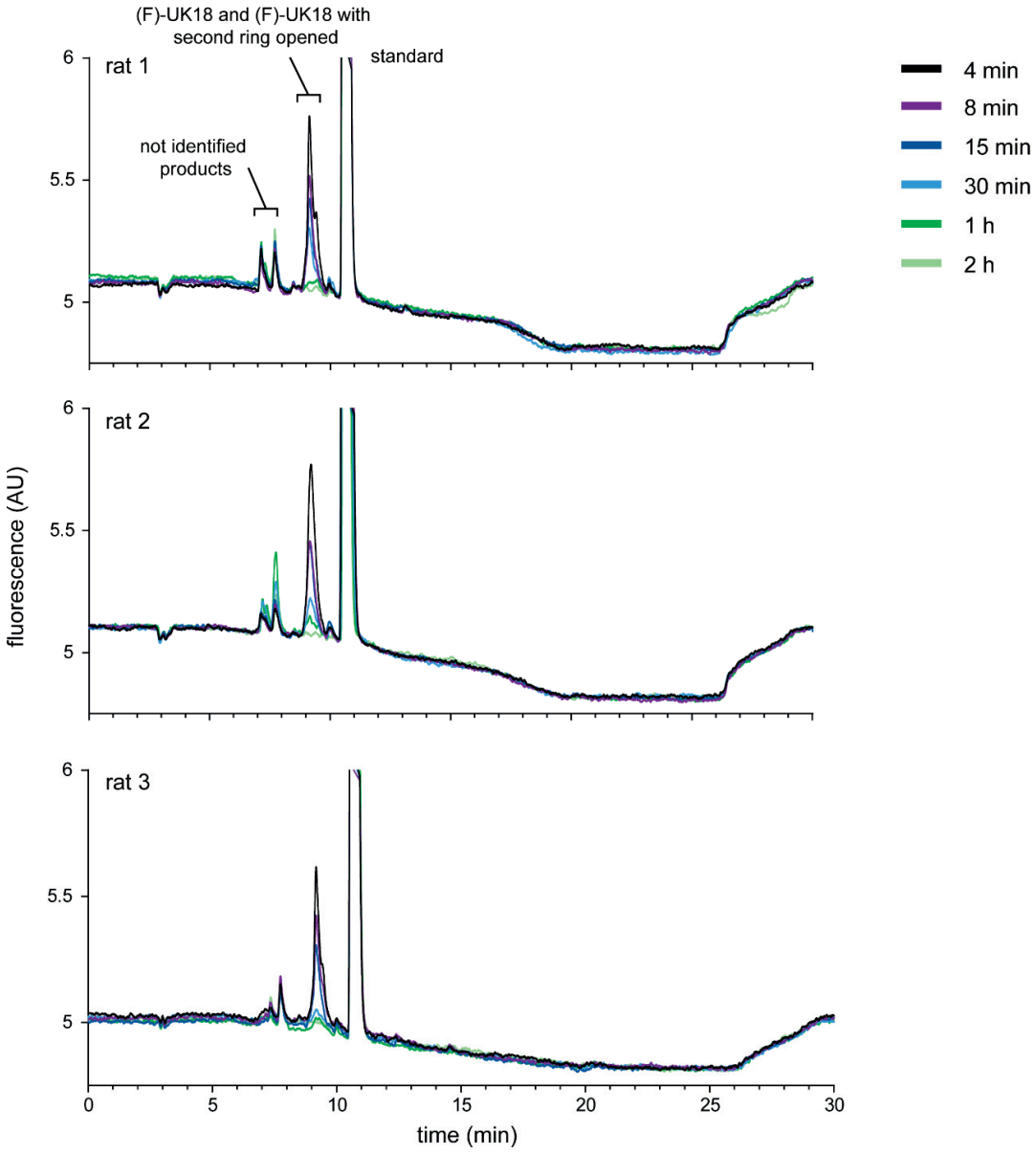

Figure S4. Pharmacokinetic study of fluorescein labeled bicyclic peptide UK18 in rats. Fluorescent peptide species in blood samples taken from three rats at the indicated time points were analyzed by RP-HPLC and fluorescence detection. The blood samples were spiked with a fluorescent standard.

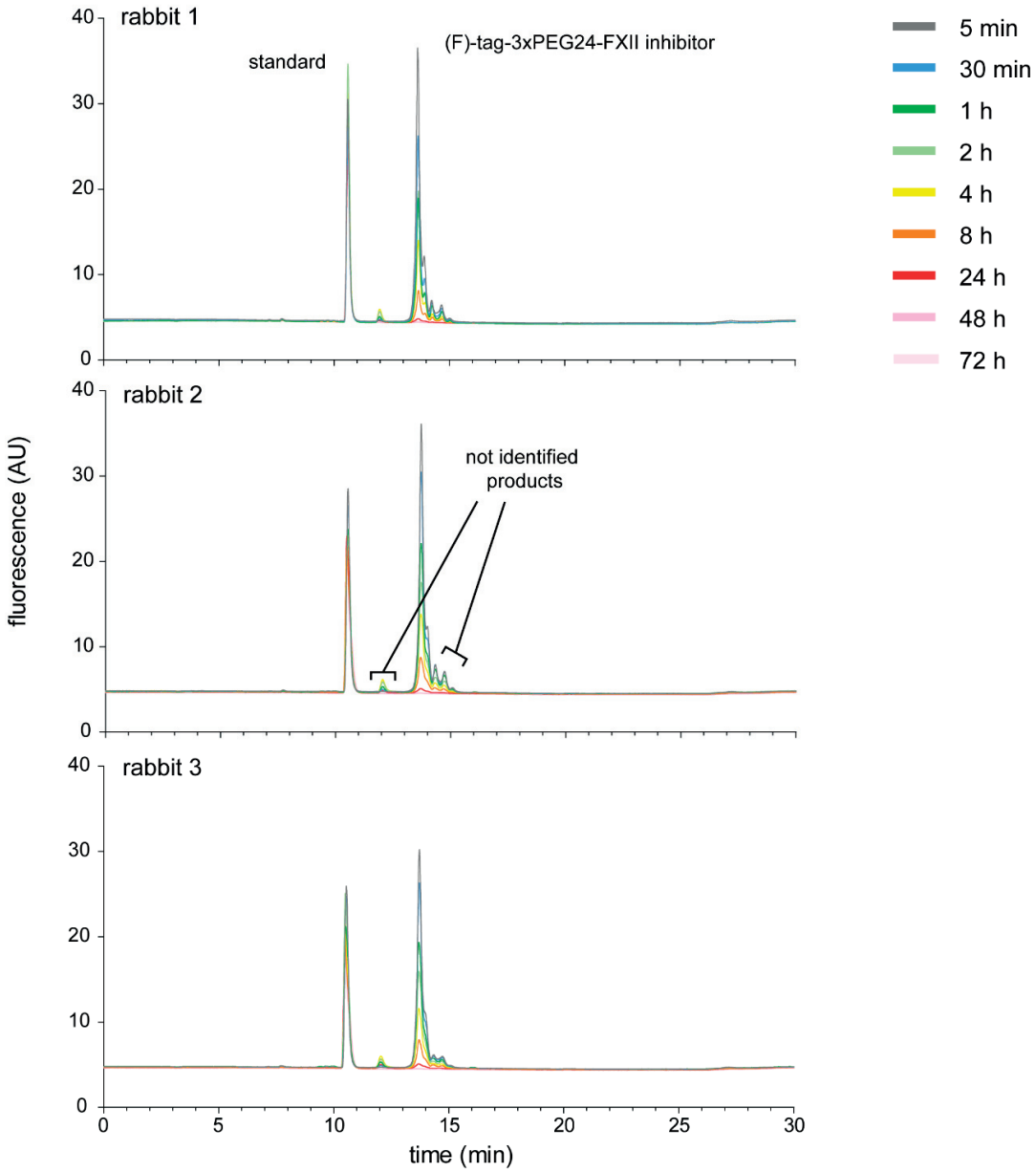

Figure S5. Pharmacokinetic study of fluorescein labeled tag-3xPEG24-FXII inhibitor in rabbits. Fluorescent peptide species in blood samples taken from three rats at the indicated time points were analyzed by RP-HPLC and fluorescence detection. The blood samples were spiked with a fluorescent standard.

Table S1. Pharmacokinetic parameters.

Name	Description	Symbol	Unit	Equation
dose	amount of drug administered	X_0	$\mu g \cdot kg^{-1}$	known parameter
plasma concentration	initial concentration after i.v. injection at time zero	$C_{p(0)}$	$\mu g \cdot ml^{-1}$	A + B
coefficients of biexponential equation	distribution phase	A		y-intercept of the determined distribution line C_p - C_p'
	elimination phase	B		y-intercept of the back extrapolate elimination line C_p'
exponents of biexponential equation (first-order rate constants)	distribution phase	α	min^{-1} or hrs^{-1}	slope of the distribution line (determine from line C_p - C_p')
	elimination phase	β		slope of the elimination line
first-order micro rate constants	transfer rate constant from the peripheral to the central compartment	K_{21}		$\frac{(A \cdot \alpha + B \cdot \beta)}{(A + B)}$
	elimination rate constant from the central compartment	K_{10}		$\frac{(\alpha \cdot \beta)}{K_{21}}$
	transfer rate constant from the central to the peripheral compartment	K_{12}		$(\alpha + \beta) - (K_{10} + K_{21})$
distribution half-life	time required for the concentration of a drug to reach half of its starting value	$\tau_{1/2}\ \alpha$	min or hrs	$\frac{\ln(2)}{\alpha}$
elimination half-life		$\tau_{1/2}\ \beta$		$\frac{\ln(2)}{\beta}$
area under the curve	integral of the plasma drug concentration vs time curve (bioavailability in plasma)	AUC	$mg \cdot min \cdot ml^{-1}$	$\frac{A}{\alpha} + \frac{B}{\beta}$
systemic clearance	volume of plasma purified from a drug per unit of time	CL	$ml \cdot hrs^{-1} \cdot kg$	$\frac{X_0}{AUC}$ *or* $V_D \cdot \beta$
volume of the central compartment	volume in which a drug distributes after i.v. injection at time zero	V_C	$ml \cdot kg^{-1}$	$\frac{X_0}{(A + B)}$
volume of distribution in the β-phase	volume in which a drug distributes during the elimination phase	V_D		$\frac{CL}{\beta}$ *or* $\frac{Xo}{AUC \cdot \beta}$

Values obtained from the biexponential equation $Cp = A \cdot e^{-\alpha \cdot t} + B \cdot e^{-\beta \cdot t}$ plotted as plasma concentration (y-axis, log scale) vs. time (x-axys).

7. References

1. Vlieghe, P., Lisowski, V., Martinez, J. & Khrestchatisky, M. Synthetic therapeutic peptides: science and market. *Drug Discov. Today* **15,** 40–56 (2010).
2. Kaspar, A. A. & Reichert, J. M. Future directions for peptide therapeutics development. *Drug Discov. Today* **18,** 807–817 (2013).
3. Craik, D. J., Fairlie, D. P., Liras, S. & Price, D. The future of peptide-based drugs: peptides in drug development. *Chem. Biol. Drug Des.* **81,** 136–147 (2013).
4. Product sales data from annual reports of major pharmaceutical companies - 2015. *http://www.pharma-compass.com/pharma-data/product-sales-data-from-annual-reports-of-major-pharmaceutical-companies-2015* (2016).
5. Uhlig, T. *et al.* The emergence of peptides in the pharmaceutical business: from exploration to exploitation. *EuPA Open Proteomics* **4,** 58–69 (2014).
6. Lax, E. R. Redefining the peptide therapeutics manufacturing industry in the 21st century (part 1) - Status and outlook in 2016. *Pharma Horiz.* **1 (1),** 64–72 (2016).
7. Henriques, S. T. & Craik, D. J. in *Peptide Chemistry and Drug Design, First Edition* (J. Wiley & Sons Hoboken, New Jersey, USA, 2015).
8. Ladner, R. C., Sato, A. K., Gorzelany, J. & de Souza, M. Phage display-derived peptides as therapeutic alternatives to antibodies. *Drug Discov. Today* **9,** 525–529 (2004).
9. Góngora-Benítez, M., Tulla-Puche, J. & Albericio, F. Multifaceted roles of disulfide bonds. Peptides as therapeutics. *Chem. Rev.* **114,** 901–926 (2014).
10. Driggers, E. M., Hale, S. P., Lee, J. & Terrett, N. K. The exploration of macrocycles for drug discovery — an underexploited structural class. *Nat. Rev. Drug Discov.* **7,** 608–624 (2008).
11. Roxin, Á. & Zheng, G. Flexible or fixed: a comparative review of linear and cyclic cancer-targeting peptides. *Future Med. Chem.* **4,** 1601–1618 (2012).
12. White, C. J. & Yudin, A. K. Contemporary strategies for peptide macrocyclization. *Nat. Chem.* **3,** 509–524 (2011).
13. Zorzi, A., Deyle, K. & Heinis, C. Cyclic peptide therapeutics: past, present and future. *Curr. Opin. Chem. Biol.* **38,** 24–29 (2017).
14. Owens, J. 2006 drug approvals: finding the niche. *Nat. Rev. Drug Discov.* **6,** (2007).
15. Hughes, B. 2007 FDA drug approvals: a year of flux. *Nat. Rev. Drug Discov.* **7,** 107–109 (2008).
16. Hughes, B. 2008 FDA drug approvals. *Nat. Rev. Drug Discov.* **8,** 93–96 (2009).
17. Hughes, B. 2009 FDA drug approvals. *Nat. Rev. Drug Discov.* **9,** 89–92 (2010).
18. Mullard, A. 2010 FDA drug approvals. *Nat. Rev. Drug Discov.* **10,** 82–85 (2011).

19. Mullard, A. 2011 FDA drug approvals. *Nat Rev Drug Discov* **11,** 91–94 (2012).

20. Mullard, A. 2012 FDA drug approvals. *Nat. Rev. Drug Discov.* **12,** 87–90 (2013).

21. Mullard, A. 2013 FDA drug approvals. *Nat. Rev. Drug Discov.* **13,** 85–89 (2014).

22. Mullard, A. 2014 FDA drug approvals. *Nat. Rev. Drug Discov.* **14,** 77–81 (2015).

23. Mullard, A. 2015 FDA drug approvals. *Nat Rev Drug Discov* **15,** 73–76 (2016).

24. Klinker, K. P. & Borgert, S. J. Beyond vancomycin: the tail of the lipoglycopeptides. *Clin. Ther.* **37,** 2619–2636 (2015).

25. Nicolaou, K. C., Boddy, C. N., Bräse, S. & Winssinger, N. Chemistry, biology, and medicine of the glycopeptide antibiotics. *Angew. Chem. Int. Ed.* **38,** 2096–2152 (1999).

26. Aguilar-Zapata, D., Petraitiene, R. & Petraitis, V. Echinocandins: the expanding antifungal armamentarium. *Clin. Infect. Dis.* **61,** S604–S611 (2015).

27. Modlin, I. M., Pavel, M., Kidd, M. & Gustafsson, B. I. Review article: somatostatin analogs in the treatment of gastro-entero-pancreatic neuroendocrine (carcinoid) tumors. *Aliment. Pharmacol. Ther.* (2009).

28. Bruns, C., Lewis, I., Briner, U., Meno-Tetang, G. & Weckbecker, G. SOM230: a novel somatostatin peptidomimetic with broad somatotropin release inhibiting factor (SRIF) receptor binding and a unique antisecretory profile. *Eur. J. Endocrinol.* **146,** 707–716 (2002).

29. Zain, J. & Jain, S. Romidepsin in the treatment of cutaneous T-cell lymphoma. *J. Blood Med.* 37 (2011).

30. Corsetti, M. & Tack, J. Linaclotide: a new drug for the treatment of chronic constipation and irritable bowel syndrome with constipation. *United Eur. Gastroenterol. J.* **1,** 7–20 (2013).

31. Busby, R. W. *et al.* Linaclotide, through activation of guanylate cyclase C, acts locally in the gastrointestinal tract to elicit enhanced intestinal secretion and transit. *Eur. J. Pharmacol.* **649,** 328–335 (2010).

32. Bryant, A. P. *et al.* Linaclotide is a potent and selective guanylate cyclase C agonist that elicits pharmacological effects locally in the gastrointestinal tract. *Life Sci.* **86,** 760–765 (2010).

33. Yaqoob, M. M. & Kaushik, T. Lessons learned from peginesatide in the treatment of anemia associated with chronic kidney disease in patients on dialysis. *Biol. Targets Ther.* 243 (2013).

34. Livnah, O. *et al.* Functional mimicry of a protein hormone by a peptide agonist: the EPO receptor complex at 2.8 Å. *Science* **273,** 464 (1996).

35. Wrighton, N. C. *et al.* Small peptides as potent mimetics of the protein hormone erythropoietin. *Science* **273,** 458 (1996).

36. Ironwood Pharmaceuticals provides fourth quarter and full year 2015 investor update. *http://investor.ironwood-pharma.com/releasedetail.cfm?releaseid=955707* (2016).

37. Srinivas, N. *et al.* Peptidomimetic antibiotics target outer-membrane biogenesis in *Pseudomonas aeruginosa*. *Science* **327,** 1010 (2010).

38. Robinson, J. A., DeMarco, S., Gombert, F., Moehle, K. & Obrecht, D. The design, structures and therapeutic potential of protein epitope mimetics. *Drug Discov. Today* **13,** 944–951 (2008).

39. DeMarco, S. J. *et al.* Discovery of novel, highly potent and selective β-hairpin mimetic CXCR4 inhibitors with excellent anti-HIV activity and pharmacokinetic profiles. *Bioorg. Med. Chem.* **14,** 8396–8404 (2006).

40. Sahu, A., Kay, B. K. & Lambris, J. D. Inhibition of human complement by a C3-binding peptide isolated from a phage-displayed random peptide library. *J. Immunol.* **157,** 884–891 (1996).

41. Chang, Y. S. *et al.* Stapled α−helical peptide drug development: a potent dual inhibitor of MDM2 and MDMX for p53-dependent cancer therapy. *Proc. Natl. Acad. Sci.* **110,** E3445–E3454 (2013).

42. Ricardo, A. *et al.* Preclinical evaluation of RA101495, a potent cyclic peptide inhibitor of C5 for the treatment of paroxysmal nocturnal hemoglobinuria. *Blood* **126,** 939–939 (2015).

43. Guillen Schlippe, Y. V., Hartman, M. C. T., Josephson, K. & Szostak, J. W. *In vitro* selection of highly modified cyclic peptides that act as tught binding inhibitors. *J. Am. Chem. Soc.* **134,** 10469–10477 (2012).

44. Bechara, C. & Sagan, S. Cell-penetrating peptides: 20 years later, where do we stand? *FEBS Lett.* **587,** 1693–1702 (2013).

45. Walensky, L. D. & Bird, G. H. Hydrocarbon-stapled peptides: principles, practice, and progress. *J. Med. Chem.* **57,** 6275–6288 (2014).

46. Passioura, T., Katoh, T., Goto, Y. & Suga, H. Selection-based discovery of druglike macrocyclic peptides. *Annu. Rev. Biochem.* **83,** 727–752 (2014).

47. Packer, M. S. & Liu, D. R. Methods for the directed evolution of proteins. *Nat. Rev. Genet.* **16,** 379–394 (2015).

48. Smith, G. Filamentous fusion phage: novel expression vectors that display cloned antigens on the virion surface. *Science* **228,** 1315 (1985).

49. Smith, G. P. & Petrenko, V. A. Phage display. *Chem. Rev.* **97,** 391–410 (1997).

50. Nixon, A. E., Sexton, D. J. & Ladner, R. C. Drugs derived from phage display: from candidate identification to clinical practice. *mAbs* **6,** 73–85 (2014).

51. Lowman, H. B. Bacteriophage display and discovery of peptide leads for drug development. *Annu. Rev. Biophys. Biomol. Struct.* **26,** 401–424 (1997).

52. Boder, E. T. & Wittrup, K. D. Yeast surface display for screening combinatorial polypeptide libraries. *Nat Biotech* **15,** 553–557 (1997).

53. Daugherty, P. S. Protein engineering with bacterial display. *Curr. Opin. Struct. Biol.* **17,** 474–480 (2007).

54. Goldflam, M. & Ullman, C. G. Recent advances toward the discovery of drug-like peptides *de novo*. *Front. Chem.* **3,** (2015).

55. Liu, C. C. *et al.* Protein evolution with an expanded genetic code. *Proc. Natl. Acad. Sci.* **105,** 17688–17693 (2008).

56. Roberts, R. W. & Szostak, J. W. RNA-peptide fusions for the *in vitro* selection of peptides and proteins. *Proc. Natl. Acad. Sci.* **94,** 12297–12302 (1997).

57. Hanes, J. & Plückthun, A. In vitro selection and evolution of functional proteins by using ribosome display. *Proc. Natl. Acad. Sci.* **94,** 4937–4942 (1997).

58. Bashiruddin, N. K. & Suga, H. Construction and screening of vast libraries of natural product-like macrocyclic peptides using *in vitro* display technologies. *Curr. Opin. Chem. Biol.* **24,** 131–138 (2015).

59. Hamzeh-Mivehroud, M., Alizadeh, A. A., Morris, M. B., Bret Church, W. & Dastmalchi, S. Phage display as a technology delivering on the promise of peptide drug discovery. *Drug Discov. Today* **18,** 1144–1157 (2013).

60. Heinis, C. & Winter, G. Encoded libraries of chemically modified peptides. *Curr. Opin. Chem. Biol.* **26,** 89–98 (2015).

61. Russel, M., Lowman, H. & Clackson, T. in *Phage Display — A Practical Approach* (eds. Clackson, T. & Lowman, H.) (Oxford University Press, 2004).

62. Cwirla, S. E., Peters, E. A., Barrett, R. W. & Dower, W. J. Peptides on phage: a vast library of peptides for identifying ligands. *Proc. Natl. Acad. Sci. U. S. A.* **87,** 6378–6382 (1990).

63. O'Neil, K. T. *et al.* Identification of novel peptide antagonists for GPIIb/IIIa from a conformationally constrained phage peptide library. *Proteins Struct. Funct. Bioinforma.* **14,** 509–515 (1992).

64. McLafferty, M. A., Kent, R. B., Ladner, R. C. & Markland, W. M13 bacteriophage displaying disulfide-constrained microproteins. *Gene* **128,** 29–36 (1993).

65. Ladner, R. C. Constrained peptides as binding entities. *Trends Biotechnol.* **13,** 426–430 (1995).

66. Chen, S. & Heinis, C. in *RSC Drug Discovery* (eds. Jones, L. & McKnight, A. J.) 241–262 (Royal Society of Chemistry, 2013).

67. Sinclair, A. Erythropoiesis stimulating agents approaches to modulate activity. *Biol. Targets Ther.* 161 (2013). doi:10.2147/BTT.S45971

68. Heinis, C., Rutherford, T., Freund, S. & Winter, G. Phage-encoded combinatorial chemical libraries based on bicyclic peptides. *Nat. Chem. Biol.* **5,** 502–507 (2009).

69. Baeriswyl, V. *et al.* Bicyclic peptides with optimized ring size inhibit human plasma kallikrein and its orthologues while sparing paralogous proteases. *ChemMedChem* **7,** 1173–1176 (2012).

70. Angelini, A. *et al.* Bicyclic peptide inhibitor reveals large contact interface with a protease target. *ACS Chem. Biol.* **7,** 817–821 (2012).

71. Angelini, A., Morales-Sanfrutos, J., Diderich, P., Chen, S. & Heinis, C. Bicyclization and tethering to albumin yields long-acting peptide antagonists. *J. Med. Chem.* **55,** 10187–10197 (2012).

72. Timmerman, P., Beld, J., Puijk, W. C. & Meloen, R. H. Rapid and quantitative cyclization of multiple peptide loops onto synthetic scaffolds for structural mimicry of protein surfaces. *ChemBioChem* **6,** 821–824 (2005).

73. Diderich, P. & Heinis, C. Directed evolution of bicyclic peptides for therapeutic application. *Chim. Int. J. Chem.* **67,** 910–915 (2013).

74. Rebollo, I. R., Angelini, A. & Heinis, C. Phage display libraries of differently sized bicyclic peptides. *Med Chem Commun* **4,** 145–150 (2013).

75. Chen, S., Morales-Sanfrutos, J., Angelini, A., Cutting, B. & Heinis, C. Structurally diverse cyclisation linkers impose different backbone conformations in bicyclic peptides. *ChemBioChem* **13,** 1032–1038 (2012).

76. Chen, S., Bertoldo, D., Angelini, A., Pojer, F. & Heinis, C. Peptide ligands stabilized by small molecules. *Angew. Chem. Int. Ed.* **53,** 1602–1606 (2014).

77. Bertoldo, D. *et al.* Phage selection of peptide macrocycles against β-Catenin to interfere with Wnt signaling. *ChemMedChem* **11,** 834–839 (2016).

78. Chen, S. *et al.* Bicyclic peptide ligands pulled out of cysteine-rich peptide libraries. *J. Am. Chem. Soc.* **135,** 6562–6569 (2013).

79. Chen, S. *et al.* Improving binding affinity and stability of peptide ligands by substituting glycines with D-amino acids. *ChemBioChem* **14,** 1316–1322 (2013).

80. Baeriswyl, V. *et al.* Development of a selective peptide macrocycle inhibitor of coagulation factor XII toward the generation of a safe antithrombotic therapy. *J. Med. Chem.* **56,** 3742–3746 (2013).

81. Baeriswyl, V. *et al.* A synthetic factor XIIa inhibitor blocks selectively intrinsic coagulation initiation. *ACS Chem. Biol.* **10,** 1861–1870 (2015).

82. Wu, Y. Contact pathway of coagulation and inflammation. *Thromb. J.* **13,** (2015).

83. Björkqvist, J., Sala-Cunill, A. & Renné, T. Hereditary angioedema: a bradykinin-mediated swelling disorder. *Thromb. Haemost.* **109,** 368–374 (2013).

84. Andreasen, P. A., Egelund, R. & Petersen, H. H. The plasminogen activation system in tumor growth, invasion, and metastasis. *Cell. Mol. Life Sci. CMLS* **57,** 25–40 (2000).

85. Angelini, A. *et al.* Chemical macrocyclization of peptides fused to antibody Fc fragments. *Bioconjug. Chem.* **23,** 1856–1863 (2012).

86. Long, A. T., Kenne, E., Jung, R., Fuchs, T. A. & Renné, T. Contact system revisited: an interface between inflammation, coagulation, and innate immunity. *J. Thromb. Haemost.* **14,** 427–437 (2016).

87. Björkqvist, J., Nickel, K. F., Stavrou, E. & Renné, T. *In vivo* activation and functions of the protease factor XII. *Thromb. Haemost.* **112,** 868–875 (2014).

88. Kenne, E. *et al.* Factor XII: a novel target for safe prevention of thrombosis and inflammation. *J. Intern. Med.* **278,** 571–585 (2015).

89. Dobrovolskaia, M. A. & McNeil, S. E. Safe anticoagulation when heart and lungs are 'on vacation'. *Ann. Transl. Med.* **3,** S11–S11 (2015).

90. Wilbs, J., Middendorp, S. J. & Heinis, C. Improving the binding affinity of *in vitro* evolved cyclic peptides by inserting atoms into the macrocycle backbone. *ChemBioChem* **17,** 2299–2303 (2016).

91. Middendorp, S. J. *et al.* Peptide macrocycle inhibitor of coagulation factor XII with subnanomolar affinity and high target selectivity. *J. Med. Chem.* (2017).

92. Di, L. Strategic approaches to optimizing peptide ADME properties. *AAPS J.* **17,** 134–143 (2015).

93. Kontermann, R. E. Half-life extended biotherapeutics. *Expert Opin. Biol. Ther.* **16,** 903–915 (2016).

94. Perea, S. E. *et al.* Antitumor effect of a novel proapoptotic peptide that impairs the phosphorylation by the protein kinase 2 (casein kinase 2). *Cancer Res.* **64,** 7127–7129 (2004).

95. Biron, E. *et al.* Improving oral bioavailability of peptides by multiple N-methylation: somatostatin analogues. *Angew. Chem. Int. Ed.* **47,** 2595–2599 (2008).

96. Wang, J., Yadav, V., Smart, A. L., Tajiri, S. & Basit, A. W. Toward oral delivery of biopharmaceuticals: an assessment of the gastrointestinal stability of 17 peptide drugs. *Mol. Pharm.* **12,** 966–973 (2015).

97. Guyton, A. C. & Hall, J. E. *Textbook of medical physiology*. (Elsevier Saunders, 2006).

98. Yamasaki, K., Chuang, V. T. G., Maruyama, T. & Otagiri, M. Albumin–drug interaction and its clinical implication. *Biochim. Biophys. Acta BBA - Gen. Subj.* **1830,** 5435–5443 (2013).

99. van Witteloostuijn, S. B., Pedersen, S. L. & Jensen, K. J. Half-life extension of biopharmaceuticals using chemical methods: alternatives to PEGylation. *ChemMedChem* **11,** 2474–2495 (2016).

100. Pasut, G. & Veronese, F. M. State of the art in PEGylation: the great versatility achieved after forty years of research. *J. Controlled Release* **161,** 461–472 (2012).

101. Knop, K., Hoogenboom, R., Fischer, D. & Schubert, U. S. Poly(ethylene glycol) in drug delivery: pros and cons as well as potential alternatives. *Angew. Chem. Int. Ed.* **49,** 6288–6308 (2010).

102. Roberts, M. J., Bentley, M. D. & Harris, J. M. Chemistry for peptide and protein PEGylation. *Adv. Drug Deliv. Rev.* **64,** 116–127 (2012).

103. Harris, J. M. & Chess, R. B. Effect of PEGylation on pharmaceuticals. *Nat. Rev. Drug Discov.* **2,** 214–221 (2003).

104. Dozier, J. & Distefano, M. Site-specific PEGylation of therapeutic proteins. *Int. J. Mol. Sci.* **16,** 25831–25864 (2015).

105. Sherman, M. R., Saifer, M. G. P. & Perez-Ruiz, F. PEG-uricase in the management of treatment-resistant gout and hyperuricemia. *Adv. Drug Deliv. Rev.* **60,** 59–68 (2008).

106. Zhang, F., Liu, M. & Wan, H. Discussion about several potential drawbacks of PEGylated therapeutic proteins. *Biol. Pharm. Bull.* **37,** 335–339 (2014).

107. Fishburn, C. S. The pharmacology of PEGylation: balancing PD with PK to generate novel therapeutics. *J. Pharm. Sci.* **97,** 4167–4183 (2008).

108. Swierczewska, M., Lee, K. C. & Lee, S. What is the future of PEGylated therapies? *Expert Opin. Emerg. Drugs* **20,** 531–536 (2015).

109. Caparrotta, T. M. & Evans, M. PEGylated insulin Lispro (LY2605541) - a new basal insulin analogue. *Diabetes Obes. Metab.* **16,** 388–395 (2014).

110. Duckworth, W. C., Bennett, R. G. & Hamel, F. G. Insulin degradation: progress and potential 1. *Endocr. Rev.* **19,** 608–624 (1998).

111. Bonneville, T. *Vectoring diabetic glucose for type 1 diabetics*. (Xlibris Corporation, 2012).

112. Riddle, M. C. Lessons from peglispro: IMAGINE how to improve drug development and affordability. *Diabetes Care* **39,** 499–501 (2016).

113. Zhou, K. *et al.* Studies of poly(ethylene glycol) modification of HM-3 polypeptides. *Bioconjug. Chem.* **20,** 932–936 (2009).

114. Liu, Z., Ren, Y., Pan, L. & Xu, H.-M. *In vivo* anti-tumor activity of polypeptide HM-3 modified by different polyethylene glycols (PEG). *Int. J. Mol. Sci.* **12,** 2650–2663 (2011).

115. Hamley, I. W. PEG–peptide conjugates. *Biomacromolecules* **15,** 1543–1559 (2014).

116. Macdougall, I. C. *et al.* Pharmacokinetics of novel erythropoiesis stimulating protein compared with epoetin alfa in dialysis patients. *J. Am. Soc. Nephrol.* **10,** 2392–2395 (1999).

117. Strohl, W. R. Fusion proteins for half-life extension of biologics as a strategy to make biobetters. *BioDrugs* **29,** 215–239 (2015).

118. Bouloux, P. M. G. *et al.* First human exposure to FSH-CTP in hypogonadotrophic hypogonadal males. *Hum. Reprod.* **16,** 1592–1597 (2001).

119. Duijkers, I. J. M. *et al.* Single dose pharmacokinetics and effects on follicular growth and serum hormones of a long-acting recombinant FSH preparation (FSH-CTP) in healthy pituitary-suppressed females. *Hum. Reprod.* **17,** 1987–1993 (2002).

120. Moradi, S. V., Hussein, W. M., Varamini, P., Simerska, P. & Toth, I. Glycosylation, an effective synthetic strategy to improve the bioavailability of therapeutic peptides. *Chem Sci* **7,** 2492–2500 (2016).

121. Joensuu, T. K. Phase I trial on sms-D70 somatostatin analogue in advanced prostate and renal cell cancer. *Ann. N. Y. Acad. Sci.* **1028,** 361–374 (2004).

122. Jain, S. *et al.* Polysialylated insulin: synthesis, characterization and biological activity *in vivo*. *Biochim. Biophys. Acta BBA - Gen. Subj.* **1622,** 42–49 (2003).

123. Knudsen, L. B. *et al.* Potent derivatives of glucagon-like peptide-1 with pharmacokinetic properties suitable for once daily administration. *J. Med. Chem.* **43,** 1664–1669 (2000).

124. Edwards, C. M. B. *et al.* Exendin-4 reduces fasting and postprandial glucose and decreases energy intake in healthy volunteers. *Am. J. Physiol.-Endocrinol. Metab.* **281,** E155–E161 (2001).

125. Meier, J. J. GLP-1 receptor agonists for individualized treatment of type 2 diabetes mellitus. *Nat. Rev. Endocrinol.* **8,** 728–742 (2012).

126. Kong, J.-H., Oh, E. J., Chae, S. Y., Lee, K. C. & Hahn, S. K. Long acting hyaluronate – exendin 4 conjugate for the treatment of type 2 diabetes. *Biomaterials* **31,** 4121–4128 (2010).

127. Greindl, A. *et al.* AGEM400 (HES), a novel erythropoietin mimetic peptide conjugated to hydroxyethyl starch with excellent *in vitro* efficacy. *Open Hematol. J.* **4,** (2010).

128. Podust, V. N. *et al.* Extension of *in vivo* half-life of biologically active molecules by XTEN protein polymers. *J. Controlled Release* **240,** 52–66 (2016).

129. Schellenberger, V. *et al.* A recombinant polypeptide extends the *in vivo* half-life of peptides and proteins in a tunable manner. *Nat. Biotechnol.* **27,** 1186–1190 (2009).

130. Podust, V. N. *et al.* Extension of *in vivo* half-life of biologically active peptides via chemical conjugation to XTEN protein polymer. *Protein Eng. Des. Sel.* **26,** 743–753 (2013).

131. Betts, J. G., OpenStax College & Rice University. *Anatomy & physiology*. (2013).

132. Roopenian, D. C. & Akilesh, S. FcRn: the neonatal Fc receptor comes of age. *Nat. Rev. Immunol.* **7,** 715–725 (2007).

133. Mitragotri, S., Burke, P. A. & Langer, R. Overcoming the challenges in administering biopharmaceuticals: formulation and delivery strategies. *Nat. Rev. Drug Discov.* **13,** 655–672 (2014).

134. Levin, D., Golding, B., Strome, S. E. & Sauna, Z. E. Fc fusion as a platform technology: potential for modulating immunogenicity. *Trends Biotechnol.* **33,** 27–34 (2015).

135. Yeung, Y. A. *et al.* Engineering human IgG1 affinity to human neonatal Fc receptor: impact of affinity improvement on pharmacokinetics in primates. *J. Immunol.* **182,** 7663–7671 (2009).

136. Andersen, J. T. *et al.* Extending serum half-life of albumin by engineering neonatal Fc receptor (FcRn) binding. *J. Biol. Chem.* **289,** 13492–13502 (2014).

137. Sockolosky, J. T. & Szoka, F. C. The neonatal Fc receptor, FcRn, as a target for drug delivery and therapy. *Adv. Drug Deliv. Rev.* **91,** 109–124 (2015).

138. Chames, P., Van Regenmortel, M., Weiss, E. & Baty, D. Therapeutic antibodies: successes, limitations and hopes for the future. *Br. J. Pharmacol.* **157,** 220–233 (2009).

139. Benjamin, W. U. & Sun, Y.-N. Pharmacokinetics of peptide–Fc fusion proteins. *J. Pharm. Sci.* **103,** 53–64 (2014).

140. Hubulashvili, D. & Marzella, N. Romiplostim (Nplate), a treatment option for immune (idiopathic) thrombocytopenic purpura. *Pharm. Ther.* **34,** 482–485 (2009).

141. Molineux, G. & Newland, A. Development of romiplostim for the treatment of patients with chronic immune thrombocytopenia: from bench to bedside. *Br. J. Haematol.* (2010).

142. Jendle, J. *et al.* Efficacy and safety of dulaglutide in the treatment of type 2 diabetes: a comprehensive review of the dulaglutide clinical data focusing on the AWARD phase 3 clinical trial program. *Diabetes Metab. Res. Rev.* **32,** 776–790 (2016).

143. Morais, S. A., Vilas-Boas, A. & Isenberg, D. A. B-cell survival factors in autoimmune rheumatic disorders. *Ther. Adv. Musculoskelet. Dis.* **7,** 122–151 (2015).

144. Hsu, H. *et al.* A novel modality of BAFF-specific inhibitor AMG623 peptibody reduces B-cell number and improves outcomes in murine models of autoimmune disease. *Clin. Exp. Rheumatol.* **30,** 197—201 (2012).

145. Scheinberg, M. A., Srinivasan, D. & Martin, R. S. The potential role of blisibimod for the treatment of systemic lupus erythematosus. *Int. J. Clin. Rheumatol.* **9,** 121–134 (2014).

146. Oliner, J. *et al.* Suppression of angiogenesis and tumor growth by selective inhibition of angiopoietin-2. *Cancer Cell* **6,** 507–516 (2004).

147. Coxon, A. *et al.* Context-dependent role of angiopoietin-1 inhibition in the suppression of angiogenesis and tumor growth: implications for AMG 386, an angiopoietin-1/2-neutralizing peptibody. *Mol. Cancer Ther.* **9,** 2641–2651 (2010).

148. Herbst, R. S. *et al.* Safety, pharmacokinetics, and antitumor activity of AMG 386, a selective angiopoietin inhibitor, in adult patients with advanced solid tumors. *J. Clin. Oncol.* **27,** 3557–3565 (2009).

149. Monk, B. J. *et al.* Anti-angiopoietin therapy with trebananib for recurrent ovarian cancer (TRINOVA-1): a randomised, multicentre, double-blind, placebo-controlled phase 3 trial. *Lancet Oncol.* **15,** 799–808 (2014).

150. Picha, K. M. *et al.* Protein engineering strategies for sustained glucagon-like peptide-1 receptor-dependent control of glucose homeostasis. *Diabetes* **57,** 1926–1934 (2008).

151. Parlevliet, E. T. *et al.* CNTO736, a novel glucagon-like peptide-1 receptor agonist, ameliorates insulin resistance and inhibits very low-density lipoprotein production in high-fat-fed mice. *J. Pharmacol. Exp. Ther.* **328,** 240–248 (2009).

152. Johnson, D. L. *et al.* Identification of a 13 amino acid peptide mimetic of erythropoietin and description of amino acids critical for the mimetic activity of EMP1. *Biochemistry (Mosc.)* **37,** 3699–3710 (1998).

153. Bouman-Thio, E. *et al.* A phase I, single and fractionated, ascending-dose study evaluating the safety, pharmacokinetics, pharmacodynamics, and mmunogenicity of an erythropoietin mimetic antibody fusion protein (CNTO 528) in healthy male subjects. *J. Clin. Pharmacol.* **48,** 1197–1207 (2008).

154. Bugelski, P. J. *et al.* CNTO 530: molecular pharmacology in human UT-7EPO cells and pharmacokinetics and pharmacodynamics in mice. *J. Biotechnol.* **134,** 171–180 (2008).

155. Mezo, A. R. *et al.* Atrial natriuretic peptide-Fc, ANP-Fc, fusion proteins: semisynthesis, *in vitro* activity and pharmacokinetics in rats. *Bioconjug. Chem.* **23,** 518–526 (2012).

156. Kim, B.-J. *et al.* Transferrin fusion technology: a novel approach to prolonging biological half-Life of insulinotropic peptides. *J. Pharmacol. Exp. Ther.* **334,** 682–692 (2010).

157. Matsubara, M. *et al.* Single dose GLP-1-Tf ameliorates myocardial ischemia/reperfusion injury. *J. Surg. Res.* **165,** 38–45 (2011).

158. Xia, C. Q., Wang, J. & Shen, W.-C. Hypoglycemic effect of insulin-transferrin conjugate in streptozotocin-induced diabetic rats. *J. Pharmacol. Exp. Ther.* **295,** 594–600 (2000).

159. Brandsma, M. E., Jevnikar, A. M. & Ma, S. Recombinant human transferrin: beyond iron binding and transport. *Biotechnol. Adv.* **29,** 230–238 (2011).

160. Pollaro, L. & Heinis, C. Strategies to prolong the plasma residence time of peptide drugs. *MedChemComm* **1,** 319 (2010).

161. DeLano, W. L., Ultsch, M. H., de, A. M., Vos & Wells, J. A. Convergent solutions to binding at a protein-protein interface. *Science* **287,** 1279 (2000).

162. Mersich, C., Billes, W. & Jungbauer, A. Identification of a ligand for IgG-Fc derived from a soluble peptide library based on fusion proteins secreted by *S. cerevisiae*. *Biotechnol. J.* **2,** 672–677 (2007).

163. Menegatti, S., Hussain, M., Naik, A. D., Carbonell, R. G. & Rao, B. M. mRNA display selection and solid-phase synthesis of Fc-binding cyclic peptide affinity ligands. *Biotechnol. Bioeng.* **110,** 857–870 (2013).

164. Sockolosky, J. T., Kivimäe, S. & Szoka, F. C. Fusion of a short peptide that binds immunoglobulin G to a recombinant protein substantially increases its plasma half-life in mice. *PLoS ONE* **9,** e102566 (2014).

165. Hutt, M., Farber-Schwarz, A., Unverdorben, F., Richter, F. & Kontermann, R. E. Plasma half-life extension of small recombinant antibodies by fusion to immunoglobulin-binding domains. *J. Biol. Chem.* **287,** 4462–4469 (2012).

166. Unverdorben, F., Hutt, M., Seifert, O. & Kontermann, R. E. A Fab-selective immunoglobulin-binding domain from streptococcal protein G with improved half-life extension properties. *PLOS ONE* **10,** e0139838 (2015).

167. Löfblom, J. *et al.* Affibody molecules: engineered proteins for therapeutic, diagnostic and biotechnological applications. *FEBS Lett.* **584,** 2670–2680 (2010).

168. Seijsing, J. *et al.* An engineered affibody molecule with pH-dependent binding to FcRn mediates extended circulatory half-life of a fusion protein. *Proc. Natl. Acad. Sci.* **111,** 17110–17115 (2014).

169. Mezo, A. R. *et al.* Reduction of IgG in nonhuman primates by a peptide antagonist of the neonatal Fc receptor FcRn. *Proc. Natl. Acad. Sci.* **105,** 2337–2342 (2008).

170. Sockolosky, J. T., Tiffany, M. R. & Szoka, F. C. Engineering neonatal Fc receptor-mediated recycling and transcytosis in recombinant proteins by short terminal peptide extensions. *Proc. Natl. Acad. Sci.* **109,** 16095–16100 (2012).

171. Penchala, S. C. *et al.* A biomimetic approach for enhancing the *in vivo* half-life of peptides. *Nat. Chem. Biol.* **11,** 793–798 (2015).

172. de Kort, M. *et al.* Conjugation of ATIII-binding pentasaccharides to extend the half-life of proteins: long-acting insulin. *ChemMedChem* **3,** 1189–1193 (2008).

173. Miltenburg, A. M. M. *et al.* Half-life prolongation of therapeutic proteins by conjugation to ATIII-binding pentasaccharides: a first-in-human study of CarboCarrier ® insulin. *Br. J. Clin. Pharmacol.* **75,** 1221–1230 (2013).

174. Lee, J. H., Engler, J. A., Collawn, J. F. & Moore, B. A. Receptor mediated uptake of peptides that bind the human transferrin receptor. *FEBS J.* **268,** 2004–2012 (2001).

175. Grönwall, C. *et al.* Affibody-mediated transferrin depletion for proteomics applications. *Biotechnol. J.* **2,** 1389–1398 (2007).

176. Zhang, J., Williams, B. A. R., Nilsson, M. T. & Chaput, J. C. The evolvability of lead peptides from small library screens. *Chem. Commun.* **46,** 7778 (2010).

177. Sleep, D., Cameron, J. & Evans, L. R. Albumin as a versatile platform for drug half-life extension. *Biochim. Biophys. Acta BBA - Gen. Subj.* **1830,** 5526–5534 (2013).

178. Peters, T., Jr. *All about albumin: biochemistry, genetics, and medical applications*. (Academic Press, 1996).

179. Fanali, G. *et al.* Human serum albumin: from bench to bedside. *Mol. Aspects Med.* **33,** 209–290 (2012).

180. Dockal, M., Carter, D. C. & Rüker, F. Conformational transitions of the three recombinant domains of human serum albumin depending on pH. *J. Biol. Chem.* **275,** 3042–3050 (2000).

181. Larsen, M. T., Kuhlmann, M., Hvam, M. L. & Howard, K. A. Albumin-based drug delivery: harnessing nature to cure disease. *Mol. Cell. Ther.* **4,** (2016).

182. Nicholson, J. P., Wolmarans, M. R. & Park, G. R. The role of albumin in critical illness. *BJA Br. J. Anaesth.* **85,** 599–610 (2000).

183. Schmidt, M. M. *et al.* Crystal structure of an HSA/FcRn complex reveals recycling by competitive mimicry of HSA ligands at a pH-dependent hydrophobic interface. *Structure* **21,** 1966–1978 (2013).

184. Sand, K. M. K. *et al.* Dissection of the neonatal Fc receptor (FcRn)-albumin interface using mutagenesis and anti-FcRn albumin-blocking antibodies. *J. Biol. Chem.* **289,** 17228–17239 (2014).

185. Kratz, F. Albumin as a drug carrier: design of prodrugs, drug conjugates and nanoparticles. *J. Controlled Release* **132,** 171–183 (2008).

186. Trujillo, J. M. & Nuffer, W. Albiglutide: a new GLP-1 receptor agonist for the treatment of type 2 diabetes. *Ann. Pharmacother.* **48,** 1494–1501 (2014).

187. Liu, Z. & Chen, X. Simple bioconjugate chemistry serves great clinical advances: albumin as a versatile platform for diagnosis and precision therapy. *Chem Soc Rev* **45,** 1432–1456 (2016).

188. Wang, W., Ou, Y. & Shi, Y. AlbuBNP, a recombinant B-type natriuretic peptide and human serum albumin fusion hormone, as a long-term therapy of congestive heart failure. *Pharm. Res.* **21,** 2105–2111 (2004).

189. Duttaroy, A. *et al.* Development of a long-acting insulin analog using albumin fusion technology. *Diabetes* **54,** 251 (2004).

190. Zhang, L. *et al.* A novel exendin-4 human serum albumin fusion protein, E2HSA, with an extended half-life and good glucoregulatory effect in healthy rhesus monkeys. *Biochem. Biophys. Res. Commun.* **445,** 511–516 (2014).

191. Baggio, L. L., Huang, Q., Cao, X. & Drucker, D. J. An albumin-exendin-4 conjugate engages central and peripheral circuits regulating murine energy and glucose homeostasis. *Gastroenterology* **134,** 1137–1147 (2008).

192. Xie, D. *et al.* An albumin-conjugated peptide exhibits potent anti-HIV activity and long *in vivo* half-life. *Antimicrob. Agents Chemother.* **54,** 191–196 (2010).

193. Muller, D. *et al.* Improved pharmacokinetics of recombinant bispecific antibody molecules by fusion to human serum albumin. *J. Biol. Chem.* **282,** 12650–12660 (2007).

194. Evans, L. *et al.* The production, characterisation and enhanced pharmacokinetics of scFv–albumin fusions expressed in *Saccharomyces cerevisiae*. *Protein Expr. Purif.* **73,** 113–124 (2010).

195. Richards, D. *et al.* A Phase 1 and pharmacologic study of MM-111, a bispecific HER2/HER3 antibody fusion protein, in combination with multiple treatment regimens in patients with advanced HER2 positive solid tumors. *Breast* **20,** 63 (2012).

196. Ascenzi, P. & Fasano, M. Allostery in a monomeric protein: the case of human serum albumin. *Biophys. Chem.* **148,** 16–22 (2010).

197. Bhattacharya, A. A., Grüne, T. & Curry, S. Crystallographic analysis reveals common modes of binding of medium and long-chain fatty acids to human serum albumin. *J. Mol. Biol.* **303,** 721–732 (2000).

198. Rustan, A. C. & Drevon, C. A. Fatty acids: structures and properties. *Encycl. Life Sci.* (2005).

199. Spector, A. A. Fatty acid binding to plasma albumin. *J. Lipid Res.* **16,** 165–179 (1975).

200. Kragh-Hansen, U., Watanabe, H., Nakajou, K., Iwao, Y. & Otagiri, M. Chain length-dependent binding of fatty acid anions to human serum albumin studied by site-directed mutagenesis. *J. Mol. Biol.* **363,** 702–712 (2006).

201. Jonassen, I. *et al.* Biochemical and physiological properties of a novel series of long-acting insulin analogs obtained by acylation with cholic acid derivatives. *Pharm. Res.* **23,** 49–55 (2006).

202. Koehler, M. F. *et al.* Albumin affinity tags increase peptide half-life *in vivo*. *Bioorg. Med. Chem. Lett.* **12,** 2883–2886 (2002).

203. Zobel, K., Koehler, M. F. T., Beresini, M. H., Caris, L. D. & Combs, D. Phosphate ester serum albumin affinity tags greatly improve peptide half-life *in vivo*. *Bioorg. Med. Chem. Lett.* **13,** 1513–1515 (2003).

204. Dumelin, C. E. *et al.* A portable albumin binder from a DNA-encoded chemical library. *Angew. Chem. Int. Ed.* **47,** 3196–3201 (2008).

205. Franzini, R. M. *et al.* Identification of structure-activity relationships from screening a structurally compact DNA-encoded chemical library. *Angew. Chem. Int. Ed.* **54,** 3927–3931 (2015).

206. Trüssel, S. *et al.* New strategy for the extension of the serum half-life of antibody fragments. *Bioconjug. Chem.* **20,** 2286–2292 (2009).

207. Muller, C., Struthers, H., Winiger, C., Zhernosekov, K. & Schibli, R. DOTA conjugate with an albumin-binding entity enables the first folic acid-targeted 177Lu-radionuclide tumor therapy in mice. *J. Nucl. Med.* **54,** 124–131 (2013).

208. Dennis, M. S. *et al.* Albumin binding as a general strategy for improving the pharmacokinetics of proteins. *J. Biol. Chem.* **277,** 35035–35043 (2002).

209. Sato, A. K. *et al.* Development of mammalian serum albumin affinity purification media by peptide phage display. *Biotechnol. Prog.* **18,** 182–192 (2002).

210. Dennis, M. S. *et al.* Imaging tumors with an albumin-binding Fab, a novel tumor-targeting agent. *Cancer Res.* **67,** 254–261 (2007).

211. Langenheim, J. F. & Chen, W. Y. Improving the pharmacokinetics/pharmacodynamics of prolactin, GH, and their antagonists by fusion to a synthetic albumin-binding peptide. *J. Endocrinol.* **203,** 375–387 (2009).

212. Nilvebrant, J. & Hober, S. The albumin-binding domain as a scaffold for proteins engineering. *Comput. Struct. Biotechnol. J.* **6,** 1–8 (2013).

213. Jonsson, A., Dogan, J., Herne, N., Abrahmsen, L. & Nygren, P.-A. Engineering of a femtomolar affinity binding protein to human serum albumin. *Protein Eng. Des. Sel.* **21,** 515–527 (2008).

214. Stork, R., Muller, D. & Kontermann, R. E. A novel tri-functional antibody fusion protein with improved pharmacokinetic properties generated by fusing a bispecific single-chain diabody with an albumin-binding domain from streptococcal protein G. *Protein Eng. Des. Sel.* **20,** 569–576 (2007).

215. Andersen, J. T. *et al.* Extending half-life by indirect targeting of the neonatal Fc receptor (FcRn) using a minimal albumin binding domain. *J. Biol. Chem.* **286,** 5234–5241 (2011).

216. Guo, R. *et al.* Fusion of an albumin-binding domain extends the half-life of immunotoxins. *Int. J. Pharm.* **511,** 538–549 (2016).

217. Li, R. *et al.* Fusion to an albumin-binding domain with a high affinity for albumin extends the circulatory half-life and enhances the *in vivo* antitumor effects of human TRAIL. *J. Controlled Release* **228,** 96–106 (2016).

218. Markussen, J. *et al.* Soluble, fatty acid acylated insulins bind to albumin and show protracted action in pigs. *Diabetologia* **39,** 281–288 (1996).

219. Nguyen, A. *et al.* The pharmacokinetics of an albumin-binding Fab (AB.Fab) can be modulated as a function of affinity for albumin. *Protein Eng. Des. Sel.* **19,** 291–297 (2006).

220. Hopp, J. *et al.* The effects of affinity and valency of an albumin-binding domain (ABD) on the half-life of a single-chain diabody-ABD fusion protein. *Protein Eng. Des. Sel.* **23,** 827–834 (2010).

221. Levy, O. E. *et al.* Novel exenatide analogs with peptidic albumin binding domains: potent anti-diabetic agents with extended duration of action. *PLoS ONE* **9,** e87704 (2014).

222. Holt, L. J. *et al.* Anti-serum albumin domain antibodies for extending the half-lives of short lived drugs. *Protein Eng. Des. Sel.* **21,** 283–288 (2008).

223. O'Connor-Semmes, R. L. *et al.* GSK2374697, a novel albumin-binding domain antibody (AlbudAb), extends systemic exposure of exendin-4: first study in humans—PK/PD and safety. *Clin. Pharmacol. Ther.* **96,** 704–712 (2014).

224. Van Roy, M. *et al.* The preclinical pharmacology of the high affinity anti-IL-6R Nanobody® ALX-0061 supports its clinical development in rheumatoid arthritis. *Arthritis Res. Ther.* **17,** (2015).

225. Adams, R. *et al.* Extending the half-life of a fab fragment through generation of a humanized anti-human serum albumin Fv domain: An investigation into the correlation between affinity and serum half-life. *mAbs* **8,** 1336–1346 (2016).

226. Davé, E. *et al.* Fab-dsFv: a bispecific antibody format with extended serum half-life through albumin binding. *mAbs* **8,** 1319–1335 (2016).

227. Kurtzhals, P. *et al.* Albumin binding of insulins acylated with fatty acids: characterization of the ligand-protein interaction and correlation between binding affinity and timing of the insulin effect *in vivo*. *Biochem. J.* **312,** 725–731 (1995).

228. Jonassen, I. *et al.* Design of the novel protraction mechanism of Insulin Degludec, an ultra-long-acting basal Insulin. *Pharm. Res.* **29,** 2104–2114 (2012).

229. Kurtzhals, P., Havelund, S., Jonassen, I. B. & Markussen, J. Effect of fatty acids and selected drugs on the albumin binding of a long-acting, acylated insulin analogue. *J. Pharm. Sci.* **86,** 1365–1368 (1997).

230. Danne, T., Lüpke, K., Walte, K., Von Schuetz, W. & Gall, M.-A. Insulin detemir is characterized by a consistent pharmacokinetic profile across age-groups in children, adolescents, and adults with type 1 diabetes. *Diabetes Care* **26,** 3087–3092 (2003).

231. Havelund, S. *et al.* The mechanism of protraction of insulin detemir, a long-acting, acylated analog of human insulin. *Pharm. Res.* **21,** 1498–1504 (2004).

232. Wang, F., Surh & Kaur. Insulin degludec as an ultralong-acting basal insulin once a day: a systematic review. *Diabetes Metab. Syndr. Obes. Targets Ther.* 191 (2012).

233. Agersø, H., Jensen, L. B., Elbrønd, B., Rolan, P. & Zdravkovic, M. The pharmacokinetics, pharmacodynamics, safety and tolerability of NN2211, a new long-acting GLP-1 derivative, in healthy men. *Diabetologia* **45,** 195–202 (2002).

234. Plum, A., Jensen, L. B. & Kristensen, J. B. *In vitro* protein binding of liraglutide in human plasma determined by reiterated stepwise equilibrium dialysis. *J. Pharm. Sci.* **102,** 2882–2888 (2013).

235. Elbrønd, B. *et al.* Pharmacokinetics, pharmacodynamics, safety, and tolerability of a single-dose of NN2211, a long-acting glucagon-like peptide 1 derivative, in healthy male subjects. *Diabetes Care* **25,** 1398–1404 (2002).

236. Novo Nordisk files for regulatory approval of once-weekly semaglutide with the FDA for the treatment of type 2 siabetes. *http://press.novonordisk-us.com/2016-12-05-Novo-Nordisk-Files-for-Regulatory-Approval-of-Once-Weekly-Semaglutide-with-the-FDA-for-the-Treatment-of-Type-2-Diabetes* (2016).

237. Lau, J. *et al.* Discovery of the once-weekly glucagon-like peptide-1 (GLP-1) analogue semaglutide. *J. Med. Chem.* **58,** 7370–7380 (2015).

238. Kapitza, C. *et al.* Semaglutide, a once-weekly human GLP-1 analog, does not reduce the bioavailability of the combined oral contraceptive, ethinylestradiol/levonorgestrel. *J. Clin. Pharmacol.* **55,** 497–504 (2015).

239. Bellmann-Sickert, K. *et al.* Long-acting lipidated analogue of human pancreatic polypeptide Is slowly released into circulation. *J. Med. Chem.* **54,** 2658–2667 (2011).

240. Shechter, Y. *et al.* Newly designed modifier prolongs the action of short-lived peptides and proteins by allowing their binding to serum albumin. *Bioconjug. Chem.* **23,** 1577–1586 (2012).

241. Edgerton, D. S. *et al.* Changes in glucose and fat metabolism in response to the administration of a hepato-preferential insulin analog. *Diabetes* **63,** 3946–3954 (2014).

242. van Witteloostuijn, S. B. *et al.* Neoglycolipids for prolonging the effects of peptides: self-assembling glucagon-like peptide 1 analogues with albumin binding properties and potent *in vivo* efficacy. *Mol. Pharm.* **14,** 193–205 (2017).

243. Lowenthal, M. S. Analysis of albumin-associated peptides and proteins from ovarian cancer patients. *Clin. Chem.* **51,** 1933–1945 (2005).

244. Gundry, R. L., Fu, Q., Jelinek, C. A., Van Eyk, J. E. & Cotter, R. J. Investigation of an albumin-enriched fraction of human serum and its albuminome. *PROTEOMICS – Clin. Appl.* **1,** 73–88 (2007).

245. Pollaro, L. *et al.* Bicyclic peptides conjugated to an albumin-binding tag diffuse efficiently into solid tumors. *Mol. Cancer Ther.* **14,** 151–161 (2015).

246. Goldfarb, A. R., Saidel, L. J. & Mosovich, E. The ultraviolet absorption spectra of proteins. *J. Biol. Chem.* **193,** 397–404 (1951).

247. Noble, J. E. & Bailey, M. J. A. in *Methods in Enzymology* **463,** 73–95 (Elsevier, 2009).

248. Anthis, N. J. & Clore, G. M. Sequence-specific determination of protein and peptide concentrations by absorbance at 205 nm: sequence-specific protein concentration at 205 nm. *Protein Sci.* **22,** 851–858 (2013).

249. Manning, M. C., Chou, D. K., Murphy, B. M., Payne, R. W. & Katayama, D. S. Stability of protein pharmaceuticals: an update. *Pharm. Res.* **27,** 544–575 (2010).

250. Freyer, M. W. & Lewis, E. A. in *Methods in Cell Biology* **84,** 79–113 (Elsevier, 2008).

251. Rossi, A. M. & Taylor, C. W. Analysis of protein-ligand interactions by fluorescence polarization. *Nat. Protoc.* **6,** 365–387 (2011).

252. Kenniston, J. A. *et al.* Inhibition of plasma kallikrein by a highly specific active site blocking antibody. *J. Biol. Chem.* **289,** 23596–23608 (2014).

253. Sturis, J. *et al.* GLP-1 derivative liraglutide in rats with *β* -cell deficiencies: influence of metabolic state on *β* -cell mass dynamics. *Br. J. Pharmacol.* **140,** 123–132 (2003).

254. Margulies, D., Melman, G. & Shanzer, A. Fluorescein as a model molecular calculator with reset capability. *Nat. Mater.* **4,** 768–771 (2005).

255. Sjöback, R., Nygren, J. & Kubista, M. Absorption and fluorescence properties of fluorescein. *Spectrochim. Acta. A. Mol. Biomol. Spectrosc.* **51,** L7–L21 (1995).

256. Bracci, L. *et al.* Synthetic peptides in the form of dendrimers become resistant to protease activity. *J. Biol. Chem.* **278,** 46590–46595 (2003).

257. Jambhekar, S. S. & Breen, P. J. *Basic pharmacokinetics*. (Pharmaceutical Pr, 2009).

258. European Medicines Agency. *Assessment report for Victoza (International non-proprietary name: liraglutide)*. Procedure No. EMEA/H/C/001026 (2009).

259. European Medicines Agency. *CHMP assessment report for Tresiba (International non-proprietary name: insulin degludec)*. Procedure No. EMEA/H/C/002498 (2012).

Alessandro Zorzi

Avenue Davel 21
1004 Lausanne
Switzerland

+41 076 608 68 18

alessandro.zorzi.7@gmail.com

12.01.1988
Monselice (Padua, Italy)
Male, Single, Italian

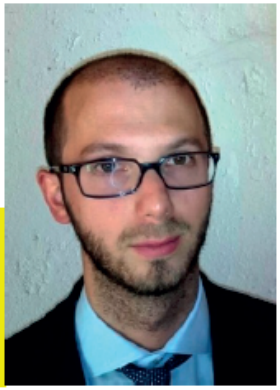

STRENGTHS

- Enterprising, passionate and hardworking biotechnologist
- Self-driven in applying my skills to handle the goal of a research project and highly involved in all project-related decisions
- Strong background in peptide synthesis, binding and inhibition assays, screening, pharmacokinetic studies

RESEARCH EXPERIENCE

01 / 2013 – 06 / 2017 — **Ph.D. candidate**
Laboratory of Therapeutic Proteins and Peptides (LPPT);
École Polytechnique Fédérale de Lausanne (EPFL), Switzerland
Dr. Christian Heinis

Developed an albumin-binding tag for prolonging the half-life of peptides:

- Optimized a ligand with high affinity and long half-life in animals;
- Established an automated synthesis of complex conjugates;
- Designed conjugates with retained bioactivity and longer half-life;
- Improved *in vivo* activity of a high-potential therapeutic peptide.

Direct responsibility for preparative and analytical RP-HPLC and LC-MS.

03 / 2012 – 09 / 2012 — **Master student**
Laboratory of Therapeutic Proteins and Peptides (LPPT);
École Polytechnique Fédérale de Lausanne (EPFL), Switzerland
Dr. Christian Heinis

- Performed phage display selection against human albumin.
- Synthesized peptides by SPPS and measured affinities by FP.

03 / 2010 – 07 / 2010 — **Bachelor student**
Laboratory of Protein Chemistry, Interdepartmental Research Center of Innovative Biotechnology (CRIBI); University of Padua, Italy
Dr. Angelo Fontana and Dr. Patrizia Polverino De Laureto

- Characterized structure and kinetics of aggregation of lysozyme.
- Developed a method to analyze the arrangement of fibrils by FRET.

WORK EXPERIENCE

09 / 2011 – 01 / 2012 — **Employee**
Cadline Software (for architectural design), Caselle di Selvazzano, Padua, Italy

- Support of corporate marketing
- Data storage
- Customer management

EDUCATION

10 / 2010 – 10 / 2012 — **Master's degree in Pharmaceutical Biotechnology**, *University of Padua, Italy; final mark 110 / 110 magna cum laude*
6-months exchange at École Polytechnique Fédérale de Lausanne (EPFL)
Advanced knowledge for development of biotechnological drugs and diagnostic tools.

10 / 2007 – 07 / 2010 **Bachelor's degree in Health Biotechnology**, *University of Padua, Italy; final mark 110 / 110 magna cum laude*
Basic knowledge essentials for the study of human and animal biology. First approach with biotechnological tools used for research, development and diagnosis.

PERSONAL SKILLS

ITALIAN — MOTHER TONGUE

OTHER LANGUAGES

	Listening	Reading	Speaking	Writing
ENGLISH	B2	B2	B2	B2
FRENCH	A2	B2	A2	A2

IT SKILLS — Competent with Microsoft Office (Word, Excel, Power Point), protein databases (PDB, Expasy), software useful in chemistry or biology (ChemDraw, MestReNova) and data editing (Sigma Plot, GraphPad Prism, Adobe Illustrator).

LABORATORY COMPETENCES

- Phage display technology
- Solid phase peptide synthesis (SPPS) and chemical or enzymatic modification of proteins and peptides (proteolysis, cyclization, labeling, click chemistry)
- Chromatography: IEX-FPLC, RP-HPLC, UPLC-MS
- Mass spectrometry: ESI-MS, MALDI-TOF
- Gel electrophoresis: SDS-PAGE, agarose
- Molecular biology: primers and gene design, PCR, library generation
- Spectroscopy: UV-Vis, FRET, circular dichroism
- Binding and inhibition assays: fluorescence polarization (FP), isothermal titration calorimetry (ITC), enzymatic activity

SOCIAL SKILLS

- Well-versed in interacting, sharing and discussing ideas with members of a diverse group.
- Seeking the opportunity to implement myself-leader scientist skills improving my autonomous capacity to understand problems, ask advices, propose and argue personal solutions.

ORGANIZATIONAL SKILLS

- Daily planning of duties and organization of outcome and protocol data.
- Constantly updated on relevant literature connected with the field of interest in order to further understand and stay current on state-of-the-art.

INTERESTS

- Football player and co-trainer in a children football team
- Runners in semi-competitive races (10-20 km)
- Swim, play football and draw during my free time

PUBLICATIONS

Zorzi, A., Middendorp, S. J., Wilbs, W., Deyle, K. & Heinis, C. Acylated heptapeptide binds albumin with high affinity and application as tag furnishes long-acting peptides. *In revision, Nat Comm.* (2017)

Zorzi, A., Deyle, K. & Heinis, C. Cyclic peptide therapeutics: past, present and future. *Curr. Opin. Chem. Biol.* **38**, 1-6 (2017).

Baeriswyl, V., Calzavarini, S., Chen, S., **Zorzi, A.**, Bologna, L., Angelillo-Scherrer, A. & Heinis, C. A synthetic factor XIIa inhibitor blocks selectively intrinsic coagulation initiation. *ACS Chem. Biol.* **10**, 1861-1870 (2015).